

JUHA LATVALA

# The Effect of Drainage on the Functionality of Railway Track Sub-ballast





JUHA LATVALA

# The Effect of Drainage on the Functionality of Railway Track Sub-ballast

ACADEMIC DISSERTATION

To be presented, with the permission of  
the Faculty of Built Environment  
of Tampere University,  
for public discussion in the RG202  
of the Rakennustalo, Korkeakoulunkatu 5, Tampere,  
on 16 February 2024, at 12 o'clock.

## ACADEMIC DISSERTATION

Tampere University, Faculty of Built Environment  
Finland

*Responsible  
supervisor  
and Custos*

Docent  
Heikki Luomala  
Tampere University  
Finland

*Supervisor*

Professor  
Pauli Kolisoja  
Tampere University  
Finland

*Pre-examiners*

Ph.D.  
Sakdirat Kaewunruen  
University of Birmingham  
United Kingdom

D.Eng.  
Kjell Arne Skoglund  
Norwegian Public Roads Administration  
Norway

*Opponent*

Professor Emerita  
Hannele Zubeck  
University of Alaska Anchorage  
United States

The originality of this thesis has been checked using the Turnitin OriginalityCheck service.

Copyright ©2024 author

Cover design: Roihu Inc.

ISBN 978-952-03-3300-3 (print)

ISBN 978-952-03-3301-0 (pdf)

ISSN 2489-9860 (print)

ISSN 2490-0028 (pdf)

<http://urn.fi/URN:ISBN:978-952-03-3301-0>



ClimateCalc: CC-000205471  
PunaMusta Printing

Carbon dioxide emissions from printing Tampere University dissertations have been compensated.

PunaMusta Oy – Yliopistopaino  
Joensuu 2024

# ACKNOWLEDGEMENTS

This doctoral dissertation is a kind of culmination of a series of long research projects related to drainage. Special thanks are due to the Finnish Transport Infrastructure Agency for making all of this possible by funding these research projects related to railway track drainage.

When I first started studying civil engineering at Tampere University of Technology, railways were not what I first had in mind. However, half by accident, I ended up taking a summer job at the construction management organisation in charge of the Seinäjoki–Oulu railway project in 2008, and since then my work has been related to railways. In 2012, I ended up taking a summer job at the Earth and Foundation Structures unit of Tampere University of Technology. That summer, a little surprisingly, I found myself building equipment for measuring the natural convection of the railway embankment and simultaneously studying this phenomenon with various aggregates. My summer job sneakily turned into a master's thesis about natural convection, and I continued my research after the completion of my thesis. I would like to thank my previous professor, Antti Nurmikolu, for introducing me to projects related to railway track drainage.

I already had an opportunity to start a collaboration with Heikki Luomala when we were building equipment to study natural convection. I would particularly like to thank Heikki for obtaining these research projects and for his major help with resolving practical issues. Once the first research projects began to come to a close, this dissertation also started to become apparent. For supervising the actual dissertation and articles, I would like to thank long-standing professor Pauli Kolisoja from Research Centre Terra, who assisted me in several ways in analysing the results on the actual subject of study and reporting the results internationally through articles. I also want to thank all of the other personnel of Terra for making Terra such an exceptionally pleasant workplace for all these years. I would like to offer particular thanks to the entire railway research team, especially Tiia, Riku and Tommi, who have worked with me for more than 11 years. Another thanks goes to the laboratory personnel, particularly Marko, with whom I have built and repaired monitoring stations out in the field on many occasions for this study as well. Likewise, I want to thank Nuutti for helping me carry out the static triaxial tests,

Antti for developing the applications for the triaxial test arrangements, and also research assistants Toni and Miikka, who was involved in carrying out the DCP and cyclic triaxial tests while working at Terra.

I would also like to thank you, D.Eng. Kjell Arne Skoglund and Ph.D. Sakdirat Kaewunruen, pre-examining this doctoral dissertation and Professor Emerita Hannele Zubeck for accepting the request to being my opponent in the public examination. It has been wonderful to have you participate in this work. Last, but not least, I would like to thank my wife, Aino, for her support and encouragement and our children, Lumi, Kaisla and Onni, for reminding me that there are many other things in life besides work.

# ABSTRACT

The significance of railway track drainage has typically been emphasised in various guidelines, but little research data exists on its actual effects. Based on the literature, water content clearly has an impact on the loading resistance of earth structures, but the occurrence of detrimental displacements and geometry deterioration depend on the actual loads. In particular, there was a lack of information on the degree to which geometry problems could be reduced by increasing the drainage depth along railway tracks.

Several shortcomings were found in the implementation of railway track drainage in Finland. For the most part, these problems are relatively simple issues, such as silted ditches, blocked culverts or subsurface drains. The original level of drainage has also been low in many places. Site drainage poses a more challenging problem, as conducting water away from the track area has been difficult in places due to reasons such as low height differences. Drainage maintenance design has largely been based on visual inspection, and maintenance contracts that call for maintenance ‘as necessary’ proved to be difficult to assess. This may have caused the functionality of drainage to have deteriorated over an extended period of time. Therefore, it is obvious that methods producing numerical data on the state of drainage should be adopted in order to optimise maintenance.

Three drainage monitoring stations were built along the Rantarata track in Southern Finland in places where the plan was to improve drainage. Material samples were collected from the sub-ballast layer at these monitoring stations and examined with several methods at the laboratory. The static triaxial tests found a clear increase in shear strength in all of the materials examined when the water content dropped below 7%. The effect of apparent cohesion was clear, and, at best, maximum shear stresses more than twice as high were achieved in a drier state. In the cyclic tests the samples with the highest water content proved to be the weakest. When the materials’ behaviour is examined in the predicted operating stress range, the Km44 and Km98 materials can withstand loading with relatively minor deformations, while the uniformly grained Km137 material, which has the smallest mean grain size, proved to be weak at high saturation degrees. However, the Km137 material also

appears to withstand the impact of the axle loads of passenger traffic, even when saturated.

Based on field measurements, the water content of the railway track sub-ballast layer is largely determined according to the level of the (ground)water table at the site. The impact of rain on water content was lower than expected, and rain was unable to increase the degree of saturation beyond 60–70% due to the effect of absorption; instead, the impact of rain was primarily evident in the rise in the (ground)water table. Water content varied by site, as expected. The drainage improvement carried out at site Km44, which previously had poor drainage, resulted in a major improvement. The high saturation degrees corresponding to seasonal variation practically disappeared entirely, and the water content decreased significantly at the sub-ballast layer.

Based on the monitoring results, no connection could be established between the vertical displacements along the railway tracks and the water content of the sub-ballast layer. The same observation was also made when examining supplementary data from frost monitoring stations. However, this observation can be explained with the laboratory tests conducted, as the load increase caused by passenger traffic in particular at the depth of the insulation layer is so small that weaker materials can also withstand the load as long as the intermediate layer is not completely saturated. The axle loads of freight traffic cause slightly more deformations, but heavy axle load (250 kN) trains usually operate only on mainly overhauled main track lines. The vertical displacements occurring at site Km44 could not be changed with the help of the drainage improvement carried out at the site. The most common causes of these displacements appear to be subgrade settlement, discontinuity points along the track or thaw softening after frost heave. Therefore, it is likely that in many places the formation of geometry irregularities cannot be prevented by improving drainage alone.

Based on the results, recommendations were issued for planning railway track drainage. In principle, drainage should always be kept operative, but draining all of the structural layers, particularly in rail sections with a low traffic volume, may be cost-ineffective. The key content of the new guidelines is that the ballast layer and intermediate layer must be drained under all circumstances. With busy or heavy traffic, the drainage level must go even deeper than this. Based on this study, the axle loads currently in use in Finland do not necessarily require the drainage of sub-ballast to be extended to the design depth of frost.

# TIIVISTELMÄ

Radan kuivatus on ollut tyypillisesti asia, jonka merkitystä on korostettu monissa eri ohjeissa, mutta sen todellisista vaikutuksista on ollut vähän tutkittua tietoa. Kirjallisuuden perusteella vesipitoisuuden vaikutus maarakenteiden kuormituskestävyyteen on ilmeistä, mutta haitallisten siirtymien syntyminen ja geometrian heikkeneminen riippuu todellisista kuormituksista. Erityisesti oli puutetta tiedosta, miten paljon geometriaongelmia voidaan mahdollisesti vähentää kasvattamalla kuivatussyvyyttä radalla.

Radan kuivatuksen toteutuksessa havaittiin Suomessa useita puutteita. Pääosin ongelmat ovat varsin yksinkertaisia, kuten liettyneitä oja tai tukkeutuneita rumpuja/salaojia. Paikoitellen alkuperäinen kuivatustaso on myös ollut matala. Haastavampi ongelma on aluekuivatus, sillä paikoitellen vesien johtaminen pois rata-alueelta on ollut hankalaa esimerkiksi vähäisten korkeuserojen vuoksi. Kuivatuksen kunnossapito on pohjautunut pitkälti silmämääräiseen arviointiin ja kunnossapitosopimusten kirjaukset ”tarpeen vaatiessa” osoittautuivat vaikeasti arvioitaviksi. Tällöin kuivatuksen toimivuus on saattanut heikentyä pitkällä aikavälillä. Tulevaisuudessa on syytä ottaa käyttöön menetelmiä, jotka tuottavat numeerista tietoa kuivatuksen tilasta kunnossapidon optimoinniksi.

Rantaradalle rakennettiin kolme kuivatuksen seuranta-asemaa kohteisiin, joissa kuivatusta oli tarkoitus parantaa. Näiltä mitta-asemilta otettiin alusrakennekerroksesta materiaalinäytteet, joita tarkasteltiin useilla menetelmillä laboratorioissa. Staattisissa kolmiakσιαalikoikeissa kaikilla tarkastelluilla materiaaleilla havaittiin selkeä leikkauslujuuden kasvu, kun vesipitoisuus laski alle 7 %. Näennäisen koheesion vaikutus oli ilmeinen ja parhaimmillaan kuivemmassa tilassa saavutettiin yli kaksinkertaisia maksimileikkausjännityksiä. Syklisissä kokeissa materiaalit käyttäytyvät eri tavalla ja eniten vettä sisältäneet näytteet osoittautuivat heikoimmiksi. Kun tarkastellaan materiaalien käyttäytymistä todennäköisellä käyttöjännitysalueella, Km44- ja Km98-materiaalit kestävät kuormitusta varsin pienin muodonmuutoksin, mutta keskiraekooltaan pienin ja tasarakeinen Km137-materiaali osoittautui heikoksi suurissa kyllästysasteissa. Kuitenkin sekin materiaali näyttäisi kestävän henkilöliikenteen akselipainojen vaikutuksen myös kyllästettynä.

Kenttämittausten perusteella radan alusrakennekerroksen vesipitoisuus määräytyy pitkälti alueellisen (pohja)vedenpinnan korkeuden perusteella. Sateiden vaikutus vesipitoisuuteen oli odotettua vähäisempi, eivätkä sateet kyenneet nostamaan kyllästysastetta yli 60–70 % kyllästysasteen imeytymisen vaikutuksesta, vaan niiden vaikutus näkyi pääasiassa kohonneen (pohja)vedenpinnan myötä. Vesipitoisuudet vaihtelivat odotetusti kohteittain. Km44-kuivatusparannuksella saavutettiin entuudestaan heikosti kuivatettuun kohteeseen erittäin suuri parannus, sillä vuodenaikaisvaihtelua vastaavat korkeat kyllästysasteet katosivat kuivatusparannuksen myötä käytännössä kokonaan ja vesipitoisuus aleni merkittävästi mittaussyvyydellä.

Seurantamittausten perusteella radan pystysuuntaisten siirtymien ja alusrakennekerroksen vesipitoisuuden välille ei kyetty muodostamaan yhteyttä. Sama havainto tehtiin myös täydentävällä routaseuranta-asemien datalla. Havainto on kuitenkin selitettävissä tehdyillä laboratoriokokeilla, sillä varsinkin henkilöliikenteen aiheuttama kuormituslisäys eristyskerroksen syvyydellä on niin pieni, että heikommatkin materiaalit kestävät, kunhan välikerros ei ole täysin vedellä kyllästynyt. Tavaraliikenteen akselipainoilla muodonmuutoksia syntyy hieman enemmän, mutta raskaiden akselipainojen (250 kN) junat operoivat yleensä vain perusparannetuilla rataosuuksilla. Km44-kohteelle tehdyllä kuivatusparannuksella ei kyetty muuttamaan kohteella muodostuvia pystysiirtymiä. Siirtymien yleisimpiä aiheuttajia näyttävät olevan joko pohjamaan painuminen, radan epäjatkuvuuskohdat tai sulamispehmeneminen. On siis todennäköistä, että monin paikoin pelkästään kuivatusta parantamalla ei voida korjata muodostuvia geometriaongelmia.

Tulosten perusteella annettiin suositukset radan kuivatuksen suunnitteluun. Kuivatus kannattaa lähtökohtaisesti pitää aina kunnossa, mutta varsinkin vähäliikenteisillä rataosilla kaikkien rakennekerrosten kuivattaminen voi olla kustannustehotonta. Uuden ohjeistuksen keskeinen sisältö on se, että tukikerros ja välikerros tulee kuivattaa kaikissa tapauksissa. Liikenteen ollessa vilkasta tai raskasta, kuivatustason tulee olla tätäkin syvempi. Alusrakenteen kuivattaminen routamitoitusvyöhyteen saakka ei ole tämän tutkimuksen perusteella kuitenkaan välttämättä tarpeellista nykyisin Suomessa käytössä olevilla akselipainoilla.



# CONTENTS

|       |   |    |
|-------|---|----|
| 1     | Introduction .....  | 1  |
| 1.1   | Background of the study.....  | 1  |
| 1.2   | Research objectives and questions .....   | 2  |
| 1.3   | Research methodologies .....  | 3  |
| 1.4   | Delimitations of the research topic.....  | 8  |
| 2     | Theoretical framework .....   | 9  |
| 2.1   | Retention of water by soil and drainage capacity .....  | 9  |
| 2.2   | Flow of water in soil.....  | 19 |
| 2.3   | The effect of water content on the strength properties of soils .....                         | 20 |
| 2.4   | The effect of water content on cyclic loading resistance .....                                | 23 |
| 2.5   | The effect of water content on frost protection design .....                                  | 30 |
| 2.6   | Drainage principles and water content in track structure .....                                | 33 |
| 3     | Results and discussion .....  | 36 |
| 3.1   | The current status of drainage and drainage maintenance on Finnish railway network .....      | 36 |
| 3.1.1 | Organization of drainage maintenance.....   | 36 |
| 3.1.2 | Observed drainage problems .....  | 38 |
| 3.2   | The effect of water to the loading resistance of sub-ballast materials .....                  | 40 |
| 3.2.1 | The grain size distribution and compaction properties of the materials studied .....          | 40 |
| 3.2.2 | Stresses in the sub-ballast.....  | 43 |
| 3.2.3 | Static triaxial tests .....   | 45 |
| 3.2.4 | DCP-method as a tool for recognizing poor quality sub-ballast materials.....                  | 49 |
| 3.2.5 | Material properties in cyclic loading triaxial tests .....                                    | 53 |
| 3.3   | Observations from the field site measurements .....   | 59 |
| 3.3.1 | Measured water contents .....   | 59 |
| 3.3.2 | Track deformation properties of monitored sites and the effect of drainage improvements ..... | 68 |
| 3.3.3 | Frost monitoring stations .....   | 74 |
| 3.4   | The effect of water content on frost protection design .....                                  | 82 |
| 4     | Conclusions .....   | 86 |
| 4.1   | Research outcomes .....   | 86 |

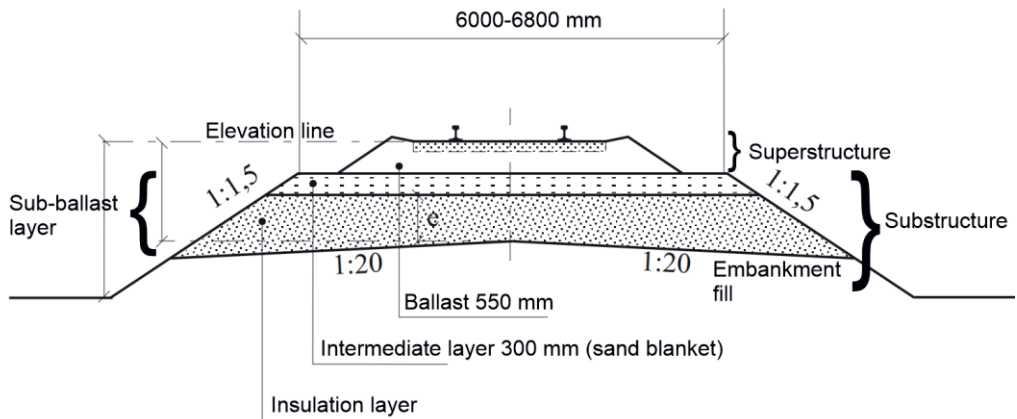
|     |   |    |
|-----|---|----|
| 4.2 | Suggestions for drainage improvement design ..... | 88 |
| 4.3 | Suggestions for further research.....             | 91 |
|     | References .....                                  | 92 |

# ABBREVIATIONS

|        |  |
|--------|--|
| $c'$   | Effective cohesion of the soil   |
| DCP    | Dynamic Cone Penetrometer  |
| $e$    | Void ratio   |
| FEM    | Finite Element Method  |
| FTIA   | Finnish Transport Infrastructure Agency  |
| grad H | Hydraulic gradient   |
| $k$    | Permeability/ Hydraulic conductivity of the material [m/s]   |
| K      | Fitting parameter used for improving correlation between measurements and forecasts (in Eq. 2–6)                   |
| K      | Height of capillary rise (in Fig. 2.13)  |
| Km44   | Monitoring site on Rantarata track   |
| Km98   | Monitoring site on Rantarata track   |
| Km137  | Monitoring site on Rantarata track   |
| MGT    | Million Gross Tons   |
| $n$    | Porosity   |
| $n_e$  | Effective porosity (~Drainable porosity)   |
| $q$    | Flux [m/s]   |
| R      | Depth of freezing point from ground level  |
| ROPE   | Routa- ja Pehmeikkökohteiden korjaushanke ( <i>Frost Damaged and Soft Soil Located Tracks Renovation Project</i> ) |
| $S_a$  | Saturation of the aqueous phase  |
| $S_r$  | Saturation degree  |
| $S_r$  | Specific retention (in Fig. 2.6)   |
| Ss     | Specific storage coefficient, which accounts for fluid compressibility   |
| $S_y$  | Specific yield   |
| $t$    | Time   |
| $u_a$  | Pore air pressure  |
| $u_w$  | Pore water pressure  |
| Z      | Depth of water table from ground level (in Fig. 2.13)  |

|                    |  |
|--------------------|--|
| $z$                | Vertical spatial dimension   |
| $\Theta$           | Normalised volumetric water content (identified from the water content versus suction curve) |
| $\theta$           | Volumetric water content   |
| $\sigma_n$         | Total normal stress on the plane of failure  |
| $\tau$             | Shear strength   |
| $\tau_f$           | Shear strength of an unsaturated soil  |
| $\phi'$            | Effective friction angle   |
| $\phi_b$           | Angle of shearing resistance relative to an increase in suction                              |
| $\psi$             | Pressure head  |
| $\psi_g$           | Gravitational potential  |
| $\psi_m$           | Matric potential   |
| $\psi_o$           | Osmotic potential  |
| $\psi_p$           | Pressure potential   |
| $\psi_t$           | Total moisture potential   |
| $(u_a - u_w)$      | Matric suction   |
| $(\sigma_n - u_a)$ | Net normal stress  |
| $(\sigma_n - u_w)$ | Effective normal stress on the plane of failure  |

# THE STRUCTURAL LAYERS OF FINNISH RAILWAY TRACK



The structural layers in the above figure are theoretical, when it comes to old track sections. In old track sections both intermediate and insulation layers are usually built using the same material and therefore that layer is called **sub-ballast** in this dissertation.

# KEY TERMINOLOGY

## Apparent cohesion

A phenomenon, where negative pore water pressure (matrix suction) increases non-cohesive soil strength in unsaturated state.

## Capillary rise

A phenomenon, where water rises in a thin tube or a porous material due to intermolecular forces between a liquid and surrounding solid surfaces.

## Confining pressure

In this work, confining pressure means the applied stress level for tested material sample in a static or cyclic triaxial test.

## Drainage depth

A depth at which drainage system keeps free water out of the structure. Defined as a distance from the elevation line.

## Horizontal stress

The stress state in horizontal direction of materials in track structure. The horizontal stresses can act on longitudinal or transversal direction and thus they are not necessarily equal. In this work, horizontal stress corresponds stress in transversal direction.

#### Insulation layer

Track layer, which is located between intermediate layer and embankment fill or subsoil. This layer is usually made of sand or crushed rock materials. In old track sections, the sub-ballast layers below the ballast are often built of the same materials.

#### Intermediate layer

Track layer, which locates first below the ballast layer. In Finland, that layer is typically 300 mm thick.

#### Loading resistance

The ability of soil structure to resist applied external loads (in this work train loads).

#### Permanent vertical displacement

The vertical displacements, which are measured from both ends of the sleeper in this study. Vertical displacements are usually directed downwards but during frost action, the displacement can be upwards. Measured vertical displacements don't include elastic responses from external loading. Permanent vertical displacements cause track geometry deterioration.

#### Saturation degree

The ratio of volume of water in the soil to the volume of voids. It defines how big proportion of the empty spaces between soil particles is filled with water.

#### Sub-ballast layer

The layer(s) below the ballast and above the embankment fill or subsoil. In new track sections these include intermediate and insulation layers, but in older track sections sub-ballast is usually built of the same material.

### Subgrade settlement

The deformation of subsoil mainly due to the consolidation settlement.

### Substructure

Sub-ballast with possible embankment fill. Basically, all layers between ballast and subsoil.

### Superstructure

The part of a railway track that consist of ballast, sleepers and rails.

### Vertical stress increase

The vertical stress addition in the structure due to an external load (in this work train load)



# ORIGINAL PUBLICATIONS

- Publication I Latvala, J., Nurmikolu, A., Luomala, H. (2016), “Problems with Railway Track Drainage in Finland”, *Advances in Transportation Geotechnics 3. The 3rd International Conference on Transportation Geotechnics (ICTG2016)*, Vol. 143, 2016, pages 1051-1058 <https://doi.org/10.1016/j.proeng.2016.06.098>.
- Publication II Latvala, J., Luomala, H., Kolisoja, P. (2020a), “Determining Soil Moisture Content and Material Properties with Dynamic Cone Penetrometer”, *The Baltic Journal of Road and Bridge Engineering*, Vol. 15 (2020), No. 5, pages 136–159 <https://doi.org/10.7250/bjrbe.2020-15.511>.
- Publication III Latvala, J., Kolisoja, P., Luomala, H. (2023) , “Water content variation of railway track sub-ballast layer in seasonal frost area: A case study from Finland”, *Transportation Geotechnics*, Vol. 38, January 2023, 100926 <https://doi.org/10.1016/j.trgeo.2022.100926>.
- Publication IV Latvala, J., Kolisoja, P., Luomala, H. (2022), “The cyclic loading resistance of old railway track sub-ballast materials at different water contents”, *Transportation Geotechnics*, Vol. 35 July 2022, 100772 <https://doi.org/10.1016/j.trgeo.2022.100772>.
- Publication V Latvala, J., Luomala, H., Kolisoja, P., Nurmikolu, A. (2020b), “Convective Heat Transfer in Crushed Rock Aggregates: The Effects of Grain Size Distribution and Moisture Content”, *Journal of Cold Regions Engineering*, Vol. 34 No. 3:04020012 [https://doi.org/10.1061/\(ASCE\)CR.1943-5495.0000219](https://doi.org/10.1061/(ASCE)CR.1943-5495.0000219).

# AUTHOR CONTRIBUTIONS

- Publication I The author of this dissertation was responsible for gathering the data, making the site inspections, literature review, analysing the results and writing the publication as corresponding author in guidance of Heikki Luomala and Antti Nurmikolu.
- Publication II The author of this dissertation was responsible for analysing laboratory and field measurement data, making the site investigations and writing the publication as corresponding author in guidance of Pauli Kolisoja and Heikki Luomala.
- Publication III The author of this dissertation was responsible for making field measurement system, analysing field measurement data, and writing the publication as corresponding author in guidance of Pauli Kolisoja and Heikki Luomala.
- Publication IV The author of this dissertation was responsible for planning and guidance of laboratory tests, analysing test results and writing the publication as corresponding author in guidance of Pauli Kolisoja and Heikki Luomala.
- Publication V The author of this dissertation was responsible for planning and manufacturing of laboratory test apparatus, making the laboratory tests, analysing test results and writing the publication as corresponding author in guidance of Heikki Luomala, Pauli Kolisoja and Antti Nurmikolu.

# 1 INTRODUCTION

## 1.1 Background of the study

The approximately 6,000-kilometre-long Finnish rail network is an infrastructure significant to the Finnish national economy. Today, its maintenance is the responsibility of the Finnish Transport Infrastructure Agency. A large proportion of this rail network was built at the turn of the 19<sup>th</sup> and 20<sup>th</sup> centuries, when the railways were developing rapidly, but the work methods used in their construction were completely different from modern methods. At the time, it was impossible to move around large amounts of earth, and the policy was to avoid making rock cuts. It is important to understand this historical background because even though the railway superstructures have been replaced several times in many places, it is still often the case that the original substructure layers remain in place under them. In many cases, these layers do not meet the current material requirements. In the future, train speeds and axle loads are expected to increase, leading to higher track evenness requirements, while at the same time the climate conditions will become more challenging. The maintenance of the Finnish rail networks is also hindered by frost and other phenomena related to high seasonal variation, in addition to rapidly changing subgrade conditions and thick and soft clay layers.

Climate change is predicted to cause a significant change in the current climate. Various extreme weather phenomena, such as floods and heavy rains, are predicted to increase in the future (Trenberth, 2011). According to studies, the intensity of individual rains is predicted to increase in Finland (Lehtonen, 2011), and total annual rainfall is expected to increase by multiple percentage points (Ruosteenoja et al., 2016). This type of change in the climate has also raised concerns internationally. For example, one study conducted in Sweden (Lindgren et al., 2009) states that the increase in unfavourable conditions on railways should be prepared for as early as possible. It is known based on international studies that cyclic loading and fine-grained materials in combination with excessive water content significantly reduce track geometry stability (Li and Selig, 1995). Excessive water content affects the sub-

ballast layer of the tracks in particular, as today the ballast layer is primarily made of coarse crushed rock materials.

Various guidelines have long stated that attention must be paid to the drainage of earth structures and that drainage must be kept operative. However, very little research data existed on the actual effects of drainage, and researchers have so far been unable to assess the measurable effects of drainage improvement, for example. In Finland, the Finnish Transport Infrastructure Agency has previously conducted various studies on unevenness problems occurring along the Finnish rail network. These studies have suspected that excessive water content contributes to the occurrence of frost heave, the development of unevenness and the weakening of loading resistance during thaw periods. All of the observations mentioned above in combination with climate change indicate a clear need to find out how railway track drainage affects the functioning of sub-ballast materials and what kinds of effects can be achieved with drainage improvement.

## 1.2 Research objectives and questions

The overall study comprises the following research objectives and questions:

### **Research objective 1.**

Identifying the most typical problems related to drainage and its maintenance in the Finnish rail network.

- What types of problems related to drainage occur along the rail network?
- What is the current situation of drainage maintenance in Finland?
- What types of methods are used to assess the functionality of track drainage?

### **Research objective 2.**

Determining the magnitudes of water content present in the track sub-ballast layer in seasonal frost areas and examining how drainage improvement affects water content.

- What magnitudes of water content are present in the sub-ballast layer in different types of locations?
- Can the impact of intensive seasonal variations be observed in the water content of the sub-ballast layer?

- Can the water content of the sub-ballast layer and its effect on loading resistance be interpreted with an indirect method, such as by using the dynamic cone resistance measured with a dynamic cone penetrometer?
- How does drainage improvement change the water content of the sub-ballast layer?

### **Research objective 3.**

Determining how a change in water content affects the functioning of the track sub-ballast materials.

- What type of effect does water content have on the loading resistance of the track sub-ballast materials, and can it be improved by reducing the degree of saturation?
- How does water content affect the heat transfer properties of the sub-ballast material from the frost protection design point of view?

### **Research objective 4.**

Using field measurement data to determine what type of connection exists between the deformation properties measured in the laboratory and the vertical displacements observed in the field.

- Can a correlation be found between the vertical displacements measured at the field sites and the water content of the sub-ballast layer?
- Under what types of conditions can the track water content reduce track geometry stability?
- Based on the measurement data, does track drainage improvement affect track geometry stability at the monitored sites?

## **1.3 Research methodologies**

When this study was first initiated, the primary question was: ‘Can the unevenness problems occurring along the railway be reduced by improving drainage?’ Both previous international studies and studies previously conducted in Finland indicated a possible connection between unevenness problems and excessive water content in the structural layers of the railway tracks. However, an answer to the question regarding the impact of drainage improvements on unevenness problems was not found in the literature. A significant amount of money is spent on railway maintenance each year, which is why major savings can be achieved with well-

targeted maintenance. Improving railway track drainage is a much more affordable measure than heavier measures, such as replacement of the sub-ballast, which makes the use of drainage improvement a very attractive option.

The structure of the study is presented in Figure 1.1. In the first phase, the theoretical aspects of this subject area were examined through a *literature review*. This review primarily focused on the impact mechanisms of water in the loading resistance and strength properties of soils, as well as the role of water availability in frost heave problems. The retention of water by soil was also studied with the help of literature, in order to better assess the effects of drainage. The results gained from the literature review were encouraging, as excessive water content reduces the loading resistance of unbound earth structures and, based on studies, also increases frost problems. The most typical drainage problems occurring in Finland were studied at the same time based on *field surveys* and *data from the Frost Damaged Tracks Renovation (ROPE) project*. Data was also gathered through an *interview study* with persons working in railway track maintenance. In the first phase of the study, the effects of various drainage solutions were primarily assessed with the help of *computer-aided modelling*.

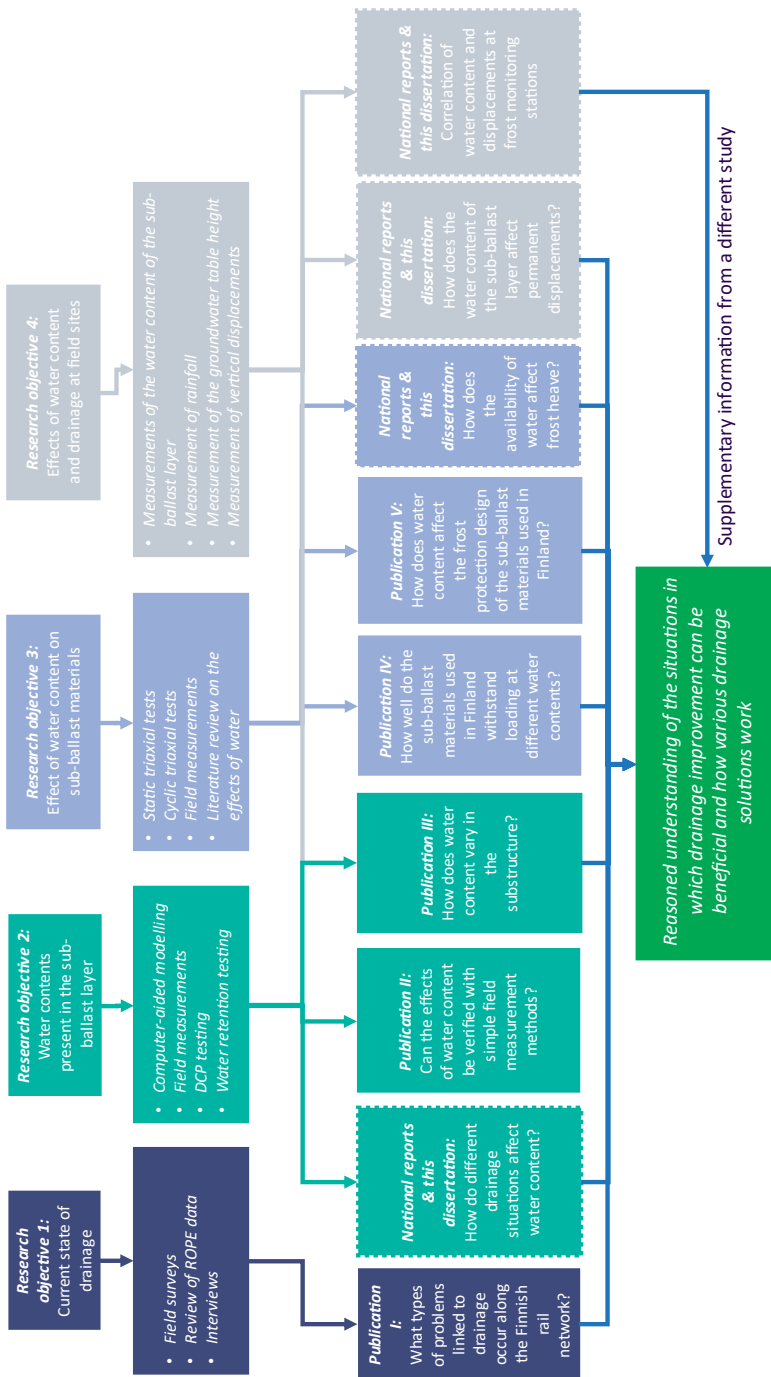


Figure 1.1. Structure of the study.

In the next phase, the goal was to find *field sites along the Finnish rail network* where drainage had been improved a few years earlier and where it was possible to analyse the functionality of the sites with the help of track inspection data. The objective was to determine how drainage improvements affected track geometry stability. However, it quickly became apparent that drainage had primarily been improved in conjunction with other relatively large measures, such as replacement of the superstructure, and only a few sites were found where drainage improvement alone had been carried out. Another thing that became apparent was that no reliable data was available on measures carried out in the past, such as tamping, because of the railway track maintenance implementation model followed in Finland. Nevertheless, a few suitable sites were found and their functioning was analysed through *field surveys* carried out as visual inspections and by analysing *track inspection data*. However, the results of these analyses were puzzling, as drainage improvement was found to have either a minor impact or no impact at all on the occurrence of geometry problems. For the present study, this was a turning point that led to the selection of a different type of approach: the construction of monitoring stations focusing on the functioning of railway track drainage.

Three *monitoring stations* were built along the Rantarata track running along Finland's southern coastline *to produce quantitative data on vertical displacements occurring along the track and the water content of the sub-ballast layer*. *Material samples* were collected from the track sub-ballast layer in conjunction with the construction of the monitoring stations, and the samples were utilised in extensive *laboratory tests*. The locations of the monitoring stations were selected based on the criteria that there were track geometry problems at or in the vicinity of the stations and that the drainage at the sites was not functional at the start of the study. The sites also differ from each other to allow the study to take account of different types of track structures. In connection with the project, the Finnish Transport Infrastructure Agency also undertook to improve drainage at the sites in order for the effects of the improvements to be verified through measurement data on the sites monitored. Additionally, other surveys, such as *field measurements conducted with a dynamic cone penetrometer*, were carried out at the sites. The purpose of these measurements was to find out whether excessive water content in the sub-ballast layer can be indirectly detected with the help of dynamic cone resistance, measured by a penetrometer.

The *tests conducted at the laboratory* played a key role in the overall study. The tests conducted at the laboratory to obtain more information about the effects of water



content on sub-ballast materials previously used in Finland include but are not limited to the following:

- Dry and wet sieving to determine grain size distributions.
- Proctor tests to identify the compaction properties of the materials.
- Determining the soil moisture characteristic curve to identify drainage capacity.
- Determining the height of capillary rise at different densities
- Static triaxial tests to determine the strength properties at different water contents.
- Large-scale cyclic triaxial tests to identify the effects of water content on railway track structures.
- Dynamic cone penetrometer tests to determine the connection between water content and dynamic cone resistance.

*Long-term monitoring* of the monitoring stations along the Rantarata track provided valuable data on the changes in the water content of the sub-ballast layer as a result of seasonal variation. In the literature, there was an obvious lack of this kind of information from northern countries with seasonal frost. Based on the observations, analyses were carried out on the connection between the vertical displacements measured and water content. However, as there were only three sites under observation, it was decided that the measurement data would be expanded by incorporating the *measurement data from frost monitoring stations* gathered by another study. A total of 16 frost monitoring stations were once built along the Finnish rail network, with eight of them capable of some type of water content measurement. At best, a set of measurement data covering a period of more than 10 years was available from these sites. This data was analysed by paying attention to water content and the occurrence of vertical displacements. The long term-data about permanent displacements from many sites is very unique and cannot be found from the literature.

Therefore, the observations presented in this doctoral dissertation are primarily based on *empirical/experimental measurements and observations*. However, they are rooted in the *conceptual* hypothesis, formed based on previous observations and literature, that reducing water content could reduce the unevenness problems occurring along the rail network. The study also includes *qualitative assessment of field sites* and an *interview study* conducted in writing with railway track maintainers.

## 1.4 Delimitations of the research topic

The railways are a complex entity combining technology from several different fields. The following delimitations have been made for this study:

- The drainage surveys primarily focus on line sections. The implementation of the drainage of turnouts and other special structures, such as rail yards, is not examined in this study. The drainage solutions for these structures differ from those used for line sections.
- The study focuses on the properties of the sub-ballast layer in particular. The study does not examine the effects of the water content of the ballast layer and subgrade on the operation of the tracks.
- With regard to the forces to which the railway tracks are subjected by rolling stock, the study is limited to the axle loads of the rolling stock currently in use in Finland, with the maximum axle load being 250 kN. For most sections of the Finnish rail network, the maximum permitted axle loads are lower than 250 kN.
- The examination of loading resistance in this study does not take account of the increase in dynamic load caused by discontinuity points along the track, such as rail defects, or the dynamic forces caused by different types of rolling stock.
- The main focus in the examination of the frost phenomenon has been on heat transfer properties, particularly convective heat transfer.

## 2 THEORETICAL FRAMEWORK

The interaction between unbound structural layers and water forms a very broad and complex whole. It is affected by several physical phenomena that simultaneously affect the functioning of the railway track substructure. The theory of a completely saturated structure is simpler, as it means that the change in loading resistance primarily arises from the pore pressure mobilised in conjunction with a rapid change in the load. In a partially saturated state, there are several different interaction forces present between water and soil particles, and the analysis and computational assessment of these forces is difficult. Several articles and books have been written about the assessment of the strength of partially saturated soil alone, which is why this chapter is not intended to be a complete review of the underlying theory. This chapter briefly goes over the most important theoretical aspects and discusses the phenomena contributing to the observations made in this study. However, even if the background of the phenomena causing track geometry deterioration are discussed in the literature, there is an obvious gap of knowledge regarding the beneficial effects of drainage that have been dealt with in this dissertation.

### 2.1 Retention of water by soil and drainage capacity

#### *Retention of water at soil particle level*

The water present in soil can be classified according to things such as the forces affecting the water, the origin of the water, flow properties or physical and chemical properties. Several different interaction forces exist between water and soil particles, and they are often in effect at the same time. Therefore, classification based on such interaction forces is not completely unequivocal. Classification also depends on the motive, as e.g. in agriculture farmers are interested in plant available water, whereas in engineering sciences the determining factor is the effect of water on the technical (strength) properties of soils. (Rétháti, 1983.)

The layer nearest to the soil particle (item 1 in Figure 2.1) is a heavily bound *layer of absorbed water* that is 1–10 water molecules thick. The next layer is a slightly less heavily bound water film less than 200 water molecules thick (item 2 in Figure 2.1). Together, these two layers form a hygroscopic layer that is primarily affected by electrostatic, polar and ionic forces. The third layer comprises *interstitial water* (item 3 in Figure 2.1), which is mainly bound by capillary forces. Factors affecting the amount of interstitial water include humidity, the grain size distribution of the soil type and the amount of colloidal matter, among other things; typically, interstitial water accounts for a larger proportion of the water in fine-grained soil types. Because of the effect of electric forces, the physical properties of interstitial water differ from normal free water: interstitial water has a higher viscosity, surface tension and boiling point and a lower freezing point. Soil particles also contain *water of crystallization*, which is structurally bound to minerals and is only removed by heating. The layer furthest away from the soil particle comprises *capillary water* (item 4 in Figure 2.1), which can be interpreted as *free water*. (Airaksinen, 1978; Rantamäki et al., 1979; Rétháti, 1983.)

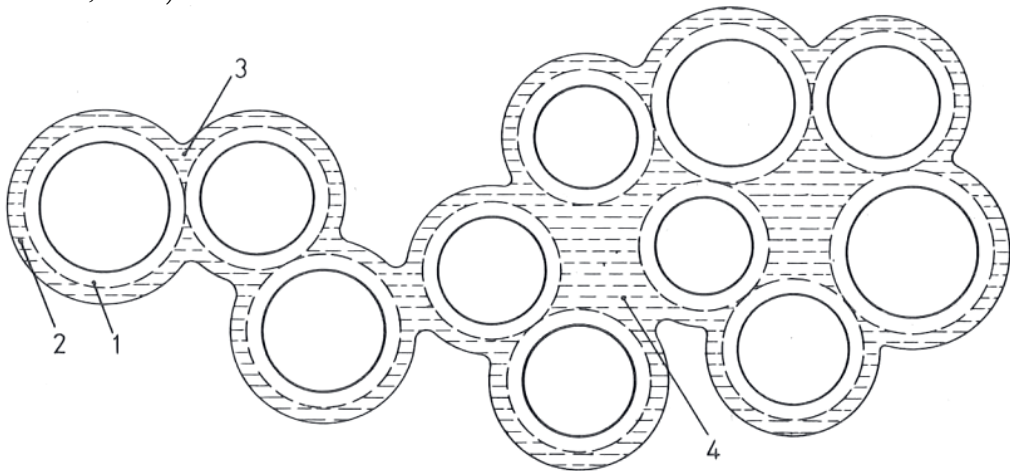


Figure 2.1. Films of water around soil particles. The layer nearest to the particle is a heavily bound hygroscopic water film (1), the second is a lightly bound hygroscopic water film (2), the third is interstitial water (3) and the fourth is fine or free capillary water (4). (Rétháti, 1983.)

As the name suggests, *capillary water* is held in the spaces between soil particles and on surfaces due to the effect of forces caused by surface tension. The cohesion of water causes water molecules to attract each other, resulting in surface tension, which is characteristic to water. In the capillary phenomenon, water molecules form an

interface with another material, and adhesive forces hold the water against the interface. As a result, the water forms curved interfaces called menisci. The pressure differentials present in the menisci lift up the water. The water continues to rise until the capillary force and gravity affecting the mass of water reach a state of equilibrium and the water reaches the capillary rise height. The capillary phenomenon occurs in thin pipes or similar pores in particular. Because of this phenomenon, the capillary rise height is also higher in fine-grained soil types. The amount of capillary water is the highest near the surface of groundwater. Capillary rise height can be calculated with the help of the equilibrium state of the forces caused by adhesion and cohesion. (Airaksinen, 1978; Daintith, 2009; Fredlund and Rahardjo, 1993; Kirkham and Powers, 1972.)

### *Soil moisture potential*

The classification of soil moisture into different types of zones provides a rough understanding of the nature of soil moisture. However, this zone model makes it necessary to make simplifications, as in practice, water is always affected by several different interaction forces. A more precise way of describing soil moisture retention is the soil moisture potential theory, which measures the potential energy of water at different points. According to the theory, water has both potential energy and kinetic energy, but when the flow of water is slow, kinetic energy is practically meaningless. Total soil moisture potential is often calculated based on equation 2–1. This equation takes account of the generally most important factors, but as potential may also be affected by other factors, an ellipsis is included on the right side of the equation. (Airaksinen, 1978; Hillel, 1971.)

$$\Psi_t = \Psi_m + \Psi_o + \Psi_g + \Psi_p + \dots \quad (2-1)$$

where

$\psi_t$  = total moisture potential

$\psi_m$  = matric potential

$\psi_o$  = osmotic potential

$\psi_g$  = gravitational potential

$\psi_p$  = pressure potential

According to the basic laws of physics, water tries to reach a state of equilibrium, thereby balancing out the potential differences. The soil moisture potential theory claims that the differences in potential energy cause water to move in search of a lower potential level until a state of equilibrium is reached. As the soil moisture

potential theory takes account of several factors affecting potential energy, it can be used to efficiently assess the movement of water in soil. Additionally, the theory takes account of the potential differences caused by differences in soil material. In many cases, potential energy is represented by hydraulic head, which expresses the potential energy as the height of a column of water. As the potential energies present in soil can be high, the height of a column of water can be represented by the pF value, which expresses the height of a column of water in centimeters as a base 10 logarithm. (Airaksinen, 1978; Hillel, 1971.)

The *pressure potential* of water represents the hydrostatic pressure of water. On a free water surface, the water pressure is as high as the prevalent atmospheric pressure, as shown in Figure 2.2. Water pressure increases below the surface, as the point examined is affected by both atmospheric pressure and the pressure caused by the weight of the water. Above the surface, the pressure potential is negative and the water is subjected to tensile stress or suction. Negative pressure potential is commonly referred to as **matric potential** or matric suction, but the term capillary potential is also used. Matric potential and pressure potential cannot be present in the same place at the same time, as one represents suction pressure while the other represents positive pressure. Negative pressure binds water with the help of suction/tension. Thus, matric potential represents the adhesion of water to soil materials. Capillary forces account for a significant proportion of matric potential, but this potential also includes other forces that hold water molecules around a soil particle. Matric potential reduces the total potential energy of water so much that water does not start flowing downwards gravitationally, despite the higher gravitational potential. In sandy soil types, most of the matric potential comes from capillary forces, whereas e.g. in fine-grained, clay-rich soil types absorption forces account for a large proportion of the potential. From a drainage perspective, matric potential is highly important, as it has a major impact on the soil moisture status of an unsaturated zone. (Hillel, 1971.)

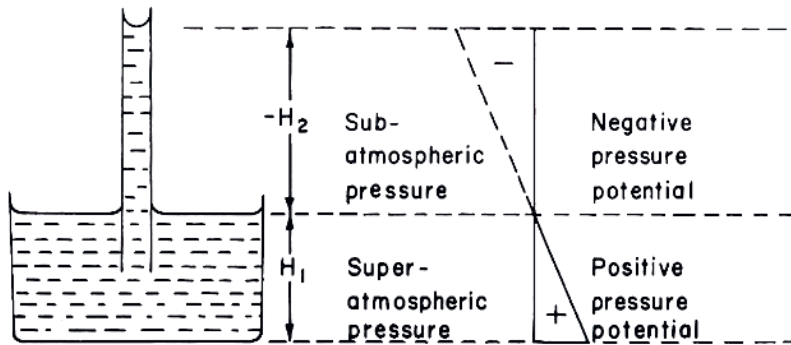


Figure 2.2. Pressure potentials above and below the surface of water. (Hillel, 1971.)

### Concepts related to water releasability

The pore spaces or voids in soil contain water, which is why it is important to define **porosity** unequivocally. **Porosity (n)** is defined as the ratio of the volume of voids to the total volume of the soil. **Void ratio (e)** refers to the ratio of the volume of voids to the total volume of solids. The porosity of soil can also be examined from the perspective of flow, in which case the term **effective porosity (n<sub>e</sub>)** is used. Effective porosity only takes into account pores that allow water to flow through them, such as interconnected pores, cracks and crevices. The definition excludes dead-end pores and stagnant pockets. Pore types also affect water movement, as pores that are narrower at one end may, in practice, prevent the flow of water. (Bear and Braester, 1972.)

Thanks to the various water binding forces and pore spaces, it is possible to determine a curve between porosity and water content, as shown in Figure 2.3, as well as limit values related to the curve, for different soil materials. **Specific yield**, which under certain conditions means the same thing as effective porosity (given as n<sub>e</sub> in Figure 2.3), refers to the volume of water that drains from saturated soil when the groundwater table is lowered due to the effect of gravity. Specific yield is usually expressed as a percentage of volume, and it varies between 1% and 30%. In accordance with the definition of effective pores, water must be able to drain away from the pores due to the effect of gravity. Specific yield corresponds to effective porosity when the soil layer is uniform and the groundwater table is sufficiently far after the change. In non-homogeneous soil and near the groundwater table, these concepts no longer mean exactly the same thing, which is why the term drainable

porosity may be used. **Field capacity** is important for drainage, as it indicates the water content left in the soil after excess water has drained from saturated soil due to the effect of gravity. As a result, the effective pores in the soil have emptied of water, and the water contained by dead-end pores or similar pores remains in the soil. Usually, the pF value 1.5–2.0 corresponds to the effect of gravity. Field capacity is affected by factors such as the grain size distribution and structure of soil. (Airaksinen, 1978; Bear, 1972.)

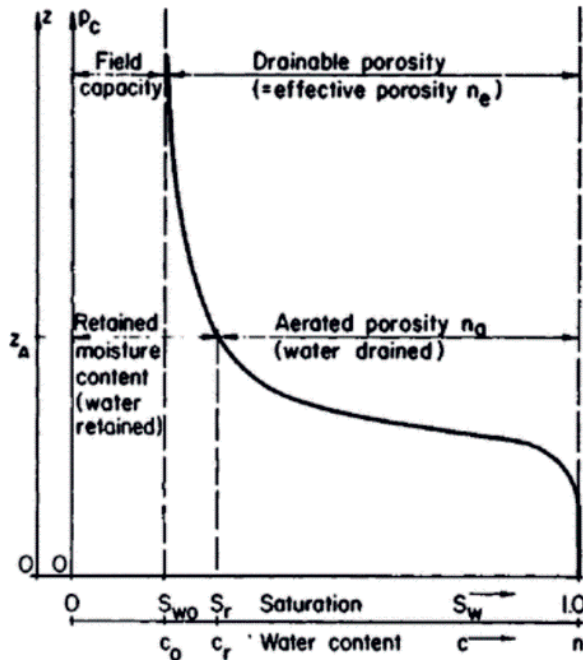


FIG. 9.4.8. Field capacity and effective porosity.

Figure 2.3. Relationship between water content and porosity. (Bear, 1972.)



The water content of soil is often expressed relative to the pF value with the help of a *soil moisture characteristic curve*, which represents the water content of soil relative to matric suction. Figure 2.4 presents a typical curve. The relationship between the matric potential of water and water content is not completely unequivocal, as the magnitude of matric potential depends on whether the soil is drying or absorbing water. This phenomenon is referred to as *soil moisture hysteresis*. Figure 2.5 shows a typical situation caused by hysteresis, in which matric suction pressure is clearly higher while the soil is drying than while the soil is getting wet. In practice, this means that the water is more heavily bound while the soil is drying and thus more difficult to release. The measurement shown in the figure was carried out by increasing the suction pressure on a saturated sample on the drying path while reducing the suction pressure on the dry sample on the wetting path. (Hillel, 1971.)

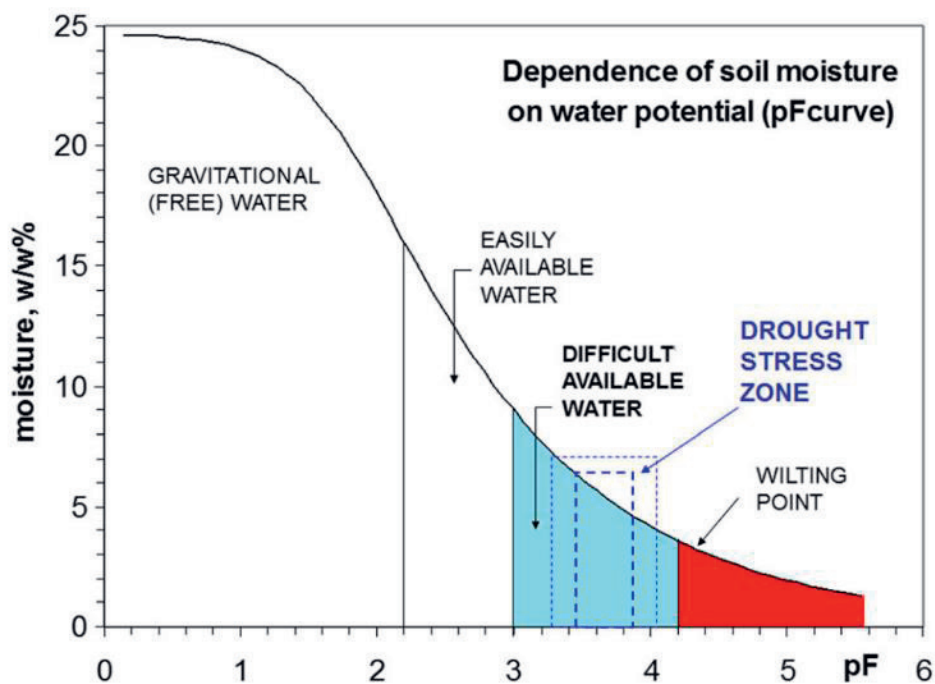


Figure 2.4. The relationship between the pF value and water content in a certain material. (Mikolajczak et al., 2016.)

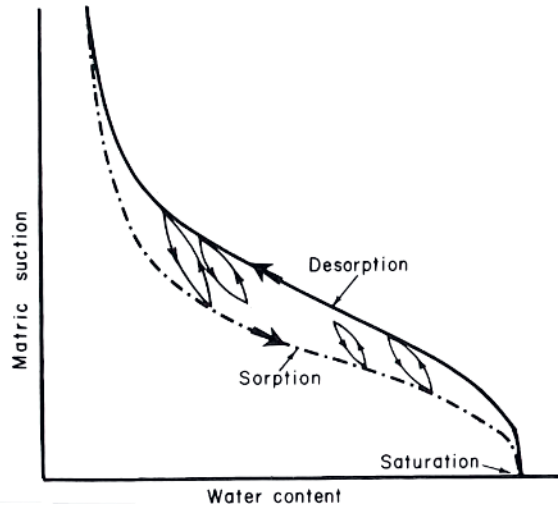


Figure 2.5. Variation in matric suction pressure while the material is absorbing (sorption) and releasing (desorption) water as a function of water content. (Hillel, 1971.)

The physical background of the hysteresis phenomenon is not completely unequivocal, and the phenomenon is likely to have several causal factors. The most significant cause is likely to be the geometric diversity of individual pores, which means that the shape of individual pores varies significantly, thus causing the 'ink-bottle effect'. Based on capillarity, the pipe diameter affects suction pressure. In the ink-bottle effect, drying depends on the diameter at the section of pore with the smallest diameter, while wetting depends on the diameter of the section of pore with the largest diameter. As a result, the suction pressure caused by the capillary phenomenon varies, and it is more difficult to release water from pores through drainage. Another cause of hysteresis is the contact angle effect. A droplet of water forms a certain contact angle, often called meniscus, on the surface of the solid. The size of the contact angle is affected by the properties of the liquid, solid and surrounding gas. Pure water on inorganic matter forms a contact angle that is close to zero. However, the contact angle increases if the surface is coarse or contains hydrophobic substances. The direction of the flow of water also affects the behaviour of the droplet, as the angle becomes larger as the meniscus progresses (as the material gets wet) compared to when the material drains of water. Therefore, this phenomenon can cause soil moisture hysteresis, which means that the matric potential is higher while the material is drying. Due to this phenomenon, the soil

moisture characteristic curve may also be surprisingly sharp for coarse-grained soil types with a relatively uniform pore size. Another possible cause of hysteresis is the presence of air in the earth structure, which prevents an actual state of equilibrium between water and air from being achieved as soon as the soil becomes wet. Changes in the soil moisture conditions may also cause soil shrinkage, swelling and ageing, i.e. changes in the earth structure itself. Generally speaking, the hysteresis effect occurs in coarse soil types at low suction pressures in particular. In suitable conditions, hysteresis may cause '*Haines jumps*', which refers to water being discharged in occasional bursts. This phenomenon can also happen the other way around: if the suction pressure on the soil decreases to a sufficient degree, the material may suddenly absorb water in its pores. Therefore, it can be noted that the absorption or discharge of water does not necessarily occur completely linearly as a function of suction pressure and that there can be significant jumps in the curve. (Hillel, 1971)

Different soil types have different water retention capacities. The water retention capacity of the material is strongly linked to the amount of fines contained by the material, and it can be said that the higher the fines content of the material, the better its water retention capacity. In Figure 2.6, Korkka-Niemi & Salonen (1996) have presented porosities, specific yields and specific retentions occurring in various soil types. The figure clearly shows how fine-grained soil types, such as clay and silt, have a relatively low specific yield and a high specific retention. This means that gravity drainage leaves a great amount of water in the soil. For coarse-grained soil types, such as sand and gravel, there is a clear increase in specific yield and reduction in specific retention, which means that it is possible to drain a great amount of water from the soil materials through drying. The situation is different for finer-grained soil types. For example, only 3–10% of the water content of clay can be drained. Therefore, it is clear that drying this type of material is difficult. Moreover, the capillary rise height of fine-grained materials is high, leading to new water constantly flowing into the structures unless capillary rise can be stopped. Figure 2.7 presents pF curves typical for various materials. The figure shows that sand releases most of its water content at a low suction pressure, whereas clay still retains a great amount of water at a similar pressure. The pF curves vary according to the soil type and degree of compaction examined. The degree of compaction mostly determines the

amount of pore space and the pore size of the material, which correlate with maximum water content.

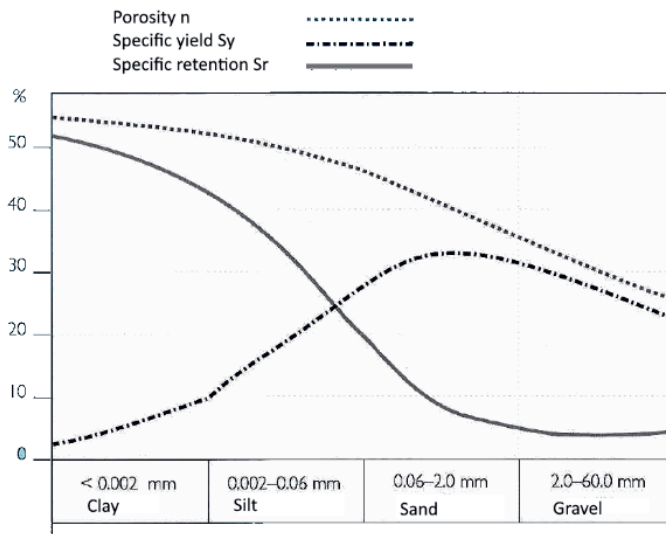


Figure 2.6. Porosities, specific yields and specific retentions for different soil types. The figure shows that clay retains a great amount of water, which is difficult to remove. (Korkka-Niemi and Salonen, 1996.)

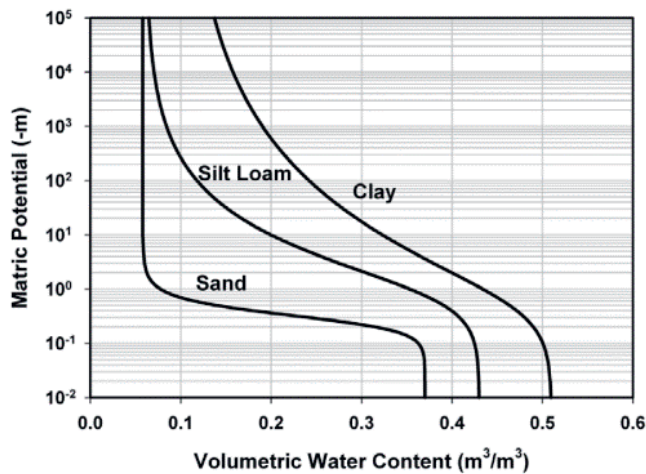


Figure 2.7. A typical soil moisture characteristic curve for clay, silt and sand. (Tuller and Or, 2003.)

## 2.2 Flow of water in soil

Understanding the flow of water in soil is a key part of the functioning of railway track drainage. In the 19th century, Henry Darcy studied the flow of water through horizontal layers of sand. His studies clearly showed that the volume of water flowing through a layer of sand is directly proportional to the water pressure and inversely proportional to the thickness of the sand layer. This is referred to as **Darcy's law**. *It can be presented* in the form of equation 2-2 and is the foundation of modern groundwater hydraulics. Darcy's law can be used to determine the volume of water flowing through a porous layer of soil as long as the area, permeability and hydraulic gradient of the soil layer are known. The original version of the equation only concerns one-dimensional flow, but it is possible to derive an equation for three-dimensional flow from the equation. Darcy's law is not directly valid at high flow velocities, as a flow with a high velocity differs from a (laminar) flow that moves smoothly in layers. However, the flow of groundwater is almost always laminar in nature. In very fine-grained soil types (such as clay), it is possible for flow to not occur at all until the threshold gradient characteristic to the soil type is exceeded. (Airaksinen, 1978; Miyazaki, 2005.)

$$q = -k \cdot \text{grad } H \quad (2-2)$$

where

|         |                    |
|---------|--------------------|
| q=      | flux [m/s]         |
| k=      | permeability [m/s] |
| grad H= | hydraulic gradient |

In the drainage of earth structures, water flow is usually not limited only to the saturated zone, which is why the flow occurring in the unsaturated zone must also be taken into account. The flow in the unsaturated layer can be modelled with the help of the Richards equation, for example. This differential equation created by Lorenzo Richards in 1931 is presented in equation 2-3. The equation takes account of the degree of saturation, based on which flow can be calculated. However, as algebraic use of the equation is not easy, several publications have presented solutions to the equation. Today, certain modelling

programs are also capable of solving the Richards equation, which also allows these programs to be used to analyse the flow of water in the unsaturated zone. It is not necessary to discuss the use of the equation in more detail in this context, as in any case its use requires a suitable modelling program, for example. These calculation programs are also able to take into account the different types of flow in different zones. (Tocci et al., 1997.)

$$S_s S_a(\psi) \frac{\partial \psi}{\partial t} + \frac{\partial \theta}{\partial t} = \frac{\partial}{\partial z} [K(\psi) \left( \frac{\partial \psi}{\partial z} + 1 \right)] \quad (2-3)$$

where

$S_s$  = specific storage coefficient, which accounts for fluid compressibility

$S_a$  = saturation of the aqueous phase

$\psi$  = pressure head

$t$  = time

$z$  = vertical spatial dimension

$K$  = hydraulic conductivity of the material

$\theta$  = volumetric water content

## 2.3 The effect of water content on the strength properties of soils

The water content of earth structures is known to affect the loading resistance of the structure. Clay is a good example of a material sensitive to water, as its strength is high when dry, but a sufficient amount of water causes soil liquefaction, and the material can almost completely lose its strength. The effect of water is smaller on coarser-grained soil types. It is known based on international studies that cyclic loading and fine-grained materials in combination with excessive water content significantly reduce track geometry stability (Li and Selig, 1995). For example, Bilodeau & Doré (2012) have stated in their article that water has a major impact on the mechanical properties of unbound structural layers. Repeated cyclic loading and vibration in railway environments also increase loading impact, as cyclic loading can cause mud pumping and increase pore pressure. On railways, the direction of the load changes due to the effect of moving trains, meaning that the effect of the load is greater compared to solely vertical repeated loading.

The shear strength of soil is traditionally determined with equation 2-4, presented by Terzaghi (1936). This equation describes the shear strength of soil as a linear function of the effective stress in the soil material. Terzaghi's basic equation is suitable for use in a saturated or dry state. However, the soil is often only partially saturated, hence the equation must be expanded to take account of the suction pressure that increases the strength of soil in a partially saturated state. Fredlund et al. (1978) presented equation 2-5, which is also suitable for assessing a partially saturated state. This equation, which takes the saturation state into account, is in practice an extension of Terzaghi's equation. The part of equation 2-5 that is provided after the + sign expresses the increase in strength caused by suction pressure, which is often referred to as apparent cohesion. (Fredlund et al., 1996, 1978; Vanapalli et al., 1998.)

$$\tau = c' + (\sigma_n - u_w) \tan \phi' \quad (2-4)$$

where

- $\tau$  = shear strength
- $c'$  = effective cohesion
- $\phi'$  = effective friction angle
- $\sigma_n$  = total normal stress on the plane of failure
- $(\sigma_n - u_w)$  = effective normal stress on the plane of failure
- $u_w$  = pore water pressure

$$\tau_f = [c' + (\sigma_n - u_a) \tan(\phi')] + [(u_a - u_w) \tan \phi^b] \quad (2-5)$$

where

- $\tau_f$  = shear strength of an unsaturated soil
- $c'$  = effective cohesion of the soil
- $\phi'$  = effective angle of shearing resistance for a saturated soil
- $u_a$  = pore air pressure
- $u_w$  = pore water pressure
- $(\sigma_n - u_a)$  = net normal stress
- $(u_a - u_w)$  = matric suction
- $\phi^b$  = angle of shearing resistance relative to an increase in suction

The equations presented above show how the suction pressure of soil in a partially saturated state increases the shear strength of the soil. However, as the equation cannot be used as is, it has been developed further to allow the soil moisture characteristic curve representing the suction pressure properties of soil to be used in calculating strength properties. Fredlund et al. (1996) and Vanapalli et al. (1996) have

studied this topic, and equation 2-6 presents a version of the equation that uses normalised volumetric water content identified from the soil moisture characteristic curve. However, use of this equation requires further integration and editing of the equation, among other things. Nevertheless, the significant role played by water in strength properties is evident in the equation.

$$\tau_f = [c' + (\sigma_n - u_a)\tan\phi'] + (u_a - u_w)\{\Theta(u_a - u_w)\}^K(\tan\phi') \quad (2-6)$$

*where*

K= fitting parameter used for improving correlation between measurements and forecasts

Θ= normalized volumetric water content (identified from the water content versus suction curve)

The basic assumption in the equation presented by Fredlund et al. (1978) is that the strength properties of soil increase as suction pressure increases. However, this is not the case for every material. For example, tests carried out on silty sand achieved the highest total shear strength at a saturation degree of 10–20%, as shown in Figure 2.8. The same tests also found that a sample on the drying path had higher strength than a sample on the wetting path at the same water content. (Leal-Vaca et al., 2012) Cohesive soil types in particular are sensitive to the effects of water content (Bláhová et al., 2013). Hence, it is very difficult to describe the strength properties of soil with only a few parameters.



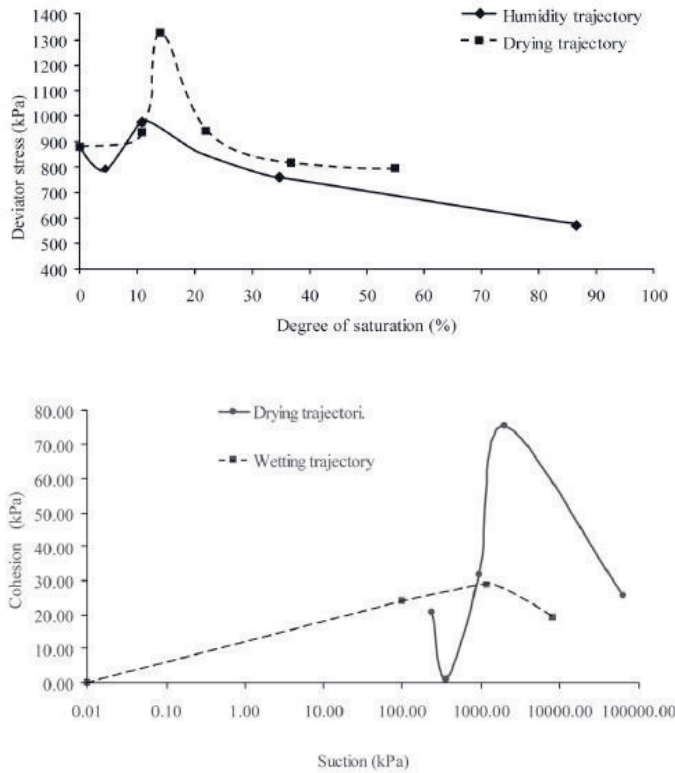


Figure 2.8. Change in the strength of silty sand based on water content (upper part) and whether the sample is on the drying or wetting path (lower part). (Leal-Vaca et al., 2012.)

## 2.4 The effect of water content on cyclic loading resistance

The cyclic loading resistance of earth structures is a complex entity. In static loading, effective stresses and the cohesive forces between particles are easier to assess. Water table increases total stress and accumulated pore water pressure reduces effective stresses when soil is in a saturated state, but the situation is the most difficult in partially saturated soil, as several concurrent phenomena affect the ultimate loading resistance. The nature and duration of the cyclic loading are also factors. The mechanisms affecting loading resistance include variable matric suction, friction between particles or potential overpressure. For these reasons, cycling loading has largely been examined with the help of tests, and this chapter presents important observations from the perspective of railway environments. Most of the studies on

this subject area that were found in literature focus either on cyclic loading of structures loaded by traffic or deformations caused by earthquakes. High-amplitude vibration, which often occurs during earthquakes, can cause pore pressure to increase rapidly, leading to soil liquefaction. In contrast, lower amplitude vibration at a high number of repetitions can, over an extended period of time, cause deformations that increase the need for maintenance along railway tracks, for example (Wichtmann et al., 2005).

Permanent deformations in unbound structural layers that are caused by cyclic loading are often described using the shakedown theory, which Theyse et al. (2007) have illustrated in Figure 2.9. According to this theory, the occurrence of deformations is divided into different zones based on the stress level and the number of load repetitions. At low stress levels, the occurrence of deformations per load repetition slows down over time, thereby falling below the plastic shakedown limit. At higher stress levels that fall below the plastic creep limit, there is linear growth in the accumulation of deformations relative to the loading cycles. At stress levels exceeding the plastic creep limit, deformations increase uncontrollably and, in practice, the material collapses or breaks down. Therefore, when examining the effects of water content, it is important for the loading conditions to not end up in the unstable area and instead preferably stay below the plastic shakedown limit.

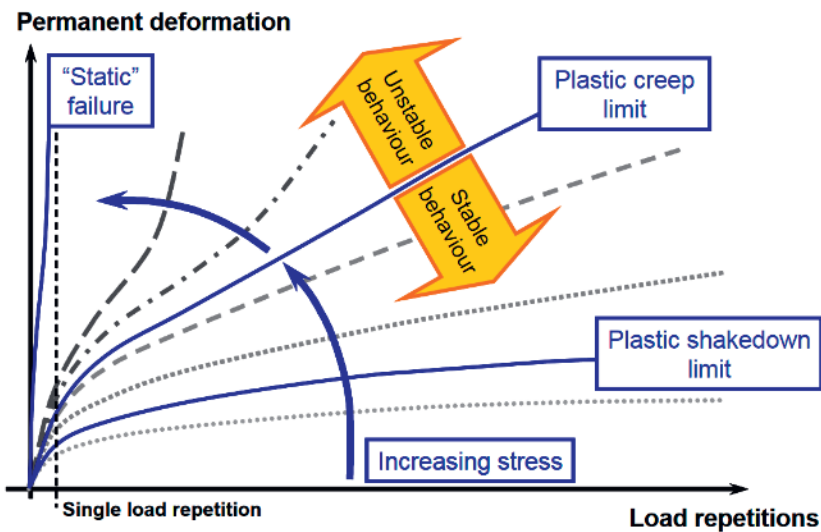


Figure 2.9 The shakedown theory, which illustrates the various collapse mechanisms of soil materials under cyclic loading. (Theyse et al., 2007.)

Fine-grained materials and excessive water content in particular are a bad combination with regard to cycling loading (Li and Selig, 1995). Materials that are sensitive to cycling loading typically include silts and fine sand (Lee and Fitton, 1969). In unbound materials, coarse granularity generally improves the ability of the structure to withstand repeated loading. However, the role of fines in loading resistance is not unequivocal, as a reasonable amount of fines can also reinforce the material. One example of this is a study by Soliman & Shalaby (2015) that examined the properties of limestone and gravel with different fines contents at different water contents. The results for gravel are presented in Figure 2.10. The fines content of the gravel material used varied between 4.0% and 14.5%, and the dry bulk density was 2,170–2,223 kg/m<sup>3</sup>, respectively. The optimum water content was 7.9% at a fines content of 4%, 7.0% at a fines content of 9.0% and 8.3% at a fines content of 14.5%. The best loading resistance against permanent deformations was achieved at a fines content of 10.5%; at amounts higher and lower than 10.5%, the deformations were greater. Moreover, the results showed that a water content only 2% lower than the optimum water content reduced the amount of permanent deformations. Based on these results, the increase in fines content increased the amount of permanent deformations, particularly when the water content was higher. In gravel materials, fines also typically increase the volume of water absorbed, and at least in some crushed gravel materials there appears to be a relatively linearly growing relation between water content and fines content (Kolisoja et al., 2002).

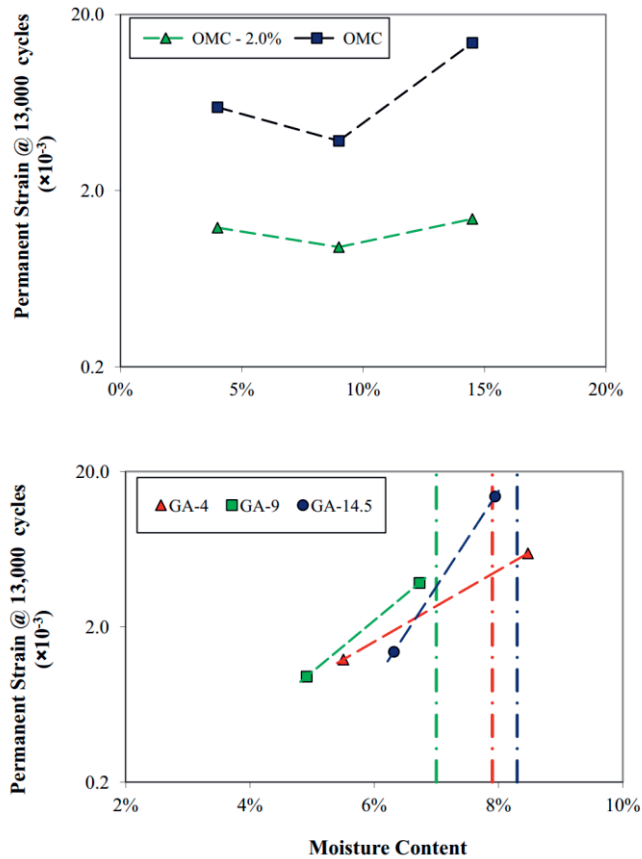


Figure 2.10. Test results of Soliman & Shalaby. The figure on the upper part shows the effect of fines content on the accumulation of permanent deformations, while the figure on the lower part shows the effects of water content. (Soliman and Shalaby, 2015.)

The effect of cyclic loading ultimately manifests as displacements detrimental to the structure. In the worst case scenario, excessively high water contents in railway environments can lead to derailments or severe damage during flooding, for example (Hasnayn et al., 2015). In the Roadex project, Dawson & Kolisoja (2005) studied the effect of water content on the cyclic loading resistance of road structural layer materials at different water contents. The results of this study are compiled in Figure 2.11. The results presented in the figure are based on cyclic loading triaxial tests, and it should be noted that the occurrence of deformations speeds up greatly once the saturation degree exceeds 60–70%. The differences between different water contents

are smaller at saturation degrees of less than 60%. The detrimental nature of the saturated state was also highlighted in a study by Trinh et al. (2012) on worn ballast material. This material, of which 18% comprised fines smaller than 100  $\mu\text{m}$ , could not withstand cyclic loading for very long in a saturated state. Moreover, a change in water content from 4% to 6% increased permanent axial deformations from 0.4% to 1.4%. In unbound structures, coarse granularity generally improves the material's ability to withstand external loading. There are also differences in loading resistance between natural materials and crushed materials, as the particles in crushed materials have sharper edges and do not slide past each other as easily as in rounded natural materials. The dry bulk density of materials also has a significant impact on loading resistance, as the soil skeleton is usually dense at high dry bulk densities, and it is more difficult for particles to relocate. However, a dense soil skeleton can lead to low permeability, which may cause the pore pressure to increase under cyclic loading. In other words, with regard to resistance against repeated loading, studies have found that permeability should remain at a sufficient level. (Altun et al., 2005; Kolisoja, 1997; Lee and Fitton, 1969; Trask, 1959.)

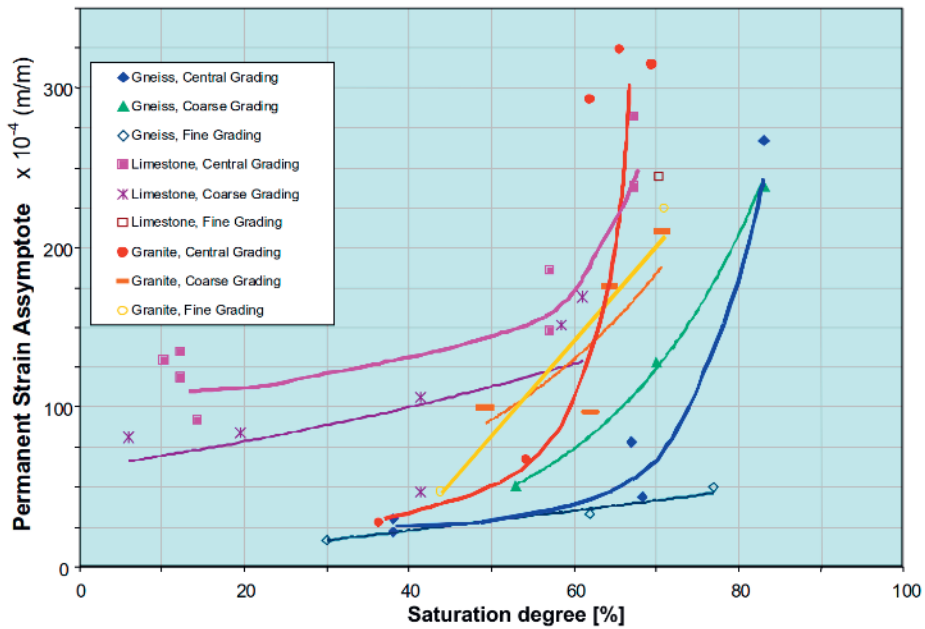


Figure 2.11. The effect of water content on permanent deformations for the materials tested in conjunction with the Roadex project. (Adapted from Dawson & Kolisoja, 2005.)

The effect of water content on cyclic loading resistance has often been examined with the help of the material's resilient modulus. The resilient modulus is useful in design because it describes the resilient deformations occurring in the material relative to external loading. Several studies have clearly found that an increase in water content reduces the resilient modulus, particularly when the material approaches a saturated state (Drumm et al., 1997; Khoury and Zaman, 2004; Yang et al., 2005). With regard to Finnish aggregates, Kolisoja et al. (2002) have studied the mechanical properties of the materials used in the base-course layer of roads at various water contents. Figure 2.12 presents the resilient moduli of the unbound crushed materials used in road structures relative to the amount of fines under different conditions. For most of the materials, the resilient moduli were significantly higher in dry samples compared to condition when the material had been allowed to absorb water. Freeze-thaw cycles also weakened the resilient moduli of several materials. When the materials were measured in a dry state, the highest resilient moduli were found in samples with the highest fines content. In contrast, an increase in fines content reduced the resilient modulus in more moist samples. Additionally,

the fines increased the volume of water absorbed by the material, which was evident in the permanent deformation tests as larger permanent displacements. Duong et al. (2013) have also noted a similar phenomenon, in which an increase in the amount of fines increased the amount of permanent deformations, particularly in a wet or saturated state. This observation is interesting, as old materials often contain an excessive amount of fines compared to current material guidelines for infrastructures.

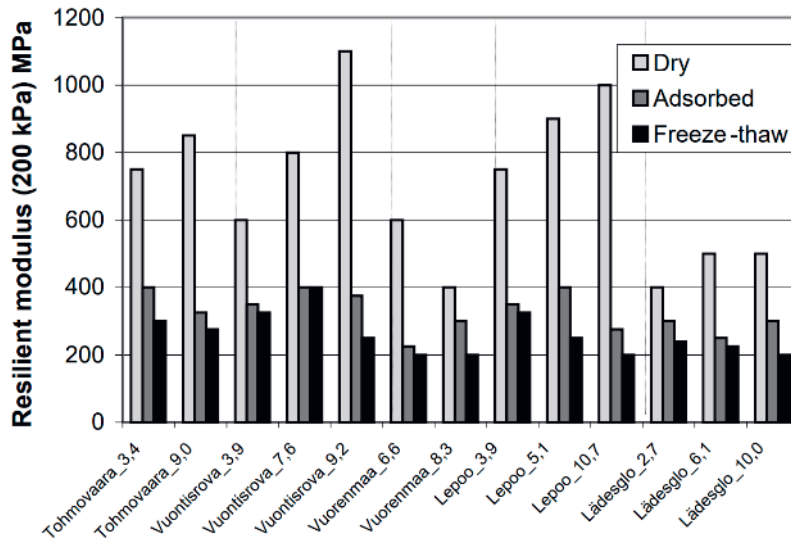


Figure 2.12. Results of the cyclic loading triaxial tests conducted by Kolisoja et al. In dry samples, the resilient modulus was significantly higher compared to wet samples. (Kolisoja et al., 2002)

Water content is one of the factors that significantly reduces loading resistance, but as the loading resistance of earth structures is affected by several different factors, the actual effects are challenging to assess. The frequency used in loading tests is significant because the frequency in railway environments is estimated to vary between 0.5 Hz and 2,000 Hz (Esveld, 2001). According to some studies, such as Steenbergen et al. (2015), low frequencies in particular would be detrimental due to excessive deformations. However, high frequencies do not have as strong an effect as lower frequencies at the depth of the track sub-ballast layer, which is why e.g. Suiker et al. (2005) and Trinh et al. (2012) used the loading frequency of 5 Hz in their tests. Another significant factor besides frequency is principal stress rotation. The

results presented in the previous chapter were largely based on vertically applied cyclic loading, but in reality the rolling stock in railway environments causes rotation of principal stress directions. The effect of principal stress rotation has been studied by Mamou (2013), Cai et al. (2016) and Thevakumar et al. (2021), among others. These studies have found that principal stress rotation can generally cause larger permanent deformations than vertical loading alone. However, the effect of principal stress rotation is significantly reduced as the depth increases (Powrie et al., 2007).

## 2.5 The effect of water content on frost protection design

Frost heave as a phenomenon has been studied extensively both in Finland and around the world. Frost heave is a relatively complex phenomenon, but the basic requirements for its occurrence include a material susceptible to frost action, freezing temperatures and the availability of water. In materials susceptible to frost action, ice lenses form in the soil, increasing the material's volume and causing frost heave. Another form of frost heave is 'in-situ frost heave', which is also significant because of the high track evenness requirements in railway environments. In in-situ frost heave, frost heave occurs as a result of the increase in volume (approximately 9%) caused by the freezing of water in the pores in soil, but no actual ice lenses form in the soil. In northern areas, protecting railway tracks from frost problems has been a topic of discussion for a long time, and the frost problems occurring along the Finnish rail network and potential solutions to their prevention were already discussed in an article written in 1940. Today, crushed rock aggregates are used extensively in railway construction in place of natural materials. According to studies, their thermal properties differ from those of naturally sorted materials. The use of these types of materials adds new perspectives to frost protection design, such as the possibility of convective heat transfer. (Kallio, 2022; Nixon, 1982; Nurmikolu and Kolisoja, 2002.)

The effect of water availability on frost heave has been studied for a long time. For example, McGaw (1972) has noted that the rate of heave and the segregation potential were both linked to the water table depth and the rate of freezing in the materials studied. Similarly, Guthrie & Hermansson (2003) noted in their laboratory tests that the water content of their samples of various materials was 3–70% higher after freezing tests than before freezing. On average, water content increased by



29%. The higher amount of water in the samples could be linked to the greater frost heave observed in the frost heave test. Frost heave began to increase on average above a saturation degree of 60% in particular, though frost heave also occurred at lower saturation degrees. In their later study, Hermansson & Guthrie (2005) found in a laboratory setting that lowering the water table height of external water led to a lower rate of frost heave, and there were also clear differences in the amount of additional water absorbed by the sample. These results prove that drainage improvement could reduce frost heave in the substructure. There also exists the 'Freiberg frost heave criterion', which can be expressed in the form of Figure 2.13 (Rantamäki et al., 1979). This equation is not widely used, but it shows how water flow  $Q$  is clearly affected by the material's permeability coefficient, the capillary rise height and the distance of the groundwater table from the surface of the ground. According to this equation, with commonly used parameters even a small increase in drainage depth can significantly reduce the flow of water into an ice lens. However, the article by Hermansson & Guthrie (2005) states that frost heave can also occur without extra external water in some conditions if the existing water in the material is redistributed. A similar phenomenon has also been observed in Finnish road structures (Vuorimies et al., 2004). Similar tests to those conducted by Guthrie & Hermansson have been carried out on Finnish railway track materials by Isohaka (2014). These tests also found that the availability of extra external water increases segregation potential, depending on the material. However, such a clear connection could not be established based on the measurement data on the field sites.

$$Q = k \cdot \frac{K - (Z - R)}{(Z - R)}$$

$k$  = coefficient of permeability  
 $K$  = height of capillary rise  
 $Z$  = depth of water table from ground level  
 $R$  = depth of freezing point from ground level

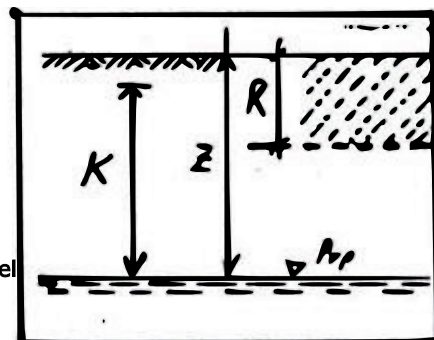


Figure 2.13. Freiberg frost heave criterion. This method assesses frost heave with the help of permeability, capillary rise height and the distance between the water table and the ground surface, among other things. Translated from (Rantamäki et al., 1979.)

Heat transfer can occur in three different ways: by conduction, by radiation and by convection. Heat transfer in soil is a complex process that is materially affected by water content. Another factor that complicates the process is the fact that water can exist as a liquid, gas or ice, which affects heat transfer. Figure 2.14, prepared by Johansen (1977), presents the relationship of the granularity and saturation degree of soil with the different types of heat transfer, in addition to which conduction also occurs. The figure shows that the role of water in heat transfer differs between different soil types. The granularity of materials also affects the primary type of heat transfer. For example, convective heat transfer can be the primary type of heat transfer in coarse crushed or blasted rock materials. In frost protection design, effective thermal conductivity is usually used to calculate heat flow, as it incorporates all heat transfer types. The frost protection design of structures can be carried out either by designing the permitted frost heave or designing the structures so that there are no frost-susceptible materials within the frost penetration depth. In railway environments, the evenness requirements are high, particularly at the current operating speeds. For this reason, a design method based on the magnitude of frost heave cannot be used. Hence, heat conduction in soil plays a critical role in the design of the structures so that frost is prevented from penetrating the frost-susceptible layers of soil at the desired level of certainty. Several optional methods exist. In Finland, a combination of the Watzinger, Kindem and Beskow methods, as well as the Skaven-Haug-Watzinger method, have been used. Thermal conductivity plays a key role in these methods. (Farouki, 1981; Nurmikolu and Kolisoja, 2002; Young et al., 1996.)

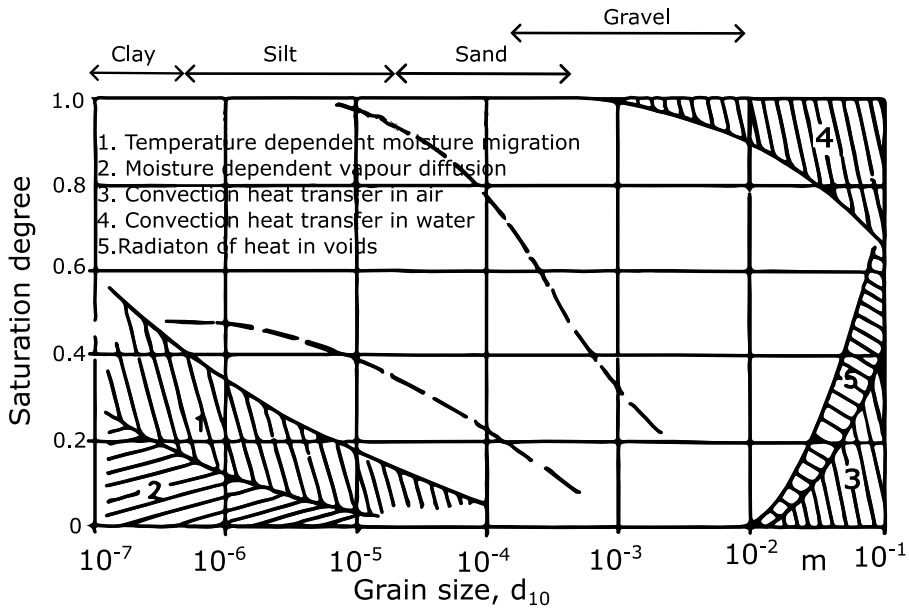


Figure 2.14. Types of heat transfer in different soil types. Redrawn from (Johansen, 1977.)

## 2.6 Drainage principles and water content in track structure

A ballasted track is always exposed to the effects of water from many different directions, as evident in Figure 2.15. The top section of the railway track is exposed to rain and melting waters, water can flow into the embankment from outside the track, the groundwater table can extend to near the structural layers, and water can also flow out of saturated subgrade due to capillary action. In the implementation of drainage, drainage can be divided into internal and external drainage. The objective in internal drainage is for water to efficiently flow away from the track structures, while the purpose of external drainage is to prevent water from penetrating the track structures. The ballast layer and its drainage play a particularly important role in maintaining the track operative, as e.g. the permeability of a degraded ballast material is significantly weaker than that of a new equivalent material. Additionally, the interface between the ballast layer and sub-ballast layer is essential for drainage. (Li et al., 2015.)

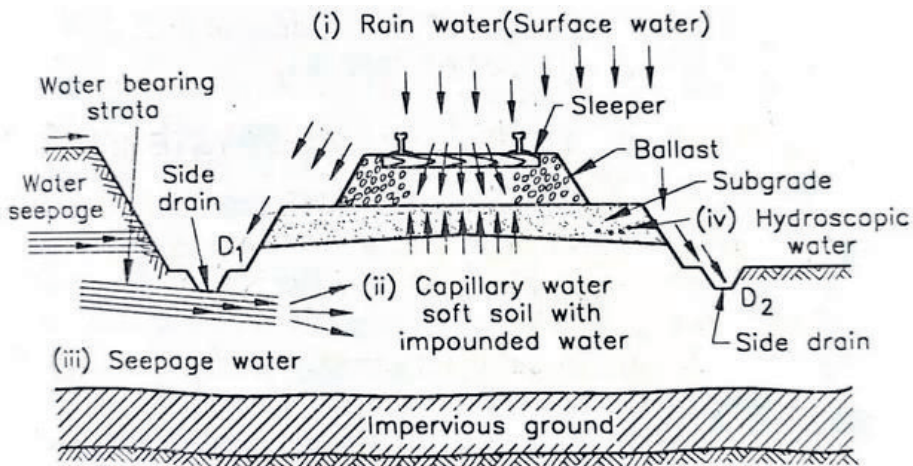


Figure 2.15. Water sources of a ballasted track. (Saxena and Arora, 2004.)

Functional drainage comprises many different drainage solutions. In external drainage, ditches and slopes form one of the most important tools of drainage. The depth of ditches is usually designed so that the drainage depth extends at least to the bottom of the sub-ballast layer. Various methods that take account of height differences and flow rates are available for drainage design. In principle, the longitudinal drainage gradient should be 0.5%, but a gradient of 1–2% is recommended. However, a gradient exceeding 2% should not be used due to erosion. Another highly important factor from the perspective of functional track structure drainage is the use of a coarse-grained material with adequate permeability in the structure. These methods allow water to be directed in the desired manner, but attention must also be paid to preventing the coarse-grained layers from being contaminated by fines. Possible protection methods include geotextiles, for example. A third important element in functional drainage is different types of pipes, including culverts and subsurface drains. A sufficient gradient and design flow rate must also be ensured for these structures. Additionally, attention must be paid to proper diversion of surface water away from the railway track. (Li et al., 2015.)

In Finland, guidelines for railway track drainage are primarily found in the Finnish Transport Infrastructure Agency’s track construction guidelines and the Finnish general quality requirements for infrastructure (InfraRYL). At the time of writing this dissertation, the guidelines on railway track drainage were being updated. The proposal on design drainage depths presented in Chapter 4.2 was drawn up based on the results of this dissertation in connection with the update. In accordance with

the old guidelines, surface drainage of railway tracks is primarily carried out by using side ditches, cess drains, catch drains and mitre drains. What is most relevant from the perspective of the present study is the requirement included in the previous guidelines that *the bottom of side ditches must be at least at the level of the lower surface of the structural layers or below them*. With regard to maintenance, the track maintainer is tasked with ensuring that track drainage is operative. The structural layers, ballast layer and track shoulder must always be kept clear of vegetation, which must also not prevent the operation of the track drainage system. This means that culvert ends, side ditches and other drains must be kept clear of vegetation that could hinder operation. Slopes must be cleared of brushwood according to the requirements for the service level class but at least twice every five years. Vegetation must primarily be removed by mechanical means; herbicides are to be used if necessary. In other words, much attention is paid to the functioning of the drainage system when the guidelines are followed. (Finnish Transport Infrastructure Agency, 2018, 2002, 2002, 1999.)

## 3 RESULTS AND DISCUSSION

### 3.1 The current status of drainage and drainage maintenance on Finnish railway network

#### 3.1.1 Organization of drainage maintenance

For a long time, the operation and maintenance of the Finnish rail network and rail traffic were the responsibility of a single state-owned company. It was not until 1995 that the Finnish Rail Administration was established (Finnish Rail Administration, 2009), at which point control of the rail network was transferred to a government agency and the companies in charge of maintenance began to be decided through a tendering process. This significant change in railway track maintenance partly explains the current situation and challenges in gathering maintenance data, for example. Today, the Finnish rail network is controlled by the Finnish Transport Infrastructure Agency, which has divided the maintenance of the rail network into 12 maintenance areas that are grouped into four management areas. Currently, there are several companies in charge of maintenance in these areas, and maintenance services are tendered regularly, typically every five years, but several of the maintenance contracts also include a two-year extension option. The fact that the parties responsible for maintenance keep changing has caused clear challenges for the retention of ‘tacit knowledge’, as the data on things such as past measures and problem areas has partly been lost. Short maintenance periods are also presumed to have had an effect on the measures carried out, as during short maintenance periods it may not necessarily be worthwhile for track maintainers to carry out measures that will not yield benefits until much later.

Drainage maintenance can be carried out either as necessary or periodically, for example. The implementation of drainage management along the Finnish rail network is defined in the RAMO 15 (Technical rules and guidelines for fixed installations of railway) guidelines (Finnish Rail Administration, 2002):

*“The side drains, catch drains, mitre drains, cess drains and subsurface drains, as well as side drains connected to level crossings, that are located on land managed by the Finnish Rail Administration must be maintained in the condition required by their original purpose of use, clear of vegetation and obstacles that could block the drains and thereby materially reduce flow.”*

The idea behind these guidelines was good, but qualitative assessment, which is primarily carried out as visual inspections, is often problematic (Graybeal et al., 2002; Moore et al., 2001; See, 2012). Maintenance practices in Finland are discussed in Publication I. According to the interview study with track maintainers, conducted in the form of a survey, the examination of drainage continues to be based on visual inspections in practice. This makes it difficult to say e.g. at which point the flow in a ditches has deteriorated *materially*, as vegetation and mild silting are practically always found along railways. In previous maintenance contracts, the principle was to carry out drainage maintenance specifically when needed. This has led to a situation in which the condition of the drainage systems may have been deteriorating for an extended period of time.

Fortunately, maintenance contracts have been developed to make them more unequivocal. In more recent maintenance contracts, the expression ‘as necessary’ has been replaced by a clearer model that defines a minimum amount of annual ditch cleaning. Furthermore, at least one maintenance contract at the time of the study included a mention that all ditches and drains must be cleaned during the maintenance contract. This type of maintenance model is clearer because it removes the problem of qualitative assessment, but on the other hand, this approach may lead to resources being wasted. From the perspective of the environment, structures and economy, the ideal would be to focus measures and resources on the right places in order to obtain the most benefits. However, this type of optimisation is impossible in a time of short-term contracts and without prior maintenance records. During the study, data was gathered from sites in different rail sections that were problematic from a drainage perspective, and one track maintainer also provided a response that aptly describes the situation in Finland: *“Five years ago, I threw away all of the information covering a 20-year period.”*

Although no methods that provide numerical data were used in drainage assessment in daily maintenance, there have been pilot projects in Finland that have made use of more modern technology. One example of these projects is the ROPE project, in which problematic sites were analysed with the help of several different information sources, such as ground penetrating radar data, video taken of the tracks, laser

scanning data and data produced by a track recording car data. The same project also more boldly sought new repair methods, such as drainage improvement. It is recommended that new inspection methods be developed and adopted in order to produce continuous measurement data about the development of drainage conditions. This would also make it possible to optimise drainage maintenance at the different rail sections and sites.

### 3.1.2 Observed drainage problems

A significant proportion of the most typical drainage problems identified along the Finnish rail network were related to basic drainage solutions. Drainage problems are discussed in Publication I and the key points are summarized in this chapter. Based on site visits, ROPE data and the interview study conducted with track maintainers, the problems were found to primarily be related to drainage maintenance. In the interview study, one track maintainer wrote the following apt account: *“Some sites deteriorate so rapidly that one or two years after the repairs it is difficult to believe that any work has been carried out on them at all.”* Based on the analyses, the following problems can be said to be the most typical drainage problems in Finland:

- Blockage/silting of ditches. Strong growth of vegetation also blocks ditches.
- The original level of drainage is too low. There are old sites along the rail network where the drainage system has never been able to keep the structure dry.
- Blockage of culverts/subsurface drains. Confirming the operating condition of subsurface drains in particular is challenging, as information on the locations and past maintenance of old subsurface drains may not necessarily be available any longer.
- Site drainage problems related to an inability to direct water away from the track area. In flat areas in particular, the condition of external ditches has a major effect on track drainage and the planning of drainage system should be performed carefully when height differences are low.

The problems identified are solvable, primarily from the perspective of technical implementation. The most challenging factor is the improvement of site drainage. Its implementation can be challenging both in technical and legal terms, as it may be necessary to extend the drainage improvement far beyond the track area and to areas owned by other property owners.



## *Discussion about observed drainage related issues*

The drainage problems identified along the Finnish rail network proved to be reasonably simple, and many of the problems are caused by shortcomings in maintenance. In countries where seasonal frost occurs, the structural layers of the track are usually thicker. According to the guidelines in force in Finland, tracks without frost insulation must have structural layers at least 2.15 m thick that are not susceptible to frost action, and they must be even thicker in Northern Finland. The total thickness of structural layers not susceptible to frost action can be reduced by using frost insulation, but this solution is always secondary and requires permission. (Finnish Transport Infrastructure Agency, 2018) Although the old track structures do not meet the current guidelines, they are still exceptionally thick by international comparison. Excessive water content in a ballasted track can often lead to subgrade containing fines (clay, silt) being ejected (mud pumping) under cyclic loading. These types of problems have been found to occur in southern Britain, for example (Hudson et al., 2016). In many cases, this mud pumping phenomenon is related to degradation of the ballast layer and, through it, weakened permeability. The mud pumping problem has also been found to occur elsewhere, such as in Australia, where this problem has often been linked to poor drainage capacity of side drains (Nguyen and Indraratna, 2022). Mud pumping is not usually a problem in Finland because the structures beneath the ballast layer are exceptionally thick and the ballast layer is located very far from subgrade that contains fines.

International literature offers few sources about actual defects in track drainage systems because studies have focused more on the phenomena that occur as a result of poor drainage. This has also been pointed out by Usman et al. (2017), who have developed a fault tree model for track drainage problems. According to the authors of said study, drainage problems are usually poorly recognised because poor drainage is caused by a combination of several different factors. In the fault tree model, drainage failure modes are divided into blocked drainage, collapsed drainage, clogged filter media and inadequate capacity (hydraulic surcharging). Inadequate capacity refers to a situation in which the drainage structures are unable to conduct sufficiently high volumes of water despite being operative. This can occur as a result of reasons such as climate change, which Baker et al. (2010) predict will increase loading on drainage systems. In their article, Usman et al. (2017) also more closely describe how the model works and list several drainage problems in more detail, but the problems related to blockages and capacity in particular appear to be similar to those that occur in Finland. Researchers from other parts of the world have also paid

attention to the operation and maintenance of drainage systems. For example, in Croatia poor drainage and drainage maintenance have been identified as causes of stability problems at individual sites (Kovacevic et al., 2016). In Australia, erosion and the spillage of coal from freight trains and other fines originating from outside of the track structures have been found to reduce track drainage (Nguyen and Indraratna, 2022). Old rail sections in Brazil have also experienced drainage-related problems in which water is prevented from flowing from the ballast layer to the side ditches and instead remains in the contaminated ballast material (Paiva et al., 2015). In France, drain calcite scaling has occurred on high-speed lines (Jia et al., 2016). In conclusion, drainage problems occurring on railway tracks are often the sum of several factors, and typical drainage problems vary by structure.

## **3.2 The effect of water to the loading resistance of sub-ballast materials**

### **3.2.1 The grain size distribution and compaction properties of the materials studied**

The materials studied include three actual sub-ballast material samples collected from the Rantarata track, as well as a high-quality reference material that meets the grading requirements. The grain size distribution curves determined by wet sieving are presented in Figure 3.1 and the grading parameters are presented in Table 3.1. The grading limits presented in the figure were valid at the time of sampling in 2017, but they were later changed to requiring a more coarse-grained material to be used for the intermediate and insulation layers due to loading resistance design.

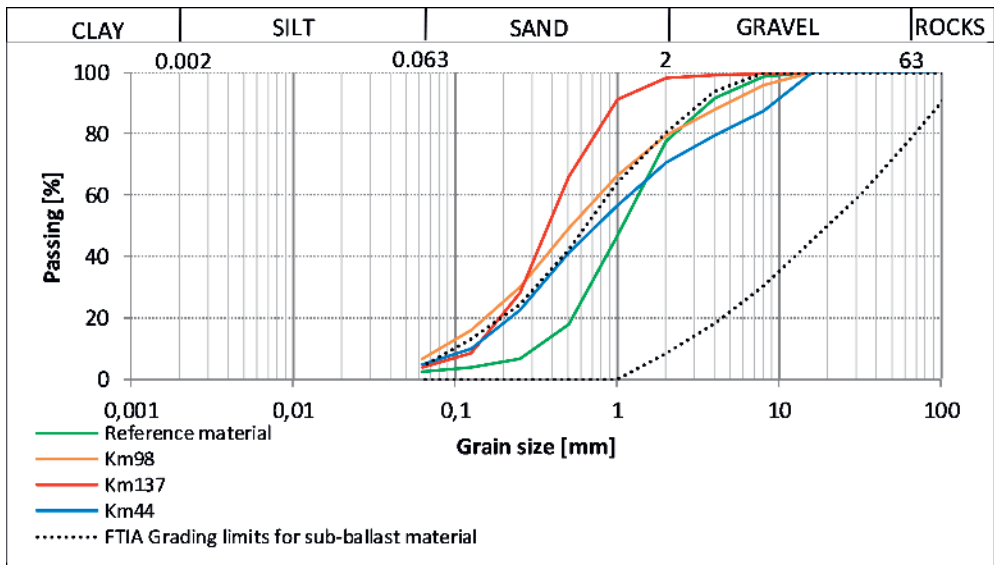


Figure 3.1. The grain size distributions of the actual sub-ballast materials and high-quality reference material examined in this study and the grading limits for sub-ballast materials valid in 2017. (Publication II.)

The grain size distribution curves of the actual sub-ballast materials studied deviate from the design grading curve. The grain size distribution curve for both the reference material and the Km44 material only barely stayed within the grading limits, but the grain size distribution curve tended heavily towards the fine-grained direction. Particularly the mean grain size of 0.4 mm in the Km137 material, which was collected from a sand esker-like site, was too small and the material's coefficient of uniformity was low. Due to these properties, the material has low compaction. This was also evident in the Proctor tests conducted, the results of which are presented in Figure 3.2. The Km98 material had the highest fines content (6.7%) and the highest compaction. The compaction of the reference material was slightly better than the compaction of the Km137 material.

Table 3.1. Grading parameters of the studied materials. (Publication III)

| Sample             | Average particle diameter $d_{50}$ [mm] | Coefficient of uniformity [-] | Content of fines <0.06 mm [%] |
|--------------------|---|-------------------------------|-------------------------------|
| Reference material | 1.1                                     | 4.7                           | 2.5                           |
| Km44               | 0.7                                     | 10.0                          | 4.9                           |
| Km98               | 0.5                                     | 10.0                          | 6.7                           |
| Km137              | 0.4                                     | 3.5                           | 3.7                           |

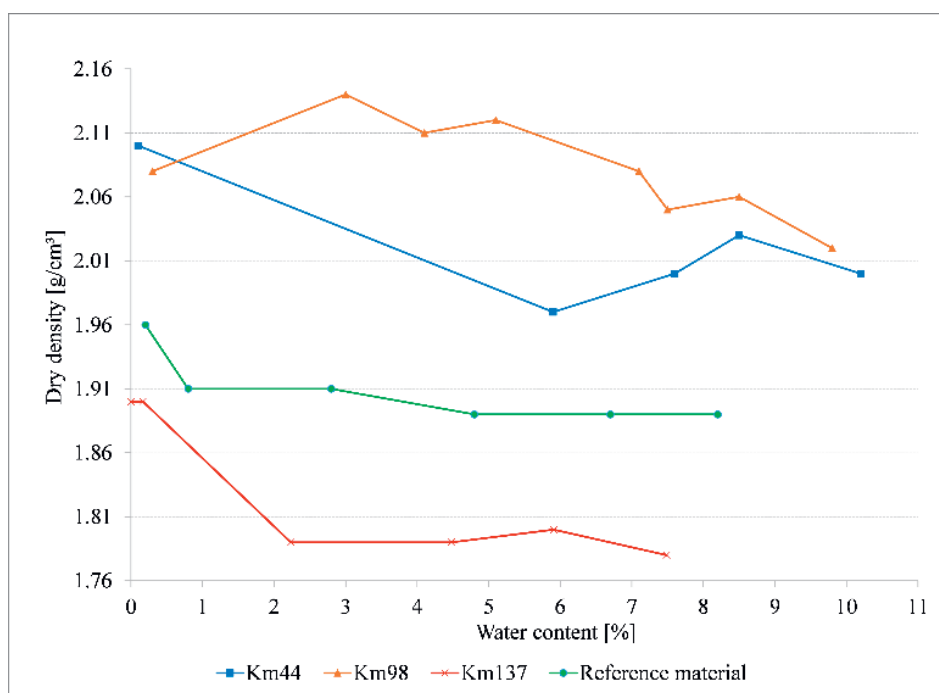


Figure 3.2. Proctor tests conducted on the sub-ballast materials studied. (Publication II.)

### 3.2.2 Stresses in the sub-ballast

The strength properties of granular unbound structural layers are affected by vertical and horizontal stresses. In order for the results of the static and cyclic triaxial tests to be compared to the operating situation, it is necessary to identify the stresses occurring in the sub-ballast layer (Publication IV). Back when Finland was considering adopting axle loads of 250 kN, Kolisoja et al. (2000) examined the magnitude of vertical stress by conducting analyses based on computer-aided multi-layer linear elastic modelling (BISAR) and field measurements. The results of these analyses are presented in Figure 3.3. A vehicle with an axle load of 250 kN caused an increase in vertical stress of up to 80 kPa at a depth of 0.5 m from the bottom surface of the sleeper. The magnitude of this increase in stress decreases rapidly as the depth increases: at a depth of 1.0 m from the bottom surface of the sleeper, the increase in stress only amounted to 20–30 kPa. The modelling data produced with the BISAR program and the field measurement data are highly similar to the FEM modelling data reported by Peltomäki (2020), which is presented in Figure 3.4. Similarly, the recent measurements carried out by Pelho et al. (2022) found that the vertical stress increase caused by a train when measured at a depth of -0.65 m from the surface of the ballast layer was generally less than 60 kPa, but wheel defects clearly increased the force of the impacts. Therefore, the vertical stress addition in the sub-ballast layer is very likely between 40 and 80 kPa in Finland. The vertical stress increases estimated in Finland are similar in magnitude to those found in studies conducted elsewhere, the results of which are discussed in more detail in Publication IV.

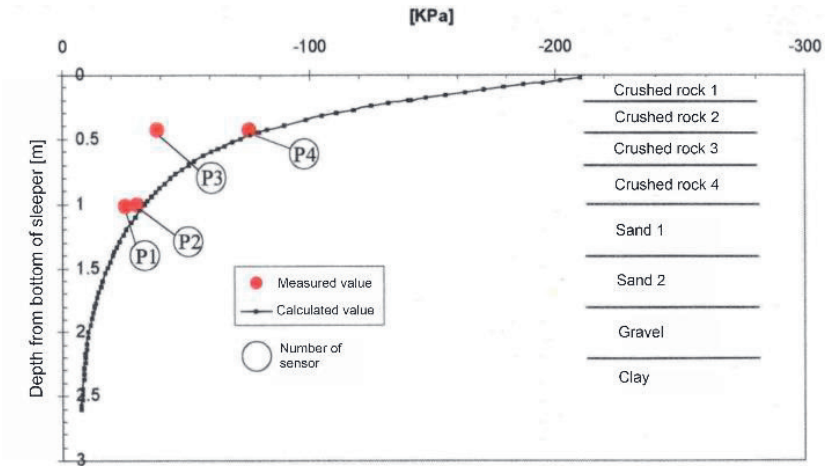


Figure 3.3. Calculated and measured vertical stresses as a function of depth below the sleeper under a 250 kN axle load. (Publication IV, original source (Kolisoja et al., 2000.))

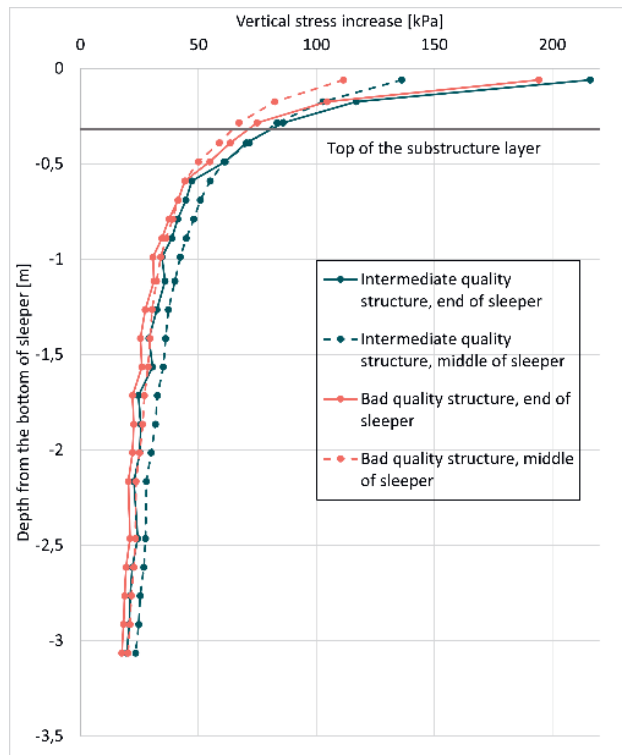


Figure 3.4. FEM modelling results on the vertical stress increase caused by a 250 kN axle load as a function of depth. (Peltomäki, 2020.)

The horizontal stresses occurring in the track sub-ballast layer are more difficult to define than vertical stresses. Based on a FEM model previously developed by Kalliainen et al. (2016), a confining pressure of 30 kPa was chosen for the cyclic triaxial tests conducted in the present study because it was estimated to correspond to the typical horizontal stress in the sub-ballast layer. A similar confining pressure was used by Trinh et al. (2012) in their study on the properties of an old ballast material. Longitudinal and horizontal stresses have also been measured by Peltomäki (2021) in Finland, and they have been compared to the obtained results by using a calculation model. According to the measurements, a longitudinal and horizontal stress increase of approximately 15 kPa resulting from a train load was detected at a depth of 0.75 m from the bottom surface of the sleeper. When this is increased by the approximate weight ( $16 \text{ kN/m}^3$ ) of the roughly one-metre-thick overlying structures, multiplied by a coefficient of earth pressure at rest of 0.5, the total horizontal earth pressure measured is approximately 23 kPa. The confining pressure of 30 kPa used based on different methods of analysis is in the right size range. In the actual structure, however, stress varies according to the site's material properties, depth and the direction examined.

### 3.2.3 Static triaxial tests

A broad series of triaxial tests was conducted on the materials studied in order to determine the relationship between moisture content and strength properties. The aim was to identify the moisture contents at which apparent cohesion begins to strengthen the samples. The implementation and outcomes of the tests are examined in Publication II and the key points are presented on this chapter. The saturated samples were otherwise prepared according to the standard SFS-ISO 17892-9:2018 Geotechnical Investigation and Testing. Laboratory Testing of Soil. Part 9: Consolidated Triaxial Compression Tests on Water Saturated Soils (2018), but the degree of saturation was not confirmed through the B value. The samples were first compacted at near their optimum moisture content, i.e. 4.1–8.7% depending on the material, in order for the bulk dry density to remain constant in the same material. Next, the samples were saturated and consolidated. Following the consolidation, the samples to be tested in an unsaturated state were dried by sucking air through them at a negative pressure of 3.5–5.0 kPa. The drying time and vacuum level were adjusted based on the samples' properties to achieve the desired range of different

moisture contents. The maximum shear strengths measured at a confining pressure of 40 kPa at different moisture contents are compiled in Figure 3.5. The confining pressure used in the static tests differed from the pressure used in the cyclic tests, as the objective was to identify differences between moisture contents rather than examine the absolute shear strength based on the stress in the sub-ballast layer. The results indicate that the maximum shear strength measured by the tests begins to increase when the moisture content of the studied samples is below 7%. There are, however, differences between the materials, since with the Km44 material the growth starts at a moisture content of 6.8%, whereas with the Km137 material it starts at below 4.3%. When the same material is examined, the increase in shear strength is very significant, as the difference between the moist and the drier samples is above 100 kPa. The results of the tests carried out in a saturated state are compiled in Table 3.2, which presents the friction angles and cohesion values determined for the materials. The letter identifiers in the table represent results obtained at different confining pressures (20 kPa, 40 kPa, 80 kPa). Some of the tests had to be repeated, which is why there are numbers after the letters. Based on observations, the strength properties of the materials studied improve significantly in the dry samples compared to a completely saturated state.



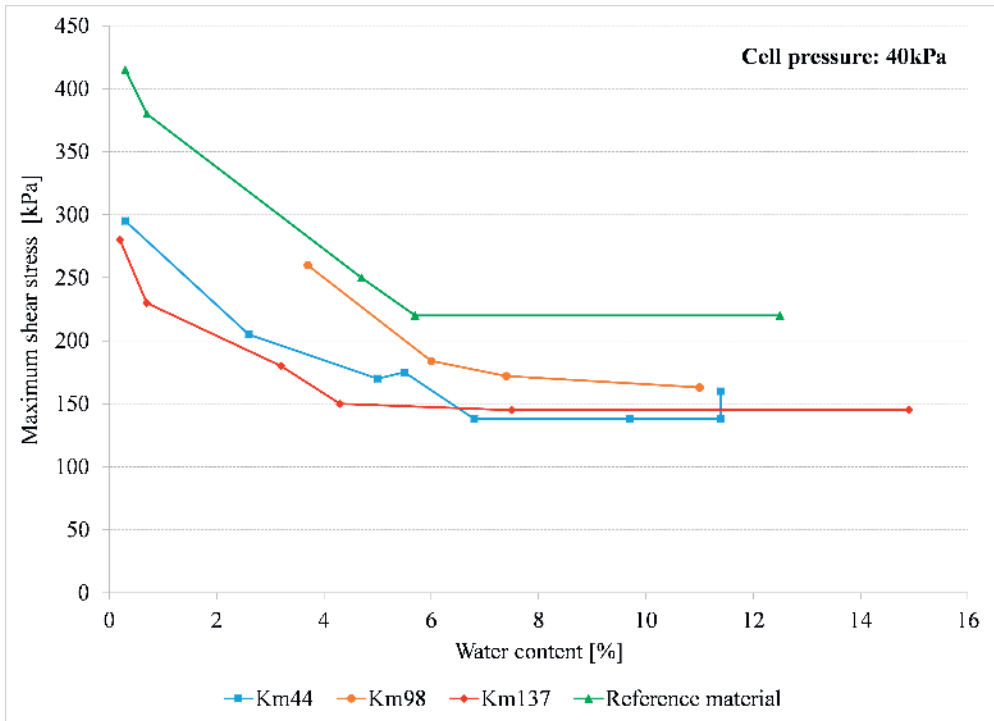


Figure 3.5. Maximum shear strengths of the materials studied at different moisture contents, determined through triaxial tests (Publication II.).

Table 3.2. Parameters of the static triaxial tests and the properties measured. (Publication II)

| Sample ID             | Cohesion,<br>kPa | Friction<br>angle,<br>° | Cohesion<br>after<br>failure,<br>kPa | Friction angle<br>after failure<br>° | Strain level<br>at maximum<br>shear stress,<br>% |
|-----------------------|------------------|-------------------------|--------------------------------------|--------------------------------------|--|
| km98                  | 10.9             | 49.4                    | 4.8                                  | 38.6                                 |  |
| A1                    |                  |                         |                                      |                                      | 1.00   |
| B                     |                  |                         |                                      |                                      | 1.80   |
| C2                    |                  |                         |                                      |                                      | 2.60   |
| km44                  | 18.8             | 45.6                    | 3.9                                  | 39.1                                 |  |
| A1                    |                  |                         |                                      |                                      | 1.20   |
| B2                    |                  |                         |                                      |                                      | 1.30   |
| C1                    |                  |                         |                                      |                                      | 1.70   |
| km137                 | 4.1              | 49.5                    | 6.1                                  | 37.2                                 |  |
| A2                    |                  |                         |                                      |                                      | 2.80   |
| B                     |                  |                         |                                      |                                      | 2.40   |
| C                     |                  |                         |                                      |                                      | 2.40   |
| Reference<br>material | 10.2             | 55.4                    | 9.6                                  | 40.2                                 |  |
| A                     |                  |                         |                                      |                                      | 2.60   |
| B1                    |                  |                         |                                      |                                      | 2.30   |
| C                     |                  |                         |                                      |                                      | 3.10   |

Summary of the results of the static triaxial tests:

- In each of the materials studied, a decrease in moisture content significantly increased the maximum shear strength.
- The ‘critical’ moisture content below which strength started to increase was 5–6% (equal to 40–50% saturation degree) for the materials studied.
- The increase in strength observed in the static tests is primarily caused by apparent cohesion. The maximum shear strength of the tested materials can almost double when the material dries.
- An increase in moisture content no longer reduced maximum shear strength at moisture contents of over 5–6%. This deviates from the strength behaviour observed in the cyclic tests described in Chapter 3.2.5.

## *Discussion about static triaxial test results*

The results achieved in the static triaxial tests were very much as expected and consistent with the theory presented in Chapter 2.3. No decrease in shear strength was detected in the materials studied when the moisture content increased to a point at which matric suction no longer had an effect on particles. In static condition, the change in strength is primarily caused by apparent cohesion, which increases effective stress between particles. Studies show that, in a silty soil type, cohesion decreases greatly when moisture content exceeds a saturation degree of 80% (Yoshida et al., 1991). As shown in Figure 3.5, in coarser-grained materials the increase in strength caused by matric suction was already lost at lower moisture contents. The observed increase in maximum shear strength is in the same size range as in the study by Yoshida et al. with silty sand material, which found that, at the same axial deformation level, the ability of the material to withstand deviatoric stress increases from approximately 30 kPa to over 250 kPa between the saturation degrees of 100% and 12%, respectively. Similar observations have also been made by Azam et al. (2013) on unbound granular materials (UGM) and by Wang et al. (2015) on loose accumulation soil induced by an earthquake through a direct shear test. However, the studies indicate that the material studied by Wang et al. appears to have an optimal moisture content, above and below which the shear strength is reduced. The non-linearity of the change in strength seems to be a well-known phenomenon also identified in older studies, such as by Gan & Fredlund (1988), who found that the failure envelope is non-linear in a partially saturated area. Based on observations and sources, the static tests were therefore successful, and the expected change in strength was demonstrated. However, the identified threshold moisture content is very low, potentially making it difficult to achieve an increase in strength in field conditions, particularly in the bottom section of the sub-ballast.

### **3.2.4 DCP-method as a tool for recognizing poor quality sub-ballast materials**

The properties of the sub-ballast materials were determined with the help of material samples in a laboratory in a typical manner. The laboratory tests found that the static maximum shear strength of the actual sub-ballast materials studied changed significantly depending on the moisture content (Publication II). Penetrometers of different types are some of the oldest devices used to study soil (Spagnoli, 2007).

Thanks to the advancement of technology, current dynamic cone penetrometers are lightweight field measurement devices that are easy to use, and the results are also automatically recorded by the terminal device. On account of these factors, this study decided to find out whether a dynamic cone penetrometer (DCP) can be used to detect the increase in shear strength caused by a change in moisture content by using material samples prepared in a laboratory and along the track in field conditions. The theory behind the dynamic cone resistance measured by the device is presented in Publication II.

At the laboratory, the DCP tests were carried out with the same four materials that were used in triaxial tests. The key results are presented in Figure 3.6. For the samples containing water, the dynamic cone resistance varied according to the dry bulk density and moisture content in particular. The differences between the materials tested were considerable, and the lowest dynamic cone resistance was measured in the reference material, which had the highest maximum shear strength in the triaxial test. For each of the materials, the highest dynamic cone resistance was achieved at the lowest moisture content. The coarser-grained reference material was also the least sensitive to a change in moisture content.

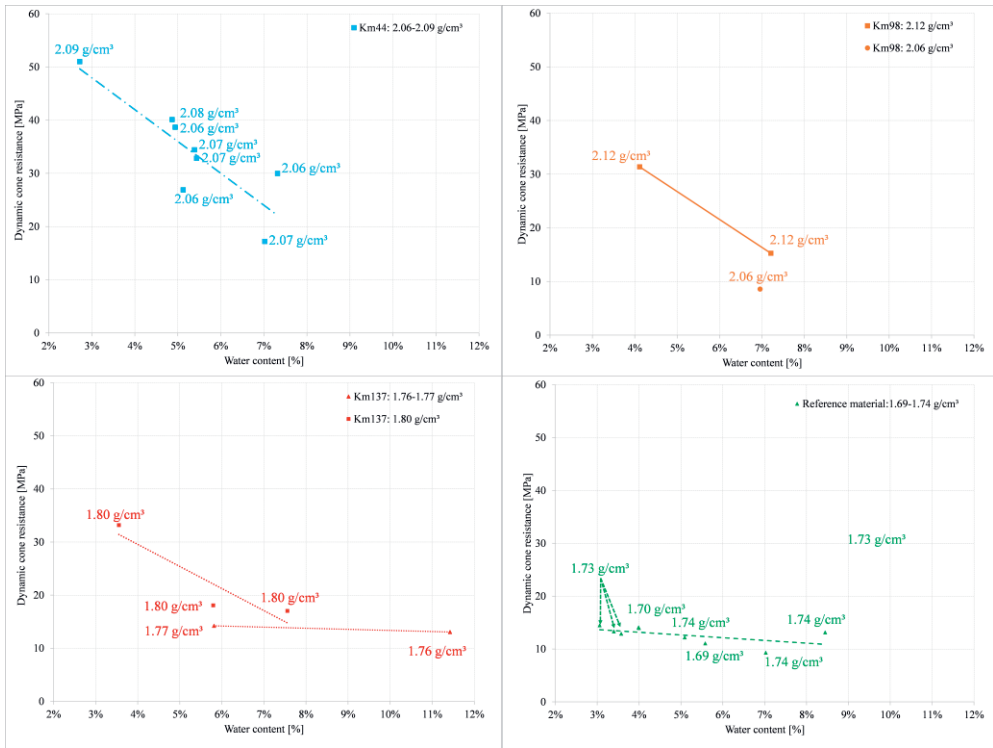


Figure 3.6. The effect of moisture content on dynamic cone resistance (Publication II.)

The dynamic cone resistances were clearly higher when measured at the laboratory than when measurements were conducted on the same materials at the field sites. The tests carried out at the laboratory used a plastic tube with an inner diameter of 235 mm and a height of 800 mm. The tube diameter was apparently so small that the rod penetrating the sample caused a horizontal stress similar to confining pressure in the material. This stress in combination with skin friction increased the dynamic cone resistance measured by the DCP device. There are several methods available for eliminating skin friction, but they are not particularly easy to use. Another problem identified at the actual field sites was the ballast and its partial penetration into the sub-ballast layer. It was found at the field sites that the device's 14-mm-thick drive rods could not withstand ballast properly and started to bend. With regard to the sub-ballast layer, the device identified clear layer boundaries (the results are presented in more detail in Publication II). However, the results indicate that the material's dry bulk density appears to play the most important role in determining dynamic cone resistance, which makes it practically impossible to

identify differences in moisture content from the field site measurement data. Moreover, it is difficult to assess the quality of the materials because the laboratory tests indicate that dry bulk density does not describe the ability of the materials to withstand static or cyclic loading.

Conclusions about the DCP tests:

- There was a noticeable relation between moisture content and the dynamic cone resistance measured by the device.
- The dry bulk density of the material was found to be the key factor in determining the dynamic cone resistance. The static and cyclic triaxial tests indicated, however, that dry bulk density alone does not describe the loading resistance of the material, as the reference material had a low dry bulk density and the best loading resistance. Therefore, the study was unable to assess the quality of the material based on dynamic cone resistance.
- The 14-mm-thick drive rods of the portable, lightweight DCP device could not properly withstand the ballast, which can be found in surprisingly thick layers along old rail sections. The rods began to bend sideways.
- The magnitude of the dynamic cone resistance is affected by several factors, and moisture content plays such a small role compared to dry bulk density that it is not possible to reliably identify the materials in a saturated state with the device in field conditions due to elements of uncertainty.

### *Discussion about DCP-testing results*

The tests carried out with the portable, lightweight DCP device did not progress completely as expected. The greatest issue in the measurements carried out in the field was ballast, which posed significant problems for the 14-mm-thick drive rods. However, Haddani et al. (2016) used the same device to conduct similar tests directly through the ballast layer in France. It later turned out based on discussions with the manufacturer that Haddani et al. also had spare rods in case the original ones were damaged during the studies. Thus, penetrating the ballast appears to be possible but not easy based on studies by the author of this dissertation. In field conditions, the large ballast particles bent the rods, which lent itself to increase skin friction. The effects of skin friction proved to be greater than anticipated both in the laboratory and out in the field. Based on the literature review, it turned out that e.g. in the study by Bolton et al. (1999) dynamic cone resistance more than doubled when the diameter of the container containing the material relative to the diameter of the cone

was reduced to a sufficient degree. This observation is consistent with the measurement results obtained by the author of this dissertation. Several different methods exist for eliminating skin friction or taking it into account. For instance, Livneh (2000) has presented a method originally proposed by Dahlberg & Bergdahl (1974) in which the rod is rotated at regular intervals and the torque required by this is measured in order to correct the dynamic cone resistance. Other methods are based on minimizing skin friction with e.g. the method proposed by Meardi & Gadsby (1971) on the use of a protective pipe or the method presented by Baudrillard (1974), in which drilling fluid is injected between the rod and the ground (Abuel-Naga et al., 2011). In their article, Abuel-Naga et al. propose a method in which the rod is raised at regular intervals and then driven down again to allow the proportion accounted for by skin friction to be measured. In conclusion, many options are available for taking skin friction into account, but compared to the idea of the original DCP test, they are not easy to carry out in field conditions.

In the studies, the dynamic cone resistance increased strongly relative to dry bulk density. This observation is consistent with other studies, such as Escobar et al. (2016) or Chaigneau et al. (2000), both of which found that dynamic cone resistance reacts sensitively to even small changes in dry bulk density. In the studies by the author of this dissertation, the effect of moisture content was smaller but recognizable. This observation is also supported by the studies carried out by Morvan & Breul (2016) and Byun & Kim (2020). The observations and discussion concerning the DCP device are presented in more detail in Publication II.

### 3.2.5 Material properties in cyclic loading triaxial tests

The static triaxial tests detected a clear change in the strength properties of the materials as the moisture content increased. However, trains operating on the tracks subject the substructure to cyclic loading. For this reason, the actual sub-ballast materials were also studied with the help of a cyclic triaxial test, which is covered in its entirety in Paper IV and in this chapter. The cyclic tests used a confining pressure of 30 kPa, which was estimated to correspond to the horizontal stress occurring at the depth of the sub-ballast layer, as explained in Chapter 3.2.2. The tests conducted were divided into three different series:

- In the A series tests, each test was conducted at the compaction water content.

- In the B series tests, the sample was prepared at the compaction water content and conditioned. After this, the sample was saturated by feeding water into it through the bottom of the cell. The resilient moduli were determined and the permanent displacement tests were carried out at this water content.
- In the C series tests, the sample was prepared and saturated similarly to the B series tests, but it was then allowed to drain gravitationally through the bottom of the cell prior to the actual tests.

The dry bulk densities and water contents of the tested samples are presented in Table 3.3.

Table 3.3. Parameters of the samples used in the cyclic triaxial tests. (Publication IV.)

Dry densities and water contents of tested specimens.

| Test label         | Dry density<br>[g/<br>cm <sup>3</sup> ] | Void ratio | Saturation degree<br>[%] | Water content bottom<br>[%] | Water content middle<br>[%] | Water content top [%] |
|--------------------|---|------------|--------------------------|-----------------------------|-----------------------------|-----------------------|
| Reference material |   |            |                          |                             |                             |                       |
| 1A1*               | 1.768                                   | 0.50       | 40                       | 8.7                         | 6.3                         | 6.2                   |
| 1A2                | 1.786                                   | 0.50       | 40                       | 8.7                         | 5.6                         | 4.8                   |
| 1B                 | 1.733                                   | 0.53       | 70+                      | 17                          | 7.6                         | 17                    |
| 1C                 | 1.782                                   | 0.49       | 30-                      | 6.6                         | 4.9                         | 4.3                   |
| Km137              |   |            |                          |                             |                             |                       |
| 2A                 | 1.764                                   | 0.50       | 35                       | 7.4                         | 7.0                         | 5.8                   |
| 2B                 | 1.751                                   | 0.51       | 65+                      | 14.1                        | 13.1                        | 8.0                   |
| 2C                 | 1.733                                   | 0.53       | 50-                      | 13.4                        | 8.3                         | 5.4                   |
| Km98               |   |            |                          |                             |                             |                       |
| 4A*                | 2.083                                   | 0.27       | 60                       | 6.9                         | 6.3                         | 4.7                   |
| 4B                 | 2.083                                   | 0.27       | 70+                      | 7.0                         | 7.0                         | 6.7                   |
| 4C                 | 2.062                                   | 0.29       | 55-                      | 6.5                         | 6.2                         | 5.5                   |
| Km44               |   |            |                          |                             |                             |                       |
| 3A                 | 2.071                                   | 0.28       | 65                       | 7.1                         | 6.7                         | 5.1                   |
| 3B                 | 2.137                                   | 0.24       | 80+                      | 7.4                         | 6.5                         | 6.9                   |
| 3C*                | 2.069                                   | 0.28       | 70-                      | 7.4                         | 7.3                         | 6.3                   |

\* Resilient deformation test was not successful because of sensors failure.

The key results of the tests are presented in Figure 3.7, which illustrates the axial deformation of the materials at different water contents per load pulse at different loading levels. The area indicated in yellow in the figure represents the probable



vertical stress increase in the sub-ballast layer (Chapter 3.2.2). In each of the four materials, the largest deformations were measured in the samples with the highest water content, while the smallest deformations were measured in the driest samples. The loading behaviour of the Km44 and Km98 materials was relatively similar, though the Km44 material reached a slightly higher loading resistance. In the driest state, the reference material withstood a vertical stress increase of 200 kPa without significant deformation, whereas in a saturated or almost saturated state a deformation on a similar scale already began to occur at a vertical stress increase of 100 kPa. Within the predicted operating stress range from 40 to 80 kPa in Finland, deformation began to occur to a detrimental degree in the test conducted in a saturated state on the Km137 material in particular, while the other materials can withstand the operating stress range with very little deformation. The dry bulk densities of the Km137 material and reference material were low, but dry bulk density alone is not enough to explain the poor loading resistance of the material, as the reference material had the best loading resistance among the materials studied. The small mean grain size and uniform granularity of the Km137 material clearly caused problems with regard to loading resistance.

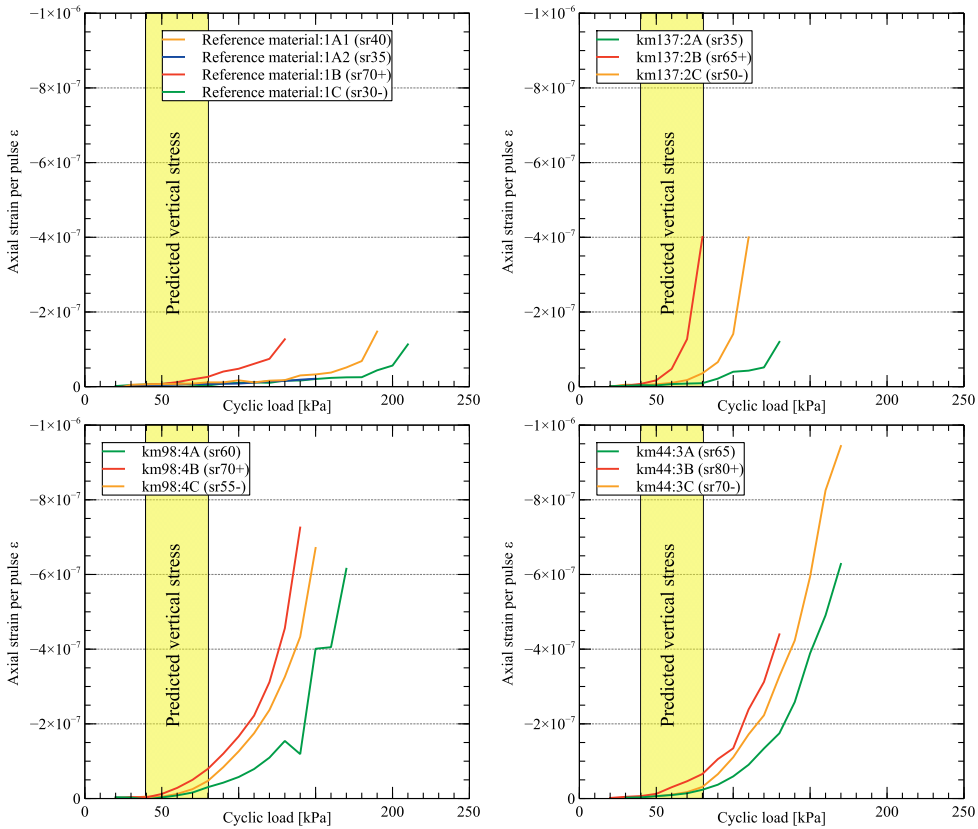


Figure 3.7. The axial deformation of the sample per loading cycle in the cyclic triaxial tests. The yellow area represents the expected vertical stress increase at the depth of the sub-ballast layer. (Publication IV.)

Summary of the results of the cyclic tests:

- An increase in water content reduced the cyclic loading resistance in each of the materials examined.
- Within the predicted operating stress range (40–80 kPa), the studied materials functioned well for the most part, with the exception of the Km137 material in a completely saturated state.
- An excessively small mean grain size in combination with uniform granularity in particular is a problem in terms of loading resistance.
- The cyclic loading resistance of the material cannot be deduced based on dry bulk density alone.

- Similarly, it is not possible to reliably estimate cyclic loading resistance based on the measured resilient modulus of the materials.
- With passenger traffic axle loads, the vertical stress increase comes closer to the lower limit of the operating stress range, so the structure should withstand repeated loading almost indefinitely in these types of loading situations.
- The freight traffic trains with the axle load of 225/250 kN start to utilize the strength properties of substructure materials more intensively. However, 250 kN axle load trains usually operate only on overhauled main track lines.

### *Discussion about observed effects of water content on cyclic loading*

The results of the cyclic tests are interesting because they provide a better understanding of the deterioration of the track condition. Old materials usually have excessive fines content, and Lee & Fitton (1969) say that fine-grained and silty sands are generally sensitive to cyclic loading. On the other hand, Steenbergen et al. (2015) claim that track wear can be reduced in the Netherlands by up to 23% by controlling the magnitude of dynamic loading. The effect of water content on the functioning of infrastructures has largely been examined through a change in the resilient modulus. However, the differences between the resilient moduli measured in this test series, as presented in Publication IV, did not explain the behaviour of the sample in the actual cyclic test series. The behaviour is explained by the lengths of the test series and the loading frequency used: in the determination of the resilient moduli, a frequency of 1 Hz was used, and the series was only 100 pulses long. These values differ significantly from the frequency of 5 Hz and series of 10,000 pulses used in the cyclic test series. If the weakening of the loading resistance is based on reduced matric suction or the formation of local pore water pressure, this is more likely to occur cumulatively at the higher loading frequency during the long test series. Some of the samples clearly discharged water during loading, which indicates a change in the sample volume.

Suiker et al. (2005) have conducted relatively similar tests to those carried out in this study. They compared cycling loading to the relative deviatoric stress achieved in a static test at a loading frequency of 5 Hz. While the relative cyclic stress was 0.495 compared to the state in the static test, hardly anything occurred in the material during one million pulses. At higher stress levels, the axial deviatoric deformations

increased but remained relatively small at approximately 0.02 until the relative cyclic stress of 0.95–0.96 was reached. At the higher relative cyclic stress levels of 0.975 and 0.995, the displacements grew significantly, and the axial deviatoric deformation was approximately 0.04. Thus, the results of the cyclic tests presented in this chapter resembled the results obtained by Suiker et al. However, the difference between the two methods was that in the results presented in this dissertation, the loading level continued to be increased after the 10,000 pulses until the sample was damaged. Nevertheless, even a smaller number of pulses may be enough to cause deformations in actual structures with excessive water content, as can be deduced from Figure 3.8, originally presented by Li & Read in 1995 (according to Li et al. (2015)). In the situation illustrated by the figure, a ballast layer with a thickness of 0.3 m and the underlying sub-ballast layer with a thickness of 0.45 m could not withstand the loss of loading resistance caused by heavy rain because the sub-ballast layer became liquefied, forcing traffic to be stopped.

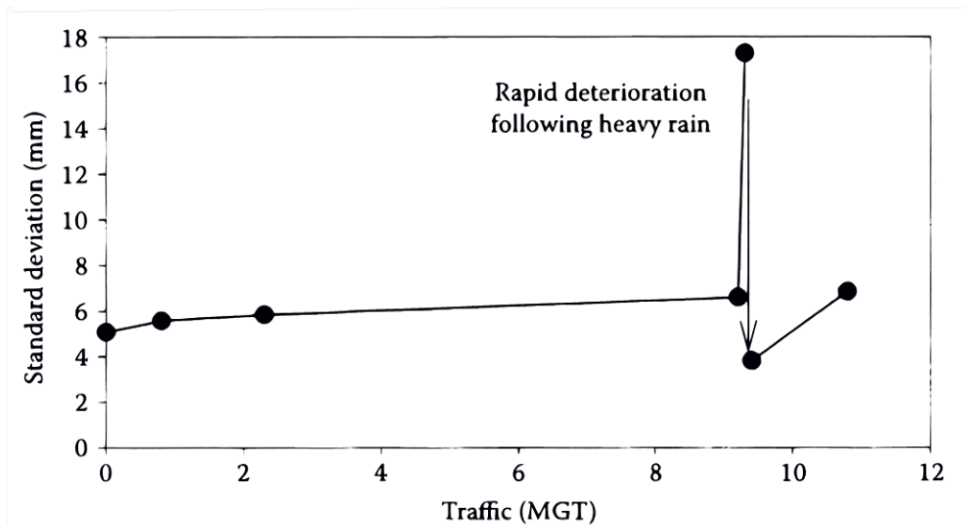


Figure 3.8. A change caused by the liquefaction of the sub-ballast layer in the vertical profile of the railway track (Read & Li (1995), according to Li et al. (2015)).

## 3.3 Observations from the field site measurements

### 3.3.1 Measured water contents

The laboratory tests presented in the previous chapters provided a clear picture of the deterioration of the loading resistance and maximum strength of the sub-ballast materials studied as the water content increases. However, assessment of the actual functioning of the track substructures requires information about the actual water contents present in Finnish track sub-ballast layer. The water contents of the three test sites along the Rantarata track are examined in Publication III and the main results are presented in this chapter. Because it was not possible to dismantle the track structures for this study, sensors measuring water content were installed vertically at regular intervals along the edge of the sub-ballast layer under the track shoulder. The Publication III provides a more detailed description of the measurement arrangements in a cross section.

With regard to possible permanent deformations occurring in the structure over time, the water contents present in the structure over a long period of time play the key role. Figure 3.9 presents the saturation degrees of the Km44 site's sub-ballast layer. The white boxes/areas are caused by sensor failures or frozen structure, because the sensors cannot measure the amount of frozen water correctly. Prior to the implementation of a drainage improvement at the turn of 2019 and 2020, high water contents were present in the area. The saturated zone extended to a depth of -1.0 m from the track elevation line. Periods with a high saturation degree have occurred both in autumn and summer. The drainage improvement eliminated periods with a high saturation degree, and since then the sub-ballast layer has, for the most part, stayed at a saturation degree below 60% throughout the year. The sensor located at the greatest depth, at -1.56 m, has at times detected saturation degrees of 70–80%, indicating that the groundwater table is now located just below the lowest sensor.

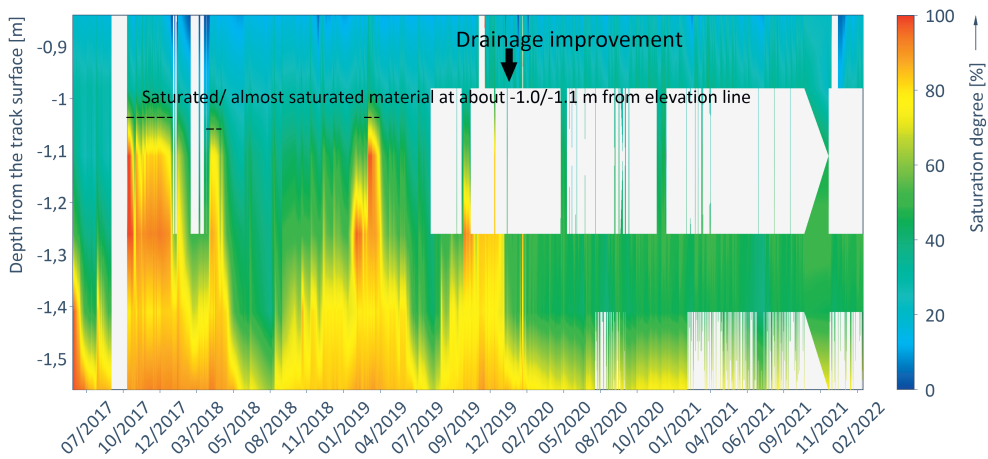


Figure 3.9. Long-term saturation degrees of the sub-ballast of the Km44 site. The white boxes and areas are caused by sensor failures or frost. (Publication III.)

At the second monitored site, i.e. Km98, the variation in water content was different from the Km44 site. Figure 3.10 presents the saturation degrees of the site's sub-ballast layer, which indicate that the water content has remained surprisingly constant during the measuring period. In autumn 2017 and 2018, high water contents were detected at depths of -1.0 m and -1.2 m from the track elevation line, and the saturation degree at the top section of the sub-ballast layer also increased to 50–70% at the time. At times, the structure has also dried to a saturation degree of 70–80% at a depth of -1.4 m, but this drying is not particularly apparent in the measurement data on the top section. This indicates that the sub-ballast layer includes clay-rich/silty layers that have better soil moisture retention capacity. The effects of rain can be seen in the top and bottom sections of the sub-ballast layer, but their impact is not particularly large.

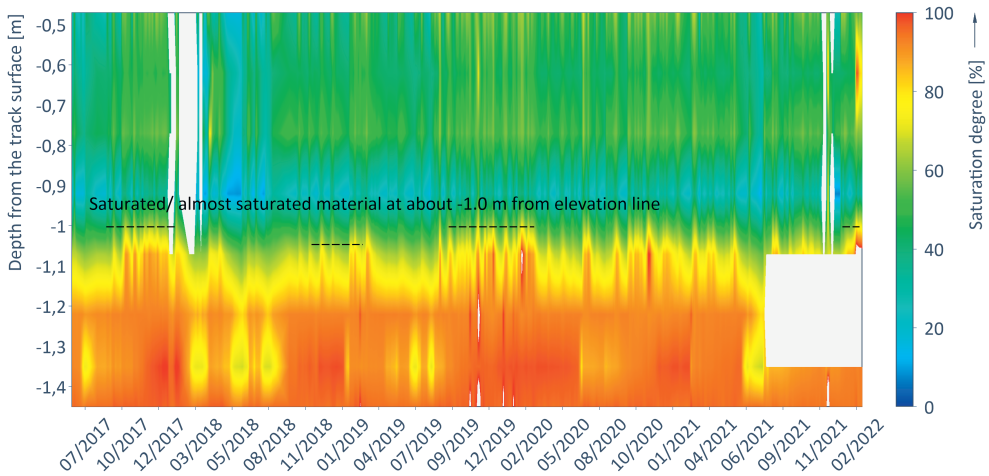


Figure 3.10. Long-term saturation degrees of the sub-ballast of the Km98 site. The white boxes and areas are caused by sensor failures or frost (Publication III.)

The third test site, Km137, proved to be the driest of the sites studied, as shown in Figure 3.11. During the measuring period, the water content remained low, mostly below a saturation degree of 60%. However, the effects of rain were clear and easy to see in the sand material with high permeability. At this site, a state of complete or almost complete saturation was only detected during thaw periods in spring, when the water content of the top section of the sub-ballast exceeded a saturation degree of 70%. However, these periods were of very short duration, for the most part only lasting a couple of days.

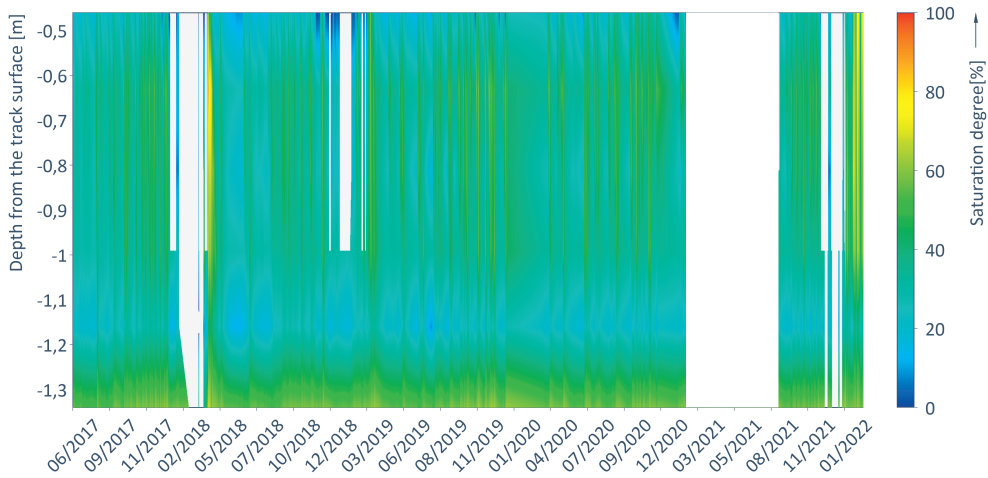


Figure 3.11. Long-term saturation degrees of the sub-ballast of the Km137 site. The white boxes are caused by frost and failure of sensors. (Publication III.)

In addition to the long-term water contents, more short-term phenomena were also examined based on the measurement data. Figure 3.12 examines the situation in autumn 2017, as the period from September until the end of the year was very rainy. The monthly precipitation measured at the site that year was 106 mm in October and even higher than that in November, at 140 mm. The rainy period affected the water content of the sub-ballast layer by rapidly increasing the saturation degree at the upper part of sub-ballast from 20–30% to 50–60%. In practice, the saturated zone rose from a depth of -1.5 m to -1.05 m. This increase in water content at the lower part of sub-ballast was more due to the rise of the local water table than the retention of rainwater by the top section of the structure.



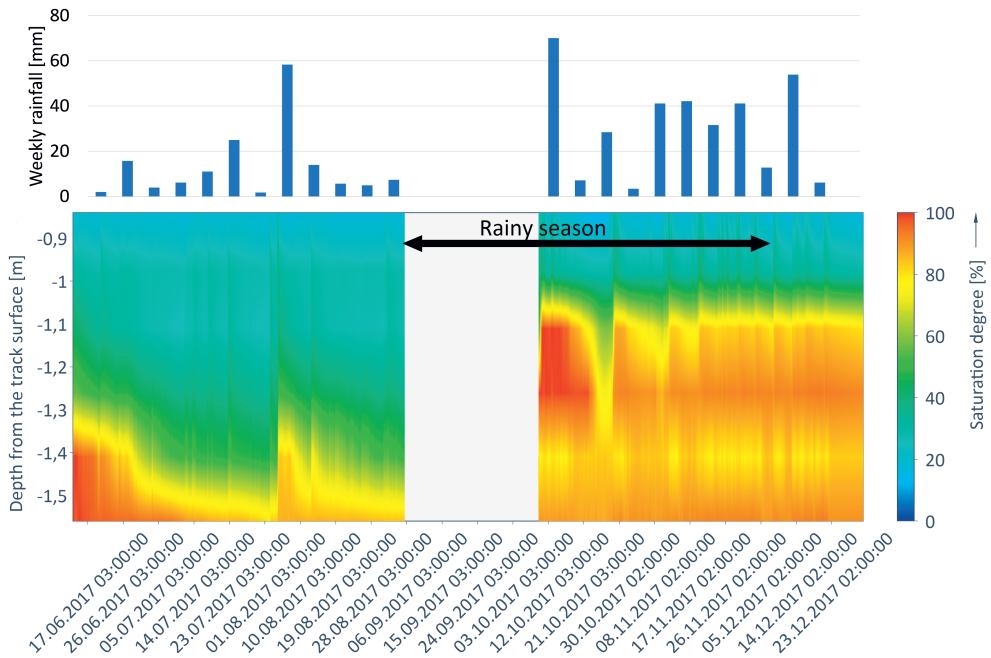


Figure 3.12. Short-term saturation degrees of the Km44 site. (Publication III.)

A similar analysis was also conducted at site Km98, as shown in Figure 3.13. In autumn 2019, rains caused the saturation degree of the top section of the sub-ballast layer to rise to approximately 70%, and the measurement data produced by the water content sensor located at the greatest depth showed that the water table had risen. The sub-ballast material at the Km98 site clearly has better soil moisture retention capacity than the material at the Km44 site. That better retention capacity also makes it more difficult to see the penetration of individual rains, because the distribution of water content is much smoother than in the other sites. The water penetration time at site Km98 is somewhere between a day or two while at sites Km44 and Km137 it is only a few hours.

The short-term survey conducted at the Km137 site focused on thaw periods, and its results are given in Figure 3.14. In spring 2018, the thawing of frost caused a saturation degree of approximately 80% to occur below the ballast layer for a period of 10 days. Water content also increased deeper in the sub-ballast. In other words, water content increased in an area where load increases caused by train traffic are still moderate.

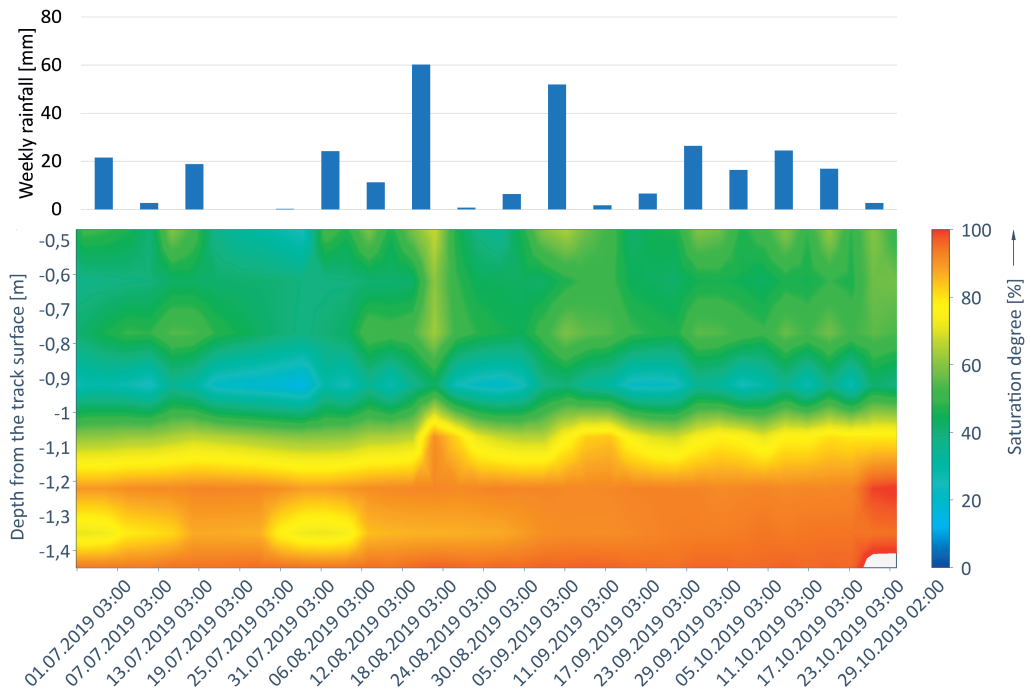


Figure 3.13. Short-term saturation degrees of the Km98 site. (Publication III.)

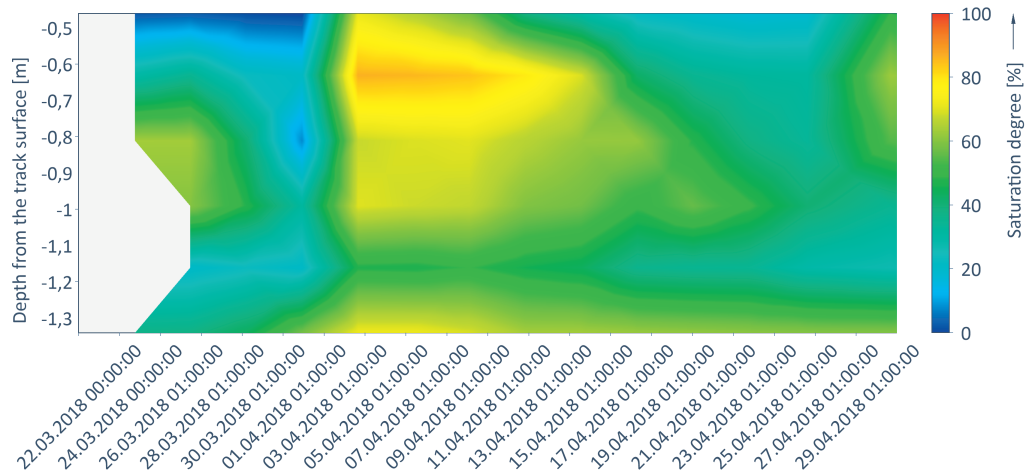


Figure 3.14. Short-term saturation degrees of the Km137 site. The white area is caused by frost. (Publication III.)

Based on the measurement data on the water contents of the sub-ballast layer at the monitored sites, the following conclusions can be drawn:

- The degree of saturation varies between 20% and 100% at the test sites but usually remains below 70% above the groundwater table. Beneath the ballast layer, where the vertical stress increase is still moderate, surprisingly few instances of almost a fully saturated state have been detected, even though the track structure is exposed to rain. The high amount of fines increases water content to a saturation degree of over 50%.
- High water contents may occur in the sub-ballast layer during thawing, but the measurements indicate that these periods last for 10 days at most.
- Rains affected the water content of the sub-ballast layer by increasing the saturation degree above the water table to up to 60–70% at the Km44 and Km98 sites, which have finest contents of 4.9% and 6.7%, respectively. The effect of a long rainy period is primarily evident in the rise in the local (ground)water table.
- The effect of capillary rise was smaller than expected in the sub-ballast materials studied. Higher water contents are primarily found within 20–30 cm above the water table, and the saturation degree decreases rapidly as the distance to the water table increases.
- The drainage improvement carried out at the Km44 site resulted in a significant decrease in the site's water contents, as the periods of high water content consistent with seasonal variation were practically eliminated entirely, and since then the structure has remained at a clearly lower degree of saturation down to a depth of -1.55 m.

### *Discussion about measured water contents*

The changing climate and increasing precipitation pose a clear challenge to the functioning of infrastructures. In the worst case scenario, excessive water content may cause the railway track to suffer extensive damage and even result in train derailment (Hasnayn et al., 2015). Based on the results presented in this dissertation, the effects of track drainage appear to vary by site, which was largely to be expected. However, the differences between sites were significant. For example, the sand esker-like Km137 site generally had a very low water content, even though its drainage system is severely lacking and the track runs by a steep and high sandy slope

that descends right to the track. Similarly, the water content of the Km98 site constantly remained at a higher level, most likely because the sub-ballast material retains an excessive amount of water and there is some type of groundwater / perched groundwater layer below the track. Rainfall had a smaller effect than expected. For instance, Ghataora & Rushton (2012) have found that on single-track sections it can take longer than four days for water to be conducted from the track structure to the subsurface drain, whereas on double-track sections drained only on one side, this can take more than 10 days. The challenges with one-sided drainage were also recognised in a model of various drainage situations that was presented in a Finnish national report (Latvala, 2018). The permeability of the sub-ballast layer has a considerable effect on track drainage. One solution proposed by Ghataora & Rushton (2012) in their study is to install a geocomposite with high permeability in the sub-ballast layer.

In the structure of a ballasted track, the difference in permeability between the ballast and the underlying material typically poses challenges for drainage. For example, Youngs & Rushton (2009) have computationally examined the height of the water table when water pours into a two-layer structure heavily from above. In their article, they describe the risk that the water table can, under unfortunate circumstances, rise to the height of the sleepers, which would cause problems and restrictions for traffic. Based on practical studies, on the other hand, Wang et al. (2017) noticed in their ground-penetrating radar studies that the water content is often higher in transition structures than in line sections. They also proposed the solution that the drainage of these types of transition structures be made more efficient than the drainage of line sections. This idea matches the results presented in this chapter, as different sites clearly require different types of drainage solutions. Ferreira & Teixeira (2011) have modelled a few different drainage solutions and identified differences between them in their study. Their methods are largely based on restricting the access of rainwater to the structure by using surface drainage or a bituminous sub-ballast layer or by covering the embankment's slopes with a layer with low permeability, for example. Based on their modelling data, each of the methods reduced water content in the structure.

The effect of capillary rise was lower than originally expected for the materials and sites studied. The degree of saturation rapidly decreased as the distance to the surface of free water increased. Early on in the study, water contents were also examined with the help of a computer model created with the SEEP/W program. This

modelling is explained in more detail in the national report drawn up by Latvala et al. (2018). Figure 3.15 presents an example model featuring poor-quality sub-ballast materials (excessive amount of fines, relatively high capillary rise height). Figure 3.16 examines the significance of the height of the water table to the saturation degree of the structural layers using the same materials. The results show that the degree of saturation decreases to below 60–70% in the material of the intermediate layer and insulation layer at a distance of 20–30 cm from the water table. These results are similar to the capillary rise test results presented in Publication III and the observations made at the field sites along the Rantarata track. Thus, it would appear that keeping the water table sufficiently low in the structure is an adequate drainage solution for sandy materials that are near to the fine-grained end of the FTIA’s grading limits (in Fig. 3.1).

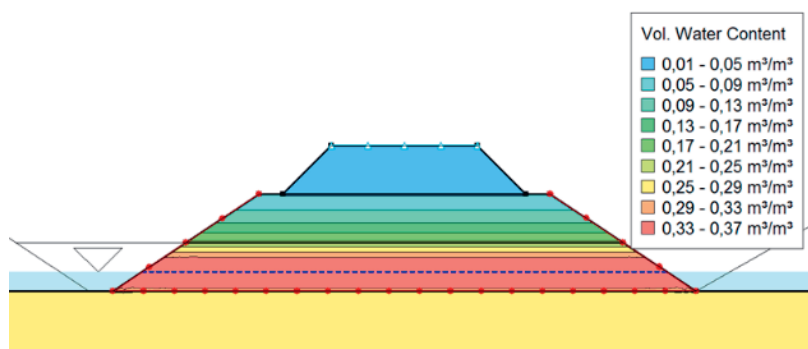


Figure 3.15. The modelled water contents of the track embankment when the sub-ballast materials are of poor quality (and the capillary rise height is high). (Latvala, 2018.)

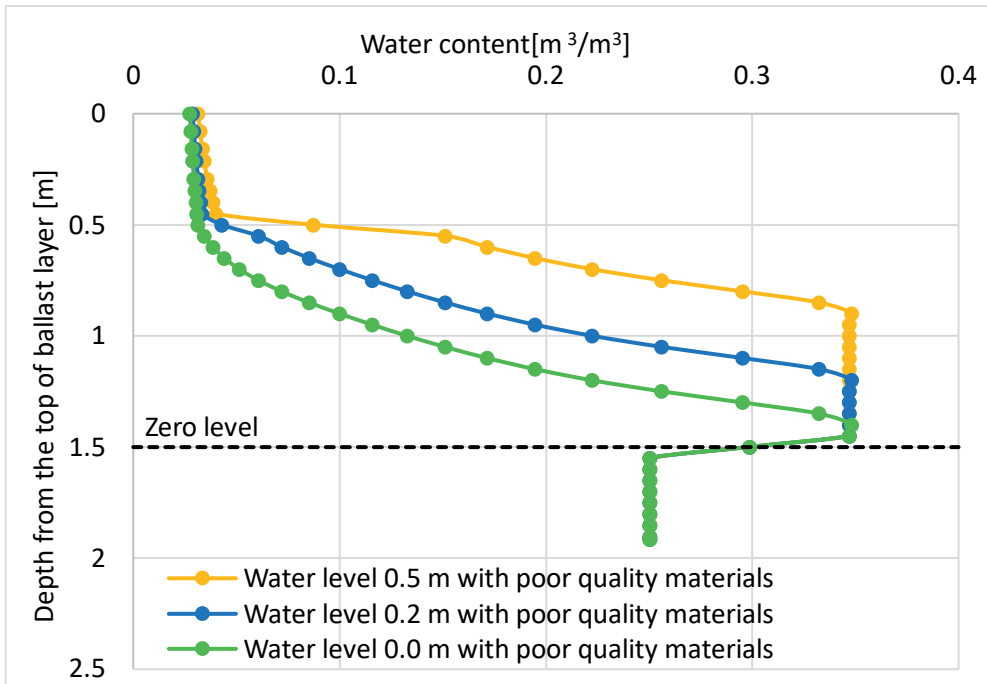


Figure 3.16. The effect of the height of the water table on the water content of the embankment based on computer modelling. The water table (zero level) is located at the lower surface of the insulation layer.

### 3.3.2 Track deformation properties of monitored sites and the effect of drainage improvements

The effects of the water content and loading resistance of the track sub-ballast layers and potential frost problems ultimately manifest as displacements of the railway track, which cause track geometry defects. Although the laboratory tests provide interesting and important data on material properties and enable the analysis of various conditions, the vertical displacements measured along the track have played a key role in this study. The results presented in this chapter have yet to be published in international research articles, but reports have been published about them in the publication series of the Finnish Transport Infrastructure Agency (Latvala, 2023a,

2023b, 2021). At the monitored sites and frost monitoring stations, displacements have been measured at each end of the sleeper. At the monitored sites, the measurement has been carried out in relation to the auger drill rods installed in the stiff subgrade layer whereas at the frost monitoring stations the measurement has been carried out in relation to the anchor installed either in the stiff subgrade layer or at a depth of three metres. All measured displacements are permanent, elastic responses have not been measured in this study.

The vertical displacements at the monitored site Km44 along the Rantarata track for the entire measuring period are shown in Figure 3.17. In 2018, the superstructure was replaced (rails, sleepers and ballast layer), which is why the measurement data is missing for that period. The site was immediately tamped during the measuring period. This typically increases the rate of displacement until the structure usually stabilizes. At this site, however, the rate of displacement remained almost constant until the replacement of the superstructure. When the displacement measurement continued in 2019, the rate of displacement was slightly lower than before the superstructure was replaced, but since tamping was carried out in early 2021, the rate of displacement once again appears the same as before. Based on the results, the track settles by more than 7 mm per year, which is a relatively high rate of settlement compared to the volume of traffic on the Rantarata track (approx. 3 MGT/year). It can also be deduced from the results that this problem has not been caused by the superstructure, as its replacement had no significant effect on the occurrence of displacements. Similarly, the sub-ballast drainage improvement carried out in early 2020 also had no effect on the occurrence of displacements.

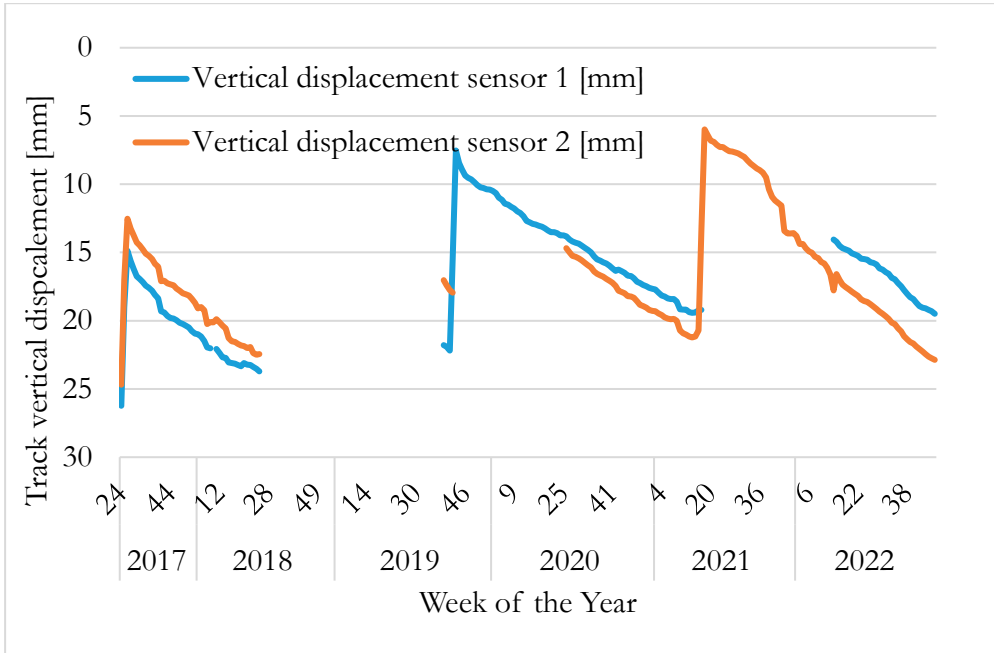


Figure 3.17. Vertical displacements measured at site Km44 during the monitoring period.

Figure 3.18 presents the monthly vertical displacements at site Km44 in relation to water content for the entire monitoring period. For the sake of clarity, the figure only shows the negative displacements, i.e. the settlement of the track. There does not appear to be a relation between water content and displacements, and the occurrence of displacement is more like random. The figure shows some individual larger monthly displacements that may be due to even a small amount of thawing or rapid initial settlement following tamping, for example. The observations made at the other sites have been very similar.



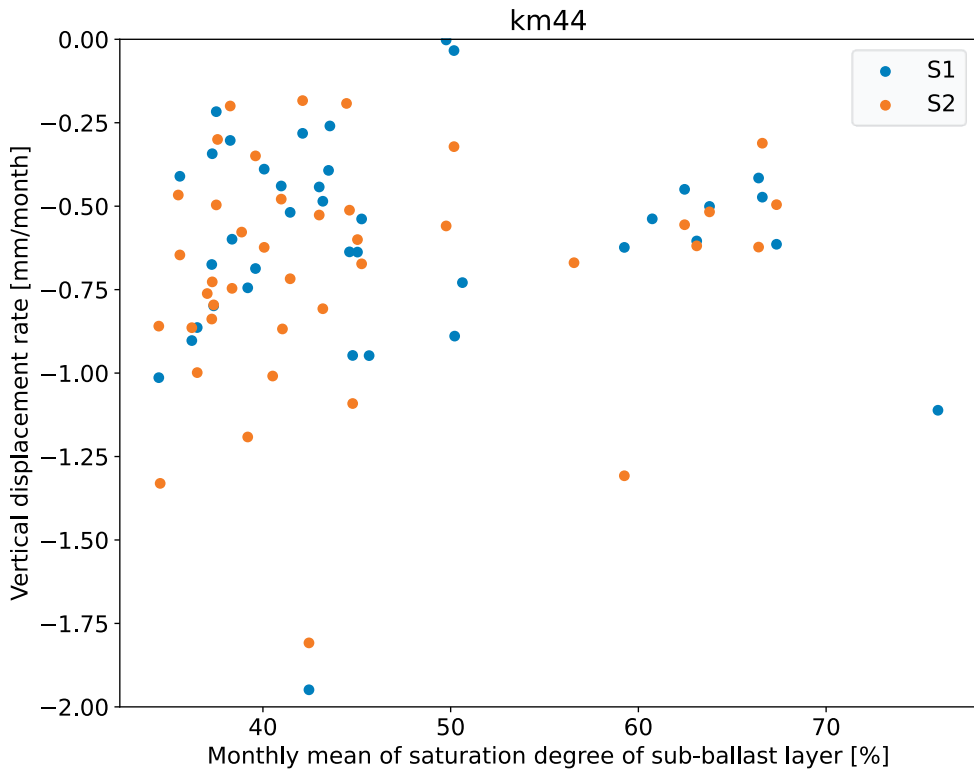


Figure 3.18. Comparison of displacements rates and saturation degrees at the Km44 site. S1 and S2 are displacement sensors on both sides of track.

At the Km98 site, the displacements were clearly smaller than at the Km44 site throughout the measuring period. The results for the entire measuring period are presented in Figure 3.19. At the end of 2018, the measurement was interrupted due to the replacement of the superstructure. The rate of displacement has been constant at this site. Prior to the replacement of the superstructure, the rate of displacement was 3–4 mm/year, whereas after the replacement the rate was 1–1.5 mm/year. However, this is partly explained by the tamping carried out in 2017, which led to the occurrence of residual settlement. In early 2021, the structure froze to some extent and a frost heave of 1–2 mm occurred, following which the structure has apparently loosened and displacements have occurred at a higher rate. Unfortunately, the stabilisation of the phenomenon cannot be observed because the

track was tamped again in spring 2021. After this tamping, the rate of displacement increased for a short period of time, but since then the rate of displacement has been very low. Minor frost heave was also detected in 2022, but it has not led to the kind of increase in the rate of displacement that occurred the year prior. With regard to displacements, it can be concluded that they are not a particular problem at the site.

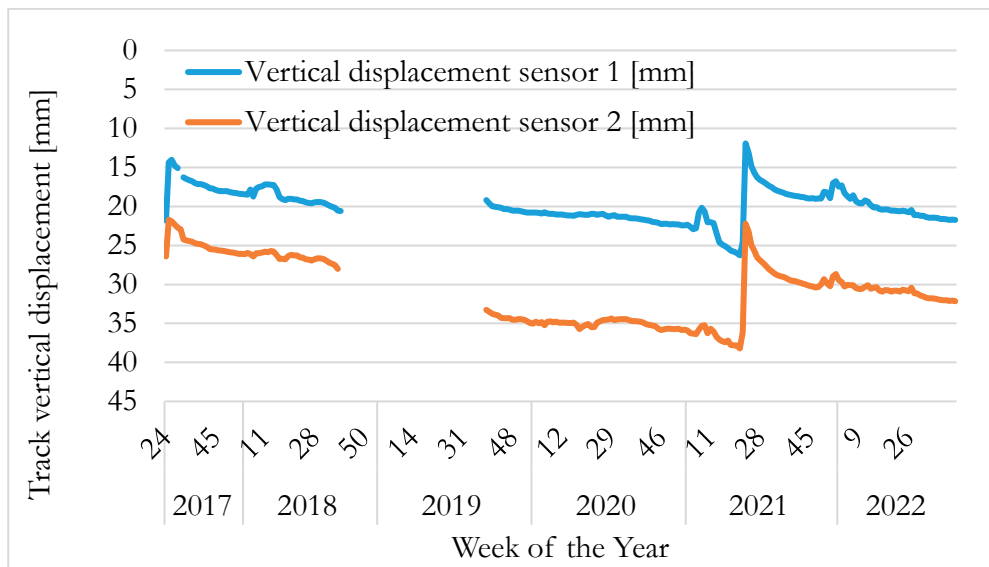


Figure 3.19. Vertical displacements measured at site Km98 during the monitoring period.

The total displacements for site Km137 are presented in Figure 3.20. At the start of the measuring period in 2017, the track was tamped on two occasions within a short period of time, which was followed by a rapid initial settlement period. This period ended in early 2018, and since then the rate of displacement has been low. In 2019, there was an interruption in the measurement process, and the railway track was tamped again at the end of the same year. This tamping operation was also followed by initial settlement. At the time of examination, the rate of displacement was approximately 1 mm per year in 2020 and 2021. At this site, the displacement sensors also partly react to temperature, as the displacements appear to have grown when the weather cooled in late 2021. This phenomenon is evident, as the rates of displacement measured are low, and the structure is situated on a dry sand embankment where the temperatures change rapidly. Based on the measurement data, the structure appears to function as expected.

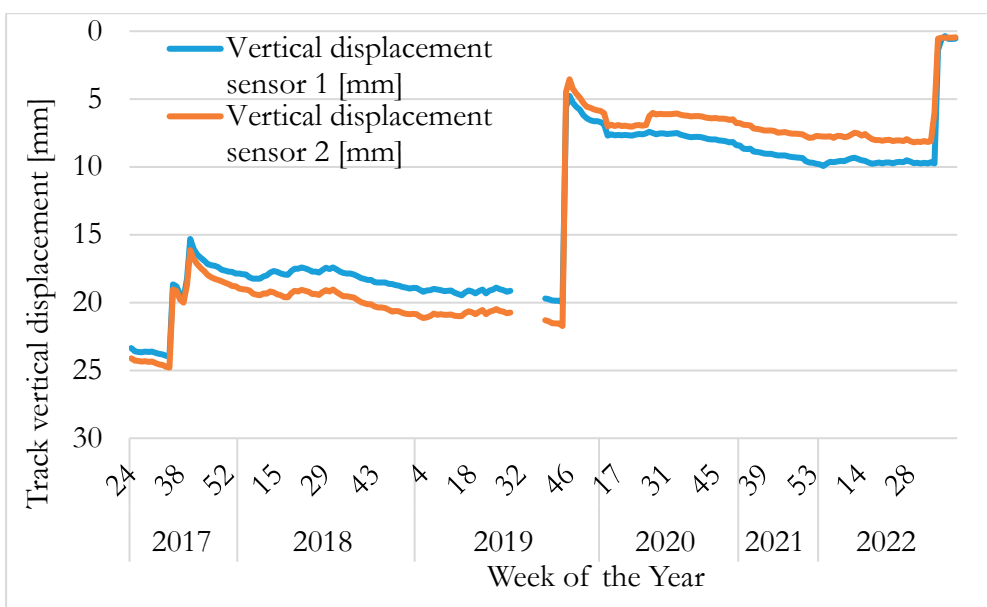


Figure 3.20. Vertical displacements measured at site Km137 during the monitoring period.

The following conclusions can be drawn about the monitoring measurements focused on displacements:

- Based on the vertical displacements measured at the test sites along the Rantarata track, there is no indication that water content has an effect on the rates of displacement measured at the monitored sites.
- The observations made indicate that the higher than usual rate of displacement occurring at the Km44 site (several millimetres per year), are most likely caused by consolidation settlement of the subgrade. Consolidation settlement also occurs at the Km98 site.
- The displacements at the Km137 site have been small throughout the measuring period. It is likely that the geometry problems that have occurred in the vicinity of the site are caused by problems in the transition structures, as the sand esker-like site is surrounded by rock cuttings on each side.
- No frost problems occurred at the test sites during the measuring period. At the Km98 site, a frost heave of 1–2 mm was detected in three winters.

### 3.3.3 Frost monitoring stations

The observations made at the Rantarata test sites were verified by expanding the observation data to include frost monitoring station data. Tampere University has maintained frost monitoring stations along the Finnish rail network since 2008. The 17 frost monitoring stations were built primarily for frost research purposes, and they have measured frost depth with the help of temperature sensors as well as vertical displacement along the track. Some of the sites have also measured water content, but this measurement is not as comprehensive as the water content measurement carried out at the Rantarata test sites. The structure and site characteristics of these stations are described in a report by Nurmikolu & Pylkkänen (2015), and a closer analysis of the water contents and displacements at the sites is presented in a research report by the Finnish Transport Infrastructure Agency (Latvala, 2023a). The site characteristics are presented in Table 3.4. A project related to this study examined the occurrence of vertical displacements and the water content of structures in particular at the frost monitoring stations.

Table 3.4. Locations of the frost monitoring stations and their structural properties. (Latvala, 2023a)

| Monitoring point and location |                  | Name   | Structural layer thicknesses [m] |                   |                   | Instrumentation: sensors [pcs] (measurement depth min–max) [m] |              |
|-------------------------------|------------------|--|----------------------------------|-------------------|-------------------|--|--------------|
| section                       | km+m             |  | ballast                          | sub-ballast       | total             | temperature  | moisture     |
| TOR-KLI                       | 899+498          | Tornio km899   | 0.6                              | 2.0               | 2.6               | 12 (0.1–2.8)   | no           |
|                               | 909+600          | Tornio km909   | 0.6                              | 1.6               | 2.2               | 12 (0.1–3.1)   | no           |
|                               | 921+050          | Tornio km921 (Niemenpää 2)   | 0.5                              | 1.1               | 1.6               | 36 (0.1–3.2)   | 4 (1–1.6)    |
|                               | 925+610          | Tornio km925 (Niemenpää 1)   | 0.5                              | 1.5               | 2.0               | 36 (0.1–2.6)   | 4 (0.6–1.2)  |
|                               | 932+135          | Ylitornio km932  | 0.5                              | 0.9               | 1.4               | 32 (0.1–2.8)   | 10 (0.2–2.2) |
|                               | 945+060          | Ylitornio km945  | 0.5                              | 0.8               | 1.3               | 32 (0.1–2.7)   | 10 (0.2–2.3) |
| SK-OL                         | 732+527          | Liminka  | 0.9 <sup>3)</sup>                | 0.5               | 1.5 <sup>3)</sup> | 12 (0.1–3.1)   | no           |
| SK-OL                         | 429+370          | Hippi E  | 0.55                             | 1.8 <sup>4)</sup> | 2.35              | 51 (0.1–2.35)  | no           |
| SK-OL                         | 429+495          | Hippi P  | 0.55                             | 1.8               | 2.35              | 34 (0.1–2.25)  | 5 (0.1–1.7)  |
| PM-KUO                        | 442+260          | Kuopio   | 0.5 <sup>3)</sup>                | 0.7               | 1.2 <sup>3)</sup> | 36 (0.2–2.0)   | 10 (0.2–1.7) |
| PM-JNS                        | 445+300          | Varkaus  | 0.6                              | 0.5               | 1.1               | 36 (0.2–2.4)   | 10 (0.2–1.8) |
| PAR-JNS                       | 441+725          | Kitee  | 0.6                              | 0.9               | 1.5               | 36 (0.2–2.7)   | 10 (0.1–2.0) |
| LLH-KKI                       | 225+266          | Karkku   | 0.7                              | 0.5               | 1.2               | 12 (0.1–2.9)   | no           |
| RI-TPE                        | 156+287          | Viiala   | 0.7                              | 0.5 <sup>2)</sup> | 1.2 <sup>3)</sup> | 12 (0.1–3.1)   | no           |
| OL-KON                        | 898+050          | Paltamo  | 0.6                              | 1.5               | 2.1               | 36 (0.2–3.1)   | 10 (0.2–1.9) |
| KE-HLT                        | 65+079           | Mäntsälä   | 0.6                              | 2.0               | 2.6               | 12 (0.1–2.6)   | no           |
| superstructure category:      | electrification: | <sup>1)</sup> EPS sheet with a thickness of 50 mm below the ballast layer<br><sup>2)</sup> XPS sheet with a thickness of 100 mm below the sub-ballast<br><sup>3)</sup> includes a frost protection sheet<br><sup>4)</sup> structure made of crushed rock aggregate |                                  |                   |                   |  |              |
| D                             | yes              |  |                                  |                   |                   |  |              |
| C <sub>1</sub>                | no               |  |                                  |                   |                   |  |              |
| C <sub>2</sub>                |                  |  |                                  |                   |                   |  |              |

The test site at the Varkaus frost monitoring station provides a good example of an analysis between water content and displacements. Annual vertical displacements of more than 3 mm have typically been found at the site, even though the annual traffic

volume is only 0.7 MGT on average. Monthly displacements are presented in Figure 3.21, with the scale capped at a maximum monthly displacement of 4 mm. Vertical displacements reflect the frost heaving of the structure, which has occurred frequently at this site. After the thawing of frost, the occurrence of displacements is very consistent. The water contents, which are presented in Figure 3.22, remain low in the ballast layer and intermediate layer at the site but are higher at depths below -0.85 m from the track elevation line. Figure 3.23 examines the relationship between displacements and the water contents of the structure during the period when the ground is unfrozen (from June to November). There is clear variation in water contents, but the occurrence of displacements does not appear to be connected to water content. The figure includes a few larger displacements that can be explained by tamping activities, for example.

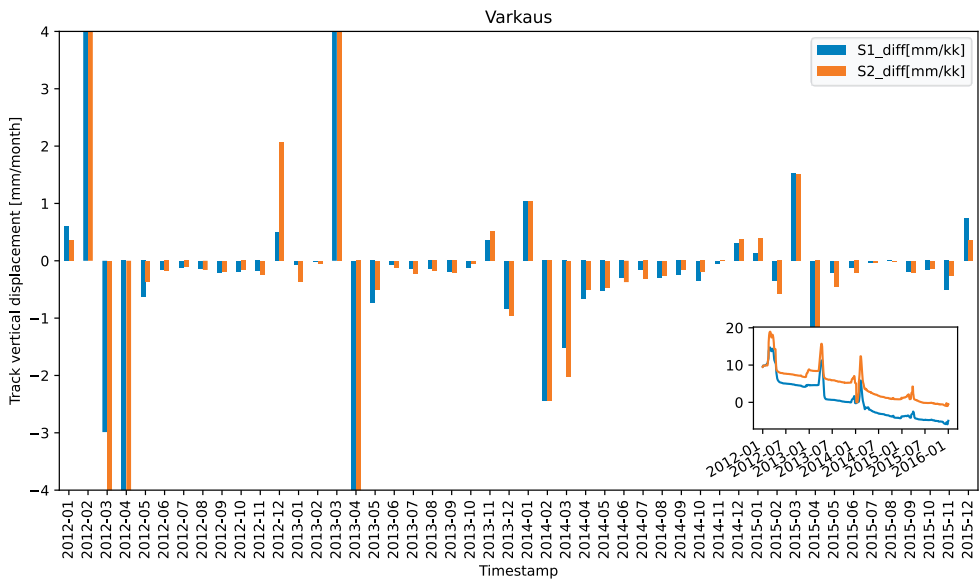
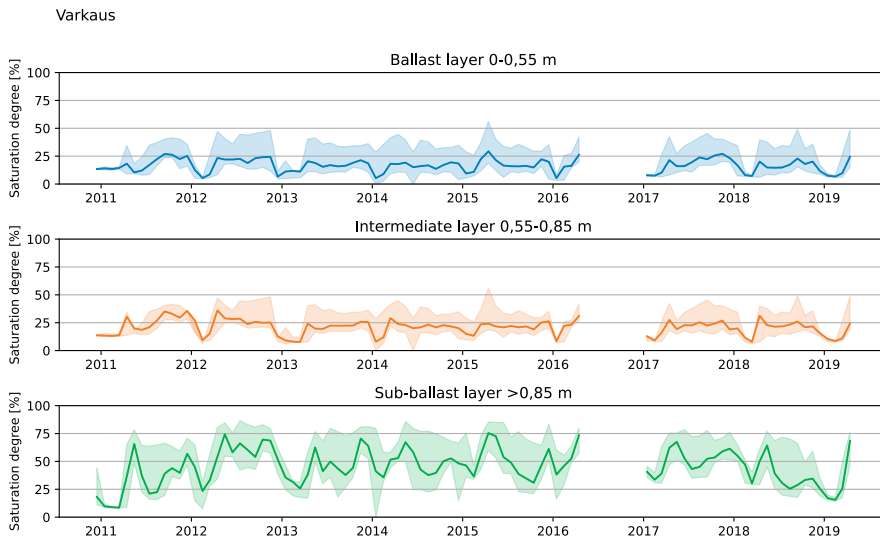


Figure 3.21. Displacements in Varkaus frost monitoring station at a monthly level. (Latvala, 2023a.)



*Figure 3.22. Water contents at the Varkaus frost monitoring station as a monthly average. The shaded area represents the minimum and maximum values for the month. (Latvala, 2023a)*

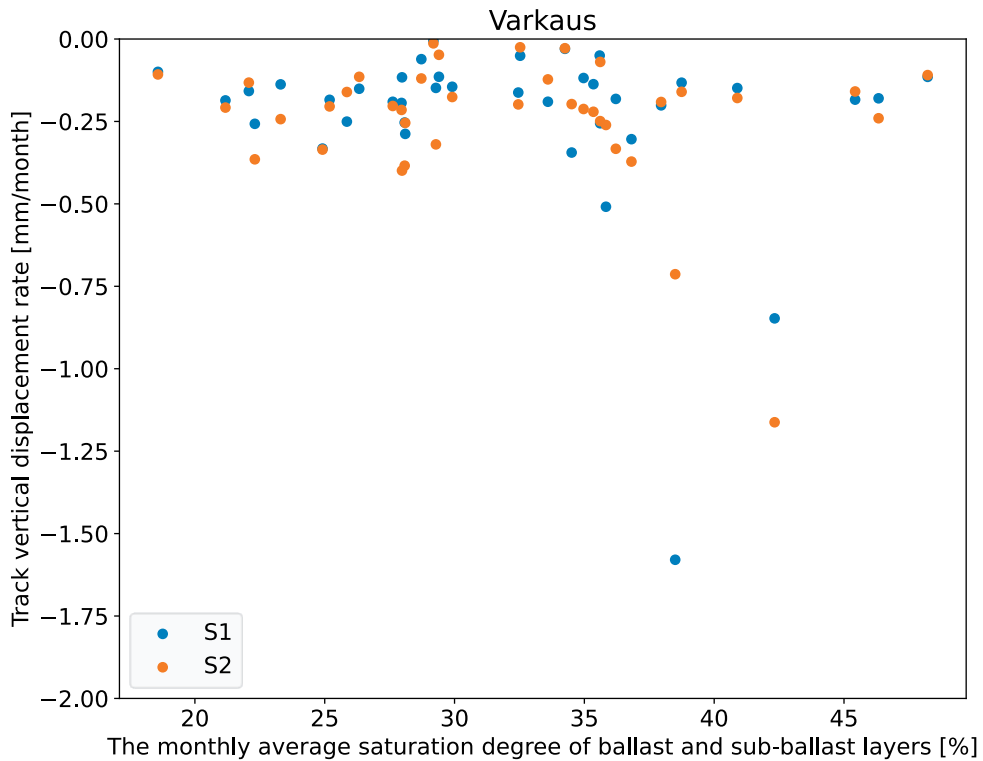


Figure 3.23. The relationship between displacement rate and the degree of saturation at the Varkaus test site. (Latvala, 2023a.)

A wide variety of analyses was conducted at each site, and they are summarised in Table 3.5. The typical rate of displacement varied by site, but the displacements were generally surprisingly small, considering that the frost monitoring stations were originally built at rail sections found to be susceptible to frost action. The rates of displacement varied by site, even though there were no significant differences in traffic volumes. In many places, the measured vertical displacements are already explained by wear of the ballast layer. No clear connection could be established between water content, the materials of the sub-ballast layer and the typical rate of displacement. In fact, it appears that the site’s individual characteristics play a key role. It must be noted, however, that the traffic data indicates that the percentage of traffic with an axle load of more than 17.5 tonnes was low. For this reason, the amount of significant loading cycles remains low. Tamping of the railway track was found to cause a higher rate of displacement lasting for several months or even years at some sites.



Table 3.5. Summary of the observations made at the frost monitoring stations. (Latvala, 2023a.)

| Site            | Typical annual rate of displacement<br>[mm/year] | Traffic                   |                  | Superstructure                 |                                | Substructure   |   | Typical depth of a saturation degree of 70–80% |  | Occurrence of frost heave          |
|-----------------|--|---------------------------|------------------|--------------------------------|--------------------------------|--|---|--|--|------------------------------------|
|                 |  | Traffic volume 2019 [MGT] | Number of tracks | Rails and sleepers             | Ballast                        | Thickness of the structural layers (ballast + sub-ballast) [m] | Grain size range of the sub-ballast layer | Average [m]                                    | During thaw periods [m]                |                                    |
| Tornio km899    | >2   | 1.0                       | 1                | 60E1 / 2008                    | 2008 additional ballast        | 2.6  |   |  |  | Moderately                         |
| Tornio km909    | <1   | 1.0                       | 1                | 60E1 / 2008                    | 2008 additional ballast        | 2.2  |   |  |  | Rarely                             |
| Tornio km921    | >3   | 1.0                       | 1                | 60E1 / 2009                    | 2009 additional ballast        | 1.6  |   | 1.6 (not within the measurement range)         |  | Frequently                         |
| Tornio km925    | >1   | 1.0                       | 1                | 60E1 / 2009                    | 2009 additional ballast        | 2.0  |   | 1.2  | 0.9                                    | Moderately                         |
| Ylitornio km932 | <1   | 1.0                       | 1                | 60E1 / 2009                    | 2009 additional ballast        | 1.4  |   | 1.8  | 1.8                                    | Never                              |
| Ylitornio km945 | <1   | 1.0                       | 1                | 60E1 / 2009                    | 2009 additional ballast        | 1.3  |   | 2.25 (not within the measurement range)        | 2.2                                    | Never                              |
| Liminka         | >3   | 12.9                      | 1                | Old at the time of measurement | no data                        | 1.5  |   |  |  | Frequently                         |
| Hippi E         | < 2  | 7.8 / 2*                  | 2                | 60E1/2012                      | 2012 new                       | 2.4  |   |  |  | Often 2–3 mm                       |
| Hippi P         | <2   | 7.8 / 2*                  | 2                | 60E1/2012                      | 2012 new                       | 2.4  |   | 1.7  | 1.5                                    | Moderately 2–3 mm                  |
| Kuopio          | -  | 8.2                       | 1                | Old at the time of measurement | Old at the time of measurement | 1.2  |   | 1.3  | 1.1                                    | Yes (short measuring period)       |
| Varkaus         | >3   | 0.7                       | 1                | 54E1(V)/2002                   | 1963 additional ballast        | 1.1  |   | 1.6  | 0.9                                    | Often over 5 mm                    |
| Kitee           | >2   | 6.6                       | 1                | 54E1/1965                      | 1964–66 additional ballast     | 1.5  |   | 2.0 (not within the measurement range)         | 2.0 (not within the measurement range) | Moderately                         |
| Karkku          | -  | 8.6                       | 1                | Old at the time of measurement | Old at the time of measurement | 1.2  |   |  |  | Moderately                         |
| Viiala          | Could not be determined                          | 20.6/2*                   | 2                | 60E1/1998                      | 1999 new                       | 1.2  |   |  |  | Often over 5 mm                    |
| Paltamo         | -  | 9.8                       | 1                | Old at the time of measurement | Old at the time of measurement | 2.1  |   | 1.8  | 1.0 (groundwater table unclear)        | Cannot say, short measuring period |
| Mäntsälä        | -  | 10.6                      | 2                | 60E1/2004                      | 2004 new                       | 2.6  |   |  |  | No displacement measurement        |
| Good/low        |  | Moderate                  |                  | Bad/high                       |                                |  |   |  |  |                                    |

The following conclusions can be made based on the analysis of the frost monitoring stations:

- The vertical displacements measured at the sites are small, for the most part, and in many cases they can be explained almost entirely by wear of the ballast layer.
- The highest water contents were typically measured from the structure during the thaw period in spring.
- No correlation between the water content of the structure and vertical displacement rates was found at the sites. Similarly, no increased rates of displacement were found to occur during rainy periods in autumn at sites where no water content measurement was carried out.
- The frost action of the track and its subsequent thaw softening were the most recognizable factors that weaken the vertical geometry of the track.
- Frost action typically occurs in the subgrade or the embankment fill, the drainage of which is difficult to improve.

### *Discussion about observed deformation properties*

The displacements that occur in track structures are ultimately evident in weakened track geometry, which hinders rolling stock operation. Several different mechanisms contribute to displacements. In order for geometry defects to be predicted, functional models are needed of several track components (Melo et al., 2020). This chapter does not discuss extreme deformations that occur during flooding or structural collapse.

Excessive water content in the structural layers of the track have been suspected of at least contributing to track geometry problems in Finland. Based on studies, even small increases in water content can cause additional need for maintenance in certain conditions (Ferreira and Teixeira, 2011). In Finland, this subject has been discussed in works such as the master's thesis by Malassu (2016), which examined the loading resistance of railway tracks and the factors affecting it. The sub-ballast and subgrade moisture indexes were found to affect the deviation of longitudinal level occurring along the tracks, and the depth of the drainage was also found to have a similar effect. Based on measurements, thaw softening occurring in spring has been suspected of causing further weakening of the geometry, at least in some sites (Metsovuori, 2013). A dissertation completed in 2023 (Sauni, 2023) sought to

identify the causes of track geometry deterioration with the help of a track geometry deterioration modeling and data mining. According to the results achieved through data mining, there are indications that the water content of the structural layers and the resulting increase in deflection are linked to geometry deterioration, particularly in thinner structures. However, the study found that the moisture index determined with the help of a ground penetrating radar sometimes showed high water contents even when sampling indicated that the sub-ballast material was dry and contained little fines. (Sauni et al., 2020)

There was no indication based on the measurements conducted at the Rantarata drainage sites and the supplementary measurement data from the frost monitoring stations that there is a connection between the water content of the sub-ballast and displacements. This means that higher displacement rates were not occurring during the autumn rainy periods than during the dry summer months, for example. While this observation was surprising from the perspective of the initial presumptions, this study also provides grounds for it. In the Finnish rail network, only few rail sections experience high volumes of traffic. For example, the traffic volume at the Rantarata drainage monitoring sites is only approx. 3 MGT/year, and the traffic volumes are also low for the most part at the frost monitoring stations, with a few exceptions (the traffic volumes are presented in Table 3.5). Thus, the amount of significant loading cycles is low. The study also obtained train load data on some of the rail sections, based on which a large proportion of the traffic comprises lightweight passenger traffic, and even the axle loads of freight trains are rarely close to the maximum axle load permitted for the rail section. Therefore, based on the cyclic triaxial tests described in Chapter 3.2.5, the axle loads to which the railway tracks are subjected are so low that there would have to be an unusually large number of repetitions for measurable displacements to occur. This phenomenon is also partly linked to the thick substructures and intermediate layer used in Finland. The additional sand blanketing located below the ballast layer corresponding to intermediate layer in Finnish track structures has also been found to improve track geometry stability elsewhere around the world (Duong et al., 2014; Hasnayn et al., 2020). Additionally, old rail sections in Finland usually contain a significant number of sandy layers below the ballast layer, above the subgrade.

The measurements indicated that subgrade settlement and thaw softening contributed the most to displacements. Subgrade stiffness has long been considered one of the key factors in the occurrence of displacements, but the thickness of the

substructure has also been found to play an important role in the stiffness of the entire railway track (Shahu et al., 1999). This observation supports the measured displacement behaviour. If subgrade settlement and thaw softening are not taken into account, the majority of the studied sites functioned very well, and the displacements were small. This is a surprising finding, as e.g. the frost monitoring stations were originally usually placed at rail sections found to function particularly poorly. The study also examined Finnish track inspection data collected near the monitored sites, which indicated that problems usually occur at various transition zones. This phenomenon has been observed around the world, also on high-speed lines where the condition of the railway track deteriorates particularly either at stiff sections, such as culverts, or various transition zones of embankments and bridges (López-Pita et al., 2007).

The observations presented by Trinh et al. (2012) are highly illustrative with regard to the study of displacements and track drainage in France. Poor track drainage was also previously considered to be a cause of track deformations in France, which is why its role was emphasised in the modernisation of railway tracks. However, it was soon discovered that even old structures could function very well without proper drainage, based on which Trinh et al. ended up presenting a proposal on how material-specific differences in the effect of water content should be taken into account in maintenance and maintenance planning. The same thing appears to have happened in the study featured in this dissertation. A similar conclusion can also be drawn about this dissertation: the significance of drainage is strongly linked to the materials, their water content and the increase in stress caused by the train load.

### 3.4 The effect of water content on frost protection design

The frost problems occurring along the rail network have long been a topical subject in Finland. Most of the rail network was built at the turn of the 19<sup>th</sup> and 20<sup>th</sup> centuries, and very soon after that discourse arose about what should be done about frost problems and how the structures should be repaired (Kallio, 2022). The problems began very soon after construction, and the operating speeds of the rolling stock have increased significantly since then, making the current evenness requirements much more demanding than they were a century ago.

Traditional frost protection design has primarily been based on the principle of preventing frost from penetrating the subgrade. The thickness of the substructure has been determined based on heat transfer by conduction. Recently, crushed rock aggregates have been used increasingly in the structural layers of the railway track, which is why the study by Nurmikolu (2004) related to this topic ended up increasing the thickness of the structural layers by 15% due to the different thermal properties of crushed rock aggregates. However, Johansen (1977) already observed in 1977 that natural convection increased the thermal conductivity of an open-graded rock material of grain size 20/80 mm by up to 2.5 times compared to when heat was only transferred by conduction and radiation. For these reasons, this subject has also been researched in Finland, as the risk of convection is not only theoretical. In Norway in the 1990s, a substructure made of a material that was too coarse and open-graded caused significant frost problems because convection had not been taken into account (Jernbaneverket, 1999). The natural convection of crushed rock aggregates and the effect of water content are studied in Publication V and the main results are presented in this chapter.

For the study, laboratory equipment was built for analysing three different types of crushed rock aggregates. The first aggregate type was a ballast material, while the second was crushed rock with a grain size of 5/16 mm, and the third was crushed rock that met the grading requirements for sub-ballast material. An interesting observation with regard to the drainage study was that adding water to the material led to a very significant increase in the thermal conductivity measured by the testing equipment. The measurement results for the sub-ballast material are presented in Figure 3.24. When dry material was tested with top heating, in which convection does not occur, the thermal conductivity measured was approximately 0.4 W/mK. With bottom heating, in which the warm medium rises up due to differences in density, the thermal conductivity measured was approximately 0.6 W/mK. However, the addition of water changed the situation significantly, increasing thermal conductivity to approximately 1.2 W/mK. A similar phenomenon was also observed in the other materials studied.

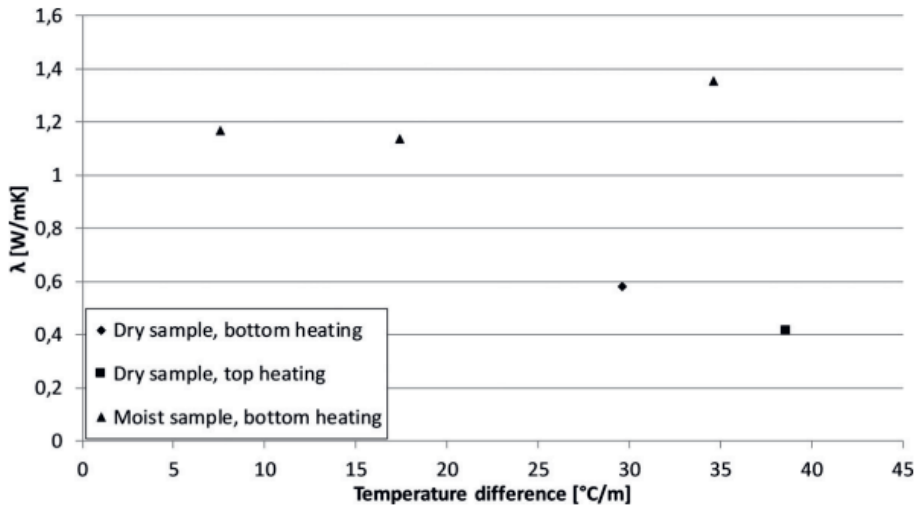


Figure 3.24 Thermal conductivities measured in the sub-ballast material with convection equipment. (Publication V.)

The following key conclusions can be drawn about the convection study:

- An increase in the water content of open-graded crushed rock aggregates can cause a very strong natural convection phenomenon, in which the thermal conductivity of the material increases many times over compared to the initial situation with conductive heat transfer.
- Open-graded crushed rock aggregates are excellent materials in terms of loading resistance, and they are not sensitive to an increase in water content. However, the use of open-grained materials requires the thermal properties to be taken into account to ensure adequate frost protection of layers below crushed rock materials.

### *Discussion about frost-heave and water availability related issues*

From the perspective of railway track drainage and loading resistance, the use of coarse-grained crushed rock aggregates is highly recommendable. They contribute to high loading resistance, even if it is not possible to implement an ideally functioning drainage system at the site. Furthermore, sufficiently coarse crushed rock aggregate does not retain water, which also makes it an ideal material from the perspective of frost. However, there appear to be restrictions related to the use of

these materials, as their heat transfer properties deviate significantly from those of naturally sorted materials. The literature offers several examples of tests on convective heat transfer in materials ((Côté et al., 2011; Farouki, 1981; Goering et al., 2020; Johansen, 1977; Rieksts, 2018; Wang and Ma, 2012), but these tests have typically been carried out using dry air. This study clearly highlighted the properties of the moving medium, as the addition of water significantly increased convective heat transfer. This observation is relevant because water is always present at some amount at the field sites. For example, heat transfer increased by 0.2 W/mK in a crushed rock aggregate with the grain size distribution of the insulation/intermediate layer material in the dry state, whereas the addition of water increased thermal conductivity by 0.8 W/mK from the initial situation. The key conclusion of this chapter is that different perspectives must be considered closely when building structures with materials that differ from those used previously. For example, replacing the sub-ballast materials with crushed rock aggregate at a site where drainage is difficult may be a good solution if the subgrade is not susceptible to frost action, whereas the use of crushed rock aggregate that is too coarse-grained may lead to unexpected frost problems at sites where the subgrade is susceptible to frost action.

# 4 CONCLUSIONS

The objective of the present study was to understand how railway track drainage and water content affect the functioning of old sub-ballast materials, and whether the unevenness problems currently occurring along the rail network could be reduced by improving railway track drainage. After this comprehensive study, there are many new findings regarding the effects of track drainage and water content. This chapter compiles the key conclusions of the study and proposals for further research.

## 4.1 Research outcomes

Railway track drainage has been studied by using several different testing methods. The study also examined several sites. Based on all of the analysis methods presented in this study, the following observations can be listed as answers to the research questions:

### **Research objective 1. Drainage problems and maintenance in Finland**

- There is much room for improvement in railway track drainage in Finland. Many drainage problems are very simple, and drainage conditions can be improved by taking simple measures. Examples of drainage problems include blocked ditches, ditches that were too shallow from the start, and non-functional subsurface drains and site drainage.
- Drainage maintenance has largely been based on visual inspection, and it is recommended that drainage assessment methods that are based on numerical, measurable data, for example, be adopted in the future. One potential method is a regular laser scanning to measure depth of ditches. Many of the drainage problems identified were related to maintenance of the drainage structures.



## **Research objective 2. Water contents present in the track sub-ballast and the effect of drainage improvement**

- The water content of the sub-ballast layer varies considerably by site. In general, the degrees of saturation occurring above the groundwater table or perched groundwater table are less than 70%. Higher water contents above ground water table may occur for a few days when frost thaws.
- At the monitored sites, rain was unable to raise the degree of saturation above the water table beyond 60–70%. The most significant effect on the degree of saturation is caused by fluctuation in the (ground)water table level.
- The drainage improvement carried out at the Km44 site resulted in a significant reduction in the site's water contents, and the periods of high water content caused by seasonal variation were practically eliminated entirely.
- The dynamic cone resistance measured with a dynamic cone penetrometer was found to react to the water contents of materials in a laboratory setting, but water content clearly has a smaller impact on dynamic cone resistance than dry bulk density. In field conditions, the effect of water content could not be observed with a DCP device because skin friction proved to be a significant disturbing factor. Moreover, the drive rods of the lightweight DCP device were easily damaged by the ballast layer.

## **Research objective 3. The effect of water content on the functioning of the track sub-ballast materials**

- The literature review and the laboratory tests conducted in this study indicate that reducing the water content of the sub-ballast layer improves loading resistance and also prevents frost problems. In principle, improving drainage is always recommended when technically and financially possible.
- There are large differences in the loading resistance properties of old sub-ballast materials. Sand materials with a small mean grain size and/or high fines content in particular are sensitive to high water contents. Based on the laboratory tests, problems are likely to start occurring if the water content is high (above 70–80 % in terms of saturation degree) at the height of the intermediate layer and if the rolling stock comprises heavy freight traffic with an axle load of 225/250 kN.
- If the total traffic volume on the railway is low and the axle load used is not particularly heavy (e.g. passenger traffic), insulation and intermediate layer

materials slightly outside of the design range can withstand the loading conditions well, even if the drainage is not in working order.

- The water content of the sub-ballast layer also has an effect on frost protection design. The crushed rock aggregates often used today can be susceptible to convective heat transfer if they are too coarse-grained. Crushed rock aggregate for the insulation and intermediate layers that meets the guidelines valid at the time of the study may be susceptible to convective heat transfer, particularly if the material is subject to sorting during construction.

#### **Research objective 4. Deformation properties identified based on field measurements and laboratory tests**

- Based on the measurement data from the field sites along the Rantarata track and the frost monitoring stations, no loading resistance problems related to high water content occurred at the sites. No connection was found between the vertical displacements measured and the water content of the sub-ballast layer. With regard to the measurement data from the frost monitoring stations, it was found that vertical geometry is particularly weakened by frost heave, which causes permanent settlement during the thaw period.
- At sites where severe geometry stability problems occur, the problems are often caused by something other than the functioning of the sub-ballast materials. The desired outcome most likely cannot be achieved with drainage improvement alone at these types of sites.

## **4.2 Suggestions for drainage improvement design**

Based on the results obtained in this study, keeping the water content of the sub-ballast layer at a low level almost always improves the layer's ability to withstand cyclic or static loading. With regard to guidelines, it is therefore reasonable to claim that drainage must generally extend to the bottom surface of the sub-ballast layer and also cover a reasonable safety distance. At rock cut sites where the structures are usually thinner, all of the structural layers must always be drained. However, there are sites along the rail network where this goal cannot be met for either financial or technical reasons, in which case a reduced drainage depth can be applied at traffic sites of the low requirement level. The new proposal for track drainage dimensioning

presented in Figure 4.1 has been drawn up based on this study. It describes various drainage situations according to the traffic requirement level and establishes minimum drainage depth requirements for different types of structures. The guidelines also take account of the quality of the sub-ballast material. The guidelines are grounded in the laboratory testing and field measurements carried out in this study, based on which the study found no deterioration of the loading resistance of the structures that would be attributable to water content and manifest as vertical displacements.

**PRINCIPLE: Drainage is extended to the bottom surface of the structures + 100 mm or, in a rock cut, all structural layers are ALWAYS drained when possible / financially sensible. If this is not possible, a reduced drainage depth is used according to the table below.**

| Type of structure   | Embankment / earth cut   | Rock cut  | Embankment / earth cut   | Rock cut                     |
|---|--|---|--|------------------------------|
| <b>Traffic with a low requirement level</b><br>Distinctive characteristics: <ul style="list-style-type: none"> <li>• Maximum speed 160 km/h</li> <li>• Low traffic volume (&lt;3 MGT/year) or typical axle load less than 200 kN</li> <li>• Side tracks</li> <li>• No recurring discontinuity points</li> </ul>   | Minimum drainage depth <b>-1.0 m from the track elevation line</b> | Minimum drainage depth <b>-1.0 m from the track elevation line</b> (or all structural layers if the structure is thinner) | Minimum drainage depth <b>-1.0 m from the track elevation line</b> | <b>All structural layers</b> |
| <b>Traffic with a high requirement level</b><br>Distinctive characteristics: <ul style="list-style-type: none"> <li>• Speed &gt;160 km/h</li> <li>• Axle load 250 kN</li> <li>• High volume of 225 kN freight traffic</li> <li>• High traffic volume (&gt;3 MGT/year)</li> <li>• Critical main tracks</li> </ul>  | Minimum drainage depth <b>-1.4 m from the track elevation line</b> | Minimum drainage depth <b>-1.4 m from the track elevation line</b>  | Minimum drainage depth <b>-1.4 m from the track elevation line</b> | <b>All structural layers</b> |
| <b>High-quality sub-ballast material</b><br>Distinctive characteristics (all must apply): <ul style="list-style-type: none"> <li>• Grain size of d60 &gt;0.7 mm</li> <li>• Grain size of d10 &gt;0.1 mm</li> <li>• Meets the Infraray grading requirements</li> </ul>   | Minimum drainage depth <b>-1.2 m from the track elevation line</b> | <b>All structural layers</b>  | <b>The normal drainage depth is used</b>                           |                              |
| <b>Poor-quality sub-ballast material</b><br>Distinctive characteristics (one or more apply): <ul style="list-style-type: none"> <li>• Amount of &lt;0.063 mm particles &gt; 5%</li> <li>• Grain size of d60 &lt;0.7 mm</li> <li>• Grain size of d10 &lt;0.1 mm</li> <li>• Does not meet the Infraray grading requirements</li> <li>• The curve does not match Infraray design curves</li> <li>• Classified as susceptible to frost heave</li> </ul> | <b>All structural layers</b>                                       | <b>All structural layers</b>  | <b>The normal drainage depth is used</b>                           |                              |

Figure 4.1. Determination of drainage depth according to the conditions.

## 4.3 Suggestions for further research

This study examined drainage problems along the Finnish rail network, the state of maintenance, the properties of actual sub-ballast materials, and observations made at field sites. The majority of the field site observations were based on three monitored sites along the Rantarata track, but confirmation for the findings was also sought from measurement data produced by frost monitoring stations. However, even all successful studies always highlight the need for further research, and the present study identified at least the following needs for further research:

- The majority of the monitoring measurements at the test sites were carried out along the Rantarata track, which is primarily used for passenger traffic and which has an annual traffic volume of only approximately three million gross tonnes. It would be useful to conduct a similar study on rail sections operated by heavy freight trains (>225 kN), where the annual volume of traffic is also higher.
- This study primarily used triaxial tests to examine the change in strength caused by the water content of materials. In these tests, the loading was axisymmetric in the vertical direction. It would be interesting to study the effects of the rotation of principal stress directions caused by actual train traffic, as well as the correlation of the results of such a study with cyclic triaxial tests.
- Setting up a long-term monitoring station for generating high-quality data on heavy rail traffic in order to study the effects of rolling stock properties on the functioning of the railway track. This monitoring station can also produce reliable data on the stresses in the different structural layers of the track and the deformations that occur in them.
- The effect of discontinuity points along the track and of the dynamic loading occurring in them on track geometry deterioration.

# REFERENCES

- Abuel-Naga, H.M., Holtrigter, M., Pender, M.J., 2011. Simple method for correcting dynamic cone penetration test results for rod friction. *Géotechnique Lett.* 1, 37–40.
- Airaksinen, J.U., 1978. *Maa- ja pohjavesihydrologia*. Pohjoinen, Oulu.
- Altun, S., Göktepe, A.B., Akgüner, C., 2005. Cyclic shear strength of silts and sands under cyclic loading, in: *Earthquake Engineering and Soil Dynamics*. pp. 1–11.
- Azam, A.M., Cameron, D.A., Rahman, M.M., 2013. Model for prediction of resilient modulus incorporating matric suction for recycled unbound granular materials. *Can. Geotech. J.* 50, 1143–1158. <https://doi.org/10.1139/cgj-2012-0406>
- Baker, C.J., Chapman, L., Quinn, A., Dobney, K., 2010. Climate change and the railway industry: a review. *Proc. Inst. Mech. Eng. Part C J. Mech. Eng. Sci.* 224, 519–528.
- Bear, J., 1972. *Dynamics of fluids in porous media*. Elsevier, New York.
- Bear, J., Braester, C., 1972. On the flow of two immiscible fluids in fractured porous media, in: *Developments in Soil Science*. Elsevier, pp. 177–202.
- Bilodeau, J.-P., Doré, G., 2012. Water sensitivity of resilient modulus of compacted unbound granular materials used as pavement base. *Int. J. Pavement Eng.* 13, 459–471.
- Bláhová, K., Ševelová, L., Pilařová, P., 2013. Influence of water content on the shear strength parameters of clayey soil in relation to stability analysis of a hillside in Brno region. *Acta Univ. Agric. Silvic. Mendel. Brun.* 61, 1583–1588.
- Bolton, M.D., Gui, M.-W., Garnier, J., Corte, J.F., Bagge, G., Laue, J., Renzi, R., 1999. Centrifuge cone penetration tests in sand. *Géotechnique* 49, 543–552.

- Byun, Y.-H., Kim, D.-J., 2020. In-situ modulus detector for subgrade characterization. *Int. J. Pavement Eng.* 1–11. <https://doi.org/10.1080/10298436.2020.1743291>
- Cai, J.Q., Liu, S.X., Fu, L., Feng, Y.Q., 2016. Detection of railway subgrade moisture content by GPR, in: 2016 16th International Conference on Ground Penetrating Radar (GPR). Presented at the 2016 16th International Conference on Ground Penetrating Radar (GPR), pp. 1–5. <https://doi.org/10.1109/ICGPR.2016.7572613>
- Chaigneau, L., Gourves, R., Boissier, D., 2000. Compaction control with a dynamic cone penetrometer, in: *Proc. of International Workshop on Compaction of Soils, Granulates and Powders*, Innsbruck. pp. 103–109.
- Côté, J., Fillion, M.-H., Konrad, J.-M., 2011. Intrinsic permeability of materials ranging from sand to rock-fill using natural air convection tests. *Can. Geotech. J.* 48, 679–690.
- Daintith, J. (Ed.), 2009. *A dictionary of physics*, 6th ed. ed. Oxford University Press, Oxford ; New York.
- Dawson, A., Kolisoja, P., 2005. Permanent deformation. Report on task 2.1. Roadex II North. Periphery.
- Drumm, E.C., Reeves, J.S., Madgett, M.R., Trolinger, W.D., 1997. Subgrade Resilient Modulus Correction for Saturation Effects. *J. Geotech. Geoenvironmental Eng.* 123, 663–670. [https://doi.org/10.1061/\(ASCE\)1090-0241\(1997\)123:7\(663\)](https://doi.org/10.1061/(ASCE)1090-0241(1997)123:7(663))
- Duong, T.V., Cui, Y.-J., Tang, A.M., Dupla, J.-C., Canou, J., Calon, N., Robinet, A., 2014. Investigating the mud pumping and interlayer creation phenomena in railway sub-structure. *Eng. Geol.* 171, 45–58. <https://doi.org/10.1016/j.enggeo.2013.12.016>
- Duong, T.V., Tang, A.M., Cui, Y.-J., Trinh, V.N., Dupla, J.-C., Calon, N., Canou, J., Robinet, A., 2013. Effects of fines and water contents on the mechanical behavior of interlayer soil in ancient railway sub-structure. *Soils Found.* 53, 868–878. <https://doi.org/10.1016/j.sandf.2013.10.006>
- Escobar, E., Navarrete, M.B., Gourvès, R., Haddani, Y., Breul, P., Chevalier, B., 2016. Dynamic characterization of the supporting layers in railway tracks using the dynamic penetrometer Panda 3®. *Procedia Eng.* 143, 1024–1033.

- Esveld, C., 2001. Modern railway track. MRT-productions Zaltbommel.
- Farouki, O.T., 1981. Thermal properties of soils. Cold Regions Research and Engineering Lab Hanover NH.
- Ferreira, T.M., Teixeira, P.F., 2011. Impact of different drainage solutions in the behavior of railway trackbed layers due to atmospheric actions. 9th World Congr Railw Reserach-May 22 26, 1–14.
- Finnish Rail Administration, 2009. Vuosikertomus 2009 (in English: The Annual Report of 2009), Publications of FRA. Finnish Rail Administration.
- Finnish Rail Administration, 2002. Ramo 15: Radan kunnossapito (in English: Track Maintenance).
- Finnish Transport Infrastructure Agency, 2018. Ratatekniset ohjeet (RATO) osa 3 Radan rakenne (in English: Track building guidelines, part 3, Track structure). Liikennevirasto.
- Finnish Transport Infrastructure Agency, 1999. Rautatien maanrakennustöiden yleinen työselitys ja laatuvaatimukset (RMYTL) osa 4 Kuivatus-työt, D3.
- Fredlund, D.G., Morgenstern, N.R., Widger, R.A., 1978. The shear strength of unsaturated soils. *Can. Geotech. J.* 15, 313–321.
- Fredlund, D.G., Rahardjo, H., 1993. Soil mechanics for unsaturated soils. John Wiley & Sons.
- Fredlund, D.G., Xing, A., Fredlund, M.D., Barbour, S.L., 1996. The relationship of the unsaturated soil shear strength to the soil-water characteristic curve. *Can. Geotech. J.* 33, 440–448.
- Gan, J.K.M., Fredlund, D.G., Rahardjo, H., 1988. Determination of the shear strength parameters of an unsaturated soil using the direct shear test. *Can. Geotech. J.* 25, 500–510.
- Ghataora, G.S., Rushton, K., 2012. Movement of Water through Ballast and Subballast for Dual-Line Railway Track. *Transp. Res. Rec.* 2289, 78–86. <https://doi.org/10.3141/2289-11>



- Goering, D.J., Instanes, A., Knudsen, S., 2020. Convective heat transfer in railway embankment ballast, in: *Ground Freezing 2000-Frost Action in Soils*. CRC Press, pp. 31–36.
- Graybeal, B.A., Phares, B.M., Rolander, D.D., Moore, M., Washer, G., 2002. Visual inspection of highway bridges. *J. Nondestruct. Eval.* 21, 67–83.
- Guthrie, W.S., Hermansson, Å., 2003. Frost Heave and Water Uptake Relations in Variably Saturated Aggregate Base Materials. *Transp. Res. Rec. J. Transp. Res. Board* 1821, 13–19. <https://doi.org/10.3141/1821-02>
- Haddani, Y., Breul, P., Saussine, G., Navarrete, M.A.B., Ranvier, F., Gourvès, R., 2016. Trackbed mechanical and physical characterization using PANDA®/geoendoscopy coupling. *Procedia Eng.* 143, 1201–1209.
- Hasnayan, M. m., Medero, G. m., Woodward, P. k., 2015. Railway track performance during and post flooding, in: *Geotechnical Engineering for Infrastructure and Development, Conference Proceedings*. ICE Publishing, pp. 379–384. <https://doi.org/10.1680/ecsmge.60678.vol2.037>
- Hasnayan, M.M., McCarter, W.J., Woodward, P.K., Connolly, D.P., 2020. Railway subgrade performance after repeated flooding – Large-scale laboratory testing. *Transp. Geotech.* 23, 100329. <https://doi.org/10.1016/j.trgeo.2020.100329>
- Hermansson, Å., Spencer Guthrie, W., 2005. Frost heave and water uptake rates in silty soil subject to variable water table height during freezing. *Cold Reg. Sci. Technol.* 43, 128–139. <https://doi.org/10.1016/j.coldregions.2005.03.003>
- Hillel, D., 1971. *Soil and water: physical principles and processes*. Academic Press, New York.
- Hudson, A., Watson, G., Le Pen, L., Powrie, W., 2016. Remediation of mud pumping on a ballasted railway track. *Procedia Eng.* 143, 1043–1050.
- Isohaka, M., 2014. *Veden saatavilla olon vaikutus radan routimiseen* (Master's Thesis). Tampere University of Technology, Tampere.
- Jernbaneverket, 1999. *Laerebok i jernbaneteknikk, L521, Kapittel vol 6, Frost*.

- Jia, N., Tassin, B., Calon, N., Deneele, D., Koscielny, M., Prévot, F., 2016. Scaling in railway infrastructural drainage devices: site study. *Innov. Infrastruct. Solut.* 1, 42. <https://doi.org/10.1007/s41062-016-0042-7>
- Johansen, O., 1977. Thermal conductivity of soils. Cold Regions Research and Engineering Lab Hanover NH.
- Kalliainen, A., Kolisoja, P., Nurmikolu, A., 2016. 3D finite element model as a tool for analyzing the structural behavior of a railway track. *Procedia Eng.* 143, 820–827.
- Kallio, K., 2022. Ratajätkätkät: Rautatienrakentajien kokemukset 1857–1939. SKS Kirjat, Helsinki.
- Khoury, N.N., Zaman, M.M., 2004. Correlation between resilient modulus, moisture variation, and soil suction for subgrade soils. *Transp. Res. Rec.* 1874, 99–107.
- Kirkham, D., Powers, W.L., 1972. *Advanced soil physics*. Wiley, New York.
- Kolisoja, P., 1997. Resilient deformation characteristics of granular materials. Tampere University of Technology Finland, Publications.
- Kolisoja, P., Järvenpää, I., Mäkelä, E., Levomäki, M., 2000. Ratarakenteen instrumentointi ja mallinnus, 250 kN: n ja 300 kN: n akselipainot (in English: Instrumentation and modelling of Track Structure, 250 kN and 300 kN axle loads). Finnish Rail Administration.
- Kolisoja, P., Saarenketo, T., Peltoniemi, H., Vuorimies, N., 2002. Laboratory Testing of Suction and Deformation Properties of Base Course Aggregates. *Transp. Res. Rec.* 1787, 83–89. <https://doi.org/10.3141/1787-09>
- Korkka-Niemi, K., Salonen, V.-P., 1996. *Maanalaiset vedet: pohjavesigeologian perusteet*. Turun yliopisto.
- Kovacevic, M.S., Gavin, K., Oslakovic, I.S., Bacic, M., 2016. A new methodology for assessment of railway infrastructure condition. *Transp. Res. Procedia* 14, 1930–1939.
- Latvala, J., 2023a. Ratarakenteen vesipitoisuuden vaikutus pysyvien siirtymien muodostumiseen 50/2023 (in English: Effect of the track structure's water

- content on the formation of permanent displacements), Publications of FTIA. Finnish Transport Infrastructure Agency, Helsinki.
- Latvala, J., 2023b. Rantaradan kuivatuksen parannuskohteiden seurantamittaukset 66/2023 (in English: Follow-up measurements of Rantarata drainage improvement sites), Publications of FTIA. Finnish Transport Infrastructure Agency.
- Latvala, J., 2021. Kuivatusratkaisujen toimivuuden ja vaikutusten arviointi 8/2021 (in English: The functionality and effects of drainage solutions), Publications of FTIA. Finnish Transport Infrastructure Agency, Helsinki.
- Latvala, J., 2018. Radan kuivatuksen toimivuuden arviointi ja parantaminen olemassa olevilla radoilla 50/2018 (in English: Cost efficiency of drainage improvements on existing railway tracks), Publications of FTA. Finnish Transport Agency, Helsinki.
- Latvala, J., Kolisoja, P., Luomala, H., 2023. Water content variation of railway track sub-ballast layer in seasonal frost area: A case study from Finland. *Transp. Geotech.* 38, 100926. <https://doi.org/10.1016/j.trgeo.2022.100926>
- Latvala, J., Kolisoja, P., Luomala, H., 2022. The cyclic loading resistance of old railway track sub-ballast materials at different water contents. *Transp. Geotech.* 35, 100772. <https://doi.org/10.1016/j.trgeo.2022.100772>
- Latvala, J., Luomala, H., Kolisoja, P., 2020a. Determining Soil Moisture Content and Material Properties with Dynamic Cone Penetrometer. *Balt. J. Road Bridge Eng.* 15, 136–159.
- Latvala, J., Luomala, H., Kolisoja, P., Nurmikolu, A., 2020b. Convective heat transfer in crushed rock aggregates: the effects of grain size distribution and moisture content. *J. Cold Reg. Eng.* 34, 04020012.
- Latvala, J., Nurmikolu, A., Luomala, H., 2016. Problems with railway track drainage in Finland. *Procedia Eng.* 143, 1051–1058.
- Leal-Vaca, J.C., Gallegos-Fonseca, G., Rojas-González, E., 2012. The decrease of the strength of unsaturated silty sand. *Ing. Investig. Tecnol.* 13, 393–402.
- Lee, K.L., Fitton, J.A., 1969. Factors affecting the cyclic loading strength of soil, in: *Vibration Effects of Earthquakes on Soils and Foundations*. ASTM International.

- Lehtonen, I., 2011. Äärisademäärien muutokset Euroopassa maailmanlaajuisten ilmastomallien perusteella (Master's Thesis). University of Helsinki.
- Li, D., Hyslip, J., Sussmann, T., Chrismer, S., 2015. Railway geotechnics. CRC Press.
- Li, D., Selig, E.T., 1995. Evaluation of railway subgrade problems. *Transp. Res. Rec.* 1489, 17.
- Lindgren, J., Jonsson, D., Carlsson Kanyama, A., 2009. Climate Adaptation of Railways: Lessons from Sweden. *Eur. J. Transp. Infrastruct. Res.* 9. <https://doi.org/10.18757/ejtir.2009.9.2.3295>
- Livneh, M., 2000. Friction correction equation for the dynamic cone penetrometer in subsoil strength testing. *Transp. Res. Rec.* 1714, 89–97.
- López-Pita, A., Teixeira, P.F., Casas, C., Ubalde, L., Robusté, F., 2007. Evolution of track geometric quality in high-speed lines: ten years experience of the Madrid-Seville line. *Proc. Inst. Mech. Eng. Part F J. Rail Rapid Transit* 221, 147–155.
- Malassu, E., 2016. Esiselvitys radan kuormituskestävyyssmitoituksen kehittämisestä (Master's Thesis). Tampere University of Technology, Tampere.
- Mamou, A., 2013. Effects of principal stress rotation and drainage on the resilient stiffness of railway foundations (PhD Thesis). University of Southampton.
- McGaw, R., 1972. Frost heaving versus depth to water table. *Highw. Res. Rec.*
- Melo, A.L.O.D., Kaewunruen, S., Papaalias, M., Bernucci, L.L., Motta, R., 2020. Methods to Monitor and Evaluate the Deterioration of Track and its Components in a Railway in-Service: A Systemic Review. *Front. Built Environ.* 6, 118.
- Metsovuori, L., 2013. Sulamispainuminen radan epätasaisuuden aiheuttajana (Master's Thesis). Tampere University of Technology, Tampere.
- Mikolajczak, K., Kuczyńska, A., Krajewski, P., Sawikowska, A., Surma, M., Ogrodowicz, P., Adamski, T., Krystkowiak, K., Górny, A., Kempa, M., Szarejko, I., Guzy-Wrobelska, J., Gudyś, K., 2016. Quantitative trait loci for plant height in Maresi × CamB barley population and their associations with yield-related traits under different water regimes. *J. Appl. Genet.* 58. <https://doi.org/10.1007/s13353-016-0358-1>

- Miyazaki, T., 2005. *Water flow in soils*. Boca Raton : Taylor & Francis.
- Moore, M., Phares, B.M., Graybeal, B., Rolander, D., Washer, G., Wiss, J., 2001. Reliability of visual inspection for highway bridges, volume I. Turner-Fairbank Highway Research Center.
- Morvan, M., Breul, P., 2016. Optimisation of in-situ dry density estimation, in: E3S Web of Conferences. EDP Sciences, p. 09002.
- Nguyen, T.T., Indraratna, B., 2022. Rail track degradation under mud pumping evaluated through site and laboratory investigations. *Int. J. Rail Transp.* 10, 44–71. <https://doi.org/10.1080/23248378.2021.1878947>
- Nixon, J.F., 1982. Field frost heave predictions using the segregation potential concept. *Can. Geotech. J.* 19, 526–529.
- Nurmikolu, A., 2004. Murskatun kalliokiviaineksen hienoneminen ja routivuus radan rakennekerroksissa: kirjallisuusselvitys [Degradation and frost susceptibility of the crushed rock aggregate in track structure, literature review]. Publications of the Finnish Rail Administration A4/2004.
- Nurmikolu, A., Kolisoja, P., 2002. Ratarakenteen routasuojaus (in English: Frost Protection of the Track Structure). Publications of the Finnish Rail Administration, Helsinki.
- Paiva, C., Ferreira, M., Ferreira, A., 2015. Ballast drainage in Brazilian railway infrastructures. *Constr. Build. Mater., Railway Engineering-2013* 92, 58–63. <https://doi.org/10.1016/j.conbuildmat.2014.06.006>
- Pelho, A., Luomala, H., Huhtala, T., Takala, M., 2022. The effect of fibre-reinforced foamed urethane sleepers and under sleeper pads on low-frequency vibration caused by freight traffic on soft soil areas, in: *The Effect of Fibre-Reinforced Foamed Urethane Sleepers and under Sleeper Pads on Low-Frequency Vibration Caused by Freight Traffic on Soft Soil Areas*. Presented at the World Congress of Railway Research, Birmingham UK.
- Peltomäki, M., 2021. Radan alusrakenteen ja pohjamaan kuormituskestävyyssmitoituksen kehittäminen: Laskennallinen lähestymistapa (in English: Development of railway track substructure and subsoil bearing capacity design methods). Publications of FTTA, Helsinki.

- Peltomäki, M., 2020. Ratarakenteen kuormituskäyttäytymisen mallintaminen (in English: Modeling the loading behavior of railway structure) (Master's Thesis). Tampere University, Finland.
- Powrie, W., Yang, L.A., Clayton, C.R., 2007. Stress changes in the ground below ballasted railway track during train passage. Proc. Inst. Mech. Eng. Part F J. Rail Rapid Transit 221, 247–262.
- Pylkkänen, K., Nurmikolu, A., 2015. Routa ja routiminen ratarakenteessa (in English: Freezing and seasonal frost action of railway track). Research reports of the Finnish Transport Agency.
- Rantamäki, M., Jääskeläinen, R., Tammirinne, M., 1979. Geotekniikka. 20. painos. Hels. Otatieto.
- Rétháti, L., 1983. Groundwater in civil engineering. Elsevier, Amsterdam.
- Rieksts, K., 2018. Heat Transfer Characteristics of Crushed Rock and Lightweight Aggregate Materials (Doctoral thesis). NTNU.
- Ruosteenoja, K., Jylhä, K., Kämäräinen, M., 2016. Climate projections for Finland under the RCP forcing scenarios. Geophysica 51.
- Sauni, M., 2023. Application of Track Geometry Deterioration Modelling and Data Mining in Railway Asset Management. Tampere University.
- Sauni, M., Luomala, H., Kolisoja, P., Turunen, E., 2020. Determining sampling points using railway track structure data analysis, in: Information Technology in Geo-Engineering: Proceedings of the 3rd International Conference (ICITG), Guimarães, Portugal 3. Springer, pp. 841–856.
- Saxena, S.C., Arora, S.P., 2004. A text book of railway engineering. Eng. Stud. 7th Ed. Dhanpat Rai Publ. P Ltd New Delhi.
- See, J.E., 2012. Visual inspection: a review of the literature. Sandia National Laboratories (SNL), Albuquerque, NM, and Livermore, CA ....
- SFS-ISO 17892-9:2018 Geotechnical Investigation and Testing. Laboratory Testing of Soil. Part 9: Consolidated Triaxial Compression Tests on Water Saturated Soils, 2018.

- Shahu, J.T., Rao, N.K., Yudhbir, 1999. Parametric study of resilient response of tracks with a sub-ballast layer. *Can. Geotech. J.* 36, 1137–1150.
- Soliman, H., Shalaby, A., 2015. Permanent deformation behavior of unbound granular base materials with varying moisture and fines content. *Transp. Geotech.* 4, 1–12.
- Spagnoli, G., 2007. An empirical correlation between different dynamic penetrometers. *Electron. J. Geotech. Eng.* 12.
- Steenbergen, M., Jong, E.D., Zoeteman, A., 2015. Dynamic axle loads as a main source of railway track degradation, in: *Geotechnical Safety and Risk V*. IOS Press, pp. 243–249.
- Suiker, A.S., Selig, E.T., Frenkel, R., 2005. Static and cyclic triaxial testing of ballast and subballast. *J. Geotech. Geoenvironmental Eng.* 131, 771–782.
- Thevakumar, K., Indraratna, B., Ferreira, F.B., Carter, J., Rujikiatkamjorn, C., 2021. The influence of cyclic loading on the response of soft subgrade soil in relation to heavy haul railways. *Transp. Geotech.* 100571.
- Theyse, H.L., Legge, F.T.H., Pretorius, P.C., Wolff, H., 2007. A Yield Strength Model for Partially Saturated Unbound Granular Material. *Road Mater. Pavement Des.* 8, 423–448.  
<https://doi.org/10.1080/14680629.2007.9690082>
- Tocci, M.D., Kelley, C.T., Miller, C.T., 1997. Accurate and economical solution of the pressure-head form of Richards' equation by the method of lines. *Adv. Water Resour.* 20, 1–14.
- Trask, P.D., 1959. Effect of grain size on strength of mixtures of clay, sand, and water. *Geol. Soc. Am. Bull.* 70, 569–580.
- Trenberth, K.E., 2011. Changes in precipitation with climate change. *Clim. Res.* 47, 123–138.
- Trinh, V.N., Tang, A.M., Cui, Y.-J., Dupla, J.-C., Canou, J., Calon, N., Lambert, L., Robinet, A., Schoen, O., 2012. Mechanical characterisation of the fouled ballast in ancient railway track substructure by large-scale triaxial tests. *Soils Found.* 52, 511–523. <https://doi.org/10.1016/j.sandf.2012.05.009>

- Tuller, M., Or, D., 2003. Hydraulic functions for swelling soils: pore scale considerations. *J. Hydrol.* 272, 50–71.
- Usman, K., Ghataora, G., Burrow, M., Eskandari Torbaghan, M., Wehbi, mohamed, Musgrave, P., 2017. Fault tree for poor drainage mechanisms of railway ballasted track: *Railway Engineering* 2017.
- Vanapalli, S.K., Fredlund, D.G., Pufahl, D.E., Clifton, A.W., 1996. Model for the prediction of shear strength with respect to soil suction. *Can. Geotech. J.* 33, 379–392.
- Vanapalli, S.K., Sillers, W.S., Fredlund, M.D., 1998. The meaning and relevance of residual state to unsaturated soils, in: 51st Canadian Geotechnical Conference. Edmonton, pp. 4–7.
- Vuorimies, N., Kolisoja, P., Saarenketo, T., 2004. In-situ Monitoring of Road Pavement and Subgrade at Koskenkylä in Rovaniemi, Finland, in: NGM 2004 XIV Nordic Geotechnical Meeting, May 19th-21st 2004, Swedish Geotechnical Society. Svenska Geotekniska Föreningen, p. s-C.
- Wang, A., Ma, W., 2012. The optimal design principles and method of crushed-rock based embankment in cold regions, in: *Cold Regions Engineering 2012: Sustainable Infrastructure Development in a Changing Cold Environment*. pp. 1–11.
- Wang, H., Silvast, M., Markine, V., Wiljanen, B., 2017. Analysis of the Dynamic Wheel Loads in Railway Transition Zones Considering the Moisture Condition of the Ballast and Subballast. *Appl. Sci.* 7, 1208. <https://doi.org/10.3390/app7121208>
- Wang, J.-J., Zhang, H.-P., Wen, H.-B., Liang, Y., 2015. Shear Strength of an Accumulation Soil from Direct Shear Test. *Mar. Georesources Geotechnol.* 33, 183–190. <https://doi.org/10.1080/1064119X.2013.828821>
- Wichtmann, T., Niemunis, A., Triantafyllidis, T., 2005. Strain accumulation in sand due to cyclic loading: drained triaxial tests. *Soil Dyn. Earthq. Eng.* 25, 967–979.
- Yang, S.-R., Huang, W.-H., Tai, Y.-T., 2005. Variation of resilient modulus with soil suction for compacted subgrade soils. *Transp. Res. Rec.* 1913, 99–106.



- Yoshida, Y., Kuwano, J., Kuwano, R., 1991. Effects of Saturation on Shear Strength of Soils. *Soils Found.* 31, 181–186.  
<https://doi.org/10.3208/sandf1972.31.181>
- Young, H.D., Freedman, R.A., Sandin, T.R., Ford, A.L., 1996. *University physics*. Addison-wesley Reading, MA.
- Youngs, E.G., Rushton, K.R., 2009. Steady-state ditch-drainage of two-layered soil regions overlying an inverted V-shaped impermeable bed with examples of the drainage of ballast beneath railway tracks. *J. Hydrol.* 377, 367–376.  
<https://doi.org/10.1016/j.jhydrol.2009.08.034>



# PUBLICATION

I

Problems with Railway Track Drainage in Finland

Juha Latvala, Antti Nurmikolu and Heikki Luomala

Advances in Transportation Geotechnics 3. The 3<sup>rd</sup> International Conference on  
Transportation Geotechnics (ICTG2016), Vol. 143, 2016, pages 1051-1058  
<https://doi.org/10.1016/j.proeng.2016.06.098>

Publication is licensed under a Creative Commons Attribution 4.0  
International License CC-BY-NC-ND





## Problems with Railway Track Drainage in Finland

Juha Latvala, Antti Nurmikolu and Heikki Luomala  
*Tampere University of Technology, Finland.*

*juha.latvala@tut.fi, antti.nurmikolu@tut.fi, heikki.luomala@tut.fi*

### Abstract

Several studies have shown that water plays a significant role in phenomena that weaken track geometry. For instance, water may cause frost heave, thaw softening, attrition of ballast, and weakening of the load bearing capacity of a track. Functioning drainage can prevent water damage, but no researched data on the magnitude of the impacts exist.

Most of the Finnish rail network has been built in times when earthworks were kept to a minimum. Drainage generally functions well along new and renovated rail sections, but the situation is quite different with old tracks. If unevenness problems can be dealt with adequately by improving drainage, it is considerably more advantageous compared to massive renovation. The aim is to find out whether systematic improvement of drainage can produce significant savings in rail network maintenance.

The study examines the unevenness problems discovered along the Finnish rail network where the functioning of drainage is thought to be a major factor, while seeking solutions to the problems. This article presents the technical and administrative problems related to drainage in the Finnish rail network. Based on observations made so far, even basic drainage solutions are beset with problems since e.g. ditches are not cleaned with sufficient regularity.

The on-going study aimed to determine the impact of drainage on track unevenness at monitored sites. However, the method did not work as expected since no suitable sites, where other significant measures had not been carried out in connection with drainage renovation, could be found along the rail network. Moreover, it was difficult to get information about earlier renovation measures.

It can be said already at this phase of the study that drainage maintenance should be improved. There are also problems with drainage assessment methods which consist mainly of visual inspection instead of more sophisticated methods. Subjective assessment methods and maintenance contracts that call for maintenance 'as required' easily lead to postponement of maintenance measures.

*Keywords:* drainage, drainage monitoring, track maintenance, frost heave, track geometry

# 1 Introduction

In recent years Finnish rail networks have suffered from unevenness problems that have significantly disturbed rail traffic. Frost heave and thaw softening – which lowers the load bearing capacity of the track during thaw periods – are among the phenomena that cause track deformations. For instance, recent studies at TUT have shown that the moisture condition of a railway embankment has a significant impact on track frost heave (Isohaka, 2014: Impact of water availability on frost heave) and can lower load bearing capacity especially during thaw periods due to softening (Metsovuori 2013: Thaw settlement as the cause of track unevenness). Many international studies also verify the role of water in the behaviour of soil materials (e.g. McGaw 1972; Guthrie & Zhan 2002; Guthrie & Hermansson 2003; Selig & Waters 1994; Hermansson & Guthrie 2005; Otter 2011; Mamou 2013). In connection with the *Frost damaged tracks renovation project (ROPE)* of the Finnish Transport Agency, inadequate drainage was almost always found to contribute to frost heave to some extent.

The assessment/quantification of the benefits of more effective drainage has, however, proved challenging. For instance, it is difficult to devise assessment and classification methods for the functioning of drainage, and to determine the magnitude of the change in the moisture condition attainable by more effective drainage and the advantageousness of different renovation alternatives. The overall aim of the on-going ‘Technical and economic efficiency of improved drainage of existing rail lines’ study at Tampere University of Technology is to provide a reasoned assessment of the impacts improved drainage can have, and the conditions under which it is technically and economically justifiable to repair track unevennesses by improving drainage. The study began in autumn 2014 by an examination of the present state of drainage, and it will continue until the summer of 2016. The study was commissioned by the Finnish Transport Agency which also finances it. The results and methods presented in this paper are an interim report on the state of the research project.

Monitored sites are used to examine the impact of different drainage solutions and the most common drainage-related problems along the rail network. The functioning of track maintenance is examined from the administrative and technical viewpoints. The situation in track maintenance has been examined e.g. by interviewing railway track managers/maintainers. The data produced by the *Frost damaged tracks renovation project (ROPE)* of the Finnish Transport Agency were also utilised. Computational modelling was also used in an effort to model a track structure drainage system. Its aim was to reveal the impact of different drainage solutions on the moisture condition of the railway embankment.

## 2 Impact of Water on Behaviour of Track Structures

Natural materials always contain water. The amount of water influences significantly the behaviour of materials and thereby the functioning and durability of an entire earth structure. The impacts of water can be divided into deformations due to frost heave and phenomena related to deformation of unfrozen soil.

Guthrie & Hermansson (2003) examined the impact of water on frost heave by laboratory tests. Their results indicated that the water required for frost heave to occur originated mainly from an external source. However, in some instances the water contained in a material may become redistributed as it freezes so that actual frost heave may occur within the material without extra external water. The water content of the sample also plays a role. Guthrie & Hermansson continued their study in 2005 as they looked more closely at the impact of the distance to the water surface on frost heave. It involved testing frost heave in a silty sample using different water levels from 300 mm to 150 mm measured from the bottom of the sample. Lowering of the water level by 150 mm decreased frost heave by 24.1% which is a significant result. Naturally, without extra water the

difference was even greater. Based on the results, they also concluded that improved drainage can reduce frost heave considerably in embankment structures. Corresponding results have also been received earlier e.g. by McGaw (1972) who tested the impact of the distance to water surface on frost heave in several materials.

The matter has been examined in Finland e.g. by Isohaka (2014) in his study *Impact of availability of water on frost heave*. He used frost heave tests and field data to provide a comprehensive explanation of the impact of extra water on frost heave. The frost heave test results showed the significance of the distance between the frost limit and the water level for frost heave in a material. On the other hand, in the case of materials highly susceptible to frost heave, their moisture content could also cause detrimental frost heave. Thus, the results were very similar to those of Guthrie & Hermansson.

The thawing of a frozen structure in spring also increases the risk of unevenness problems. As thawing begins, the deeper structural layers are still frozen which prevents water from flowing down from the upper layers which may result in oversaturated soil (Guthrie & Zhan, 2002). That naturally lowers the bearing capacity of the structure. Metsovuori (2013) has investigated the matter as it relates to the Finnish rail network. His study also indicated that reduced stiffness due to extra moisture causes permanent deformations.

Water content does not have an impact only on things related to the freezing of soil. Surplus water in a structure may cause "mud pumping" which weakens it and leads to attrition of ballast (Selig & Waters, 1994; Nurmikolu, 2005). Clay pumping in subsoil is not a common problem in Finland because of thick structure layers. Water also affects the behaviour of the materials of a structure – which is a quite extensive and complex subject area. In any case, it can be said that moisture content affects e.g. the suction pressures occurring in the unsaturated zone (Otter 2011, Mamou 2013) and friction between soil particles. It is also clear that through these various impact methods water content also affects the shear strength of soil. Based on the literature review by Brecciaroli & Kolisoja (2006), an increase in water content also weakens the durability of a structure against repeated loading.

### 3 Present State of Drainage

The drainage arrangements of new and renovated rail sections are generally in good condition unlike those of old sections. A significant portion of Finnish tracks were built at a time when keeping earthworks to a minimum was important, which is why tracks were often laid on flat ground on top of thin structural layers. The properties of old tracks were sufficient for the speeds and axle loads of their day. Then delays did not block completely the flow of traffic and prevention of permanent deformations was not considered as important as today. The great structural differences are the reason for the various types of drainage-related problems.

The *Frost damaged tracks renovation project (ROPE)* carried out in the last few years by the Finnish Transport Agency has systematically mapped sites where track unevenness problems occur repeatedly (Silvast et al. 2013). The situation at the sites has been examined by modern methods (ground penetrating radar, digital video, laser scanning and track inspection data) and traditional field inspections. In the ROPE project problems at the sites were classified and more attention was paid to the functioning of drainage than earlier. Bold experimentation with lighter renovation alternatives was also experimented with in planning renovations, such as improved drainage, in case drainage at the site was clearly inadequate. This study assesses the site-specific results and related problems revealed by ROPE analyses conducted in two different years. Currently, site-specific reports give the most accurate picture of the problems besetting the Finnish rail network.

It is important to understand that problem sites often suffer from many problems, drainage being one of them. Often it also difficult to estimate how the situation changes if an attempt is made to

remedy a defect. Many of the sites of the ROPE analyses also often suffered from several different problems.

Many problems are related to soil and rock cuts where structural layers are thin and drainage depth is shallow (Fig. 1). Old materials also cause problems since they may include water-retaining layers. At places drainage is missing completely or does not function as planned. The drainage systems of stations also have major shortcomings. Many sites were also located on soft ground where the track sank creating an unevenness problem in the transition zone. Moreover, points of discontinuity, such as culverts and transition wedges of bridges, often caused unevenness problems.

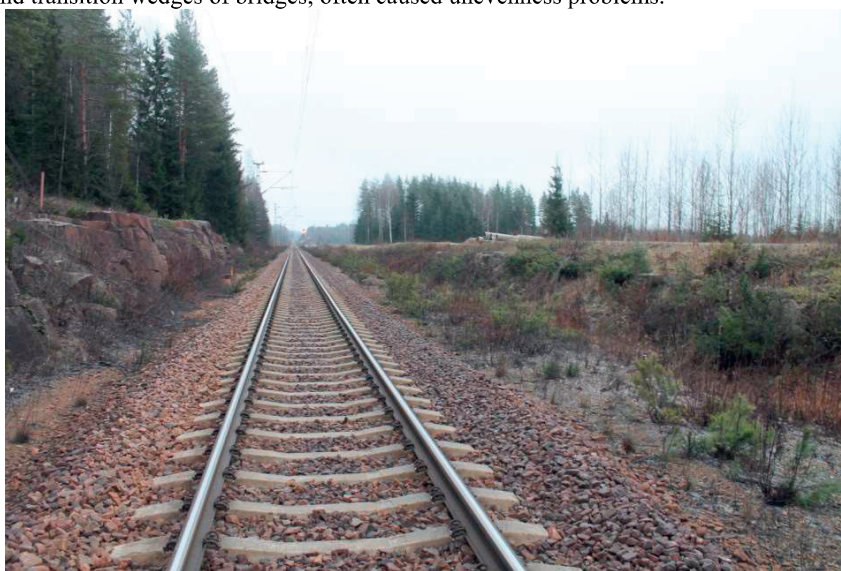


Fig. 1. Track in a cut. Drainage of the area is inadequate and recurrent problems of unevenness have been observed at the site.

A questionnaire study concerning drainage directed at maintainers in early 2015 revealed various problem sites. The problems varied by rail section, which was to be expected, since the level of maintenance varied and conditions differed by geographical location. The study found numerous problem sites along the network in need of renovations which had been ignored. The existence of ditches beyond the track area is problematic for drainage since cleaning and maintaining of just the ditches within the track area is then not sufficient. It requires assessing, planning and making functional the present overall drainage system of the entire area. There are also sites along the rail network where ditches cleaned a few years ago look like they had not been cleaned in ages. That would seem to indicate that cleaning should be considerably more regular, and it should be studied whether it is possible to improve the sites' drainage so that the problems do not recur in a few years. The functioning of covered drains and ensuring their condition is also problematic. The study also indicated that more attention needs to be given to sprouting by the track and beyond. In favourable conditions sprouting occurs very quickly and the current clearing rate is not necessarily sufficient. The study did not determine whether the sprouting problem was due to contractual reasons or prioritisation by the maintainer. However, there were indications that sprouting was not being dealt with as required by the general maintenance guidelines. Thus, many of the problems are related to tasks that should already be performed based on existing maintenance contracts.



## 4 Assessment of Drainage Solutions Based on Monitored Sites

In connection with the study, sites were sought along the track which would allow examining the impact of improved drainage on unevenness. The aim was to find sites where drainage had been improved 2–10 years earlier with no other major measures having been performed at the sites. Another aim was to compare the difference between the impacts of light drainage improvement (e.g. cleaning of ditches) and large-scale drainage improvement.

The intention was to use non-destructive methods like field inspections, the track image service, and the Rail Doctor program developed by Roadscanners. Depending on the site, the program can use laser scanning data, ground penetrating radar data, a geological map, digital videos shot from several different angles, and EMMA measurement data. Of the data produced by the EMMA track inspection vehicle, mainly the elevation deviation data were used, but in some instances also the deviation in alignment data.

The finding of monitoring sites proved more challenging than expected. It became apparent that drainage had often been systematically improved, generally in connection with renovations, when other heavy maintenance measures on the track structure had also been carried out, such as sieving of the ballast layer. It is clear that in the case of sites like that, it is difficult to point out the impacts of a change in drainage on the performance of a structure. It was also surprisingly difficult to find the actual data on the sites. That is probably mainly due to the fact that the various actors responsible for maintenance are replaced by others as a result of competitive tendering. Railway track managers have also changed whereby memory-based history data on suitable sites are lost. The situation can also probably be partially explained by the content of maintenance contracts since drainage structures are renovated primarily only e.g. when flow has weakened essentially. Then the extent of renovation is generally quite small. There were also clear indications that the priority given drainage maintenance had at some sites been quite low. Yet, some sites were investigated, but based on the results, their problems were mainly due to factors other than drainage.

Part of the sites of the ROPE surveys are well suited for use as monitored sites since data on well performed measures and preceding problems exist. Yet, the challenge of ROPE sites from the viewpoint of this study is that there is not yet enough data on the change in the situation after the performance of a measure. However, these sites should be used in follow-up studies to verify the true effects of changes in drainage.

## 5 Development of Drainage Methods

Traditionally, drainage surveys have been based primarily on visual inspection. Measurements have been made mainly in connection with planning. This type of assessment makes comparison of sites and monitoring of the development of the situation problematic. Modern technology provides more opportunities for assessing the functioning of drainage so that it is not based merely on the competence and view of the assessor. Laser scanning is the new method that appears most useful for drainage assessment as it allows creating a clear digital terrain model of the site. It also allows collecting numerical data on e.g. the depths of ditches and changes in them over time.

The Finnish Transport Agency's *Rato 13 Track inspection guidelines (2004)* define the compulsory inspections for the rail network. The number of inspections varies by maintenance level, but all rail sections are generally subject to a walking inspection at least 1–2 times per year. Inspections are also made from rolling stock. As far as drainage is concerned, inspections are to focus e.g. on the functioning of side ditches and culverts, vegetation and the condition of embankments. Thus, the functioning of drainage is, at least in principle, assessed several times a year. A questionnaire study was also directed at railway track managers and maintainers to further clarify the

matter. The responses indicated that assessment of drainage was based on the visual inspection methods set in the guidelines. No more advanced inspection methods were used.

The attitudes of track managers and maintainers toward current inspection methods and their development revealed by the questionnaire study divided roughly in two categories. Some considered the existing drainage inspection methods adequate with no need for more regular and thorough assessment. Others wanted to improve drainage monitoring. These differences of opinion are probably, at least partly, the result of regional differences since the situation with the high volume and high maintenance level tracks in the Capital Region is completely different from that of the low volume tracks up north.

The responses of regional managers and maintainers reflect the typical problem related to visual inspection: perceptions of the functioning and quality of drainage vary according to the assessor. It is also difficult to issue guidelines since it is hard to determine when the flow in the ditch has weakened substantially or there is too much vegetation in the ditch. Definitions are also partly site-specific as the consequences of drainage problems differ by site. Yet, the study indicates that drainage problems need to be studied further. Other methods, independent of the view of an assessor, are also necessary to allow objective assessment of changes in the drainage system based on measurements.

## 6 Administrative Problems in Drainage Maintenance

The Finnish rail network is divided into 12 maintenance areas. The level of track maintenance varies by rail sections: high volume main lines are maintained better than low volume sections. Maintenance companies are selected by rail sections on the basis of competitive tendering which means that companies assume responsibility for maintenance for the term of their contract. Maintenance is done under supervision of track managers. The Finnish Transport Agency has prepared instructions for maintenance, which together with a maintenance contract, set out the tasks to be performed as part of maintenance. Consequently, there has been considerable variation in the maintenance of drainage structures.

The study analysed seven maintenance contracts from the viewpoint of drainage. Five of them call for maintenance only 'as necessary'. The Transport Agency's general guidelines define the criteria for when maintenance is required which include substantial weakening of flow or sprouting. In two more recent contracts the issue has been clarified as to contractual practice by setting distinct minimum requirements for ditch cleaning. Only one contract calls for the cleaning of all ditches during the contract period. In the best contract other factors promoting drainage have also been improved, such as removal of trees too close to the track. The contracts awarded for maintenance areas that were not examined in connection with the study are similar to the five analysed ones where maintenance is performed only 'as necessary'. Accurate recording of the tasks to be performed is in the interest of both the client and the maintainer, as it leaves no ambiguity about the actual number of required tasks, which makes tender calculation and work supervision more straightforward. The new maintenance contracts should be used as models also in other maintenance areas while mere need-based definition should be abandoned.

## 7 Conclusions and Next Phases of the Study

It is clear already at this phase of the study that several sites along the Finnish rail network suffer from drainage problems. The exact impact of these problems is still difficult to assess since the study of the monitored sites proved difficult. However, the situation will improve in a few years as data on the renovated ROPE sites becomes available. The next phase of the study will deal largely with modelling aimed at determining the extent to which functioning drainage can affect the moisture

condition of the embankment. Computational modelling will be used to determine e.g. the impact of ditch depth or one-sided drainage on the embankment, as well as the influence of different materials on the moisture condition. The results will be used to assess the true role of drainage problems in the occurrence of unevenness problems.

It is also clear that drainage management is inadequate at many sites. That is partly due to the conditions of maintenance contracts as well as the ambiguity of guidelines. Yet, it can be stated that the measures to be performed 'as necessary' have not been performed even when the set criteria are met. In future, new assessment methods should be introduced, such as laser scanning, in order to be able to produce numerical data on the state of drainage. Thereby a change in the state of drainage can be reliably established which makes it easier to target measures. Another alternative is to draw up maintenance contracts that clearly define the minimum number of ditches to be cleaned annually. The current 'as necessary' contracts should be abandoned unless they are tied e.g. to data and limit values produced by laser scanning.

## References

- Brecciaroli, F. & Kolisoja, P. 2006. Deformation behaviour of railway embankment materials under repeated loading: Literature review. Publications of Finnish Rail Administration A 5/2006. Helsinki, Finnish Rail Administration. 201 p.
- Finnish Transport Agency. 2004. Ratatekniset ohjeet (RATO) osa 13 Radan tarkastus (in Finnish). 51 s. + 23 liites.
- Guthrie, W.S. & Hermansson, Å. 2003. Frost heave and water uptake relations in variably saturated aggregate base materials. *Transportation Research Record: Journal of the Transportation Research Board* 1821, 13–19. 22 p.
- Guthrie, W., & Zhan, H. 2002. Solute effects on long-duration frost heave behavior of limestone aggregate. *Transportation Research Record: Journal of the Transportation Research Board* (1786). pp. 112–119.
- Hermansson, Å. & Guthrie, W.S. 2005. Frost heave and water uptake rates in silty soil subject to variable water table height during freezing. *Cold Regions Science and Technology*, Volume 43, Issue 3, pp. 128–139.
- Isohaka, M. 2014. Influence of water availability on frost action in railway track structures. Master of science thesis (in Finnish). Tampere University of Technology, Dept. of Civil Engineering. 132 p. + 7 p. app.
- Mamou, A. 2013. Effects of principal stress rotation and drainage on the resilient stiffness of railway foundations. Doctoral dissertation. University of Southampton.
- McGaw, R. 1972. Frost Heaving Versus Depth to Water Table. In *Highway Research Record* 393. Washington DC, Highway Research Board, National Research Council. pp. 45–55.
- Metsovuori, L. 2013. Thaw settlement as cause of railway track unevenness. Master of science thesis (in Finnish). Tampere University of Technology, Dept. of Civil Engineering. 93 p.
- Nurmikolu, A. 2005. Degradation and frost susceptibility of crushed rock aggregates used in structural layers of railway track. Doctoral dissertation, Tampere University of Technology.
- Otter, L. 2011. The influence of suction changes on the stiffness of railway formation. Doctoral dissertation. University of Southampton.
- Selig, E.T. & Waters, J.M. 1994. *Track geotechnology and structure management*. London, Thomas Telford Publications. 446 p.
- Silvast, M., Nurmikolu, A., Wiljanen, B. & Mäkelä, E. 2013. Efficient track rehabilitation planning by integrating track geometry and GPR data. Proceedings of the 10th International Heavy Haul Conference, New Delhi, India, February 4–6, 2013.



# PUBLICATION II

Determining Soil Moisture Content and Material Properties with Dynamic  
Cone Penetrometer

Juha Latvala, Heikki Luomala and Pauli Kolisoja

The Baltic Journal of Road and Bridge Engineering, Vol. 15 (2020), No. 5, pages 136–159  
<https://doi.org/10.7250/bjrbe.2020-15.511>

Publication is licensed under a Creative Commons Attribution 4.0  
International License CC-BY



## DETERMINING SOIL MOISTURE CONTENT AND MATERIAL PROPERTIES WITH DYNAMIC CONE PENETROMETER

JUHA LATVALA<sup>1\*</sup>, HEIKKI LUOMALA<sup>2</sup>, PAULI KOLISOJA<sup>3</sup>

<sup>1-3</sup>*Research Centre Terra, Tampere University, Tampere, Finland*

Received 21 October 2019; accepted 12 May 2020

**Abstract.** This study utilised static triaxial and dynamic cone penetration tests to examine the identification of changes in strength in soil materials as a result of an increase in moisture content. The applicability of a light dynamic cone penetrometer device in railway environments was also studied. On a broader scale, the aim was to find an investigation method suited to field locations that identify low-quality or persistently moist materials directly from the structure. The triaxial tests found an apparent increase in shear strength when the water content dropped below 7%. Based on the series of laboratory tests, the dynamic cone penetrometer reacted strongly to material density, but the impact of moisture content was also evident. Furthermore, the results showed that dynamic cone resistance is a reasonably unfeasible metric for assessing the structural quality of materials consisting primarily of sand, due to the number of factors affecting the resistance. In the laboratory tests, the lowest dynamic cone resistances were measured in the material with the highest structural quality.

**Keywords:** dynamic cone penetrometer (DCP), Panda2, railway embankments, soil moisture, soil shear strength, substructure, triaxial test.

---

\* Corresponding author. E-mail: [juha.latvala@tuni.fi](mailto:juha.latvala@tuni.fi)

Juha LATVALA (ORCID ID 0000-0001-6306-9310)  
Heikki LUOMALA (ORCID ID 0000-0002-7113-3527)  
Pauli KOLISOJA (ORCID ID 0000-0001-7709-180X)

Copyright © 2020 The Author(s). Published by RTU Press

This is an Open Access article distributed under the terms of the Creative Commons Attribution License (<http://creativecommons.org/licenses/by/4.0/>), which permits unrestricted use, distribution, and reproduction in any medium, provided the original author and source are credited.

## Introduction

In the future, climate change is predicted to steer the global climate towards extreme phenomena, leading to increasingly frequent floods, heavy rains and, in some locations, extreme drought (Trenberth, 2011). In Finland, this shift is expected to increase annual rainfall by multiple percentage points, depending on the method of calculation (Ruosteenoja, Jylhä, & Kämäräinen, 2016). The intensity of individual instances of rainfall is also predicted to increase (Lehtonen, 2011). Increased moisture content is known to deteriorate the functionality of earth structures. As reported by Li & Selig (1995), the combination of cyclic loading, fine-grained soils, and excessive moisture content is a very harmful combination for a railway track. Thus, climate change exposes earth structures to accelerated deterioration. The Finnish Transport Infrastructure Agency and Tampere University have initiated a research project that examines the effect of moisture conditions on the bearing capacity of track earth structures and the possible benefits obtainable by drainage. One goal of the research efforts is to develop the field testing of soil materials and the identification of low-grade substructure materials. The suitable in-situ test methods vary depending on soil type. For sandy materials, Selig & Waters (1994) have listed functional methods such as standard penetration test (SPT), cone penetration test (CPT), borehole shear test (BST) and dilatometer test (DMT). One of the easiest and lightest to operate is the dynamic cone penetrometer (DCP).

Brough, Ghataora, Stirling, Madelin, Rogers, & Chapman (2003) have also been interested in track subgrade quality in their research (part 1/2) because they assumed a relationship between track-bed stiffness and track quality deterioration. Dynamic cone penetrometer was identified as one potential tool for determining the bearing capacity of subgrade. After a case study (part 2/2), Brough, Ghataora, Stirling, Madelin, Rogers, & Chapman (2006) considered that DCP is suitable for recognising subgrade heterogeneity at least. Kennedy (2011) has also mentioned DCP as a potential in-situ testing device for railway track substructures and recommends further research because there is some scatter in the results of DCP. In this study, the Panda2, which is a light hand-operated DCP manufactured by the French company Sol Solution, was selected as one of the potential examination methods. The device measures the dynamic cone resistance of the auger rod in proportion to depth, based on the stroke intensity and rod penetration. The Panda2 records the measurements automatically and enables them to be exported to a computer. The benefits of the device include ease of use and compact size. In light of the research project as a whole, the following research questions were identified:



1. Is dynamic cone resistance measured by the DCP suitable quantity to identify materials that have low bearing capacity?
2. Is the DCP accurate enough to detect changes in strength resulting from the changes in the moisture content of materials?
3. Is a light hand-operated DCP practically feasible for the Finnish railway environment?

Answers to the research questions were sought through an extensive series of laboratory tests and field measurements. Static triaxial tests were conducted on the materials being studied at varying moisture content levels to determine the impact of moisture, and the results were compared to the DCP measurement results.

## 1. Theoretical framework

Various penetrometers have been used in soil surveys for quite some time, and the method is regarded as the oldest geotechnical in-situ test (Spagnoli, 2007). As reported by Vanags, Minasny, & McBratney (2004), Parker & Jenny (1945) were the first to introduce a precursor to the DCP. In their tests, they measured the energy required to drive a test pipe into the soil by using a 9.1 kg weight dropped from a height of 30 cm and measuring the pipe penetration per stroke. This technique revealed the soil resistance in Joules per centimetre. The development of the method



**Figure 1.** The Panda2 device

continued, and the modern penetrometer was introduced in studies by the Australian engineer Scala (1956). Panda2 device by Soil Solution Ltd is a further developed version of the penetrometer that works with variable impact strength as it also measured. The French scientist Dr Roland Gourves of Blaise Pascal University has been developing Panda since 1991 (Langton, 1999).

Langton (1999) described the operating principle of the device in a technical article. Figure 1 presents the device in working order at a field location. The Panda2 device generates the impact energy using a recoil-free hammer and measures it with a connecting piece attached to the top end of the rod. The penetration of the cone-tipped rod into the soil is measured automatically with a self-spooling measuring tape attached to the connecting piece at the top of the rod. The connecting piece features an acceleration sensor that determines the impact speed. The terminal device records the results. The weight of the recoil-free hammer used in the Panda is 2.0 kg.

As reported by Langton (1999), the  $q_d$  is calculated using the “Dutch formula”, which has been modified from the original form presented by Cassan 1988 (as cited in Langton, 1999). The calculation of  $q_d$  is based on the following equation:

$$q_d = \frac{1}{A} \cdot \frac{0.5 MV^2}{1 + \frac{P}{M}} \cdot \frac{1}{x_{90^\circ}},$$

where  $q_d$  – dynamic cone resistance;  $x_{90^\circ}$  – penetration caused by a single strike with a  $90^\circ$  cone;  $A$  – cone area;  $M$  – weight of the striking mass;  $P$  – weight of the struck mass;  $V$  – impact speed of the hammer.

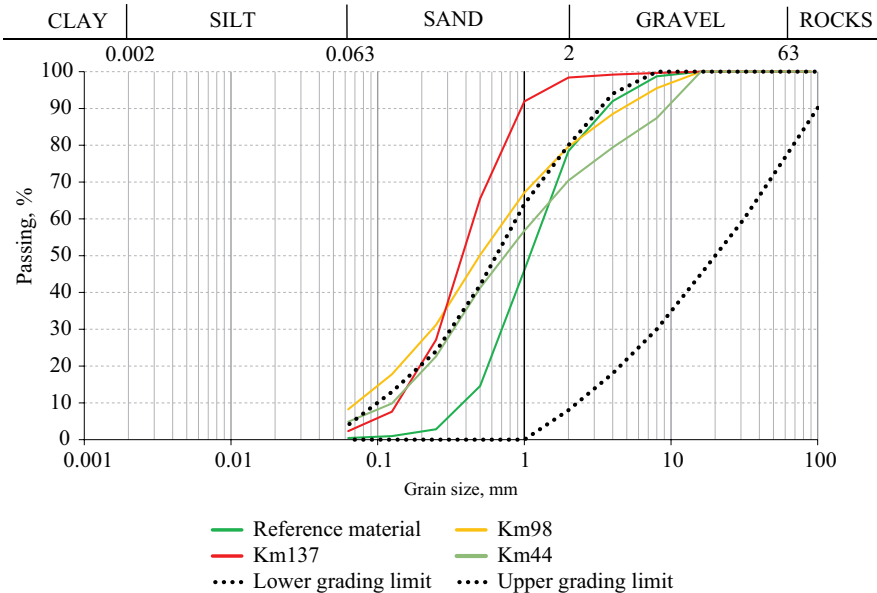
The variables contained by the formula indicate that it does not account for the skin resistance between the rod and the soil. A third version of the device is also under development, which measures more parameters but also assumes the skin resistance to be zero (Benz-Navarrete, Escobar, Haddani, Gourves, D’Aguiar, & Calon, 2014). The diameters of the cones used at the end of the rod vary. The device uses a fixed 2 cm<sup>2</sup> cone or a larger 4 cm<sup>2</sup> sacrificial cone. The diameters of these cones are 16 mm and 22.5 mm, respectively. The diameter of the impact rods is 14 mm, and the length of a single section is 500 mm. The article written by Langton (1999) also mentions a 10 cm<sup>2</sup> cone for special cases. The angle for all cone pieces is  $90^\circ$ . The Panda2 device typically measures 20–30 MPa dynamic cone resistance to an approximate depth of 4–6 m. In favourable conditions, the device measures to even deeper. The dynamic cone resistance  $q_d$  is used directly in the monitoring of compaction and in soil surveys. As reported by Langton (1999), the link between dynamic cone resistance and other commonly-used parameters have been studied using a variety of well-documented test sites where

studies have been conducted using a range of methods. The commonly-used comparable parameters in those studies were SPT and other types of DCP, California Bearing Ratio (CBR) measurements and undrained shear strength.

## 2. Materials and methods

### 2.1. Materials

The laboratory tests were carried out with four different materials, for which the particle size distributions and typical geotechnical parameters are presented in Figure 2 and Table 1, respectively. Screened sand from the Kollola gravel pit, which meets the requirements of the Finnish Transport Infrastructure Agency for insulation and intermediate layer materials, was used as high-quality reference material. The three others were actual samples from the Rantarata track in southern Finland, only one of which (km44) fulfilled the particle size requirements. The field samples deviate from the reference materials mainly concerning the fine-grained end, as the reference material



Note: the particle size limits of the Finnish Transport infrastructure Agency for insulation and intermediate layer materials are illustrated with dotted lines.

**Figure 2.** Particle sizes of the materials used in the laboratory tests

Table 1. Geotechnical properties of the studied materials

| Material           | Particle size ratio |                 | Fine fraction content diameter below | Dry density and water content (Wet samples, Proctor) | Dry density (Dry samples, Proctor) |
|--------------------|---------------------|-----------------|--------------------------------------|--|------------------------------------|
|                    | $d_{50}$            | $d_{60}/d_{10}$ | 0.06 mm,                             | $\rho_{dmax}$  | $\rho_{dmax}$                      |
|                    | mm                  | -               | %                                    | $\text{g/cm}^3$ and %                                | $\text{g/cm}^3$                    |
| Reference material | 1.20                | 3.75            | 0                                    | 1.91/2.80  | 1.96                               |
| km44               | 0.75                | 9.60            | 4.90                                 | 2.03/8.50  | 2.10                               |
| km98               | 0.50                | 10.70           | 8.20                                 | 2.14/3.00  | 2.08                               |
| km137              | 0.40                | 3.60            | 2.30                                 | 1.80/5.90  | 1.90                               |

consisted of screened 0/8 mm sand, whereas the field material contained fines. The largest deviation from the guideline range was presented by the material km137, which was excessively even-grained, resulting in low compaction properties.

For laboratory testing, the compaction behaviour of the materials was studied with the improved Proctor test method (*SFS-EN 13286-2:2011 Unbound and Hydraulically Bound Mixtures. Part 2: Test*

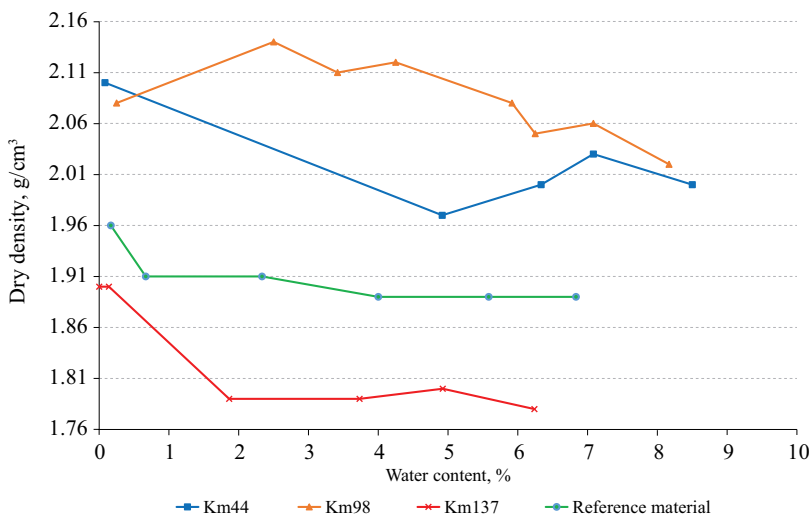


Figure 3. Results of the improved Proctor tests for the studied materials

*Methods for Laboratory Reference Density and Water Content. Proctor Compaction*). The test results are presented in Figure 3 and Table 1. The best compaction results were obtained with the km98 material, with a peak dry density of 2.14 g/cm<sup>3</sup> at a compaction water content of 3%. km44 material reached its highest dry density as oven-dried and the second-highest dry density at a moisture content of 8.5%. The reference material and the km137 sample were looser (1.96 g/cm<sup>3</sup> and 1.90 g/cm<sup>3</sup>), and for them, too, the maximum density was achieved with an oven-dry sample. The compaction curve for the reference material, in particular, shows that when the material is moist, the maximum dry density remains relatively constant across a broad moisture content range.

## 2.2. Static triaxial tests

The materials being studied have been subjected to a series of dried triaxial tests to determine the impact of moisture content on the maximum shear strength. The saturated samples were prepared by the *SFS-ISO 17892-9:2018 Geotechnical Investigation and Testing. Laboratory Testing of Soil. Part 9: Consolidated Triaxial Compression Tests on Water Saturated Soils* standard, with the exception that saturation ratio was not confirmed through the B value. The samples were first compacted at near optimum moisture content – 4.1–8.7%,

Table 2. Parameters used in the triaxial and measured material properties

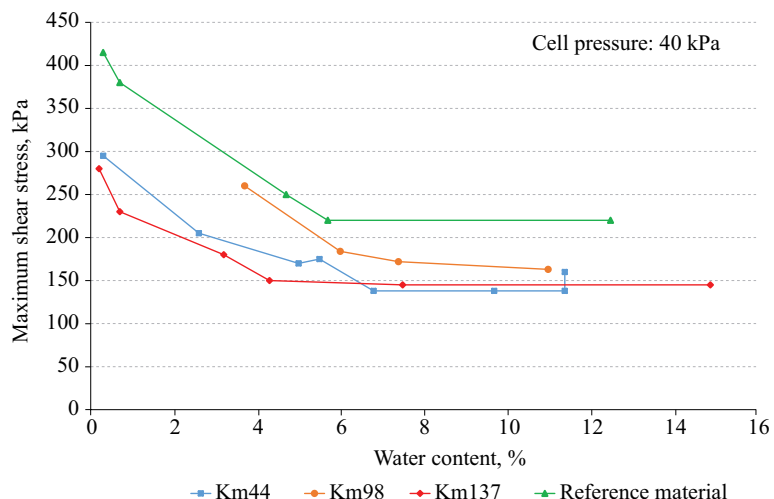
| The sample ID | Cell pressure, kPa | Moisture condition/drying procedure | Water content during compaction, % | Dry density after compaction/consolidation, g/cm <sup>3</sup> | Water content after test, % | Maximum shear stress, kPa |
|---------------|--------------------|-------------------------------------|------------------------------------|---|-----------------------------|---------------------------|
| <b>km44</b>   |                    |                                     |                                    |   |                             |                           |
| A1            | 21.0               | Saturated                           | 6.20                               | 1.96/1.96   | 11.50                       | 90                        |
| B1*1          | 41.0               | Saturated                           | 7.00                               | 1.96/1.97   | 11.40                       | 138                       |
| B2            | 41.0               | Saturated                           | 6.40                               | 1.96/1.96   | 11.40                       | 160                       |
| C1            | 81.0               | Saturated                           | 8.10                               | 1.93/1.95   | 11.00                       | 245                       |
| D1            | 41.0               | 1 d: -4.0 kPa                       | 7.30                               | 1.94/1.94   | 9.70                        | 138                       |
| E1            | 39.0               | 3 d: -4.0 kPa                       | 7.40                               | 1.92/1.92   | 6.80                        | 138                       |
| F1            | 41.0               | 5 d: -4.0 kPa                       | 7.40                               | 1.91/1.95   | 5.50                        | 175                       |
| G1            | 41.0               | 10 d: -4.0 kPa                      | 8.70                               | 1.92/1.93   | 0.30                        | 295                       |
| H1            | 41.0               | 7 d: -4.0 kPa                       | 4.90                               | 1.93/1.94   | 5.00                        | 165                       |
| I1            | 41.0               | 3.25 d: -5.0 kPa                    | 4.10                               | 1.94/1.95   | 2.60                        | 205                       |

Table 2.

| The sample ID             | Cell pressure, kPa | Moisture condition/drying procedure | Water content during compaction, % | Dry density after compaction/consolidation, g/cm <sup>3</sup> | Water content after test, % | Maximum shear stress, kPa |
|---------------------------|--------------------|-------------------------------------|------------------------------------|---|-----------------------------|---------------------------|
| <b>km98</b>               |                    |                                     |                                    |   |                             |                           |
| A1                        | 19.0               | Saturated                           | 5.60                               | 2.00/2.00   | 11.40                       | 90                        |
| B                         | 41.5               | Saturated                           | 5.80                               | 1.99/2.00   | 11.00                       | 160                       |
| C1                        | 82.0               | Saturated                           | 5.60                               | 2.02/2.03   | 11.20                       | 360                       |
| C2                        | 82.0               | Saturated                           | 6.00                               | 2.01/2.02   | 10.80                       | 285                       |
| DA                        | 40.0               | 1d: -5.0 kPa                        | 5.80                               | 1.98/2.00   | 7.40                        | 170                       |
| E                         | 41.0               | 3d: -5.0 kPa                        | 5.50                               | 2.00/2.01   | 6.00                        | 180                       |
| F                         | 41.0               | 5 d: -5.0 kPa                       | 5.10                               | 2.03/2.04   | 3.70                        | 260                       |
| <b>km137</b>              |                    |                                     |                                    |   |                             |                           |
| A2                        | 20.0               | Saturated                           | 6.10                               | 1.79/1.79   | 14.40                       | 70                        |
| B                         | 41.0               | Saturated                           | 6.30                               | 1.79/1.79   | 14.90                       | 145                       |
| C                         | 81.0               | Saturated                           | 6.60                               | 1.80/1.81   | 14.60                       | 270                       |
| D                         | 41.0               | 1 d: -5.0 kPa                       | 5.80                               | 1.77/1.80   | 4.30                        | 150                       |
| E                         | 40.0               | 3 d: -5.0 kPa                       | 6.30                               | 1.79/1.80   | 0.20                        | 280                       |
| F                         | 41.0               | 5 d: -5.0 kPa                       | 6.40                               | 1.80/1.79   | 7.50                        | 145                       |
| U                         | 41.0               | 2 d: -5.0 kPa                       | 5.30                               | 1.78/1.79   | 0.70                        | 230                       |
| U1                        | 41.0               | 2 d: -4.5 kPa                       | 7.60                               | 1.82/1.87   | 3.20                        | 180                       |
| <b>Reference material</b> |                    |                                     |                                    |   |                             |                           |
| A                         | 19.5               | Saturated                           | 5.70                               | 1.93/1.93   | 12.80                       | 130                       |
| B1                        | 40.0               | Saturated                           | 7.10                               | 1.96/1.96   | 12.50                       | 220                       |
| C                         | 80.5               | Saturated                           | 6.30                               | 1.97/1.99   | 11.11                       | 410                       |
| D                         | 40.5               | 1 d: -3.5 kPa                       | 7.00                               | 1.93/1.95   | 5.70                        | 220                       |
| E                         | 40.5               | 3 d: -4.5 kPa                       | 6.20                               | 1.93/1.95   | 0.30                        | 415                       |
| F                         | 40.0               | 3 d: -3.0 kPa                       | 6.50                               | 1.92/1.93   | 0.70                        | 380                       |
| G                         | 39.0               | n. 1 d: -4.0 kPa                    | 6.10                               | 1.95/1.96   | 4.70                        | 250                       |

Note: \*1 B1 test was repeated with B2 because dry density was above the average.

depending on the material – to obtain samples with identical densities. After this, the samples were saturated and consolidated. Following the consolidation, the air was sucked through each sample at a negative pressure of 3.5–5.0 kPa to dry the samples. The drying time and vacuum level were varied to achieve a range of different moisture contents. The values used in the tests are presented in Table 2. The



**Figure 4.** The achieved maximum shear stresses of the static triaxial tests at varying moisture content levels

**Table 3.** Parameters used in the triaxial and measured material properties

| Sample ID          | Cohesion, kPa | Friction angle, ° | Cohesion after failure, kPa | Friction angle after failure ° | Strain level at maximum shear stress, % |
|--------------------|---------------|-------------------|-----------------------------|--------------------------------|---|
| km98               | 10.9          | 49.4              | 4.8                         | 38.6                           |   |
| A1                 |               |                   |                             |                                | 1.00                                    |
| B                  |               |                   |                             |                                | 1.80                                    |
| C2                 |               |                   |                             |                                | 2.60                                    |
| km44               | 18.8          | 45.6              | 3.9                         | 39.1                           |   |
| A1                 |               |                   |                             |                                | 1.20                                    |
| B2                 |               |                   |                             |                                | 1.30                                    |
| C1                 |               |                   |                             |                                | 1.70                                    |
| km137              | 4.1           | 49.5              | 6.1                         | 37.2                           |   |
| A2                 |               |                   |                             |                                | 2.80                                    |
| B                  |               |                   |                             |                                | 2.40                                    |
| C                  |               |                   |                             |                                | 2.40                                    |
| Reference material | 10.2          | 55.4              | 9.6                         | 40.2                           |   |
| A                  |               |                   |                             |                                | 2.60                                    |
| B1                 |               |                   |                             |                                | 2.30                                    |
| C                  |               |                   |                             |                                | 3.10                                    |

maximum shear stresses at a cell pressure of 40 kPa were compiled into Figure 4. The results suggest that the maximum shear strength begins to increase when the moisture content of the studied materials is below 7%. There are, however, differences among the materials, since with km44 material the growth starts at a moisture content of 6.8%, whereas with km137 material it starts at below 4.3%. With the same material, the increase in shear strength is significant, and the difference between relatively moist and relatively dry samples is above 100 kPa. For saturated samples, the friction angles and cohesion values measured at different cell pressures are presented in Table 3. The friction angles and cohesions from saturated tests are relatively small compared to the shear strengths achieved with drier samples. That means that there is an influence of apparent cohesion component, adding the shear strength. The results of the triaxial tests indicate that reducing the moisture content substantially increases the shear strength of the soil.

### 2.3. Methods

In the laboratory, the functionality of the Panda2 device was examined using soil samples contained in plastic tubes. The interior diameter of the pipes was 235 mm, and their height was 800 mm. The bottom of each pipe was closed with a plug, which had holes for saturation and drainage. The bottom plug was covered with geotextile and a perforated plywood board for the bottom contact of the DCP rod. All material samples were compacted at the same moisture content, and the compaction procedure was kept constant. After the compaction, the samples were saturated and dried to achieve a variety of moisture contents. In the layered compaction, an efficient vibratory hammer was used for which a 200 mm diameter compaction plate had been manufactured. Figure 5 depicts an on-going measurement process from the laboratory. A unit that measures device depth is positioned at the top of the sample, and a sensor measuring impact force is visible at the end of the penetrometer rod. The samples were prepared by the following process:

1. A concrete mixer is used to moisten the dry material to a moisture content of 7–8%, i.e. near to the optimum water content.
2. A known amount of material is poured into the sample tube, resulting in a layer of approximately 50 mm after compaction.
3. The sample in the tube is compacted with a vibrating compactor. A constant compaction time of 30 s was used for each layer.
4. More sample material is added until the target sample height is reached.





**Figure 5.** Panda2 test in progress in the laboratory

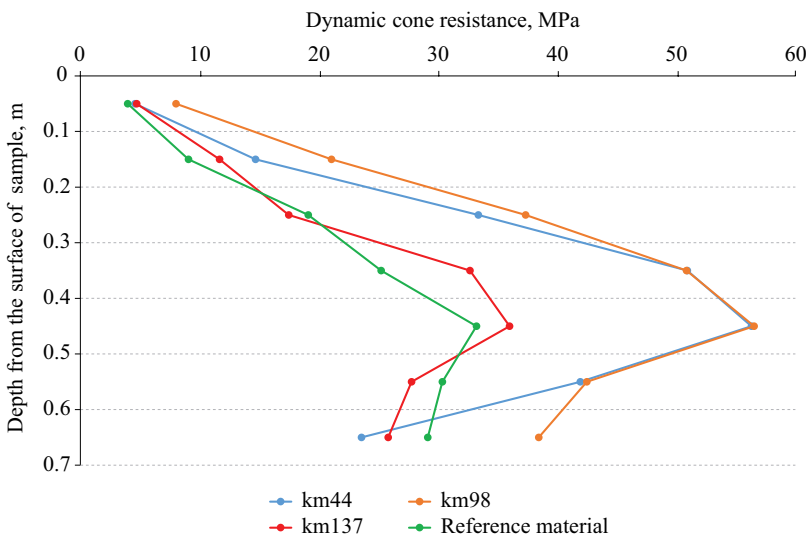
5. The compacted sample is moistened with water until it is close to the saturated state. The sample is moistened either from the top only or from the top and bottom simultaneously.
6. The sample is permitted to dry at room temperature for the duration specified in the test programme.
7. The Panda2 device is used to drive three or four penetrometer rods into the sample.
8. The sample is dismantled in layers of 100 mm. The layers are weighed, dried and weighed again to determine the moisture content of each portion.

### 3. Results

In the data directly recorded by the device, the dynamic cone resistances generated by individual impacts vary significantly due to the heterogenic properties of the soil. For this reason, the results presented here have been calculated as averages of the three rods driven into each sample, for one 100 mm section at a time. For almost all materials, the highest dynamic cone resistance was achieved at a depth of 400–500 mm. After that depth, the resistance usually began to decrease. The phenomenon was studied with a static penetrometer test, in which a computer-controlled hydraulic jack was used to drive the rod of the

Panda2 device into the sample at a constant speed. The force required for penetration was measured. The phenomenon of the dynamic cone resistance decreasing over the final 200 mm was also evident in this test, which implies that the effect is caused by skin resistance or the loosening of the base layers during the compaction of the upper layers. Therefore, the averages of dynamic cone resistance were primarily examined across the depths of 0–500 mm.

One series of tests was conducted with oven-dry materials. The oven-dry samples were prepared differently from the others in that they were compacted dry, which led to varying dry densities. The test results are shown in Figure 6, which specifies the average dynamic cone resistance of the three driven rods to depth. The results show that the measured dynamic cone resistance of all materials increases dramatically in proportion to the depth and that the highest value is achieved at an approximate depth of 450 mm. The dynamic cone resistance correlates strongly with the dry density of the samples, as km44 ( $2.23 \text{ g/cm}^3$ ) and km98 ( $2.18 \text{ g/cm}^3$ ) were denser than km137 ( $1.87 \text{ g/cm}^3$ ) and reference material ( $1.87 \text{ g/cm}^3$ ). With dry material, the median particle size does not appear to be a significant parameter in the particle size range of the materials examined based on the similarity of the curves, since the values for the km137 and reference materials were 0.4 mm and 1.2 mm, respectively.



Note: the results are averages of three tests across layers of 100 mm.

**Figure 6.** Dynamic cone resistance measured with oven-dry samples

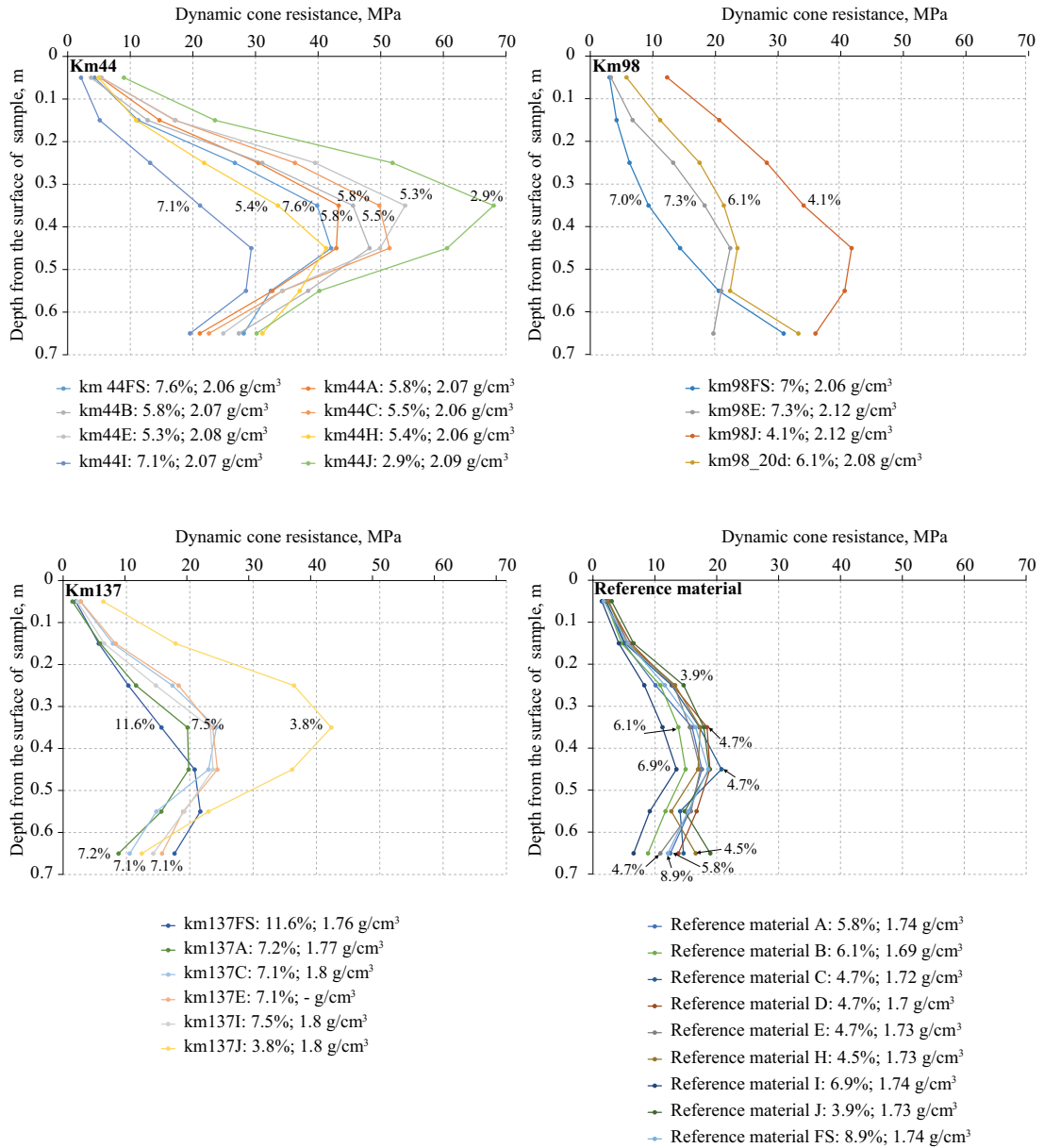
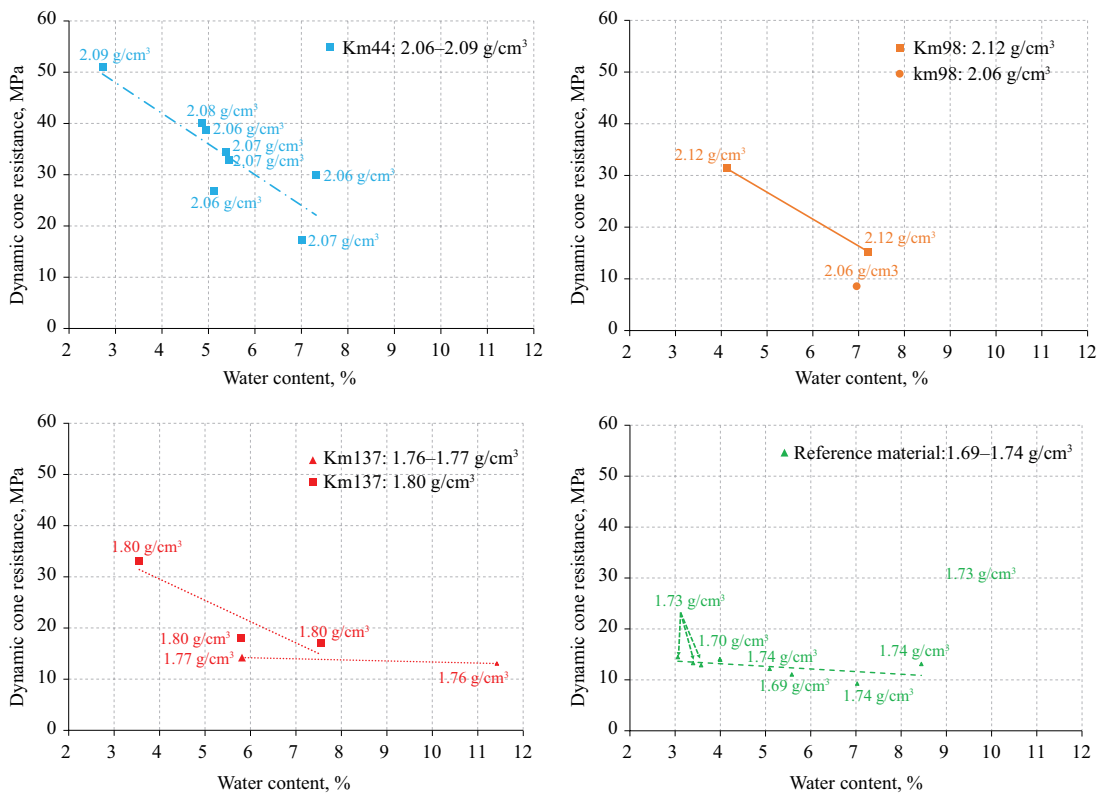


**Figure 7.** The dynamic cone resistance of entire samples at varying moisture content levels

With moist samples, the dynamic cone resistance varied noticeably according to dry density and moisture content. The moisture content indicates an average across the entire testing depth. The results are

reported in Figure 7, which presents the dynamic cone resistance to depth for the entire sample. The differences among the materials were significant, and the lowest dynamic cone resistance was measured in the reference material, which presented the highest shear strength in static triaxial tests. The highest dynamic cone resistance for all materials was reached at the lowest moisture content level, and the dynamic cone resistance generally decreased with increased moisture content. The results in Figure 7 illustrate the increase in dynamic cone resistance in proportion to depth. Moist samples, too, exhibited similar loosening of the bottom layers as oven-dry samples, but the degree varied depending on the material. Based on the results, the moisture content and dry density in km44 material caused more considerable variation of dynamic cone resistance compared to the reference material, which was the least sensitive to changes in moisture content.



Note: the depth range covered is 0–500 mm.

**Figure 8.** The impact of moisture content on dynamic cone resistance

A clearer view of the impact of moisture content is provided by Figure 8, in which the dynamic cone resistance is only presented in proportion to moisture content and which only covers a depth of 0–500 mm. This approach excludes the looser bottom section. Figure 8 divides the measuring points into separate categories based on dry density. This method of examination also revealed the reference material to be the least sensitive to increases in moisture content, even though it also exhibited slight growth. The increase is more dramatic with other materials – with km44, for example, the range of variation was above 30 MPa, depending on the dry density and moisture content. As regards material km98 and km137, the dynamic cone resistance increased with decreasing moisture content. The results show similarities with the results of the static triaxial tests, as a moisture content dropping below 7% increases dynamic cone resistance.

### 3.1. Field measurements

The purpose of the field measurements was to determine the suitability of the device to the Finnish railway environment. The field locations used were sites km44, km98, and km137 along the Rantarata track, at which substructure samples were collected for laboratory testing (at an approximate depth of 0.5 m measured from the bottom surface of the ballast layer). The field surveys were initiated at the km137 point, which is located by a sandy ridge. The substructure was examined near the footpath and on the embankment at various locations, as shown in Figure 9. The most measurements were conducted in this location as the penetrometer rod sank quickly into the soft, even-grained sand. The measured results are presented as a nine-strike average in Figure 10 since these evens out spikes caused by small rocks. The measured dynamic cone resistances were small; approximately equal to 3.0 MPa to a depth of 0.7 m. Because the dynamic cone resistances spiked immediately after that, it was clear that there was either rock or some other material that produced a higher dynamic

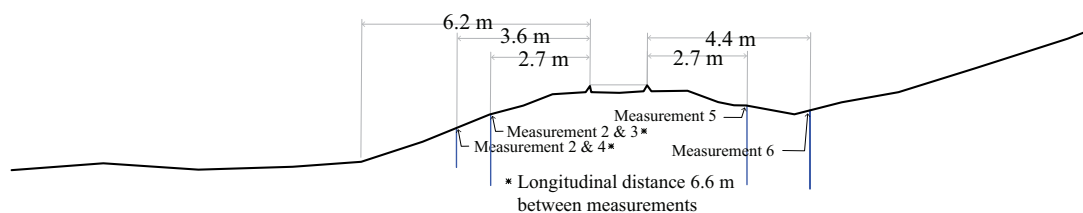


**Figure 9.** Positions of the Panda tests at the km137 point across a cross-section of the track

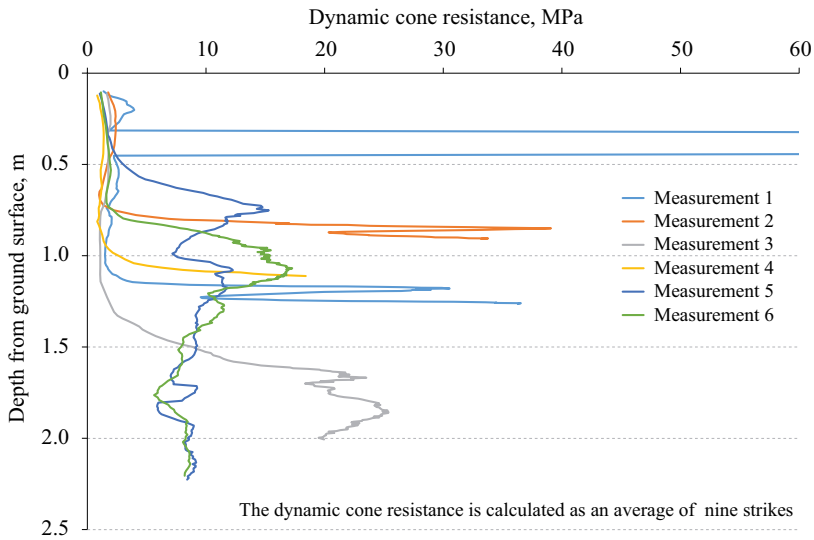


**Figure 10.** Measurement results for the km137 site

cone resistance below this layer. One measurement hit a rock near the very beginning that caused the peak value shown in the diagram at a depth of approximately equal to 0.4 m. The deepest testing point was 2.2 m. On visual observation, the nearby sandy ridge and the materials used to construct the track mostly resembled each other, and no clear distinctions between layers were identified.

The second field location examined was situated at the km98 point of the Rantarata track. Three measurements were taken at separate locations near the footpath, and the dynamic cone resistances were higher than at the previous km137 location. The results are shown in Figure 11. The dynamic cone resistance for two measurements was approximately equal to 3.0 MPa initially, before beginning an apparent increase at a depth of 1.2 m. For measurement 2, the dynamic cone resistance was immediately higher, but deeper in, the values began to correspond to the other measurements. Two measurements were successful to an approximate depth of 3.5 m, but the third was stopped at 2.0 m due to high resistance. As a technical observation relating to the tests, it was observed that the substructure in this location was more heterogeneous in terms of its particle size and also contained ballast particles. Although the dynamic cone resistance was pretty low, it was challenging to drive the rod into the ground, and long sequences of strikes were needed. The mixed-grained material that also contained ballast particles proved problematic in terms of rod durability.

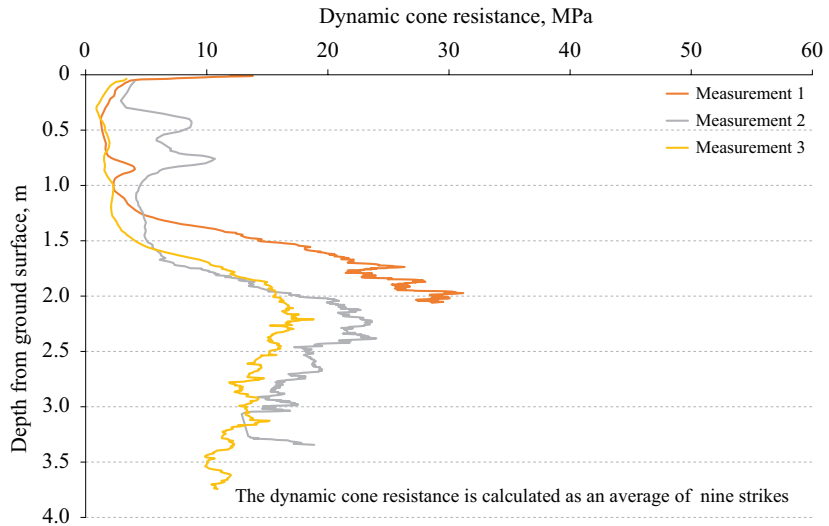


**Figure 11.** Measurement results for the km98 site

Only one test was conducted at the last test site at the km44 point. The site is situated in a soft soil area, and the track has settled somewhat over the years. The elevation has repeatedly raised with ballast to compensate the settlement. That has caused ballast material to mix with substructure materials. The DCP test was conducted on the footpath outside the actual track to avoid coarse ballast rocks. Despite this, there were significant difficulties to drive the rod into the embankment.

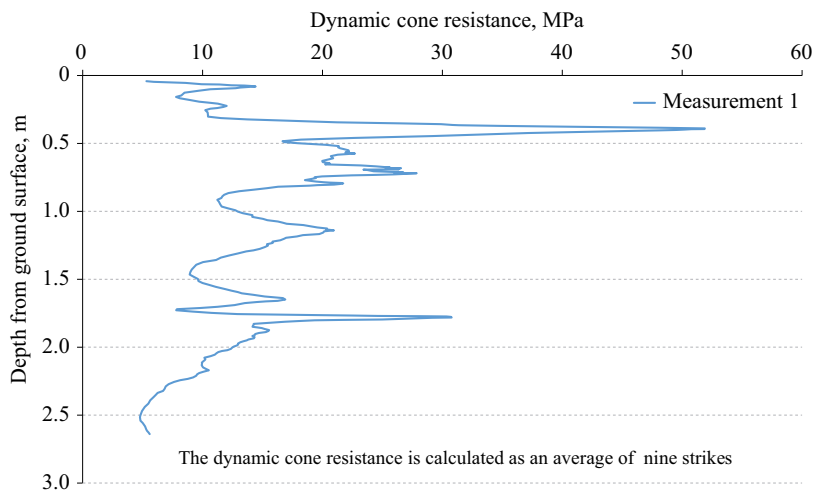


**Figure 12.** Test results for the km44 site

These difficulties are illustrated well by the results in Figure 12 since the average dynamic cone resistance rose to 10 MPa, relatively near the surface. The dynamic cone resistance increased with depth, and the soil contained rocks that caused spikes to curve. At a depth of 1.7 m, the dynamic cone resistance began to drop, which indicated a softer layer of soil than the substructure. Lifting the rod after the test was also difficult since the rocks encountered in the driving phase caused torsional stress on the rod. Conditions such as those at the site in question require significantly more robust ground surveying equipment.

## 4. Discussion

The laboratory tests indicated that all materials investigated were different, which was the intention. Based on the triaxial tests, the apparent cohesion present at low moisture content increased the shear strength of the samples examined. For the studied materials, moisture content of approximately equal to 7% appeared to be the turning point, after which the apparent cohesion begins to increase the shear strength. On the other hand, due to the nature of the undrained triaxial tests, the pore water pressure has time to dissipate. At a more rapid cyclic load, the behaviour is partially different. Repeated loading triaxial tests have also been conducted on the materials in question, and the results are presented in an upcoming article.

The Panda2 proved to be a light and easy-to-use DCP device. The series of laboratory tests indicate that the is mostly determined based on the dry density, but the moisture content also has a clear impact. The results have apparent similarities with those published by Escobar, Benz-Navarrete, Gourvès, Haddani, Breul, & Chevalier (2016), wherein a minute increase in the dry density of sand material had a surprisingly strong impact on the dynamic cone resistance measured by the Panda device. This observation is also consistent with other research results, as Chaigneau, Gourves, & Boissier (2000), for example, stated in their article that the dynamic cone resistance measured by DCP is highly sensitive to the effect of dry density. The series of tests showed that the materials brought in from the field (km44, km98, and km137) all clearly reacted to the moisture content. However, the high-quality reference material from Kollola had a relatively low response to the change in moisture content. The link between moisture content and dynamic cone resistance was also observed by Morvan & Breul (2016) in studying silt materials with the Panda device. Byun & Kim (2020) tested their in-situ modulus detector for subgrade and found that the resilient moduli of soil also decreases when the water content increases. That device had



many similarities with DCP. The median particle size of the materials did not appear to affect the dynamic cone resistance in the materials studied substantially. However, the range of particle sizes covered was relatively narrow in this study. The effect of median particle size was also small in the study of MacRobert, Bernstein, & Nchabeleng (2019), when they studied correlations between the relative density of sands and DCP. The standard error in relative density prediction was 11%, but when using median particle size with correlation, the error decreased slightly to 9%.

The dynamic cone resistances measured at the laboratory were significantly higher than those measured in the field. This effect was slightly surprising, but presumably, the plastic tube used expanded during compaction and when driving the rods into the sample. This phenomenon is likely to have caused a confining pressure akin to cell pressure in the material, which increased the resistance required for soil displacement but also resulted in substantial skin resistance affecting the penetrometer rod. Bolton, Gui, Garnier, Corte, Bagge, Laue, & Renzi (1999) had also recognised that cone resistance was above double when ratio (container diameter divided by cone diameter) was decreased from 45 to 8.85. In our test, the ratio was approximately 14. Increased dynamic cone resistance was also observed by Gansonré, Breul, Bacconnet, Benz, & Gourvès (2019) when they tested different boundary conditions with Panda DCP. The dynamic cone resistance in the small chamber was multiple compared to in-situ measurements and more extensive in the small chamber than in the larger one. In our test, materials brought in from the field were excavated by hand from the substructure below the ballast layer. That was the reason why their amount was limited, and the tests were ultimately performed inside a tubular mould. If there had been more materials available, a more extensive and shallower test container would have served the purpose better in hindsight. However, the study unequivocally indicates that skin resistance has a significant impact on the measured values, but the degree is complicated to estimate.

Apparent skin resistance also affected the penetrometer rod in the field tests, especially at the km44 site but also partially at the km98 site. This expectation must be considered in the examination of the results since skin resistance is not taken into account in the calculation of dynamic cone resistance. Using larger sacrificial cones would be a better option, but even the used 2 cm<sup>2</sup> cone proved challenging to drive into the embankment in the field. However, the problem does not appear to occur globally, as Haddani, Breul, Saussine, Navarrete, Ranvier, & Gourvès (2016) have presented measurements taken with the Panda device directly from the top of the ballast

layer in France. In Finnish conditions, it can be concluded that the device lends itself better to measuring the density of various thin layers and surveying softer materials. The same manufacturer is also developing a more heavy-duty measurement device, called Grizzly3, which is stated to be better suited to coarse-grained conditions (Benz-Navarrete, Escobar, Haddani, Gourves, D'Aguiar, & Calon, 2014). However, that is not hand-held instrument anymore, because the newest version of Grizzly EV DPSH has 63.5 kg weight of striking mass and the total mass of testing machine is 990 kg (Benz-Navarrete, Breul, & Moustan, 2019).

The relevant literature presents a variety of solutions for eliminating skin resistance in the DCP device. A method presented by Livneh (2000) where the rod struck at regular intervals, is rotated and the torque this requires is measured to enable the calculation of a corrected dynamic cone resistance value. This method was originally presented by Dahlberg & Bergdahl 1974 (as cited in Livneh, 2000). Abuel-Naga, Holtrigter, & Pender (2011) also present various methods, such as the protective pipe method developed by Meardi & Gadsby 1971. That method involves striking a penetrometer rod into the ground with a large tip, as well as a pipe that protects the penetrometer rod. This trick eliminates friction rather effectively, but fitting the protective pipe presents its own set of problems. The hybrid cone penetrometer, which was developed for evaluating railway substructures (Byun, Hong, & Lee, 2015), also have multiple rods. In that kind of test device, the outer rod is used for penetrating ballast dynamically and then the inner mini cone is used for static penetration of subgrade.

Another method of eliminating skin resistance is the process described by Baudrillard 1974 (as cited in Abuel-Naga, Holtrigter, & Pender, 2011). In that process, drilling fluid is injected into the cavity between the impact rod and the soil to reduce friction significantly. In their article, Abuel-Naga, Holtrigter, & Pender (2011) also present a method they have developed, which is based on raising the impact rod intermittently. In their method, the rod is initially raised by 1 m at the end of the test, after which it is driven back into the ground. The number of strikes required is also measured. Then, the rod is raised by 2 m and driven back in by 1 m. This method enables the measurement of the resistance caused by skin friction only, without the dynamic cone resistance. The precondition for a method of this nature is that the hole formed by the cone remains open for a while. As such, the literature indicates that there are a variety of methods for considering skin friction in a DCP test but, reportedly, they have not been applied to the Panda2 device. Skin friction requires further study before it can be reliably eliminated from the results through compensation.

Based on the laboratory results, identifying low-quality structural materials in field locations is challenging. The dynamic cone resistance measured by a DCP-type device correlates most with the dry density of materials, which does not necessarily correlate with the low bearing capacity of embankment materials. The measured dynamic cone resistance values for the Kollola reference material were low due to the low dry density. However, the km137 material had the same dry density and nearly identical dynamic cone resistance behaviour, even though the materials presented apparent differences in the static triaxial test. The laboratory tests showed that the water content and dynamic cone resistance varied significantly in the vertical sample direction. Presumably, the dry density was slightly lower at the bottom of the sample, judging by the decrease in dynamic cone resistance over the final 200 mm. A large number of variable parameters was problematic for results analysis, which is why only the averages for a 500 mm layer were examined. Based on the difficulties in the implementation of the laboratory tests, it is estimated that the dynamic cone resistance at the field sites is influenced by so many factors that it is practically impossible to identify deficiencies in material quality. Furthermore, estimating the moisture content at field locations in different seasons is nearly impossible due to the presence of too many variables.

The ballast material used in the field locations and particularly in the railway environment caused significant problems to the light device. In old track sections, ballast particles may have sunk into or mixed in with the intermediate and insulating layers, in which case more powerful equipment is needed. The DCP rods used in the device were sensitive to the sideways pull caused by boulders. As such, the device is more suitable for softer soil materials and the density monitoring as marketed by the manufacturer, which does not require long rods and where the material is equal to sand or finer in consistency and even-grained. For road structures, the device is most likely fine, if the material is not coarse-grained crushed rock.

## Conclusions

As a device, the dynamic cone penetrometer is quite simple, and Sol Solution has managed to make the Panda2 very easy to use. The lightness of the device is a clear benefit, but it also limits its applications. Based on a comprehensive series of laboratory and field tests, the following responses are provided to the original research questions:

1. A dynamic cone penetrometer type device reacts strongly to the dry density of the material, but moisture content has an impact as

well. However, the results indicate that these parameters are not directly linked to the low bearing capacity of the material, which means that the device cannot be used to identify low-quality substructure materials in railway environments reliably.

2. Drying the sample increased the strength of the material in the triaxial and laboratory tests of a dynamic cone penetrometer. However, field conditions present so many influencing factors that the proportion of moisture content in the test of dynamic cone penetrometer results is likely to not stand out sufficiently among the other factors that have an impact.
3. The light structure of the device is a benefit, but the tests in the railway environment showed that using the device in the vicinity of the ballast layer easily leads to problems. Based on the testing, more robust equipment is required for such environments.

## Acknowledgements

Finnish Transport Infrastructure Agency supported this work. Authors are also grateful for research assistant Toni Saarikoski for making the most of Panda2 tests at the laboratory.

## Funding

Finnish Transport Infrastructure Agency funded this work.

## REFERENCES

- Abuel-Naga, H. M., Holtrigter, M., & Pender, M. J. (2011). Simple method for correcting dynamic cone penetration test results for rod friction. *Géotechnique Letters*, *1*(3), 37-40. <https://doi.org/10.1680/geolett.11.00012>
- Benz-Navarrete, M. A., Breul, P., & Moustan, P. (2019, November). Servo-Assisted and Computer-Controlled Variable Energy Dynamic Super Heavy Penetrometer. In *Geotechnical Engineering in the XXI Century: Lessons learned and future challenges: Proceedings of the XVI Pan-American Conference on Soil Mechanics & Geotechnical Engineering (XVI PCSMGE), 17-20 November 2019, Cancun, Mexico* (p. 65). IOS Press.
- Benz-Navarrete, M. A., Escobar, E., Haddani, Y., Gourves, R., D'Aguiar, S. C., & Calon, N. (2014). Determination of Soil Dynamic Parameters by the Panda 3®: Railways Platform Case. In *Proc. of the Second International Conference on Railway Technology: Research, Development & Maintenance*, Civil-Comp Press, Stirlingshire, UK, Paper (Vol. 56). <https://doi.org/10.4203/ccp.104.56>

- Bolton, M. D., Gui, M. W., Garnier, J., Corte, J. F., Bagge, G., Laue, J., & Renzi, R. (1999). Centrifuge cone penetration tests in sand. *Géotechnique*, 49(4), 543-552. <https://doi.org/10.1680/geot.1999.49.4.543>
- Brough, M. J., Ghataora, G. S., Stirling, A. B., Madelin, K. B., Rogers, C. D. F., & Chapman, D. N. (2003, August). Investigation of railway track subgrade. I: In-situ assessment. In *Proc. of the Institution of Civil Engineers-Transport* (Vol. 156, No. 3, pp. 145-154). Thomas Telford Ltd. <https://doi.org/10.1680/tran.2003.156.3.145>
- Brough, M. J., Ghataora, G., Stirling, A. B., Madelin, K. B., Rogers, C. D., & Chapman, D. N. (2006, May). Investigation of railway track subgrade. Part 2: Case study. In *Proc. of the Institution of Civil Engineers-Transport* (Vol. 159, No. 2, pp. 83-92). Thomas Telford Ltd. <https://doi.org/10.1680/tran.2006.159.2.83>
- Byun, Y. H., & Kim, D. J. (2020). In-situ modulus detector for subgrade characterisation. *International Journal of Pavement Engineering*, 1-11. <https://doi.org/10.1080/10298436.2020.1743291>
- Byun, Y. H., Hong, W. T., & Lee, J. S. (2015). Characterisation of railway substructure using a hybrid cone penetrometer. *Journal of Smart Structures & Systems*, 15(4), 1085-1101. <https://doi.org/10.12989/sss.2015.15.4.1085>
- Chaigneau, L., Gourves, R., & Boissier, D. (2000, February). Compaction control with a dynamic cone penetrometer. In *Proc. of International Workshop on Compaction of Soils, Granulates & Powders, Innsbruck* (pp. 103-109).
- Escobar, E., Benz-Navarrete, M. A., Gourvès, R., Haddani, Y., Breul, P., & Chevalier, B. (2016). *Dynamic Characterisation of the Supporting Layers in Railway Tracks Using the Dynamic Penetrometer Panda 3®*. *Procedia Engineering*, 143, 1024-1033. <https://doi.org/10.1016/j.proeng.2016.06.099>
- Gansonré, Y., Breul, P., Bacconnet, C., Benz, M., & Gourvès, R. (2019). Prediction of in-situ dry unit weight considering chamber boundary effects on lateritic soils using Panda® penetrometer. *International Journal of Geotechnical Engineering*, 1-7. <https://doi.org/10.1080/19386362.2019.1698211>
- Haddani, Y., Breul, P., Saussine, G., Navarrete, M. A. B., Ranvier, F., & Gourvès, R. (2016). Trackbed Mechanical and Physical Characterisation using PANDA®/ Geoendoscopy Coupling. *Procedia Engineering*, 143, 1201-1209. <https://doi.org/10.1016/j.proeng.2016.06.118>
- Kennedy, J. (2011). *A full-scale laboratory investigation into railway track substructure performance and ballast reinforcement* (Doctoral dissertation, Heriot-Watt University).
- Langton, D. D. (1999). The Panda lightweight penetrometer for soil investigation and monitoring material compaction. *Ground Engineering*.
- Lehtonen, I. (2011). *Äärisademäärien muutokset Euroopassa maailmanlaajuisten ilmastomallien perusteella* (in Finnish)
- Li, D., & Selig, E. T. (1995). Evaluation of railway subgrade problems. *Transportation Research Record*, 1489, 17-25.
- Livneh, M. (2000). Friction correction equation for the dynamic cone penetrometer in subsoil strength testing. *Transportation Research Record*, 1714(1), 89-97. <https://doi.org/10.3141/1714-12>

- MacRobert, C. J., Bernstein, G. S., & Nchabeleng, M. M. (2019). Dynamic Cone Penetrometer (DCP) Relative Density Correlations for Sands. *Soils & Rocks*, 42(2), 201-207. <https://doi.org/10.28927/SR.422201>
- Morvan, M., & Breul, P. (2016). Optimisation of in-situ dry density estimation. In *E3S Web of Conferences* (vol. 9, p. 09002). EDP Sciences. <https://doi.org/10.1051/e3sconf/20160909002>
- Ruosteenoja, K., Jylhä, K., & Kämäräinen, M. (2016). Climate projections for Finland under the RCP forcing scenarios. *Geophysica*, 51.
- Scala, A. J. (1956). Simple methods of flexible pavement design using cone penetrometers. *New Zealand Engineering*, 11(2), 34-44.
- Selig, E. T., & Waters, J. M. (1994). *Track geotechnology and substructure management*. Thomas Telford.
- SFS-EN 13286-2:2011 Unbound and Hydraulically Bound Mixtures. Part 2: Test Methods for Laboratory Reference Density and Water Content. Proctor Compaction*
- SFS-ISO 17892-9:2018 Geotechnical Investigation and Testing. Laboratory Testing of Soil. Part 9: Consolidated Triaxial Compression Tests on Water Saturated Soils*
- Spagnoli, G. (2007). An empirical correlation between different dynamic penetrometers. *The Electronic Journal of Geotechnical Engineering*, 12.
- Trenberth, K. E. (2011). Changes in precipitation with climate change. *Climate Research*, 47(1-2), 123-138. <https://doi.org/10.3354/cr00953>
- Vanags, C., Minasny, B., & McBratney, A. B. (2004, December). The dynamic penetrometer for assessment of soil mechanical resistance. In *Proc. of the 3<sup>rd</sup> Australian New Zealand Soils Conference* (pp. 5-9).

PUBLICATION  
III

Water Content Variation of Railway Track Sub-ballast Layer in Seasonal  
Frost Area: a Case Study from Finland

Juha Latvala, Pauli Kolisoja and Heikki Luomala

Transportation Geotechnics, Vol. 38, January 2023, 100926  
<https://doi.org/10.1016/j.trgeo.2022.100926>

Publication is licensed under a Creative Commons Attribution 4.0  
International License CC-BY

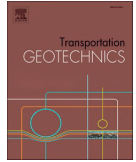






Contents lists available at ScienceDirect

# Transportation Geotechnics

journal homepage: [www.elsevier.com/locate/trgeo](http://www.elsevier.com/locate/trgeo)

## Water content variation of railway track sub-ballast layer in seasonal frost area: A case study from Finland

Juha Latvala <sup>\*</sup>,<sup>1</sup>, Pauli Kolisoja <sup>1</sup>, Heikki Luomala <sup>1</sup>

Research Centre Terra, Tampere University, Finland

### ARTICLE INFO

#### Keywords:

Drainage  
Soil moisture  
Groundwater level  
Sub-ballast layer water content  
Seasonal effects  
Precipitation  
Freezing-thawing

### ABSTRACT

Many previous international studies have found a clear relationship between railway track water content and track geometry problems. The proper drainage of substructures is important in ensuring the safe and efficient operation of tracks. This importance will be emphasized in the future with the increasing frequency of extreme weather phenomena and the raising axle weights of train traffic. In many studies, excessive water content has been found to cause excessive geometry deterioration and mud pumping. These problems are usually related to thin substructure layers. However, in this case study, Finland, track substructures are thick due to frost protection requirements and behave differently to thin substructures. In this study, the long-term water content of three instrumented test sites was monitored to study the seasonal and freeze–thaw effects, as well as the effects of drainage improvement made at one site. In a previously reported part of the same research project, the measured water contents were used in an extensive cyclic loading triaxial test series evaluating the loading resistance of substructure materials taken from the same sites. The drainage improvement resulted in a marked decrease in the average water content at the drainage improvement test site. Simultaneously, high momentary water content values also disappeared. The role of capillary water was observed to be less than expected on Finnish railways.

### Introduction

In the future, many countries intend to increase the axle weights and speeds of trains. Simultaneously, climate change is predicted to further change the global climate with extreme phenomena. Consequently, floods, heavy rains, and extreme drought will become common in some places. [12,30]. In Finland, annual rainfall has already increased and this has been predicted to continue into the coming decades [25,24]. The intensity of individual rains has also been predicted to increase [18]. The effects of a changing climate on infrastructure are causing international concern [22]. For example, a study conducted in Sweden [20] stated that the changing climate would probably increase the unfavorable conditions on Sweden's rail network, and the effects of the changing conditions should be considered as early as possible. The sustainability of infrastructures is an important target, and long-lasting climate-resilient structures save natural resources.

Excessive water weakens different kinds of earth structures. Thus, investigating the effects of track water content on loading resistance to identify the potential benefits of improved drainage is important. To

evaluate the loading resistance of track substructure materials, the long-term seasonal water content including also the freeze–thaw effects of substructure materials are needed. There is an obvious lack of that information in Nordic climatic countries like Finland. Thus, three measuring stations were built at different sites in Finland where the drainage was inoperative to determine the water content of the substructure layers. Material samples were also collected from the sub-ballast layer of these sites. These materials have been tested in the laboratory with cyclic loading triaxial tests at different water contents, and Latvala et al. [17] have reported the results.

In this paper, the measurement results of the water contents at the three monitoring stations are presented. When analyzing the results, the most important research questions are as follows:

- (1) What magnitudes of seasonal water content appear in the sub-ballast layer of an existing track in different locations?
- (2) What is the effect of rain on the water content of track sub-ballast materials?
- (3) How high values of water content capillary rise causes above the groundwater level?

<sup>\*</sup> Corresponding author.

E-mail addresses: [juha.latvala@tuni.fi](mailto:juha.latvala@tuni.fi) (J. Latvala), [pauli.kolisoja@tuni.fi](mailto:pauli.kolisoja@tuni.fi) (P. Kolisoja), [heikki.luomala@tuni.fi](mailto:heikki.luomala@tuni.fi) (H. Luomala).

<sup>1</sup> Postal address: P.O. Box 600, FI-33014 Tampere University, Finland.

<https://doi.org/10.1016/j.trgeo.2022.100926>

Received 4 November 2022; Received in revised form 13 December 2022; Accepted 21 December 2022

Available online 24 December 2022

2214-3912/© 2022 The Author(s). Published by Elsevier Ltd. This is an open access article under the CC BY license (<http://creativecommons.org/licenses/by/4.0/>).

(4) To what extent does drainage improvement influence the water content of the sub-ballast layer?

**Literature review**

The effects of the water content in the track substructure.

Cyclic loading and fine-grained materials with excessive water content are bad combination with regard to track geometry stability [19]. The effects of excessive water content appear either as an increased need for maintenance or, in flooding situations, even as derailments or significant damages [10]. Even a small increase in water content can cause a significant decrease in loading resistance [5], and severe drainage issues can lead to landslides [32]. Problems most likely occur in old sections of the track that do not meet the current requirements and design criteria [20]. However, water-related issues can also appear on high-speed tracks in cold areas [5,33]. Determining the properties of ballast, sub-ballast layers, and subsoil to distinguish the reasons for weak track geometry stability is usually necessary [1].

The relationship between track geometry problems and the water content of track substructure layers is complex. Many studies and laboratory tests have shown that a track is usually vulnerable to geometry deterioration even long after flooding [9]. According to Ghataora and Rushton [8], it can take over four days for water to dry from a single-track section but up to 10 days from a double-track section drained at one side. Wang et al. [31] observed in their ground penetrating radar (GPR) studies that high water content has been detected more in transitional structures than in line sections. This usually causes problems because the dynamic forces are increased in transition zones [27]. Consequently, Wang et al. [31] proposed that the drainages in transition structures should be more effective than in line sections. High water content can also reduce the resonance frequency of the ground and cause vibration issues when train speeds increase [14].

Development of permanent deformations are sometimes tried to be explained by the change in resilient modulus. However, in the study of Latvala et al. [17], the resilient moduli values for Finnish track sub-ballast materials could not forecast the development of permanent deformations in a long-lasting cyclic loading test series. The positive effect of sand blanketing and the intermediate layer below the ballast layer on geometry stability has been recognized Duong et al. [3] and Hasnayn et al. [11]. This layer can prevent typical problems, such as erosion and mud pumping. If the sub-ballast layer is made of coarser materials, it is more resistant to cyclic loading, even in high saturation degrees [28]. Notably, the fines content of substructural layers seems to play a dual role. Duong et al. [4] observed that with reduced water content, the increased fines content reduced permanent deformation. When saturated, the strength of the material with more fines was weakened significantly, and deformation accelerated. This observation is critical because too-high fines contents are often seen in old substructure layer

materials. In Finland, due to frost protection, the total height of non-frost susceptible materials (K) needs to be at least 2,0 m without artificial frost insulation layers, which is exceptionally large than in comparison to many other countries. In Finland, the thickness of the ballast layer is usually 550 mm and the sand blanketing below ballast is 300 mm (Fig. 1). The thickness of the sub-ballast layer varies depending on geographical location to fulfill the frost protection requirements. Even though older track sections are usually not fulfilling these requirement, there is no subsoil-related mud pumping problems in Finland.

**the measurement techniques of the water content in track substructures**

Knowing the actual water content in track substructures is critical in evaluating water content effects. The water content in earth structures can be measured using several techniques. The most traditional method is taking material samples [23]. However, this disturbs the substructure and is labor-intensive [15]. The development of technology has enabled the use of new, nondestructive methods, such as GPR [29], in substructure evaluation with faster implementation. These nondestructive methods have the advantage of gathering more measurement data. Between these methods lies the time domain reflectometer (TDR) method, where a sensor is lowered into a plastic pipe installed in the structure. This method was tested by İzvolt et al. [13] when performing calibrations for coarse-grained materials, and good accuracy was achieved.

The GPR effectively produces longitudinal data on layer structures and the water content of track substructures. However, subsequent application requires complex signal processing [21]. To reliably determine actual water content, GPR results should be calibrated using samples and test pits [31]. If the lower part of the ballast layer is contaminated with fine particles, the GPR does not penetrate this layer adequately [1]. Another method that has aroused interest is electrical resistivity tomography (ERT), which is based on changes in the earth's resistance due to the influence of water content. Chambers et al. [2] examined the water content of an old railway embankment using ERT. The results were promising and interesting, but the method was complex to implement. In the depth and lateral directions of the embankment, there was a clear variation in the water content, but the embankment was heterogeneous in terms of materials. They presented that in determining water content, petrophysical equations between the water content, the resistance, and the temperature measurement of the embankment were required since resistivity changes with temperature. In Finland and other northern countries, the water content in road substructures has been measured using Percostations, which measure dielectricity, electrical conductivity, and temperatures at different road structure depths [16].

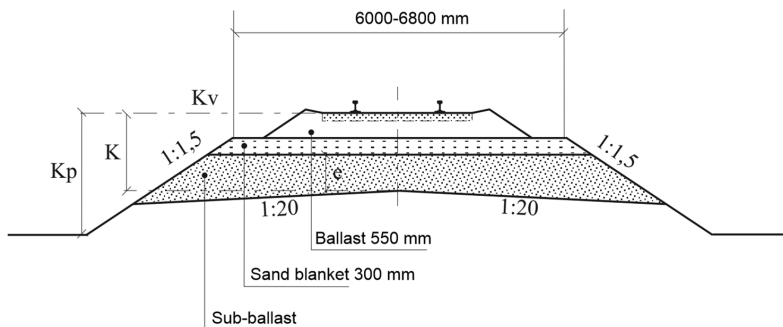


Fig. 1. The cross-section of a typical single line Finnish track [7].

**Materials and methods**

*Description of measurement sites*

Water content measuring stations were installed at three sites on the Rantarata track line, which runs along the southern coast of Finland, in various cross-sections where the drainage was assumed to be faulty. Repeated track geometry deterioration problems have occurred at all three sites or in their vicinities. The subsoil conditions in Rantarata are known to change quickly from bedrock cuts to soft clay layers over 10 m thick. The original idea was to improve the drainage of all three sites and determine the effects of drainage improvement. However, within this monitoring period, only the drainage at kilometer (Km) 44 was improved.

**Km 44**

The monitoring site at Km 44 is located in a flat area where the track is about the height of a ballast layer higher than the surrounding terrain. This is shown in an overview of the area before and after drainage improvement, taken on July 04, 2017, and January 29, 2020 (Fig. 2). The subsoil under the track is clay with a thickness of about 16–18 m.

During sensor installation, the ballast layer thickness was found to be much thicker than normal 0,55 m and the ballast particles were found up to the depth of 1 m mixed with sub-ballast material. The track has presumably sunk into the clay layer over time due to consolidation settlement. The prevailing drainage condition of the site was challenging, as the site is located on a flat area, and the surrounding terrain partly slopes in the direction of the track. There was a short ditch on one side of the track near the measuring point, and on the other side, a small ditch at the edge of the field, which was already quite far away. The water level in the ditches was high during all inspection visits, indicating that the water was not getting out of the track area. At the turn of 2019 until 2020, drainage improvement was conducted at the site by installing a drain on the side of the measuring station to the depth of –1,85 m. After that, the area was shaped, and the ditches were deepened. Simultaneously, the water drainage path outside the track area was also improved.

**Km 98**

The track at Km 98 is located on an embankment in a field (Fig. 3). The site represents a typical Finnish track. The subsoil is mainly silty clay, but there are also layers of fine sand near the measurement station.



**Fig. 2.** The areal picture of Km 44 before and after the drainage improvement from opposite perspectives. The track is on flat terrain, and the drainage was not working properly. Photos taken on May 04, 2017, and January 29, 2020.



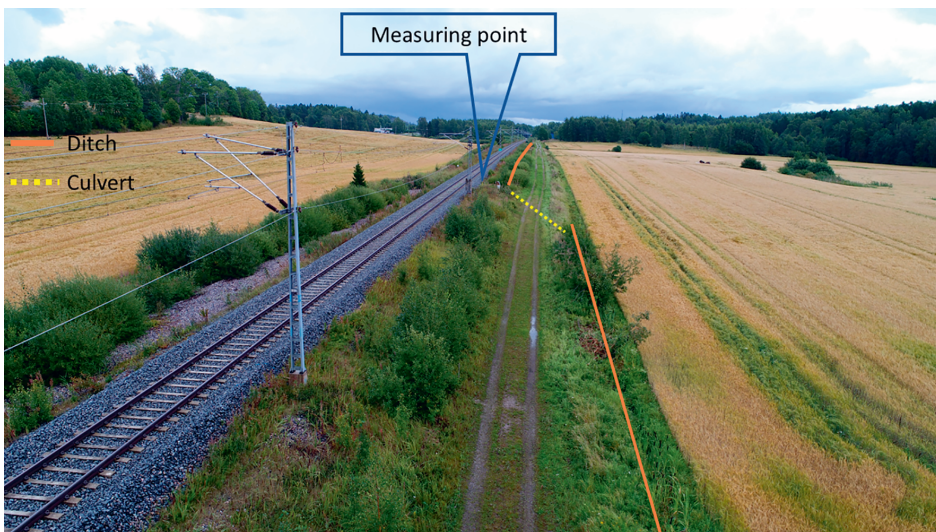


Fig. 3. The areal picture of Km 98 eastward. The track runs through a field on an embankment. The site is “average” and represents a typical Finnish track. Photo taken on August 22, 2017.

The thickness of the soft soil layer under the measuring station is 13.5–14.5 m. The drainage condition of the site can be considered typical. On the south side of the track (on the right in the picture), there is a ditch in reasonable condition, which, however, ends at the monitoring station. The water was supposed to flow from the culvert running under the service road, but the culvert was inspected to be in poor condition. On the north side of the track, there is no actual ditch between the field and the track. Improving the drainage at the site is easily possible by digging up the existing ditch, repairing the culvert, and making a proper ditch on the north side of the track.

**Km 137**

Km 137 is significantly different from the other two sites, as it is located next to a sand esker (Fig. 4). The surface of the ground is very dry. Sites like this are suspected to have some underground water flow due to the height differences and the esker. Consequently, the site was selected as one monitoring site. The thickness of the sand layer in the direction of the track varies. At the monitoring station, the sounding rods penetrated 3.9–4.0 m deep. After that, there was a hard bottom, probably a bedrock. Near the measuring station, 100–200 m away, there is a rock cut and a tunnel through the rock at the same distance on the other side. Therefore, the subsoil conditions vary rapidly at this site.



Fig. 4. The southwest areal picture of Km 137. The site is located near the sand esker that slopes in the direction of the track. Photo taken on May 04, 2017.

the measurement system

With the help of measurement stations, determining the effects of drainage arrangement changes and studying the seasonal effects is possible. The stations are equipped with sensors measuring the following quantities:

- 1) Displacement sensors measuring vertical displacements of the track
- 2) Sensors measuring the water content, temperature, and electrical conductivity of the sub-ballast layer. Temperature sensors are used to determine frost penetration depth.
- 3) Sensors measuring the suction pressure in the sub-ballast layer
- 4) Tensiometers at two different depths
- 5) Groundwater level pipes and sensors
- 6) Water level measurement in ditches
- 7) Rain gauges

Fig. 5 shows an example of the cross-section of the sensors installed at monitoring stations in the cross-section of the railway embankment. The water content measurement of the substructure was mainly based on TDR-type sensors (Decagon GS1/GS3) under the track shoulder. The suction pressure was also measured, but the system did not work as reliably as planned. The sampling rate of these sensors was 30 min so that the effects of individual rains could be detected from the data. For the water content sensors, the general coefficient provided by the manufacturer was used as the calibration coefficient. This general coefficient should be suitable for measuring all kinds of sand materials because the TDR frequency of sensor is high (70 MHz). Determining a more accurate calibration coefficient would have been challenging, as there was a noticeable vertical variation in the materials of the sub-ballast layer. Consequently, many sensors would have had to be calibrated separately. The volumetric water content was converted into saturation degrees using the measured maximum volumetric water content. The saturated state was observable in the lower sensors. For converting the upper sensors' reading to saturation degrees, the theoretical values calculated from laboratory tests were used with the help of the lower sensors' maximum water contents. Thus, the measurement resolution was assumed to be about 10 %, in terms of degree. In the cyclic loading triaxial tests, the biggest changes appeared above a 70 % saturation degree [17], and those moments could be observed from field measurement data.

Sub-ballast material properties of measurement sites

The material samples from the sub-ballast layers of the sites were collected during the installation of measurement stations. These samples

have been examined in the laboratory. One additional good-quality reference material was also included in the laboratory tests, which fulfilled the Finnish Transport Infrastructure Agency (FTIA) requirements for the sub-ballast layer at the time of the study. Fig. 6 shows the grain size distribution curves of the materials, and Table 1 shows the typical geotechnical parameters. Only one of the samples, the one taken from Km 44, fulfilled the granularity requirements. All the samples taken from the field differed from the reference material, mainly on the finer end of the grading curve. The Km 137 material was mostly out of the FTIA grading limits due to its small average particle size, and as a uniformly-grained material, it was poorly compactable.

Laboratory capillarity measurements

The determinations of the capillary rise height were performed on the material samples from the field sites in the laboratory. The tests were related to a research project that investigated the effect of capillarity on the loading resistance of materials and the differences in methods used for determining the height of capillary rise [26]. Fig. 7 shows the most important results from the capillarity tests performed in the open capillary rise pipes. These tests have been performed by adapting the SFS-EN 1097-10 standard [6], but the samples have been disassembled in layers to determine the vertical water content profile. The saturation degree above the water level seems to decrease rapidly when the distance from the water level increases. At 20 cm from the water surface, the degree of saturation was around 50–70 %, and at 35 cm above the free water level, it was less than 50 % for all the examined materials. The material density greatly affects the maximum capillary rise, as indicated by the wetting of particle surfaces in the capillary test arrangement. For example, in the Km 44 material, the difference between the very dense (2.11 g/cm<sup>3</sup>, Rc (Relative Compaction) 103 %) and loose (1.89 g/cm<sup>3</sup>, Rc 93 %) states was about 35 cm. In these tests, the maximum height of capillary rise is also time-dependent, as the water continued to rise even after 50 days with sand materials. However, the rising rate slowed significantly but continued slowly. As aforementioned, the test sites' materials differed from the current FTIA guidelines and contained too many fine particles, so their capillary rise height can be considered too high for substructure materials.

Results of water content measurements

The measurement results are continuous data from July 2017 to the beginning of 2022. Shorter periods are also examined to study the effects of individual rains. The measured water content at the sites is illustrated with heatmap-type images, where the saturation ratio of the sub-ballast layer is shown using colors. The installation depth of the sensors varied

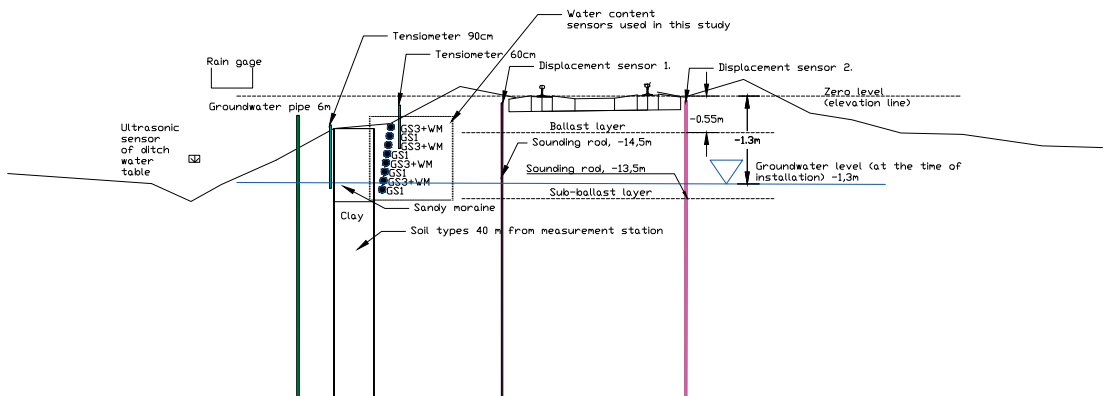


Fig. 5. An example of installed measurement instruments in track cross-section (Km 98).

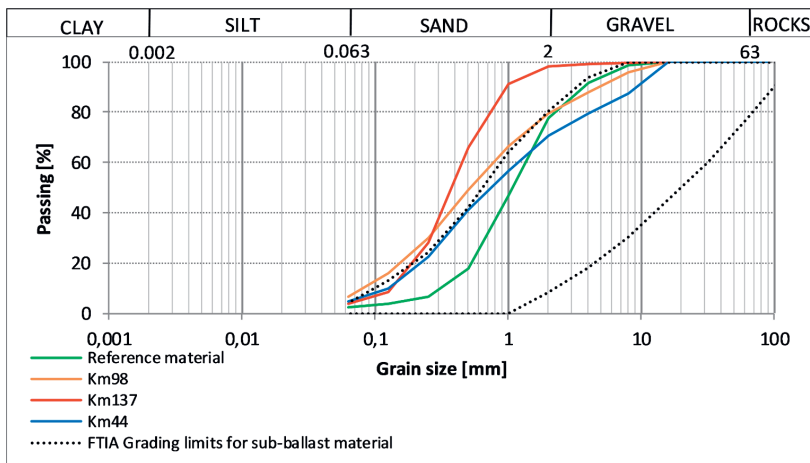


Fig. 6. The measured grain size distributions of the test materials. Dashed lines describe the grading limits of the Finnish Transport Infrastructure Agency for sub-ballast material.

Table 1  
Geotechnical properties of monitoring site material samples.

| Material               | Particle size $d_{50}$ [mm] | Uniformity Coefficient $d_{60}/d_{10}$ [-] | Fines fraction content $\phi$ less than 0.06 mm [%] | Dry density $\rho_d$ max/optimum water content $w$ [ $g/cm^3$ ] / [%] |
|------------------------|-----------------------------|--|---|---|
| Reference material 0/8 | 1.1                         | 4.7  | 2.5   | 1.91/2.8  |
| Km 44                  | 0.7                         | 10.0                                       | 4.9   | 2.03 / 8.5  |
| Km 98                  | 0.5                         | 10.0                                       | 6.7   | 2.14 / 3  |
| Km 137                 | 0.4                         | 3.5  | 3.7   | 1.80/ 5.9   |

from site to site, so different sites cannot be compared directly to each other, but all presented results are from the sub-ballast materials monitored by sensors presented in Fig. 5. Generally, it is also good to remember that TDR soil moisture sensors can measure only the volume of liquid water. Therefore, measurement results were filtered out when the sensors were below 0 °C (white areas on the heatmap in wintertime). White areas are also caused at some other times due to sensor maloperation.

Long-term water content

Fig. 8 shows the long-term water contents of the monitoring site, Km 44. During the measurement history, before the drainage improvement at the turn of 2019 until 2020, the site experienced several periods of

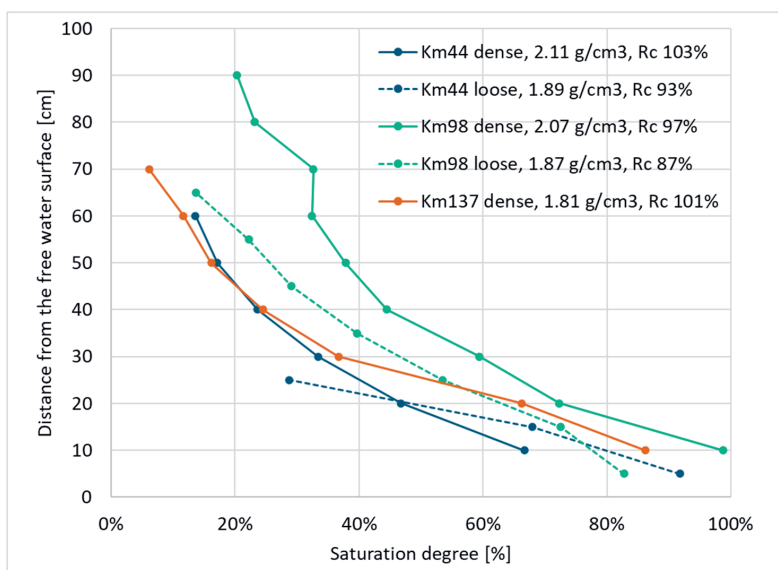


Fig. 7. Results of the height of capillary rise tests. The saturation degree decreases rapidly above the surface of the free water level.



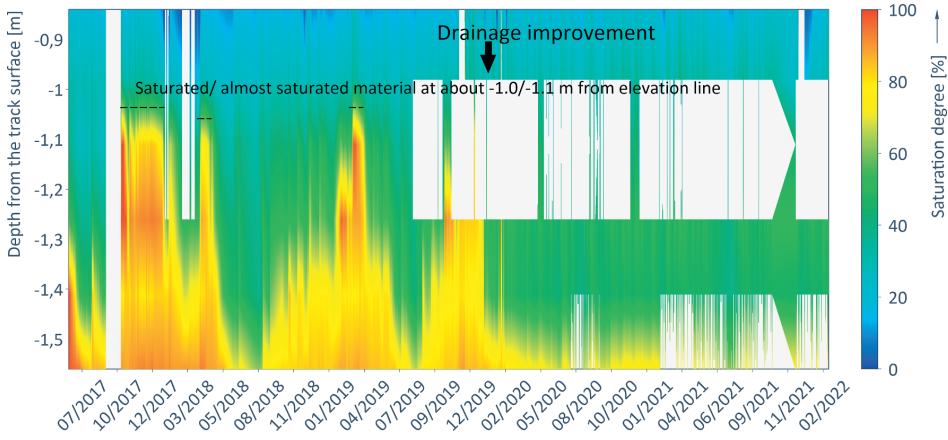


Fig. 8. The saturation degree of Km 44 sub-ballast layer. White boxes are due to intermittent malfunctions of two sensors.

high water content. The saturated zone extended to a depth of  $-1.0$  m from the track elevation line (zero level). These high water level moments appeared in autumn and summertime. In July 2017 and May 2018, the saturation ratio was at its lowest when the saturation ratio of the sub-ballast was approximately 50 % in the deeper structure and less than 20 % near the surface. After the drainage improvement, high water contents were no longer measured, and the saturation degree remained below 60 %. In the lowest sensor located  $-1.56$  m below the elevation line, there have been momentary indications of 70 %–80 % saturation degrees. Based on these measurements, the groundwater level is most likely located under the lowest sensors after the drainage improvement.

At the second monitoring site, Km 98, the water content variation cycle differed from Km 44. Fig. 9 shows the results of the long-term measurements, where the water content remained surprisingly constant during the monitoring period. In the autumns of 2017 and 2018, increased water content takes place between 1.0 m and 1.2 m below the elevation line. This can also be seen in the upper part of the sub-ballast layer, as the water content has risen to 50 %–70 % saturation degree. The variations appearing at a depth of  $-1.35$  m suggest that the material surrounding the sensor at a depth of  $-1.2$  m has better water retention capacity due to spatial variation on the layer material. The structure has also possibly dried to a saturation degree of 70 %–80 % at a

depth of  $-1.4$  m. This drying, however, is not very clearly visible in the upper part of the sub-ballast layer, indicating clayish spots in the sub-ballast layer. The effect of rain periods is visible in the upper and lower parts of the sub-ballast layer, but the magnitude of the effects is quite modest.

Fig. 10 shows the long-term measurements of the driest measurement site, Km 137. Water content generally remained low, with less than a 60 % saturation. However, the variation in water content caused by rains is evident from time to time, which is partially explained by the good water permeability of the sub-ballast material at this site. In the sub-ballast layer, high water contents caused by the melting of frost have occurred in the spring, where the water content in the upper part of the structure has risen close to the saturated state. Fortunately, these moments have been short and mostly lasted only for a few days at a time.

**Short-term water content fluctuations**

In addition to the long-term seasonal water content fluctuations, short-term phenomena were also analyzed. Fig. 11 shows an example from the autumn of 2017 at Km 44, which was very rainy from September to the end of year 2017. The precipitation measured at Km 44 was 106 mm in October and almost 140 mm in November. This rainy

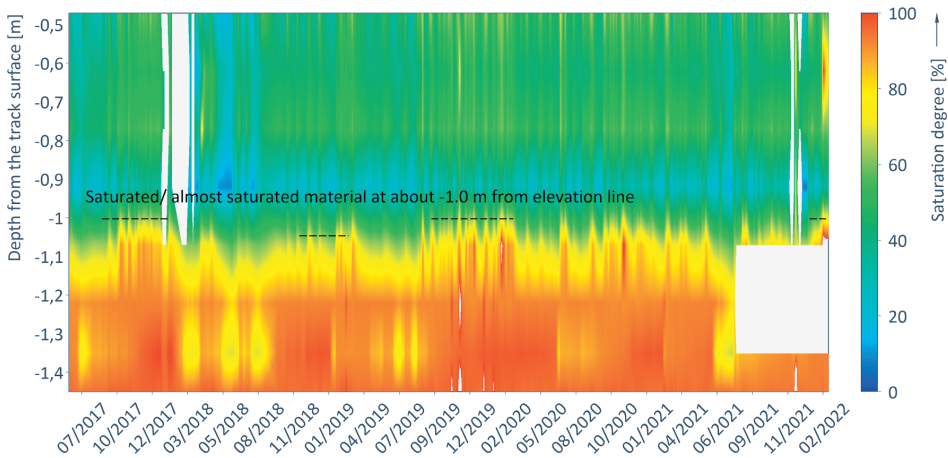


Fig. 9. The long-term saturation degrees of Km 98 sub-ballast layer. The white box is due to the malfunction of one sensor.

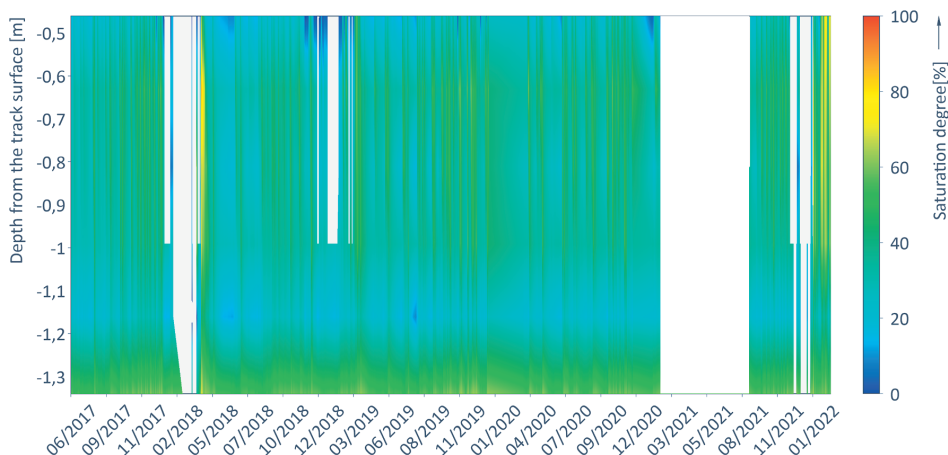


Fig. 10. The long-term saturation degrees of Km 137 sub-ballast layer. The long white area is due to the malfunction of data logger.

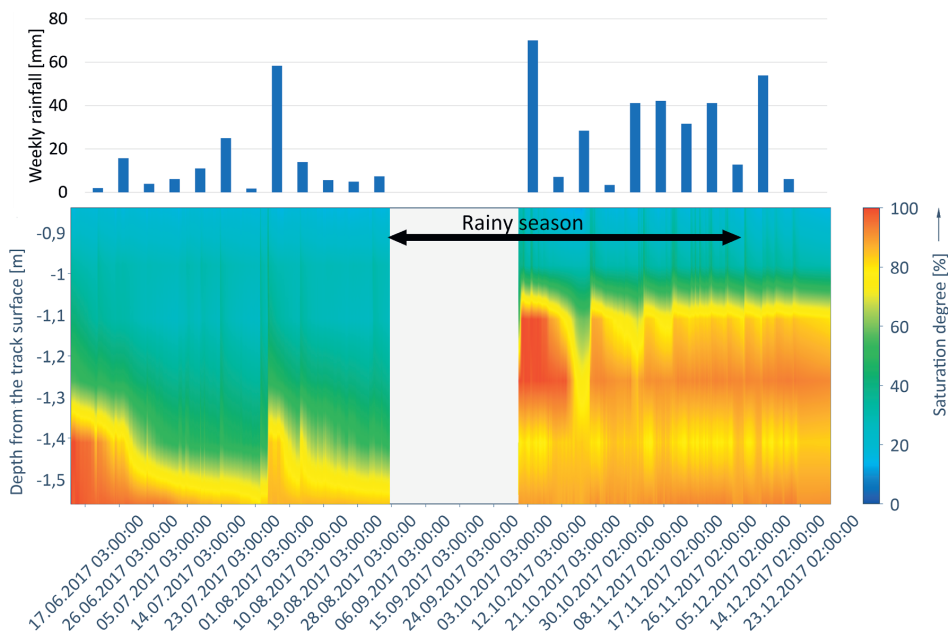


Fig. 11. Saturation degrees of Km 44 sub-ballast layer with weekly rainfalls during the summer and autumn of 2017. White area is due to total malfunction of measurement station.

season affected the water content of the upper part of the structure such that water content quickly increased from 20 to 30 % to a 50–60 % saturation degree and the practically saturated zone rose from the – 1.5 m level to the – 1.05 m level. This was due to the areal water level rather than water retained in the upper part of the structure from rains. A similar analysis was carried out for Km 98 in the autumn of 2019, and Fig. 12 shows the results. In the upper part of the sub-ballast layer, about 70 % saturation degrees have been measured to be caused by rain. Still, deeper in the sub-ballast, the surrounding water level has probably risen, which is visible in the deepest sensors’ readings. The structure of Km 98 retains water better than Km 44.

Regarding Km 137, the short-term review focused on frost thawing,

and Fig. 13 shows the respective measurement results. The white area at the beginning of the period was filtered out because the sensors could not measure the amount of frozen water correctly. In the spring of 2018, frost melting caused a period of approximately 80 % saturation, especially below the ballast layer, lasting for about 10 days. The water content of the rest of the sub-ballast has also increased significantly. The highest moisture contents are thus measured at the level where the increase of stresses caused by overpassing train loads is still moderately high.



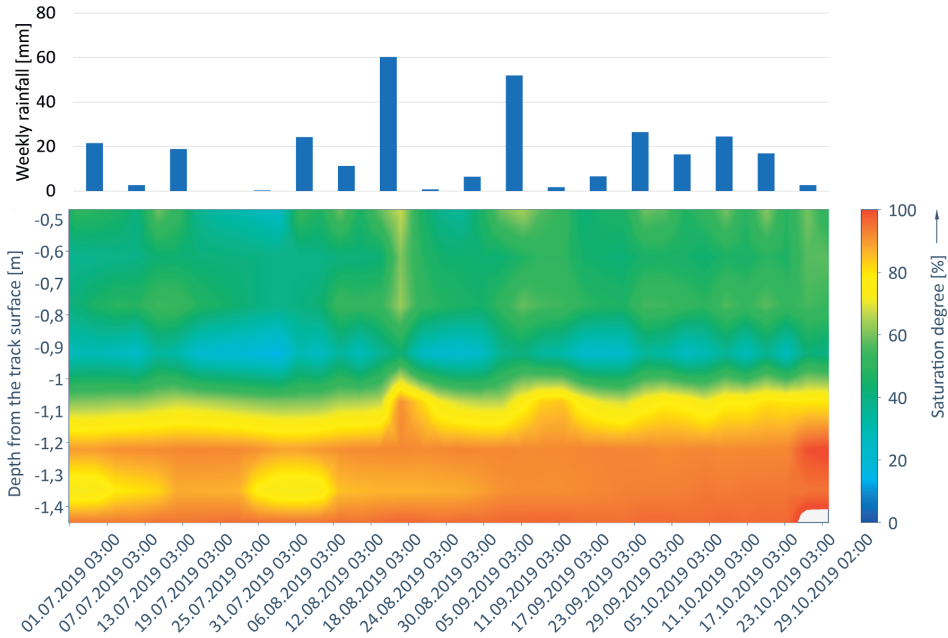


Fig. 12. Saturation degrees of Km 98 sub-ballast layer with weekly rainfalls during the rainy season of 2019.

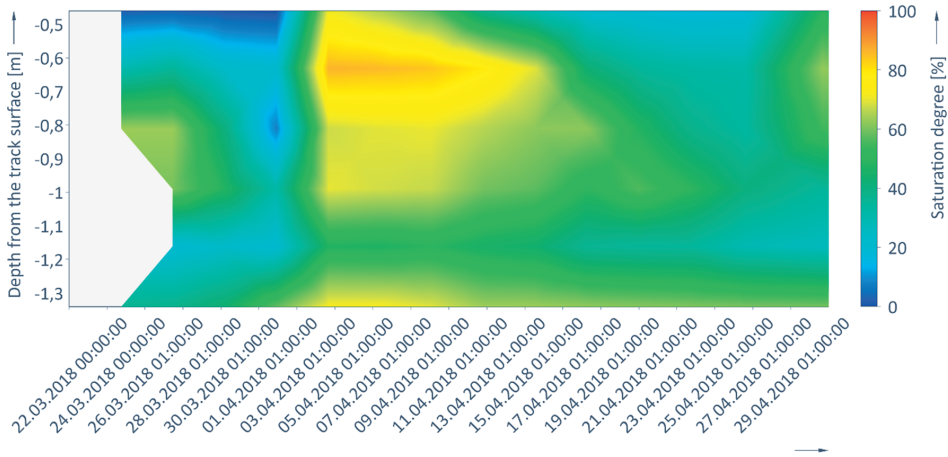


Fig. 13. Saturation degrees on Km 137 sub-ballast layer during the frost thawing period of 2018.

**Discussion and conclusion**

Based on the measurement results obtained from the monitoring sites, the water content of existing railway track embankments varies depending on the site, drainage conditions, and sub-ballast materials. At the minimum, 20 %–30 % saturation degrees were measured for the field sites. At the maximum, the sub-ballast layer was completely saturated up to – 1.0 m from the elevation line before the drainage improvement at Km 44. Almost completely saturated moments were also observed when the seasonal frost thawed. Predictably, water content varied according to the seasons. At monitoring site Km 44, the most intensive water content fluctuations were observed because the

groundwater level was close to the sub-ballast layer of the track before the drainage improvement.

Rain increases the water content in the upper part of the track sub-ballast layer but does not bring it to a completely saturated state, even if the sub-ballast materials contain a reasonably high amount of fines (>4%). Mainly, the upper part of the sub-ballast remained at a 60 % saturation degree at highest even during the rainy season, but approximately 70 % saturation was observed momentarily at the Km 98 site. However, this is due to the silt/clay-rich zones in the sub-ballast material of Km 98, which retains water. Therefore, the water content of the upper part of the sub-ballast layer has been higher than at the other two sites throughout the measurement history. A saturated/almost saturated

state detrimental to structures seems to be formed mainly due to the rise of (ground) the water level in the vicinity of the sites. This information facilitates the planning of drainage measures, as if the groundwater level will be kept at the desired level, the relatively open structure of the track does not seem to lead to particularly critical water content provided that the sub-ballast material grading is near the recommendations. However, it must be observed that the water content in this study was measured under the track shoulder, so the center of the embankment may dry slower. The almost saturated moments during the thawing period are difficult to eliminate by drainage because they are caused by melting snow and ice when the underlying structure is still partially frozen and almost impermeable.

The effect of capillary water on the sub-ballast materials of the track seems to be smaller than expected. Based on field measurements, an almost saturated capillary zone of about 10 cm appeared above the groundwater level at Km 44, where the water level has been high. In Km 98, the capillary zone has been larger, about 20–30 cm, but the water content has only been corresponding to 50 %–60 % saturation degree. Based on capillarity tests carried out in the laboratory, the degree of saturation of even low-quality materials is usually less than 70 %, around 20 cm from the free water surface. Therefore, the capillary rise would not be a problem with track sub-ballast materials classified as sand.

The drainage improvement at the monitoring site Km 44 proved to be functional. The starting point was difficult regarding site drainage, and the measurement results confirm that successful drainage improvement at a site like this is possible. The drainage improvement significantly reduced the occurrence of saturated conditions at the site, and the water content of the sub-ballast layer remained low after the improvement measures. Interestingly, also the seasonal variation disappeared almost completely, and the saturation level of the sub-ballast layer remained far from the saturated state all year round.

Significant differences in loading resistance behavior between the different sub-ballast materials were recognized in triaxial tests [17]. In the static triaxial tests, the maximum shear strength increased below a 50 % saturation degree on test site materials. This increase was due to increasing matrix suction. On the contrary, in the cyclic loading triaxial tests, differences in loading resistance were observed above 50 % saturation degrees. The different influencing methods explain this. In the static test, the matrix suction is the dominant factor, and in the cyclic tests, the development of pore water pressure decreases the loading resistance. The results of triaxial tests conducted with the test site materials led to the conclusion that over 70 % saturation degrees should be avoided on Finnish railways. However, below that, tested materials would probably work reasonably. Maintaining in-situ conditions so the saturation degree remains below 50 % to obtain the benefits of matrix suction is unlikely. Based on the water content measurements from the sites, saturation degrees lower than 70 % can be obtained by keeping the groundwater level low.

Based on this study, the following answers to the research questions can be given:

- 1) *The water content varies between 20 % and 100 % saturation degrees but usually stays below 70 % saturation degree above the groundwater level. The measurement data shows a surprisingly little saturated volume immediately below the ballast, although the track surface is exposed to rain. The water content in the top part of the sub-ballast layer significantly influences its loading resistance behavior. Sub-ballast materials containing lot of fines expose the track structure to maximum saturation degrees higher than 50 %. The melting of the frozen structure causes momentary, high but short-term water content.*
- 2) *Individual rain limitedly affects water content. In the upper part of the structure, with sub-ballast materials from Km 44 and Km 98 containing 4.9 % and 6.7 % of fine particles, rain raised the saturation level to 60 %–70 % at highest. In the monitoring sites, the most critical effect of rains is mainly a rise in the groundwater level of the area, which eventually creates a saturated state. To control the effects of rain, keeping the height of the water level under control using proper drainage methods is sufficient.*
- 3) *The effect of capillary rise is smaller than expected for the materials and structures studied. Significant capillary water content occurs mainly 20–30 cm above the free water surface, and the water content decreases rapidly as the distance increases from the free water surface. The water content measured in the field corresponds to those in the laboratory experiments, and the capillary rise could not create an almost saturated state with the examined materials.*
- 4) *At site Km 44, the drainage improvement affected the water content of the structure. After the drainage improvement, the seasonal high water content disappeared, and the sub-ballast layer was drier than before. The main impact occurred at a depth of – 1.0–1.55 m. The drainage improvement worked better than expected because the initial situation at the site was difficult.*

#### Funding and Acknowledgements

Authors are thankful for Finnish Transport Infrastructure Agency funding this study. The authors would also like to thank Enago for the English language review.

#### CRediT authorship contribution statement

**Juha Latvala:** Investigation, Data curation, Writing – original draft.  
**Pauli Kolisoja:** Supervision. **Heikki Luomala:** Supervision.

#### Declaration of Competing Interest

The authors declare that they have no known competing financial interests or personal relationships that could have appeared to influence the work reported in this paper.

#### Data availability

Data will be made available on request.

#### References

- [1] Brough M, Stirling A, Ghataora G, Madelin K. Evaluation of railway trackbed and formation: a case study. *NDT E Int. Third NDT Methods in Railway Engineering* 2003;36:145–56. [https://doi.org/10.1016/S0963-8695\(02\)00053-1](https://doi.org/10.1016/S0963-8695(02)00053-1).
- [2] Chambers JE, Gunn DA, Wilkinson PB, Meldrum PI, Haslam E, Holyoake S, et al. 4D electrical resistivity tomography monitoring of soil moisture dynamics in an operational railway embankment. *Surf Geophys* 2014;12:61–72. <https://doi.org/10.3997/1873-0604.2013002>.
- [3] Duong TV, Cui Y-J, Tang AM, Dupla J-C, Canou J, Calon N, et al. Investigating the mud pumping and interlayer creation phenomena in railway sub-structure. *Eng Geol* 2014;171:45–58. <https://doi.org/10.1016/j.enggeo.2013.12.016>.
- [4] Duong TV, Tang AM, Cui Y-J, Trinh VN, Dupla J-C, Calon N, et al. Effects of fines and water contents on the mechanical behavior of interlayer soil in ancient railway sub-structure. *Soils Found* 2013;53:868–78. <https://doi.org/10.1016/j.sandf.2013.10.006>.
- [5] Ferreira, T.M., Teixeira, P.F., 2011. Impact of different drainage solutions in the behavior of railway trackbed layers due to atmospheric actions. 9th World Congr Railw Reserach-May 22 26, 1–14.
- [6] Finnish Standards Association, 2014. SFS-EN 1097-10.
- [7] Finnish Transport Infrastructure Agency, 2018. Ratatekniset ohjeet (RATO) osa 3 radan rakenne (in English: Track construction guidelines, part 3: the structure of track).
- [8] Ghataora GS, Rushton K. Movement of Water through Ballast and Subballast for Dual-Line Railway Track. *Transp Res Rec* 2012;2289:78–86. <https://doi.org/10.3141/2289-11>.
- [9] Hasnain M, John McCarter W, Woodward PK, Connolly DP, Starrs G. Railway subgrade performance during flooding and the post-flooding (recovery) period. *Transp Geotech* 2017;11:57–68. <https://doi.org/10.1016/j.trgeo.2017.02.002>.
- [10] Hasnain M, m., Medero, G. m., Woodward, P. k., Railway track performance during and post flooding. In: *Geotechnical Engineering for Infrastructure and Development, Conference Proceedings*. ICE Publishing; 2015. p. 379–84. <https://doi.org/10.1680/ecsenge.60678.vol2.037>.
- [11] Hasnain MM, McCarter WJ, Woodward PK, Connolly DP. Railway subgrade performance after repeated flooding – Large-scale laboratory testing. *Transp Geotech* 2020;23:100329. <https://doi.org/10.1016/j.trgeo.2020.100329>.

- [12] Hosseinzadehtalaei P, Tabari H, Willems P. Climate change impact on short-duration extreme precipitation and intensity–duration–frequency curves over Europe. *J Hydrol* 2020;590:125249. <https://doi.org/10.1016/j.jhydrol.2020.125249>.
- [13] Izvolt, L., Dobeš, P., Mečár, M., 2016. Calibration of TDR Test Probes for Measuring Moisture Changes in the Construction Layers of the Railway Line. *Procedia Eng., World Multidisciplinary Civil Engineering-Architecture-Urban Planning Symposium 2016, WMCAUS 2016* 161, 1057–1063. <https://doi.org/10.1016/j.proeng.2016.08.848>.
- [14] Jiang H, Bian X, Chen Y, Han J. Impact of Water Level Rise on the Behaviors of Railway Track Structure and Substructure. *Transp Res Rec J Transp Res Board* 2015;2476:15–22. <https://doi.org/10.3141/2476-03>.
- [15] Khakiev Z, Shapovalov V, Kruglikov A, Morozov A, Yavna V. Investigation of long term moisture changes in trackbeds using GPR. *J Appl Geophys* 2014;110:1–4. <https://doi.org/10.1016/j.jappgeo.2014.08.014>.
- [16] Kolisoja P, Kurki A, Kalliainen A, Vuorimies N, Saarenketo T. Integrated Monitoring of Seasonal Variations and Structural Responses to Enable Intelligent Asset Management of Road Infrastructures. In: Correia AG, Tinoco J, Cortez P, Lamas L, editors. *Information Technology in Geo-Engineering, Springer Series in Geomechanics and Geoen지니어ing*. Cham: Springer International Publishing; 2019. p. 687–98. [https://doi.org/10.1007/978-3-030-32029-4\\_58](https://doi.org/10.1007/978-3-030-32029-4_58).
- [17] Latvala J, Kolisoja P, Luomala H. The cyclic loading resistance of old railway track sub-ballast materials at different water contents. *Transp Geotech* 2022;35:100772. <https://doi.org/10.1016/j.trgeo.2022.100772>.
- [18] Lehtonen I. *Äärisademäärien muutokset Euroopassa maailmanlaajuisten ilmastomallien perusteella*. University of Helsinki; 2011. Master's Thesis).
- [19] Li D, Selig ET. Evaluation of railway subgrade problems. *Transp Res Rec* 1995; 1489:17.
- [20] Lindgren J, Jonsson D, Carlsson Kanyama A. Climate Adaptation of Railways: Lessons from Sweden. *Eur J Transp Infrastruct Res* 2009;9. <https://doi.org/10.18757/ejitr.2009.9.2.3295>.
- [21] Liu S, Lu Q, Li H, Wang Y. Estimation of Moisture Content in Railway Subgrade by Ground Penetrating Radar. *Remote Sens* 2020;12:2912. <https://doi.org/10.3390/rs12182912>.
- [22] Palin EJ, Stipanovic Oslakovic I, Gavin K, Quinn A. Implications of climate change for railway infrastructure. *WIREs Clim Change* 2021;12:e728.
- [23] Reynolds SG. The gravimetric method of soil moisture determination Part I A study of equipment, and methodological problems. *J Hydrol* 1970;11:258–73. [https://doi.org/10.1016/0022-1694\(70\)90066-1](https://doi.org/10.1016/0022-1694(70)90066-1).
- [24] Ruosteenoja K, Jylhä K. Projected climate change in Finland during the 21st century calculated from CMIP6 model simulations. *Geophysica* 2021;56:39–69.
- [25] Ruosteenoja K, Jylhä K, Kämäräinen M. Climate projections for Finland under the RCP forcing scenarios. *Geophysica* 2016;51.
- [26] Saarikoski, T., 2020. Kapillaarisen nousukorkeuden määrittämenetelmät ja hyödynnettävyys radan alusrakennemateriaalien laadun arvioinnissa. *Capillary Rise – Determination Methods and Potential as Quality Assessment parameter for Subballast Materials of Railway Track*.
- [27] Sañudo R, dell'Olio L, Casado JA, Carrascal IA, Diego S. Track transitions in railways: A review. *Constr Build Mater* 2016;112:140–57. <https://doi.org/10.1016/j.conbuildmat.2016.02.084>.
- [28] Schulz-Poblete MV, Gräbe PJ, Jacobsz SW. The influence of soil suctions on the deformation characteristics of railway formation materials. *Transp Geotech* 2019; 18:111–23. <https://doi.org/10.1016/j.trgeo.2018.11.006>.
- [29] Silvast M, Nurmikolu A, Wiljanen B, Levomäki M. Identifying frost-susceptible areas on Finnish railways using the ground penetrating radar technique. *Proc. Inst. Mech. Eng Part F Rail Rapid Transit* 2013;227:3–9. <https://doi.org/10.1177/0954409712452076>.
- [30] Trenberth KE. Changes in precipitation with climate change. *Clim Res* 2011;47: 123–38.
- [31] Wang H, Silvast M, Markine V, Wiljanen B. Analysis of the Dynamic Wheel Loads in Railway Transition Zones Considering the Moisture Condition of the Ballast and Subballast. *Appl Sci* 2017;7:1208. <https://doi.org/10.3390/app7121208>.
- [32] Xu Q, Zhang L. The mechanism of a railway landslide caused by rainfall. *Landslides* 2010;7:149–56. <https://doi.org/10.1007/s10346-010-0195-y>.
- [33] Cai JQ, Liu SX, Fu L, Feng YQ. 2016. Detection of railway subgrade moisture content by GPR. In: 2016 16th International Conference on Ground Penetrating Radar (GPR). Presented at the 2016 16th International Conference on Ground Penetrating Radar (GPR), pp. 1–5. <https://doi.org/10.1109/ICGPR.2016.7572613>.



# PUBLICATION IV

The Cyclic Loading Resistance of Old Railway Track Sub-ballast materials  
at Different Water Contents

Juha Latvala, Pauli Kolisoja and Heikki Luomala

Transportation Geotechnics, Vol. 35 July 2022, 100772  
<https://doi.org/10.1016/j.trgeo.2022.100772>

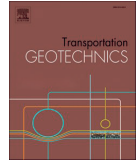
Publication is licensed under a Creative Commons Attribution 4.0  
International License CC-BY





Contents lists available at ScienceDirect

# Transportation Geotechnics

journal homepage: [www.elsevier.com/locate/trgeo](http://www.elsevier.com/locate/trgeo)

## The cyclic loading resistance of old railway track sub-ballast materials at different water contents

Juha Latvala<sup>\*</sup>, Pauli Kolisoja, Heikki Luomala

Research Centre Terra, Tampere University, P.O. Box 600, FI-33014, Finland

### ARTICLE INFO

#### Keywords:

Drainage  
Soil moisture  
Railway track substructure  
Sub-ballast layer  
Cyclic triaxial test  
Soil loading resistance

### ABSTRACT

Water content is one of the most important factors influencing the performance of earth structures. It is well known that the water content of sand has a significant effect on its shear strength and its resistance to cyclic loading. In this study, the loading resistance of four different sand materials was investigated in a cyclic load triaxial test at different water contents. Three of the four material samples were taken from the sub-ballast layer of an existing Finnish railway track. The laboratory tests confirmed that the resistance to cyclic loading decreased with an increasing saturation level for all tested materials. The weakest material in the cyclic loading triaxial test had the most uniform grain size distribution with a small median grain size. The calculation of the vertical stress increase in the sub-ballast layer revealed that even a fine-grained sand can withstand the train load well when the rolling stock is mostly passenger traffic with an axle load of 160 kN and the sub-ballast layer is not completely saturated. However, heavy freight traffic with axle loads of 225 kN and 250 kN can approach the bearing capacity of a weak sub-ballast material if the water content of the upper part of the sub-ballast layer is high. This study has shown that the top part of the sub-ballast layer should be kept below 60–70% saturation level to avoid the development of excessive permanent deformation.

### Introduction

Over time, rolling stock will cause permanent deformation of railway track. The deformation rate depends on several different factors, and appropriate models of the critical components of the track are needed to predict them [17]. The stiffness of subsoil is the most significant factor in terms of permanent deformation, but the thickness of sub-ballast layer has also been found to play a significant role in the stiffness of the entire track [21]. As a result of climate change, floods, heavy rainfall, and in some places extreme drought are predicted to increase worldwide [28]. In Finland for instance, annual precipitation is projected to increase by several percent depending on the calculation model [20]. A combination of cyclic loading, fine-grained soil, and excessive water content in the structural layers has been found to be very damaging to track durability [15].

It is known from previous studies [13] that the functionality of track drainage in Finland still needs much improvement. These factors have led to the situation where the Finnish Transport Infrastructure Agency and the Tampere University initiated a research project to investigate the effects of track water content on loading resistance to identify the

potential benefits of improved drainage. As part of the study, the shear strength of four sub-ballast material specimens were tested at different water contents in static triaxial tests. Three samples were from the sub-ballast layer of an old Finnish railway track while one sample was a reference material that fulfils the current grading requirements. Fig. 1.1 summarizes the maximum shear strengths obtained in static triaxial tests as a function of the water content. The maximum shear strength started to increase as a result of suction effect when the water content decreased below 7%. That corresponds to a degree of saturation of less than 50% with the materials studied. At higher water contents, the maximum shear strength remained constant, which, however, does not correspond to the real situation in a track environment where the loading is cyclic. More detailed results of static triaxial tests are presented in the article “Determining Soil Moisture Content and Material Properties with Dynamic Cone Penetrometer” [12]. Similar results have also been observed elsewhere, such as in the study of Trinh et al. [29] for a worn ballast layer material, the static shear strength of which increased significantly with decreasing water content.

Because of the above perspectives, it is necessary to find out how the sub-ballast materials used in old Finnish railway tracks perform with

<sup>\*</sup> Corresponding author.

E-mail addresses: [juha.latvala@tuni.fi](mailto:juha.latvala@tuni.fi) (J. Latvala), [pauli.kolisoja@tuni.fi](mailto:pauli.kolisoja@tuni.fi) (P. Kolisoja), [heikki.luomala@tuni.fi](mailto:heikki.luomala@tuni.fi) (H. Luomala).

<https://doi.org/10.1016/j.trgeo.2022.100772>

Received 22 February 2022; Received in revised form 19 April 2022; Accepted 20 April 2022

Available online 25 April 2022

2214-3912/© 2022 The Authors. Published by Elsevier Ltd. This is an open access article under the CC BY license (<http://creativecommons.org/licenses/by/4.0/>).

water contents close to the saturated state. The following research questions were set:

- (1) To what extent do the properties of the sub-ballast materials of typical existing Finnish tracks weaken under cyclic loading when the water content increases close to the saturated state?
- (2) What influence do the parameters describing the granularity of the material (fines content, median grain size, uniformity coefficient) have on the material's resistance to the cyclic loading at different water contents?
- (3) Is it possible to make a quantitative estimate of the influence of rolling stock axle load on the permanent deformations of sub-ballast?
- (4) Is the improvement of track drainage still an adequate method in the light of this study's results?

**Theoretical framework**

*Material properties that influence soil resistance to cyclic loading*

According to Li and Selig [15], cyclic loading and fine-grained materials with excessive water content establish a poor combination in terms of track geometry stability. The combination of soil and water is very complex and there are many different factors that have an effect on soil's capacity to withstand the external loading at different water contents. Typically, the considered situations are divided into saturated or unsaturated states. Especially in a saturated or almost completely saturated state, there is a risk of an increase in pore pressure, which can lead to a collapse in the soil strength.

With unbound material, coarse granularity generally improves the material's ability to withstand external loading, while uniformly grained and fine grained (silty) soils have usually been considered unsuitable for continuous cyclic loading. Crushed rock aggregates also differ from natural materials because the contacts between the particles are different. Crushed rock aggregates are formed from sharp-edged particles that do not slide as easily as rounded natural sand particles. The shape of particle size distribution curve, which also indicates the compaction characteristics of the material, also affects the resistance to

cyclic loading. Materials with a high dry bulk density also generally have a high stiffness and shear strength. This is explained by the fact that the grain structure is more stable as the smaller particles fill the voids between the large particles. However, a well-graded and very dense particle structure can result in low water permeability and make the material susceptible to the development of excess pore water pressure when exposed to cyclic loading. For this reason, some studies have recommended that the material should be sufficiently permeable under cyclic loading [1,10,14,27].

Under static load, the matrix suction pressure, which depends on the degree of the saturation, increases soil shear strength by increasing the effective stresses. Much research has been done on the subject, but estimating the additional shear strength caused by matrix suction has proven difficult. One of the best known methods is that of Fredlund et al. [6], which adds the influence of matric suction as a part of normal stress in the traditional Terzaghi formula, but other methods also exist. The direction of change in water content is also important for the development of soil strength properties, as during the hysteresis of water content the suction pressure is higher in the drying direction compared to hydration [6,7,8,30,31].

The ability of a material to withstand cyclic loading has been studied from several different perspectives. High-amplitude loading, which often occurs in earthquakes, can lead to rapidly developing large pore water pressures and total soil liquefaction. On the other hand, loading with a lower amplitude at high number of repetitions can cause long-term deformations, which cause maintenance problems, for example, on railways [32]. Typically, fine-grained sands and silty sands have been found to be sensitive to cyclic loading [14].

Trinh et al. [29] examined the properties of a worn French ballast layer, which in a way acted as a substructure layer on the track, under cyclic loading at different water contents. This material, which contained stones of 25–60 mm (44%), sand and a lot of fines (18% smaller than 100 μm), clearly deformed increasingly with increasing water content. In the experiments, they found an increase in permanent axial deformation from 0.4% to 1.4% as the water content increased from 4% to 6%. In the saturated state, the specimen collapsed with a rather small number of load repetitions. The effect of water content on the performance of the substructure layers therefore cannot be ignored. Suiker

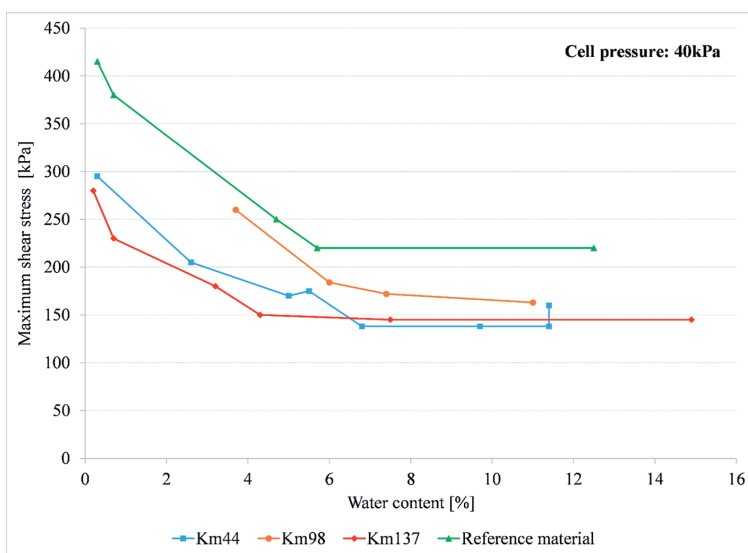


Fig. 1.1. The Results of the static triaxial tests. Three of the samples were taken from the track sub-ballast layer of an old Finnish track at kilometer poles 44, 98 and 139, respectively [12].



et al. [24] have also examined the performance of substructure material and support layer materials using both static and cyclic loading triaxial tests. The average grain size  $d_{50}$  of the substructure material they used was 0.75 mm, the coefficient of uniformity was about 11, and the fines content was about 2%. In the test process, the confining pressure was either 41.3 kPa or 68.9 kPa and the cyclic deviator stress in relation to the maximum value of deviator stress at failure in monotonous loading triaxial test ranged from 0.495 to 0.975. In this kind of loading arrangement, they found that the cyclic loading increases both the strength and stiffness of the substructure material, i.e., the cyclic loading at the applied levels did not result in immediate collapse of the test specimen. At higher loading levels some momentary deformations occurred, but their growth leveled off. In their experiments, Suiker et al. used the optimum water content of 5.5% determined for the material.

*Traffic loads on track substructure*

The interaction between the track and the rolling stock is complex. The quasi-static approach has been applied to in the traditional dimensioning, in which a load surcharge caused by a dynamic effects has been added on top of the static load. The frequency of the dynamic load varies from 0.5 Hz to up to 2000 Hz [3]. In the Netherlands, it has been estimated that it would be possible to reduce the degradation of the network geometry by up to 23%, mainly by controlling the dynamic load [23]. It is obvious that the momentary dynamic loads vary along the railway line, and especially in the vicinity of different transition zones (tunnels, bridges, railway switches, embankments) the increased dynamic load caused by rolling stock has also increased the deformation [18].

In order to be able to estimate the risk for permanent deformations in track substructure it is necessary estimate the amount of vertical stress increase that takes place in the substructure. For Finnish track structure layer thicknesses, the matter has been clarified by Kolisoja et al. [11]. In that study the effect of increasing axle loads to 250 kN was modeled with the BISAR, a multi-layer linear elastic analysis software delivered by oil company Shell. The results of the study are illustrated in Fig. 2.1, which shows both the modeling results and the measurements of vertical stress increases during the passage of a test train with an axle loads of 250 kN. Measured vertical stresses up to 80 kPa occurred at a depth of 0.5 m from the bottom surface of the sleeper. At 1.0 m from the bottom of sleeper,

the vertical stress increases were only 20–30 kPa. The stresses are very similar to the vertical stresses estimated later with a more advanced 3D FEM model [19] and shown in Fig. 2.2. The results of FEM modelling indicate that at the top of sub-ballast layer vertical stress increase is about 80 kPa, but with depth the stress increase dampens rapidly.

Vertical stress distribution in track substructure has also been studied elsewhere in full-scale laboratory experiments. Feng et al. [5] have measured stresses in structures caused by 170 kN and 220 kN axle loads

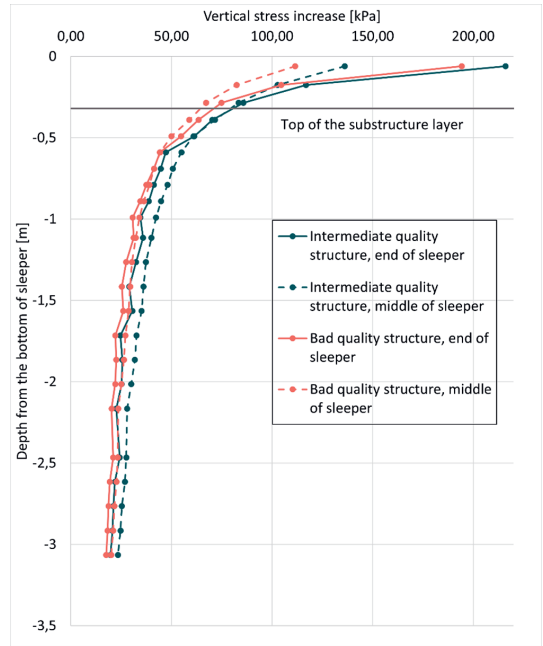


Fig. 2.2. FEM modelling results of vertical stresses caused by a 250 kN axle load in track embankment as a function of depth [19].

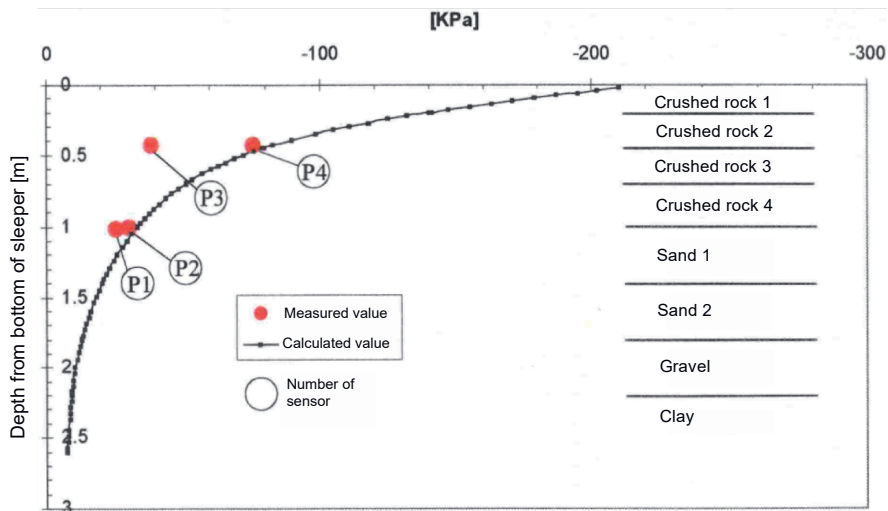


Fig. 2.1. Calculated and measured vertical stresses as a function of depth below the sleeper under a 250 kN axle load [11].

at different speeds in the full-scale laboratory test arrangement. At an axle load of 170 kN, they found a 37–81 kPa stress increase at bottom of the ballast layer. In the substructure layer, vertical stresses of 18–49 kPa were observed. At a higher axle load of 220 kN, below the ballast layer, vertical stresses of 47–109 kPa were observed. The ballast layer under the sleeper was 0.3 m and the substructure layer was 0.7 m thick. The amount of vertical stress increase depends also on the sideway location. The highest stresses in the structure were measured from the rail line and the lowest below the center of sleeper. Shahu et al. [21] found a vertical stress of 40–90 kPa at a depth of 0.4 m below the bottom of the sleeper with an axle load of 290 kN. Trinh et al. [29] concluded that the vertical stress of substructure is 40–90 kPa with the axle loads used in France. It can therefore be concluded that for a substructure, a vertical stress increase of 40–80 kPa is an appropriate estimate of the operational situation, and this range can be used to evaluate the laboratory results.

In addition to vertical stresses, there are horizontal stresses in the track embankment. The magnitude of the horizontal stress in this case was estimated using a previously developed FEM model [9]. Based on those analyses, 30 kPa was chosen as the confining pressure to be used. The same 30 kPa confining pressure has been used also in the study of ballast materials, which has been found to be close to the in-situ situation [29]. On the other hand, Touqan et al. [26] used a 90 kPa confining pressure and a vertical stress of 300 kPa. That is considerably higher than the vertical stress increases applied to the substructure in a static loading condition in Finland. The material used in Torqan et al. study was also clearly coarser ( $d_{50} = 7.4$  mm) compared to the sands used in this study.

The loading frequency used in the cyclic loading test series of this study, 5 Hz, was the same as that of Suiker et al. [24] and Trinh et al. [29]. This loading frequency is not far from the loading frequency caused by the bogies of train wagons at the speeds used in Finland. However, the speed of rolling stock on the track varies, as do the distances between wheelsets and bogies. In addition, the rolling stock causes track loads at different frequencies. Some studies have found that low dynamic frequencies are mainly causing the excessive deformation [23]. One difference between the in-situ situation and the laboratory tests lies also in the length of the load pulse series, as in Finland there is no continuous load of 10,000 pulses on the track, and there is always some time interval between trains. These discrepancies would play a significant role if the loads were to cause pore pressure build-up in the materials.

**Materials and methods**

*Materials*

The laboratory test series of this study included four different track substructure materials, three of which were taken from the sub-ballast layer of a southern Finnish track section. The samples were collected from the depth of 0.55 m to 1.35 m below the top surface of sleepers. A significant part of the Finnish rail network was built at the turn of the 19th and 20th centuries using available local materials that may not meet current material requirements. For this reason, a reference material with a low fines content and fulfilling the current granularity requirements for the substructure layer in Finland was included in the laboratory tests. The grain size distribution curves of the test materials are shown in Fig. 3.1 and the parameters describing their granularity in Table 3.1. The Km137 material is remarkably uniformly graded. The grain size distribution curves of the reference material and the Km137 sample are similar in shape, but there is a significant difference in the mean grain size, as  $d_{50}$  of Km137 is 0.4 mm and that of the reference material is 1.1 mm. The Finnish sands are usually rounded due to their glaciation-time formation history, and they usually consist of hard minerals like quartz and feldspar. The reference material particle shape was somewhat more angular than that of other samples.

*Test specimen preparation*

Test were conducted by using a specimen diameter of 200 mm and height of 400 mm. Due to the limited volume of material samples, the same material had to be used multiple times. After drying and cooling, the samples were moistened in a concrete mixer to a water content of

**Table 3.1**  
Grading parameters from tested materials.

| Sample             | Average particle diameter $d_{50}$ [mm] | Coefficient of uniformity [-] | Content of fines <0.06 mm [%] |
|--------------------|---|-------------------------------|-------------------------------|
| Reference material | 1.1                                     | 4.7                           | 2.5                           |
| Km44               | 0.7                                     | 10.0                          | 4.9                           |
| Km98               | 0.5                                     | 10.0                          | 6.7                           |
| Km137              | 0.4                                     | 3.5                           | 3.7                           |

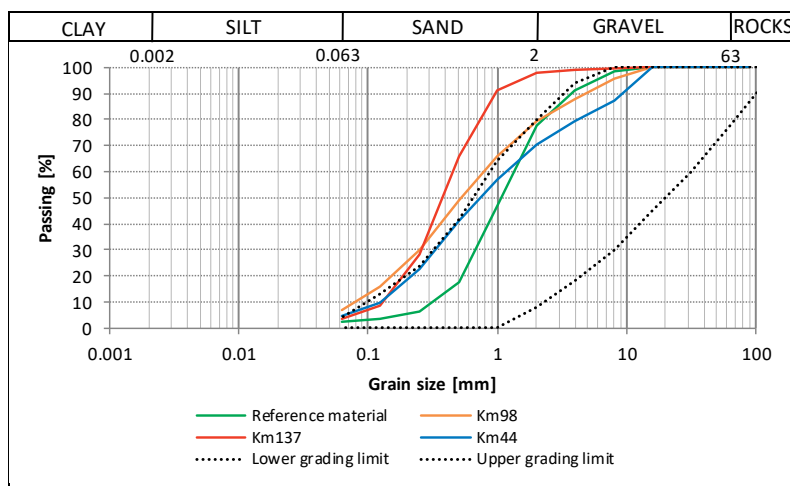


**Fig. 3.1.** The measured grain size distributions of test materials. Dashed lines describe the grading limits of Finnish Transport Infrastructure Agency for sub-ballast material.

7%, which was considered to be a suitable compaction water content based on Proctor compaction tests. However, this water content turned out to be slightly too high in some of the specimens and water was leaking out during the compaction work. Approximately 30 kg of sample material was required for each triaxial test specimen. Compaction took place in a steel mold with a vibratory compaction device in four 100 mm layers. The compaction time was about 20 s per layer, which produced the maximum compaction achieved by that method. The specimens were extruded from the steel mold into a rubber membrane, displacement sensors were installed on the specimen surface, and the specimen was placed inside the test cell. Fig. 3.2 shows the triaxial test equipment used for the large-scale cyclic loading test.

**Testing principles**

Cyclic load triaxial tests were performed as drained tests, i.e., water was allowed to drain from the specimen through the top outlet of the test cell. The tests were divided into three different series:

- In the A-series tests, the water content was the compaction water content from start to finish.
- In the B-series experiments, the specimen was prepared and conditioned at the compacting water content. The specimen was then saturated by feeding in water from the bottom of the cell. The resilient and permanent deformation test series were performed in this state.
- The C-series specimen was conditioned and saturated like in the B-series tests, but then the specimen was let to drain gravitationally before testing.

The saturation in the B- and C-series tests was carried out by introducing water from a water tank at a height of about 1.5 m into the base of test specimen. The time used for the saturation process varied considerably due to the different water permeabilities of the materials. The reference specimen and specimen Km137 were easily saturated, but the saturation of specimens Km44 and Km98 took longer. Correspondingly, more water remained in these materials in the C-series tests after saturation and gravitational drying.

The loading process started with cyclic conditioning. The purpose of the conditioning was to remove any gaps between the loading cap and test specimen and to ensure coherence of the test specimen. The

conditioning phase consisted of a cyclic vertical stress of 150 kPa applied during a 70 kPa confining pressure. The conditioning pulses were applied as long as permanent deformations developed, but not to more than 2000 load pulses. In general, significant deformations slowed down very rapidly at the beginning of the conditioning phase.

In the resilient deformation tests, a series of 100 pulses was applied to the material at a frequency of 1 Hz at different confining pressures. The loading procedure was based on the low stress level specification of EN 13286-7 [4], but the highest deviatoric stresses at all confining pressures were skipped to avoid too early destruction of the specimen. The deviator stresses used are listed in Table 3.2. The load series was interrupted if there was a permanent axial deformation of more than 0.25%. As a cumulative maximum permanent axial deformation in the resilient deformation test series, 0.5% was allowed, which means a permanent compression of 2 mm with a 400 mm high specimen.

As stated before, a confining pressure of 30 kPa was used in the permanent deformation tests. The specimens were subjected to a 10,000 pulse load series starting from a deviator stress of 20 kPa. After each series of pulses, the deviator stress was increased by 10 kPa until the specimen collapsed or the specimen deformations became critical to the test equipment.

**Results**

This chapter presents the results concerning resilient deformation behavior and permanent deformation test series performed for 13 different test specimens. The water contents of the specimens are reported as saturation degrees measured after the test. The specimen was disassembled in three parts to determine the water contents in the top, middle, and bottom parts of test specimen. These water contents have been averaged and compared to the calculated maximum water content. The calculated maximum water content has been determined using the dry bulk density and the porosity calculated on the basis of the typical solid density of Finnish rock materials (2650 kg/m<sup>3</sup>). The saturation degrees are shown in Table 4.1. Minus and plus signs after the saturation degrees are indicating the direction of latest water content change during test specimen preparation procedure. Thus the plus sign indicates that water content has been increasing from compaction water content and the minus sign indicates that test specimen has been drying from the saturation water content. In some of the test specimen there was water content variation with depth. That inevitable phenomenon was especially observed in the most coarse grained materials due to the effect of gravitation. This might have caused different behavior in different parts of the specimen and therefore the permanent deformations have been determined based on the full height of test specimen.

The results of the resilient deformation tests are summarized in Fig. 4.1, in which the resilient modulus values obtained at different water contents have been presented as a function of the sum of principal stresses. The highest resilient moduli values were obtained with the highest dry density specimens of Km44 and Km98. The differences



Fig. 3.2. Large-scale test equipment used in the cyclic load triaxial test. Specimen dimensions were d = 200 mm and h = 400 mm.

Table 3.2

The confining pressures and deviatoric stresses during the resilient deformation tests. The test was done according to EN 13286-7 [4].

|          | Confining pressure [kPa] | Deviatoric stress [kPa] | Number of pulses |
|----------|--------------------------|-------------------------|------------------|
| Series 1 | 20                       | 20                      | 100              |
|          | 20                       | 30                      | 100              |
|          | 20                       | 50                      | 100              |
| Series 2 | 35                       | 50                      | 100              |
|          | 35                       | 80                      | 100              |
| Series 3 | 50                       | 80                      | 100              |
|          | 50                       | 115                     | 100              |
| Series 4 | 70                       | 115                     | 100              |
|          | 70                       | 150                     | 100              |
| Series 5 | 100                      | 150                     | 100              |
|          | 100                      | 200                     | 100              |

**Table 4.1**  
Dry densities and water contents of tested specimens.

| Test label         | Dry density [g/cm <sup>3</sup> ] | Void ratio | Saturation degree [%] | Water content bottom [%] | Water content middle [%] | Water content top [%] |
|--------------------|----------------------------------|------------|-----------------------|--------------------------|--------------------------|-----------------------|
| Reference material |                                  |            |                       |                          |                          |                       |
| 1A1*               | 1.768                            | 0.50       | 40                    | 8.7                      | 6.3                      | 6.2                   |
| 1A2                | 1.786                            | 0.50       | 40                    | 8.7                      | 5.6                      | 4.8                   |
| 1B                 | 1.733                            | 0.53       | 70+                   | 17                       | 7.6                      | 17                    |
| 1C                 | 1.782                            | 0.49       | 30-                   | 6.6                      | 4.9                      | 4.3                   |
| Km137              |                                  |            |                       |                          |                          |                       |
| 2A                 | 1.764                            | 0.50       | 35                    | 7.4                      | 7.0                      | 5.8                   |
| 2B                 | 1.751                            | 0.51       | 65+                   | 14.1                     | 13.1                     | 8.0                   |
| 2C                 | 1.733                            | 0.53       | 50-                   | 13.4                     | 8.3                      | 5.4                   |
| Km98               |                                  |            |                       |                          |                          |                       |
| 4A*                | 2.083                            | 0.27       | 60                    | 6.9                      | 6.3                      | 4.7                   |
| 4B                 | 2.083                            | 0.27       | 70+                   | 7.0                      | 7.0                      | 6.7                   |
| 4C                 | 2.062                            | 0.29       | 55-                   | 6.5                      | 6.2                      | 5.5                   |
| Km44               |                                  |            |                       |                          |                          |                       |
| 3A                 | 2.071                            | 0.28       | 65                    | 7.1                      | 6.7                      | 5.1                   |
| 3B                 | 2.137                            | 0.24       | 80+                   | 7.4                      | 6.5                      | 6.9                   |
| 3C*                | 2.069                            | 0.28       | 70-                   | 7.4                      | 7.3                      | 6.3                   |

\* Resilient deformation test was not successful because of sensors failure.

between moduli values are not as great as observed differences in cyclic loading tests, but the measured moduli values are generally lower in the samples of high saturation degree.

The results of the cyclic loading tests are reported as the rate of accumulation of axial strain per load pulse. The advantage of that approach is that the permanent deformation developed in the track structure can then be roughly estimated when the average axle load and traffic volumes of the rolling stock on the track are known. The axial strain rate has been calculated based on the difference of vertical displacement readings at pulses number 50 and 9950, because during the pauses between the pulse series, the specimen was found to recover temporarily. The accumulation rate of axial strain has been calculated only for full-length pulse series, i.e. those in which the test specimen collapsed have not been considered. The deformations shown in this way are summarized in Fig. 4.2. Two types of collapse mechanisms were observed in the tests, as the reference material endured for a long time with low permanent deformations until the specimen became fragile and broke down, whereas in the Km44 and Km98 specimens in particular, the development of axial strain started quite early and increased continuously with increasing vertical stress.

**Discussion**

In the cyclic loading tests performed, there were clear differences in the loading resistance of the tested materials. The collapse mechanisms were also different for the materials, as the collapse of the reference material was fragile, while the collapse of the other materials was more gradual. The best cyclic load resistance was achieved with the driest specimens and the reference material was by far the most durable. Correspondingly, the highest rates of axial strain accumulation were measured in the specimens with the highest water content. In static triaxial tests, matrix suction began to increase the shear strength of test materials below saturation degree of 50%. Lower than 50% saturation degrees were observed in the cyclic loading test specimen 1A1, 1A2, and 1C of the reference material and in test 2A of the Km137 material. The differences observed in cyclic loading tests at saturation degrees of more than 50 % are not due to the effect of matrix suction.

The specimens did not achieve a calculated 100% saturation degree.

It is obvious that with a gravitational saturation process, air easily remains in some of the pores of the specimen, and this takes a long time to dissolve. In the tests performed, the saturation time varied according to the material and for the Km44 and Km98 materials, the saturation process lasted for several days, while in the reference material the water flowed through the material in less than half an hour. This was expected because the wide grain size range combined with the higher fines content in the Km44 and Km98 material samples results in low water permeability. It is also possible that the oven drying of the Km44 and Km98 materials made the silt/clay they contain very slowly saturable. It is therefore likely that with a significantly longer saturation time or other saturation methods, the air trapped in the pores would have been removed more efficiently and the loading resistance of the materials in high saturation degree would have been even weaker than what was now measured. In Finland, in-situ sub-ballast saturation degree have been measured to vary from 30 to 100 % depending on the depth and site drainage properties. More precise analysis of in-situ saturation degrees in railway substructures will be reported in an upcoming paper.

In the predicted operating vertical stress range of 40–80 kPa, the differences between the materials narrowed, but there were still clear differences. Different degrees of saturation were also found to influence the rate of deformation developed in the specimen in the operating stress range. Based on the results, a simplistic calculation was made of the total deformations formed in the sub-ballast layer. It was found that the vertical stress increase caused by passenger train axle loads is so small (near the lower limit of the operating vertical stress range) that the deformation developed in all of the materials remains very small even if the materials are close to the saturated state. This can also be clearly seen from Fig. 4.2, because with a vertical stress increase of less than 50 kPa, the axial strain accumulation rates were very low. The situation changed in the case of a vertical stress increase of the order of about 80 kPa, corresponding to an axle load of 250 kN. In this case, clear differences were observed between the materials so that much faster deformation began to occur in the materials at high saturation degree. In particular, the specimen km137 in high saturation degree caused a multiple times annual deformation in this calculation compared to the other materials.

The ability of materials to withstand cyclic loading cannot be solely predicted by using the resilient moduli. The observed differences in resilient moduli values between the different saturation levels were small. Densely packed materials km44 and km98 performed best in the resilient deformation tests, but they were still weaker than the reference material in the cyclic test. It is therefore obvious that the short-term loading series of the resilient deformation tests, with a maximum of 100 pulses, does not provide a reliable prediction of cyclic loading resistance. On the other hand, in a real loading situation, there are always intervals between trains, so a continuously propagating cyclic test series of 10,000 pulses can also overestimate the development of permanent deformations. Intervals in the cyclic loading series allow time for pore water pressure to dissipate.

Vertical cyclic loading in the triaxial test cell is a well-established test method, but it does not fully describe the situation in the actual operating environment. In a railway environment, the movement of rolling stock causes principal stress rotation. This has been investigated, for example, by Mamou [16], Cai et al. [2], and Thevakumar et al. [25]. Their studies have shown how the rotating load axis can indeed play a significant role in the deformation behavior of granular materials. This is something that should be considered more closely if laboratory tests are aimed to be used to accurately estimate permanent deformations.

The fines contained in the granular material have a divaricate effect on its performance. The fines impede the flow of water and thus easily increase the water content of the structure, but on the other hand, Soliman and Shalaby [22], for example, observed in their experiments how the loading resistance of gravel materials improved with a reasonable amount of fines. They described the phenomenon as being due to the fact that the round-grained gravel needs some fines to prevent

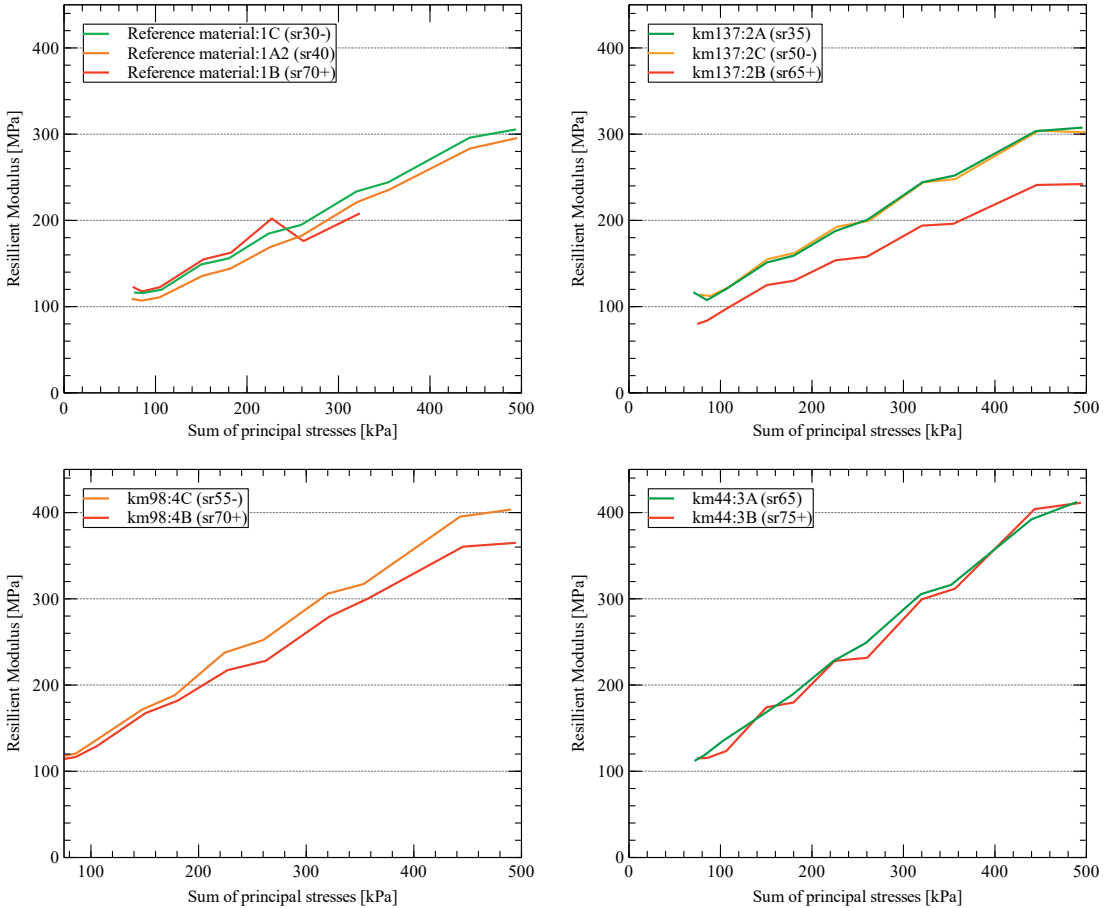


Fig. 4.1. Measured resilient modulus values of the tested specimens.

the particles from slipping past each other. This may explain the previously mentioned difference in the failure mechanisms of the specimens, as there was no fragile breakdown behavior in the specimens km44 and km98, which occurred in the reference material.

**Conclusion**

This study was part of a larger project on track drainage. The study provided indications of how the water content of the track substructure has an effect on its loading resistance. This is especially emphasized just below the ballast layer. Based on the results, drainage improvements should be directed to sites where the water level is exceptionally high. If the substructure is not saturated with water or the material is not exceptionally sensitive to the effects of water, it is unlikely that the development of deformations of the track will be significantly reduced by improving the drainage. The finding fits well with the work of Trinh et al. [29], who depict that previously track deformation has been attributed to poor drainage in France. For this reason, the importance of drainage has been emphasized in the modernization of tracks required by rolling stock with higher axle loads and speeds, but on the other hand, it has been observed how even older structures can perform quite well without proper drainage. Therefore, they also ended up stating how material-specific sensitivity to water content should be taken into

account in track maintenance and action planning.

Answers to the research questions:

- In all four materials examined, the loading resistance decreased with increasing water content. Therefore, a high saturation degree condition should be avoided. It can be concluded that if the material meets the current granularity requirements of the Finnish Transport Infrastructure Agency, its ability to withstand the cyclic load is sufficiently good at different water contents. If the material is on the finer side of the required granularity range, it is likely to have problems with its performance, especially at high water contents.
- The best-performing reference material, which clearly meets the current granularity requirements, withstood the cyclic loading tests best. The material performed well, although its dry density is low and close to the dry density of the sample Km137. In Finland, according to current regulations, the median particle size  $d_{50}$  of the sub-ballast layer must be at least 0.6 mm. Based on the study, risks of deformation increase significantly if the average grain size of the material is too small. Especially the small average grain size, low dry density, and low uniformity coefficient are a risky combination. Material with too low median grain size and uniform grain size distribution, such as Km137, should not be subjected to loads caused by heavy

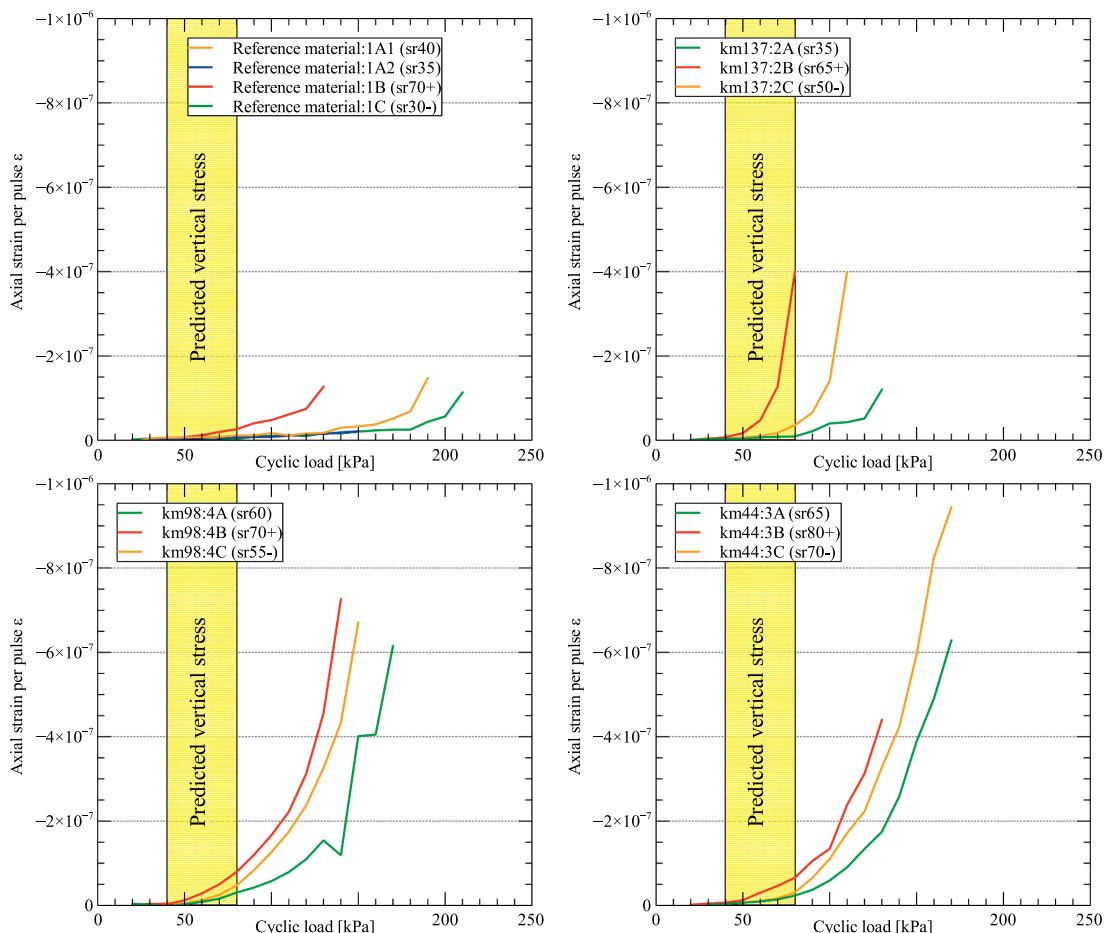


Fig. 4.2. Accumulation rate of axial strain per load pulse. The yellow area in the graphs represents the predicted level of vertical stresses in the sub-ballast layer. A confining pressure of 30 kPa was used in all cyclic loading tests. (For interpretation of the references to colour in this figure legend, the reader is referred to the web version of this article.)

axle loads in a saturated state. Moderate (less than 5%) fines contents are unlikely to cause problems.

- Based on the conducted tests, the differences in the functionality of the substructure materials in Finland are small at axle loads of about 160 kN typical for passenger traffic. This is natural, since at the depth of the sub-ballast layer, the increase in vertical stress at this axle load is small. The situation is different in freight traffic, where vehicles with axle loads of both 225 kN and 250 kN are used. Already the 225 kN axle load vehicles start to fully utilize the strength properties of substructure materials, especially with the low-quality materials mentioned above. With axle loads higher than this, the situation becomes obviously more critical. On the other hand, in Finland, traffic with an axle load of 250 kN travels mainly on high-quality sections of track which are well-built with proper drainage systems. In addition, it is also necessary to take into account the discontinuity points of the track, where the dynamic load increase can be significant and thus more of material's load resistance capacity is utilized than in line parts.
- Efficient drainage and a reasonable water content increased the loading resistance capacity of the materials in laboratory tests. Thus, the structural layers of track should be drained properly. However, it

is likely that sites with unevenness problems are multi-problematic and the benefits measurable by improving drainage alone may be small unless the track sub-ballast layer is nearly fully saturated.

**Funding**

This work was supported by Finnish Transport Infrastructure Agency.

**CRediT authorship contribution statement**

**Juha Latvala:** Investigation, Data curation, Writing – original draft. **Pauli Kolisoja:** Supervision. **Heikki Luomala:** Supervision, Writing – review & editing.

**Declaration of Competing Interest**

The authors declare that they have no known competing financial interests or personal relationships that could have appeared to influence the work reported in this paper.



## References

- [1] Altun S, Göktepe AB, Akgüner C. Cyclic shear strength of silts and sands under cyclic loading. *Earthq Eng Soil Dynam* 2005;1–11.
- [2] Cai Y, Sun Qi, Guo L, Juang CH, Wang J. Permanent deformation characteristics of saturated sand under cyclic loading. *Can Geotech J* 2015;52(6):795–807.
- [3] Esveld C. *Modern railway track*. vol. 385. MRT-productions Zaltbommel; 2001.
- [4] European Committee for Standardization. EN-13286-7. Unbound and hydraulically bound mixtures - Part 7: Cyclic load triaxial test for unbound mixtures; 2004.
- [5] Feng B, Basarah YI, Gu Q, Duan X, Bian X, Tutumluer E, et al. Advanced full-scale laboratory dynamic load testing of a ballasted high-speed railway track. *Transp Geotech* 2021;29:100559.
- [6] Fredlund DG, Morgenstern NR, Widger RA. The shear strength of unsaturated soils. *Can Geotech J* 1978;15(3):313–21.
- [7] Fredlund DG, Xing A, Fredlund MD, Barbour SL. The relationship of the unsaturated soil shear strength to the soil-water characteristic curve. *Can Geotech J* 1996;33(3):440–8.
- [8] Hillel D. *Soil and water: physical principles and processes*. Elsevier; 2012.
- [9] Kalliainen A, Kollisoja P, Nurmikolu A. 3D finite element model as a tool for analyzing the structural behavior of a railway track. *Procedia Eng* 2016;143:820–7.
- [10] Kollisoja P. Resilient deformation characteristics of granular materials. Publications: Tampere University of Technology Finland; 1997.
- [11] Kollisoja P, Järvenpää I, Mäkelä E, Levomäki M. Ratarakenteen instrumentointi ja mallinnus, 250 kN: n ja 300 kN: n akselipainot (in English: Instrumentation and modelling of Track Structure, 250 kN and 300 kN axle loads). Publications of Finnish Rail Administration; 2000.
- [12] Latvala J, Luomala H, Kollisoja P. Determining soil moisture content and material properties with dynamic cone penetrometer. *Baltic J Road Bridge Eng* 2020;15: 136–59.
- [13] Latvala J, Nurmikolu A, Luomala H. Problems with railway track drainage in Finland. *Proc Eng* 2016;143:1051–8.
- [14] Lee KL, Fitton JA. Factors affecting the cyclic loading strength of soil, ASTM International; 1969.
- [15] Li D, Selig ET. Evaluation of railway subgrade problems. *Transp Res Rec* 1995; 1489:17.
- [16] Mamou A. Effects of principal stress rotation and drainage on the resilient stiffness of railway foundations. University of Southampton; 2013. PhD Thesis.
- [17] Melo ALOD, Kaevunruen S, Papaalias M, Bernucci LL, Motta R. Methods to monitor and evaluate the deterioration of track and its components in a railway in-service: a systemic review. *Front Built Environ* 2020;6:118.
- [18] Paixão A, Varandas JN, Fortunato EC. Dynamic behavior in transition zones and long-term railway track performance. *Front Built Environ* 2021;7:29.
- [19] Peltomäki M. Ratarakenteen kuormituskäyttäytymisen mallintaminen (in English: Modeling the loading behavior of railway structure). Master's Thesis. Tampere University; 2020.
- [20] Ruosteenoja K, Jylhä K, Kämäräinen M. Climate projections for Finland under the RCP forcing scenarios. *Geophysica* 2016;51.
- [21] Shahu JT, Rao NK, Yudhbir. Parametric study of resilient response of tracks with a sub-ballast layer. *Can Geotech J* 1999;36:1137–50.
- [22] Soliman H, Shalaby A. Permanent deformation behavior of unbound granular base materials with varying moisture and fines content. *Transp Geotech* 2015;4:1–12.
- [23] Steenbergen M, Jong ED, Zoeteman A. Dynamic axle loads as a main source of railway track degradation. *Geotechnical Risk and Safety V*; 5th International Symposium on Geotechnical Safety and Risk; Rotterdam (The Netherlands), 13-16 Oct. 2015. IOS Press; 2015.
- [24] Suiker ASJ, Selig ET, Frenkel R. Static and cyclic triaxial testing of ballast and subballast. *J Geotech Geoenviron Eng* 2005;131(6):771–82.
- [25] Thevakumar K, Indraratna B, Ferreira FB, Carter J, Rujkiatkamjorn C. The influence of cyclic loading on the response of soft subgrade soil in relation to heavy haul railways. *Transp Geotech* 2021;29:100571.
- [26] Touqan M, Ahmed A, El Naggar H, Stark T. Static and cyclic characterization of fouled railroad sub-ballast layer behaviour. *Soil Dyn Earthquake Eng* 2020;137: 106293.
- [27] Trask PD. Effect of grain size on strength of mixtures of clay, sand, and water. *Geol Soc Am Bull* 1959;70:569–80.
- [28] Trenberth KE. Changes in precipitation with climate change. *Clim Res* 2011;47(1): 123–38.
- [29] Trinh VN, Tang AM, Cui Y-J, Dupla J-C, Canou J, Calon N, et al. Mechanical characterisation of the fouled ballast in ancient railway track substructure by large-scale triaxial tests. *Soils Found* 2012;52(3):511–23.
- [30] Vanapalli SK, Fredlund DG, Pufahl DE, Clifton AW. Model for the prediction of shear strength with respect to soil suction. *Can Geotech J* 1996;33(3):379–92.
- [31] Vanapalli SK, Sillers WS, Fredlund MD. The meaning and relevance of residual state to unsaturated soils. In: 51st Canadian Geotechnical Conference, Edmonton; 1998, p. 4–7.
- [32] Wichtmann T, Niemunis A, Triantafyllidis Th. Strain accumulation in sand due to cyclic loading: drained triaxial tests. *Soil Dyn Earthq Eng* 2005;25(12):967–79.





PUBLICATION  
V

Convective Heat Transfer in Crushed Rock Aggregates: The Effects of  
Grain Size Distribution and Moisture Content

Juha Latvala, Heikki Luomala, Pauli Kolisoja and Antti Nurmikolu

Journal of Cold Regions Engineering, Vol. 34 No. 3:04020012  
[https://doi.org/10.1061/\(ASCE\)CR.1943-5495.0000219](https://doi.org/10.1061/(ASCE)CR.1943-5495.0000219)

Accepted final draft. This material may be downloaded for personal use only.  
Any other use requires prior permission of the American Society of Civil  
Engineers. This material may be found at the link above.



# **Convective heat transfer in crushed rock aggregates – the effects of grain size distribution and moisture content**

Juha Latvala<sup>1</sup>, Dr.Tech Heikki Luomala<sup>2</sup>, Prof. Pauli Kolisoja<sup>3</sup> and Dr.Tech Antti Nurmikolu<sup>4</sup>,

<sup>1</sup>Faculty of Built Environment, Tampere University, Finland. Corresponding author. Email:juha.latvala@tuni.fi

<sup>2</sup>Faculty of Built Environment, Tampere University, Finland. Email: heikki.luomala@tuni.fi

<sup>1</sup>Faculty of Built Environment, Tampere University, Finland. Email: pauli.kolisoja@tuni.fi

<sup>4</sup>Laboratory of Civil Engineering, Tampere University of Technology, Finland.

## **Abstract**

This article deals with the susceptibility of the materials used in the Finnish rail network to convective heat transfer. Previous studies have found that convection clearly influences the thermal conductivity of coarse aggregates in certain conditions. The occurrence of convection may cause subsoil frost heave. This study investigated the susceptibility of three sub-ballast materials, which were made of different crushed rock aggregates, to convection: railway ballast (31.5/63 mm), sub-ballast layers of crushed rock, and 5/16 mm crushed rock. Convection was found to increase the thermal conductivity of railway ballast several-fold, while the thermal conductivity of the currently used sub-ballast material was also noted to increase clearly when the moving medium contained water. No significant increase in thermal conductivity was, however, found in the case of the 5/16 mm crushed rock. Based on these results, it is clear that it is not possible to use tremendously coarse materials in thick structure layers in the Northern area. The results of this study were one of the most important factors when the grading recommendation for sub-ballast material used in Finland was changed to include more fines, which clearly reduces the possibility of the onset of convection.

## **Keywords**

Natural convection, frost heave, railway embankment, sub-ballast material, railway ballast

## Introduction

Modern track flatness requirements are high (EN13848-6:2014), and even minor unevenness due to frost heave disturbs rail traffic. Finnish track structures are typically designed, so as to prevent seasonal frost from causing frost heave under tracks. This means that extremely thick structure layers are needed in Northern area and their dimensioning must be correct. Nowadays, crushed rock aggregate is the most commonly used material in sub-ballast in Finland, because of its price and availability. The heat properties of coarse crushed rock aggregates are different than in natural graded materials, and this issue was addressed briefly by Nurmikolu (2004), which led to an increase of 15% in layer thicknesses when the sub-ballast is made of crushed rock. The increase was based primarily on the differences of the materials with respect to dry bulk density and water content, whose impact on thermal conductivity was assessed based on Kersten's (1949) equations.

The traditional assumption in frost dimensioning has been that heat transfers in soil mainly through conduction, but international research (e.g. by Johansen 1975 and Goering et al. 2000) show that heat may also transfer by convection in coarse-grained aggregates. Johansen (1975), on the other hand, found that, in crushed aggregate of grain size 20/80 mm (notation means that the grain size of used materials varies mainly from 20 to 80 mm in diameter), natural convection increases the sample's thermal conductivity by up to 2.5 fold compared to a situation where heat transfers by conduction and radiation. The risk of higher than assumed thermal conductivity is not merely theoretical, since the so-called Sprengestein blasted rock material used in Norway in the 1990's caused major frost heave problems as the convective heat transfer made possible by the material had not been considered in determining the material's thermal conductivity (Jernbaneverket 1999). The importance of effective thermal conductivity leads to the following research questions:

- 1) Is the crushed rock aggregate used in Finnish railways adequately coarse to provide suitable conditions to natural convection?
- 2) How the moisture content of aggregate affects to of natural convection and heat transfer properties?
- 3) What the temperature gradients are in in-situ targets?

The sub-ballast material used for Finnish railways differs from materials tested elsewhere with respect to grading, meaning in that the results of such tests are not directly usable in this context. Coarse crushed rock materials have many advantageous options, e.g., good load resistance options and low moisture sorb properties considering track drainage. However, the restrictions of use for these kinds of material should be clarified. The results of this study are important for all countries where seasonal frost occurs. Based on the above factors, it was decided to study the possibility of the occurrence of convection with the help of test apparatus.

The differences between the thermal performance of tracks laid on gravel and crushed rock aggregate in the test site have also been studied in Finland. The Hippi field investigation site is located in Western Finland. Two different materials were used in the railway embankments at the site. The northern embankment used a conventional substructure of gravel, topped with a 0.3 m sub-ballast layer of crushed rock aggregate and a 0.55 m railway ballast layer. Apart from the gravel layer being substituted by crushed rock aggregate (Kalliainen et al. 2011), the structure of the southern site is otherwise similar. In the monitoring period 2011–2013, a thermal gradient of about 9 °C/m was

measured on the crushed rock embankment. However, the gradient fluctuated between measuring points, and greater thermal gradients were achieved by choosing points near the track surface. A more accurate description of Hippi's field target and the results of monitoring are going to be presented in future papers. In this paper, the thermal gradient was the most essential part of monitoring.

## Theoretical framework

### *The basic concepts of natural convection*

In order to be able to assess the susceptibility of materials to convection, it is necessary to provide a general definition of the Rayleigh and Nusselt numbers. The Rayleigh number is based on analytical studies and describes the relationship between the forces caused by buoyancy and opposing forces, which allows using it to assess the possibility of the occurrence of convection or its magnitude. Equation 1 is derived from the doctoral dissertation of Johansen (1975), except that the kinematic viscosity element has been expressed in terms of dynamic viscosity and density of the moving medium (conversion formula of Mills 1993).

$$Ra = \frac{\Delta T a g h K \rho^2 c}{\lambda \mu} \quad (1)$$

where

|            |  |
|------------|--|
| $Ra$       | = Rayleigh number, [-]                                   |
| $\Delta T$ | = temperature difference, [°C]                           |
| $h$        | = layer thickness, [m]                                   |
| $g$        | = acceleration of gravity, constant, [m/s <sup>2</sup> ] |
| $a$        | = coefficient of thermal expansion of medium, [1/K]      |
| $\mu$      | = dynamic viscosity of medium, [kg/ms]                   |
| $\rho$     | = density of medium, [kg/m <sup>3</sup> ]                |
| $c$        | = specific heat capacity of medium [J/Kg · K]            |
| $\lambda$  | = thermal conductivity excluding convection, [W/mK]      |
| $K$        | = intrinsic permeability, [m <sup>2</sup> ]              |

The critical Rayleigh number is also often used in studies. When the number reaches some critical value, the onset of convection is considered possible. The critical Rayleigh number depends on the boundary conditions, and Lapwood (1948) has calculated the following critical values for a liquid-containing, porous material in different conditions: If the material is surrounded by two impermeable heat-conducting surfaces,  $Ra_{cr} = 40$ , and if the lower surface is impermeable and the upper one open, the critical number is 27.

Another important variable to consider is the Nusselt number, which is commonly used in convection studies, since it allows assessing the actual impacts of convection. It expresses the relationship of

effective thermal conductivity (including convection) and thermal conductivity, excluding convection. It is derived from equation 2 using the critical Rayleigh number that depends on the boundary conditions. It should be noted that at large Rayleigh values, the Nusselt number no longer increases completely linearly (Johansen 1975; Côté et al. 2011).

$$Nu = \frac{Ra}{Ra_{cr}} \quad (2)$$

where

|           |  |
|-----------|--|
| $Nu$      | = Nusselt number, [-]  |
| $Ra$      | = Rayleigh number, [-]   |
| $Ra_{cr}$ | = Critical Rayleigh number beyond which onset of convection is computationally possible, [-] |

### ***Impact of convection on thermal conductivity of different materials***

The susceptibility of different materials to convection has been studied by various test apparatuses across the world. The apparatuses operate on the basis of the physical properties of natural convection. When a material is heated from below and cooled from above, warm air or some other medium starts to rise due to differences in density. Consequently, heat transfers with the air or other medium, i.e., heat transfers by conduction from one contact surface to another by radiation and convection. If a sample is heated from above and cooled from below, the medium does not move since the densest medium (air) is on the cold side of the sample at the lowest possible point.

One of the most relevant studies was conducted by Johansen (1975), who studied convective heat transfer using 20/80 mm crushed rock with a bulk density of about 1500 kg/m<sup>3</sup>. The thermal conduction of a material, excluding convection (top-heating), was about 0.45 W/mK when the average sample temperature was about 3 °C. The possibility of natural air convection was examined by using open and closed upper surface of sample, because of the different critical Rayleigh numbers. With an open upper surface and sample height of 0.48 m, the critical temperature difference was measured to be 7.8 °C and the closed surface temperature measured to be 11.6 °C. Above these temperatures, the natural air convection started and increased the effective heat conduction. With the open upper surface, Johansen achieved 1.13 W/mK effective heat conduction, which corresponds to Nusselt number of 2.5 with a temperature difference of 19.0 °C. It is obvious that the natural air convection increased the heat conductivity significantly. Johansen had also calculated the critical temperature differences for the material in question, which were 7.8 °C and 11.6 °C. The critical Rayleigh numbers calculated on the basis of measurements were 26 and 41, which are very close to the theoretical values calculated by Lapwood.

Goering et al. (2000) studied convection in a laboratory with a somewhat similar arrangement as Johansen. The material tested by Goering et al. was mixed 20/63 mm crushed rock. The grading curve of the tested material differs from that of the Finnish railway ballast, whose minimum diameter is 31.5 mm, with regard to its smallest grain size. In analyzing the results, Goering's research team aimed at modeling the pore air flow by a calculational method. The performance of the calculation model was tested, and it was discovered that pore air does not flow in the area below the critical Rayleigh number. The unidimensional temperature profile that formed was in line with the heat

conduction theory. According to the model, at Rayleigh values above 39.48 the movement of pore air increased gradually. Based on these tests, Goering et al. considered that the model performs well. The thermal conductivity of the material with top heating was 0.79 W/mK and the temperature profile of the sensors in the sample was very linear. With bottom heating, the conductivity increased significantly and temperature profile was not linear anymore.

Natural convection in structure layers is not always an unwanted phenomenon. Goering (1998) studied exploitation of convection in a permafrost area in Alaska. The idea behind the study was that an embankment releases a lot of heat into outdoor air in winter by convective heat transfer, whereby the embankment remains cooler in summer. This is possible mainly in permafrost areas. Clear convective heat transfer was detected in a test embankment composed of 50/80 mm crushed rock. The utilization of natural convection in permafrost regions is still a valid research topic. For example, the Qinghai-Tibet railway is located partly in the permafrost region. A number of studies have been carried out on this topic, mainly in China. For example, Wang & Ma (2012) investigated the most important convection-related factors in planning in relation to crushed rock embankments. Mu et al. (2012) monitored the results from different convection related substructures at Qinghai-Tibet railway and Fujun et al. (2015) continued monitoring long-term temperature profiles. Qian et al. (2012) have also made research on highway substructures. The same principles can be applied in railway structures. In short, many studies have valid evidence that the convection substructures are working well, like a thermal semiconductor in permafrost regions.

## **Materials and methods**

### ***Test Materials***

Three crushed rock materials with different grain size distribution were tested in the laboratory. The first material tested with the built apparatus was railway ballast (CrA1), which is the coarsest of the studied materials. It was assumed and corroborated by the testing that this material was coarse enough to produce natural convection. Railway ballast is used in the track support layer and its d/D grain size is 31.5/63 mm. Railway ballast contains very few fines: in the case of ballast containing class B fines, the maximum allowed percentage passing the 0.063 sieve is 1.0. In practice, there are fines mainly on top of the ballast, hardly anywhere else (EN13450:2002 & SFS-EN 13450 Aggregates for railway ballast, national guidelines). The grading of the examined railway ballast was also checked by sieving, and the results are presented in figure 1. The limits for the sub-ballast material made of crushed rock are also drawn in the figure for comparison, with all three materials' grain size curves. The continuous black lines are absolute limits for individual samples, and 90% of the results fall within the area limited by dotted lines. The densities of materials in the apparatus, bulk densities, and calculated porosities are presented in Table 1.

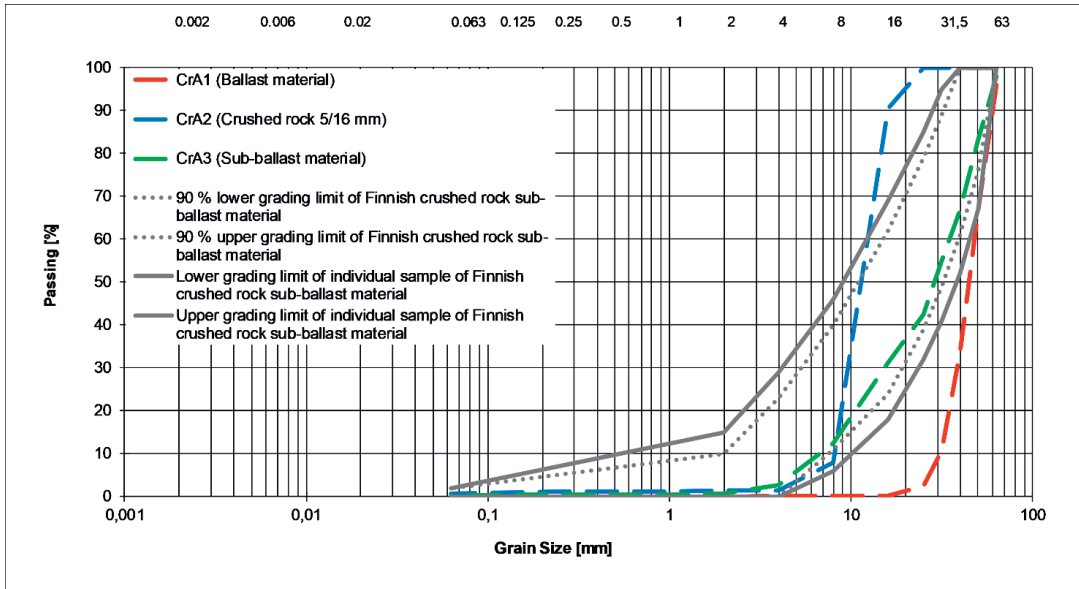


**Figure 1.** Gradings of tested materials. CrA1 (Railway ballast) was the most coarse-grained material and the CrA2 (5/16 mm crushed rock) the most fine-grained. The sub-ballast material (CrA3) fell between the two with regard to grading. The black solid lines in the figure represent the ranges of individual grading results for sub-ballast. Of the results, 90% must fall within the area bound by dashed lines.”

**Table 1.** Test material densities and aggregate bulk densities.

| Material             | Density [kg/m <sup>3</sup> ] | Bulk density [kg/m <sup>3</sup> ] | Porosity [%] |
|----------------------|------------------------------|-----------------------------------|--------------|
| CrA1 Railway ballast | 1490                         | 2690                              | 45 %         |
| CrA2 5/16 mm         | 1490                         | 2690                              | 45 %         |
| CrA3 Sub-ballast     | 1670                         | 2690                              | 38 %         |

The other tested material (CrA2) was 5/16 mm crushed rock, whose commercial names include “drainage ballast” and “capillary break ballast”. The material was chosen for testing because its grain size is clearly smaller than that of railway ballast, yet it contains no fines. 5/16 mm crushed rock is not used as such in embankments; it is also quite homogeneous, since its grain size range is quite narrow (Fig. 1). The continuous empty spaces left between the particles are smaller compared to railway ballast, but there are more of them.

The most interesting tested material from the viewpoint of convective heat transfer in the embankment was the combined sub-ballast material (CrA3), which is used nowadays in crushed rock-based track structures. The grain size distribution of the material is clearly wider compared to the two previous test materials, which usually means that it is more compact. The sieving results are presented in figure 1. Tested CrA3 material grain size distribution was close to coarse side limits of sub-ballast



materials and that is relevant for this convection study. Materials of this type proved to be highly susceptible to segregation during preparation.

### ***General structure of test apparatus***

The test apparatus of 1m<sup>3</sup> sample size was built for this study. A large sample size makes it possible to test materials as big as 63 mm particles. Côté et al. (2011) also selected an apparatus of corresponding size for their research on materials of 75/202 mm grain size. The general structure of test apparatus and its dimensions are presented in figure 2. The insulation of sample space walls is made of 100 mm XPS.

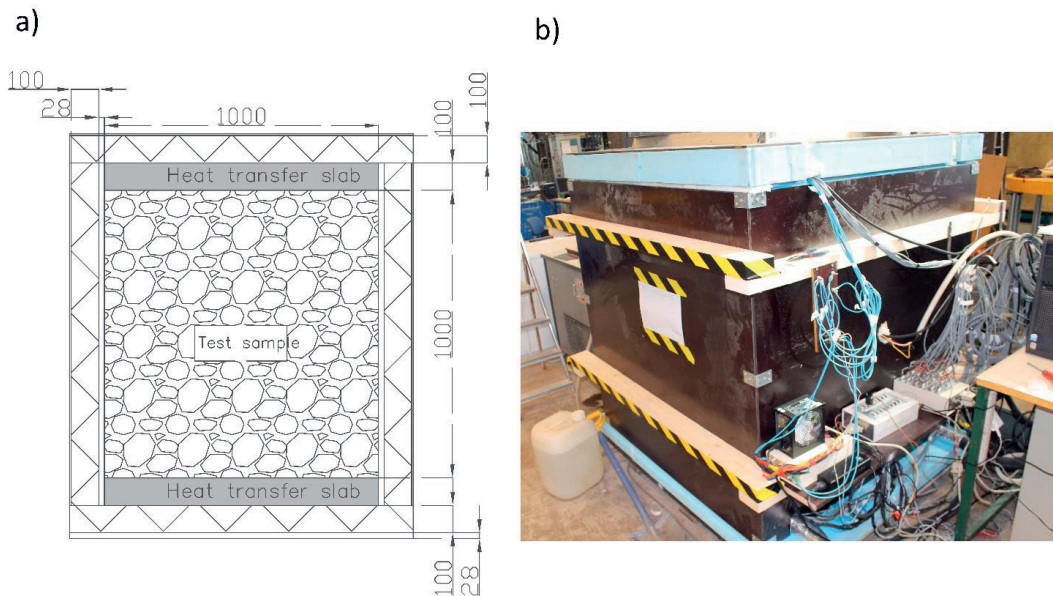


**Figure 2.** The picture a) shows the general structure and dimensions of apparatus and b) the convection measuring apparatus ready for use.

The concrete heat transfer slabs above and beneath the sample are among the key components of the convection measuring apparatus. The slabs measure 1020 mm x 1000 mm x 100 mm and weigh 250kg. Both slabs are built so that they can either cool down or heat up the sample in order to avoid changing their places during testing. A tray of 3mm thick aluminum with 50 mm high sides is built on top of the bottom heat transfer slab. The tray is intended to distribute the heat from the slab uniformly, which enables the possibility to add water to the test sample. The underside of the top heat transfer slab also has a 2mm aluminum sheet. The top or bottom slab is cooled by fluid circulation. For this purpose, a cooling coil of 10 mm copper piping is installed inside the slabs, with the in-slab portion being about 10 m long. The slabs are heated by heating cables cast within the slabs.

The operation of the convection measuring apparatus is based on a computer-controlled measurement system. The control systems maintain the temperature of both slabs in constant temperature. While the apparatus is able to heat either the full slab or half of the slab, all of the heating tests in this project involved heating the entire slab to a constant temperature. The maximum heating power is 140–150 W. Cooling is achieved by external fluid circulation cooling equipment. The cooling power was also measured but was not used for calculations.

All thermocouples used in measurements are of type T and accurate at the temperatures used. Each sample contains 30 thermocouples, as shown in Figure 3. Five sensors each are installed in six layers. The sensors in the sample indicate the distribution of temperatures in different heating situations. Both slabs incorporate comprehensive temperature measurement, with 10 LM335 sensors and five type T thermocouples. The bottom heat transfer slab involves an array of five heat flux sensors, which indicate the amount heat flowing through the bottom slab to the sample. Hukseflux HFP1 heat flux sensors are rated to be accurate by the manufacturer within  $\pm 5\%$  under normal conditions. The heat conductivity is calculated from thermal energy passing through the sample and the temperature difference of the top and the bottom slab. The measured heat flux is calculated as an average of five heat flux sensors on the bottom slab. The slabs temperatures are obtained as an average of 15 temperature sensors on each slab. The used aluminum plates on the bottom and on the top of the sample, was planned to spread the heat flux uniformly from the slab to the sample. The acquired thermal conductivity is the average of the entire sample in the testing apparatus. All measurements were taken from steady state situation. The system was considered to have reached the equilibrium, when there were not significant changes in the heat flux and in the temperatures of the sample. That certainly made the test runs more time consuming – the shortest test run was 7 days and for many of the tests it took much longer time to stabilize.

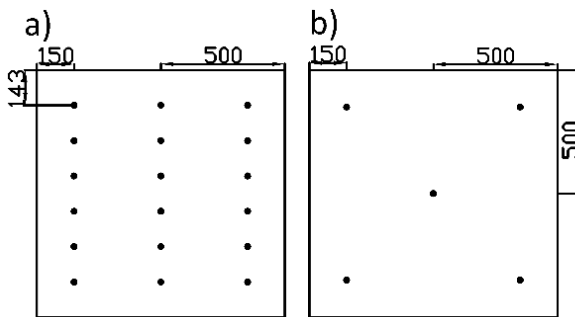


**Figure 3.** Positions of thermocouple temperature sensors in the samples. Side cross-section (a) and plan view from above (b).

The performance of apparatus was tested with bottom and top heating. The test was run out with CrAl-material. Figure 4 shows the temperature distributions in the railway ballast sample in the top heating test. Some approximations were made in plotting the left figure, because there were no temperature sensors at the edges of the sample (see Fig. 3). The left side of figure shows a cross-section of the apparatus 150 mm from the side wall towards the center. The temperature sensors in

the middle of the apparatus also appear to be on the same level, but are actually 350 mm deeper viewed from the side. The temperatures measured from the sample as a function of height are shown on the right. The curve is almost straight and the readings of sensors at the same height are very close to each other. The figure clearly shows how the isotherms settle evenly and horizontally in a top heating situation, which indicates that no flows occur in the sample.

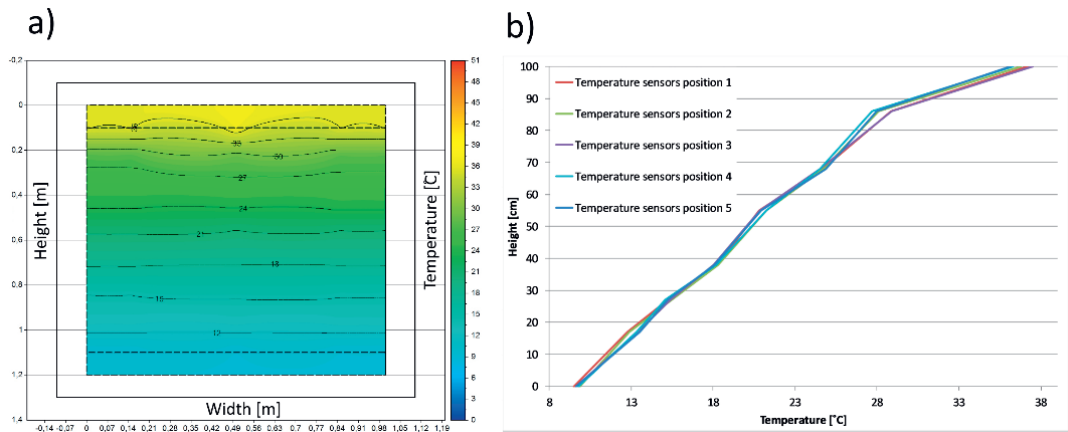


**Figure 4.** Temperatures occurring in railway ballast (CrA1) in a top heating situation. A cross-section at a temperature difference of 27 °C is shown on the figure a). Temperatures of the sample as a function of height are shown on the figure b). Both figures indicate that the change is rather linear and even throughout the sample.

With bottom heating the situation is different, as shown in Figure 5. Then, the shape of the isotherms deviates from horizontal and thermal distribution is not linear. This indicates the convection medium is flowing in the sample. The heat rose in the right side of the sample to the cold top heating slab and descended downwards with the left side of the sample. There were clear differences in temperatures across the sample. The test showed that the apparatus was functional and how the convection phenomenon was possible to recognize in the test. This observation is also supported by other studies, e.g., Goering (1998) who found uneven heat distribution caused by convection cells.

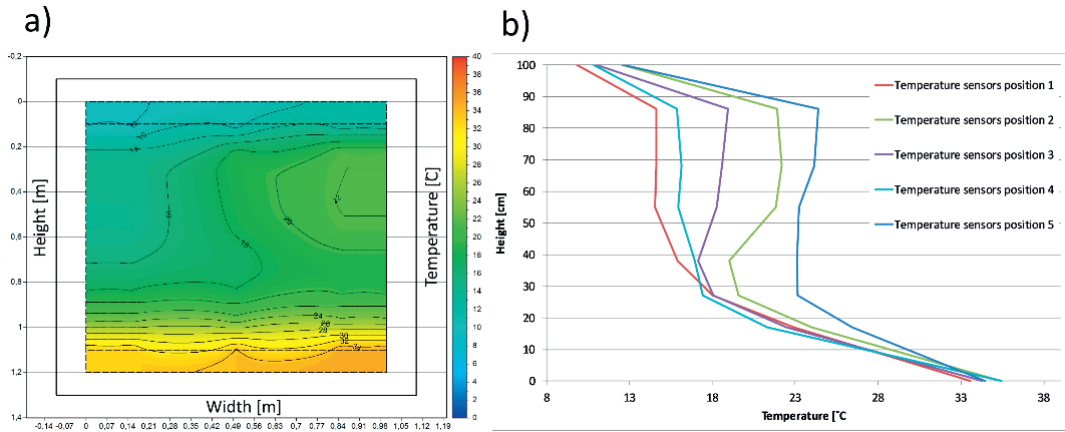


**Figure 5.** The railway ballast sample CrA1 in a convection situation. A cross-section of a wet sample with bottom heating is shown on the figure a). Temperature difference was about 23 °C. Temperatures of the sample as a function of height are shown on the figure b). The figures clearly indicate how warm air rises up on one side, cools down, and descends again.

### *Heat loss*

Although the sample space of the apparatus is insulated, heat transfers either out or in through the walls. At the start of the tests, the intention was to match the mean temperature of the sample inside with the outdoor temperature, whereby heat losses in a heat conduction situation would offset one another. However, in a convection situation, the temperature distribution deviated from linear, causing heat loss in the apparatus. Ambient temperature did not remain absolutely constant during the tests either. This difference between the ambient temperature and the mean temperature of the sample is perceivable in test parametric tables 1, 2 and 3.

Heat loss that should be accounted for in the test apparatus occurs mainly through the insulated sides, because the top and bottom slabs were maintained at a constant temperature and heat flux was measured between the sample and the bottom slab. The amount of thermal energy transferring through the sides can be calculated in principle when the thermal conductivities of wall materials and the temperature within and without the apparatus are known. An attempt was made to calculate heat loss with the help of outdoor air temperature and temperature sensors inside the sample. The method proved quite inaccurate and, therefore, absolute, unrevised values were used to arrive at the research results. The major factor of uncertainty in the heat loss calculation was probably due to the difficulty of determining actual effective conduction area between the walls and the porous material. The precise calculations of heat loss should also consider temperature change rates and the specific heat capacities of apparatus materials. Another way to approximate the heat loss was to deviate sample mean temperature from ambient temperature. That kind of arrangement was tested with a 5/16 mm crushed rock sample (CrA2). The change of mean temperature by 4.5 °C caused the thermal conductivity to drop to 0.25 W/mK from the average of 0.37 W/mK (differential test results are in table 3). Based on this test, the effect of one-degree sample mean temperature deviation from the

ambient temperature caused an error of 0.027 W/mK to heat conductivity at the most. On the second differential test, the effect of changing the mean temperature by 2.0 °C from ambient temperature was negligible to the thermal conductivity.

The differences between the ambient and mean temperature of the samples were mainly below 3 °C which means a maximum error of 0,081 W/mK to samples heat conductivity. This means that in some instances, heat loss calculations indicated that small differences in thermal conductivities are not necessarily significant.

## Test Results

The first material tested was CrA1 railway ballast aggregate, the second was CrA2 with smaller average grain size, and the third one was the most interesting material, CrA3. The most tests were conducted on railway ballast, because our aim was to also study the performance of the apparatus and how a possible occurrence of convection is evident in the results. The railway ballast sample was also tested in a situation where the top heat transfer slab was lifted 50 mm above the sample, leaving a clear air gap between the sample and the top slab. The purpose of this test was to determine the differences between open and closed space convection. The temperature differences tested were generally greater than in the real world, because a closed test apparatus caused a larger critical Rayleigh number. With greater temperature differences, the purpose was to start natural convection, if the material thermal conductivity did not otherwise grow.

The results of top heating tests of CrA1 material are in table 2 and figure 6; CrA2 material results are presented in table 3 and in figure 7; and CrA3 results are shown in table 4 and figure 8. The thermal conductivity in the top heating tests was almost the same for all materials, between 0.34–0.41 W/mK. A slightly larger value was achieved from the first test of CrA1 material, 0.52 W/mK, but that was probably caused by the remaining moisture in the heating and cooling slabs. This value was neglected in the average results as well as offset run with CrA2 material. With CrA2, greater temperature differences were also used to avoid errors from tests' arrangement. Only one top heating test was conducted for CrA3 material because the achieved thermal conductivity was similar with the other materials and Johansen's (1978) test results.

**Table 2.** Test results and parameters for CrA1 material (railway ballast).

| CrA1<br>Railway<br>ballast | Temperature<br>difference<br>[°C] | Thermal<br>conductivity<br>[W/mK] | Mean<br>temperature<br>of sample [°C] | Average<br>temperature<br>of test<br>environment<br>[°C] | Temperature<br>of top slab<br>[°C] | Temperature<br>of bottom<br>slab [°C] | Test run<br>duration<br>[d] |
|----------------------------|-----------------------------------|-----------------------------------|---------------------------------------|--|------------------------------------|---------------------------------------|-----------------------------|
| Dry sample, top heating    |                                   |                                   |                                       |  |                                    |                                       |                             |
| Test A1                    | 10,1                              | 0,52 <sup>a</sup>                 | 21,4                                  | 24,3   | 26,8                               | 16,8                                  | 11                          |
| Test A2                    | 27,1                              | 0,36                              | 20,1                                  | 20,4   | 36,7                               | 9,7                                   | 14                          |
| Test A3                    | 19,4                              | 0,32                              | 18,5                                  | 18,5   | 30,7                               | 11,3                                  | 30                          |
| Test A4                    | 9,2                               | 0,37                              | 17,7                                  | 21,5 <sup>b</sup>  | 22,7                               | 13,6                                  | 42                          |
| Test A5                    | 31,8                              | 0,37                              | 19,5                                  | 19,5   | 38,7                               | 6,9                                   | 17                          |
|                            |                                   | Mean 0,36                         |                                       |  |                                    |                                       |                             |
| Dry sample, bottom heating |                                   |                                   |                                       |  |                                    |                                       |                             |

|  |      |      |      |                   |      |      |    |
|--|------|------|------|-------------------|------|------|----|
| Test B1                                      | 10,0 | 0,81 | 22,1 | 22,8              | 16,9 | 26,9 | 13 |
| Test B2                                      | 19,4 | 1,12 | 21,4 | 23,6              | 12,3 | 31,7 | 8  |
| Test B3                                      | 14,9 | 0,99 | 21,6 | 24,0              | 14,3 | 29,3 | 7  |
| Test B4                                      | 7,1  | 0,89 | 22,6 | 22,2 <sup>b</sup> | 19,2 | 26,3 | 13 |
| Wet sample, bottom heating                   |      |      |      |                   |      |      |    |
| Test C1                                      | 12,3 | 1,69 | 14,9 | 19,7              | 9,4  | 21,8 | 10 |
| Test C2                                      | 23,3 | 3,16 | 19,7 | 21,3              | 11,3 | 34,6 | 7  |
| Test C3                                      | 13,6 | 2,44 | 20,6 | 22,0              | 15,6 | 29,2 | 8  |
| Test C4                                      | 11,1 | 2,04 | 20,0 | 21,2              | 15,6 | 26,7 | 14 |
| Test C5                                      | 5,7  | 1,52 | 21,6 | 23,0              | 19,1 | 24,8 | 13 |
| Wet sample, bottom heating, open top surface |      |      |      |                   |      |      |    |
| Test D1                                      | 5,6  | 1,46 | 21,9 | 24,9              | 19,3 | 24,8 | 12 |
| Test D2                                      | 11,4 | 1,84 | 23,0 | 25,2              | 16,9 | 34,6 | 8  |
| Test D3                                      | 17,7 | 2,61 | 22,2 | 24,6              | 18,3 | 29,7 | 7  |
| Dry sample, convection startup speed test    |      |      |      |                   |      |      |    |
| Test E1                                      | 12,9 |      | 16,1 | 19,4              | 8,9  | 21,9 | 12 |

<sup>a</sup> The result was not used in calculating the mean because it probably contains an error.

<sup>b</sup> Test environment temperature varied considerably during the test, so the mean does not indicate the success of the test reliably.

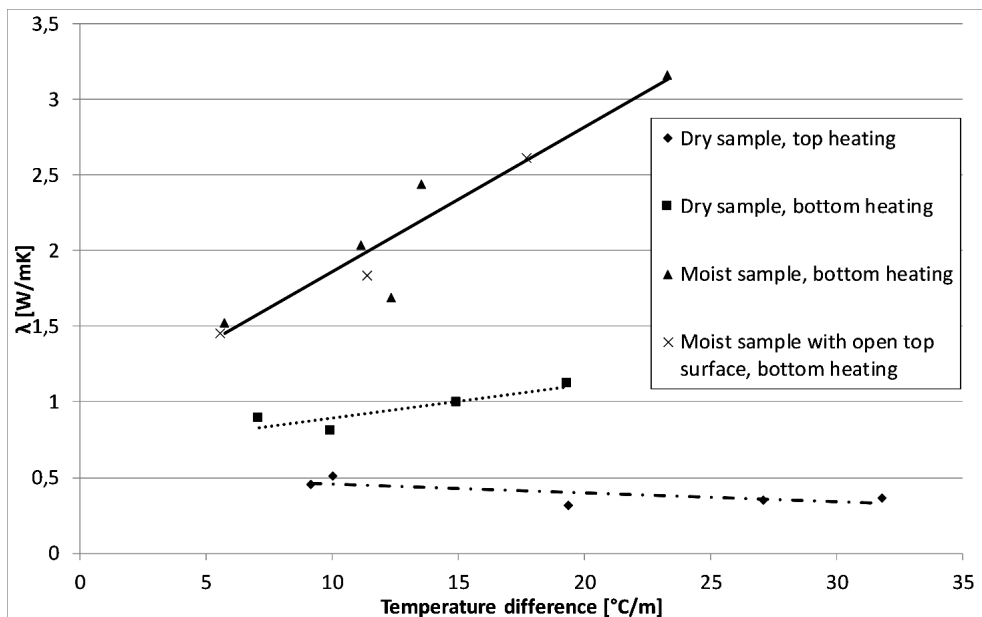


**Figure 6.** Thermal conductivities measured from the CrA1 railway ballast sample, as a function of temperature with a 1.0 m high sample.

**Table 3.** Test results and parameters for Cr2 material (5/16 mm crushed rock aggregate).

| CrA2 5/16 mm               | Temperature difference [°C] | Thermal conductivity [W/mK] | Mean temperature of sample [°C] | Average temperature of test environment [°C] | Temperature of top slab [°C] | Temperature of bottom slab [°C] | Test run duration [d] |
|----------------------------|-----------------------------|-----------------------------|---------------------------------|--|------------------------------|---------------------------------|-----------------------|
| Dry sample, top heating    |                             |                             |                                 |  |                              |                                 |                       |
| Test A1                    | 38,8                        | 0,40                        | 24,1                            | 26,3   | 44,6                         | 5,8                             | 10                    |
| TestA 2.                   | 50,1                        | 0,34                        | 23,6                            | 25,0   | 51,7                         | 1,6                             | 10                    |
| Differential <sup>b</sup>  | 53,3                        | 0,25                        | 31,1                            | 26,6   | 64,7                         | 11,4                            | 21                    |
| Differential <sup>b</sup>  | 62,4                        | 0,37                        | 25,3                            | 23,3   | 64,8                         | 2,4                             | 7                     |
| Average 0,37 <sup>a</sup>  |                             |                             |                                 |  |                              |                                 |                       |
| Dry sample, bottom heating |                             |                             |                                 |  |                              |                                 |                       |
| Test B1.                   | 29,6                        | 0,54                        | 25,0                            | 24,3 <sup>c</sup>                            | 10,0                         | 39,6                            | 14                    |
| Test B2.                   | 39,7                        | 0,55                        | 24,7                            | 24,2   | 4,9                          | 44,6                            | 8                     |
| Test B3.                   | 17,9                        | 0,49                        | 25,8                            | 27,6   | 16,8                         | 34,7                            | 8                     |
| Wet sample, bottom heating |                             |                             |                                 |  |                              |                                 |                       |
| Test C1.                   | 38,9                        | 0,86                        | 31,1                            | 26,6   | 5,6                          | 44,5                            | 21                    |
| Test C2.                   | 28,9                        | 0,99                        | 25,3                            | 23,3   | 10,7                         | 39,6                            | 7                     |

<sup>a</sup> The mean of upper heating thermal conductivity is based on two first tests only.

<sup>b</sup> In the offset run, the mean temperature of the sample was deliberately made to deviate from the mean temperature of the test environment.

<sup>c</sup> Test environment temperature varied considerably, so the mean does not represent real test conditions accurately.

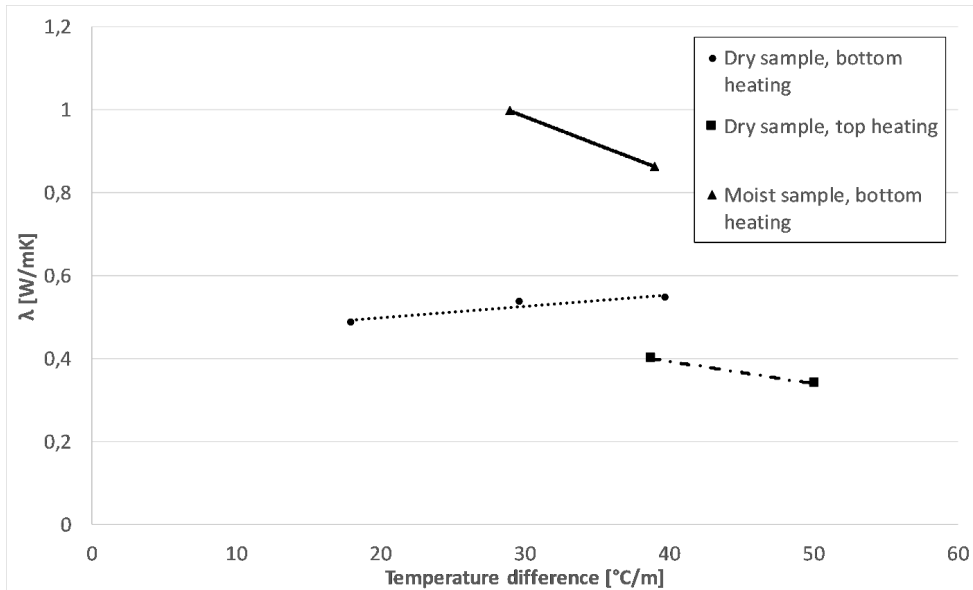


**Figure 7.** Measured thermal conductivities of CrA2 material (5/16 mm crushed rock aggregate).

**Table 4.** Test results and parameters for CrA3 material (sub-ballast)

| CrA3                       | Temperature difference [°C] | Thermal conductivity [W/mK] | Mean temperature of sample [°C] | Average temperature of test environment [°C] | Temperature of top slab [°C] | Temperature of bottom slab [°C] | Test run duration [d] |
|----------------------------|-----------------------------|-----------------------------|---------------------------------|--|------------------------------|---------------------------------|-----------------------|
| Dry sample, top heating    |                             |                             |                                 |  |                              |                                 |                       |
| Test 1.                    | 38,6                        | 0,41                        | 19,9                            | 21,3   | 42,7                         | 4,1                             | 25                    |
| Dry sample, bottom heating |                             |                             |                                 |  |                              |                                 |                       |
| Test 1.                    | 29,6                        | 0,58                        | 21,3                            | 22,6 <sup>a</sup>                            | 5,0                          | 34,6                            | 20                    |
| Wet sample, bottom heating |                             |                             |                                 |  |                              |                                 |                       |
| Test 1.                    | 34,6                        | 1,35                        | 24,0                            | 21,8   | 4,9                          | 35,6                            | 26                    |
| Test 2.                    | 17,4                        | 1,13                        | 23,0                            | 19,9   | 13,3                         | 30,7                            | 21                    |
| Test 3.                    | 7,6                         | 1,17                        | 21,3                            | 20,2   | 17,2                         | 24,8                            |                       |

<sup>a</sup> Since the hall temperature varied considerably, the mean does not represent real test conditions accurately.



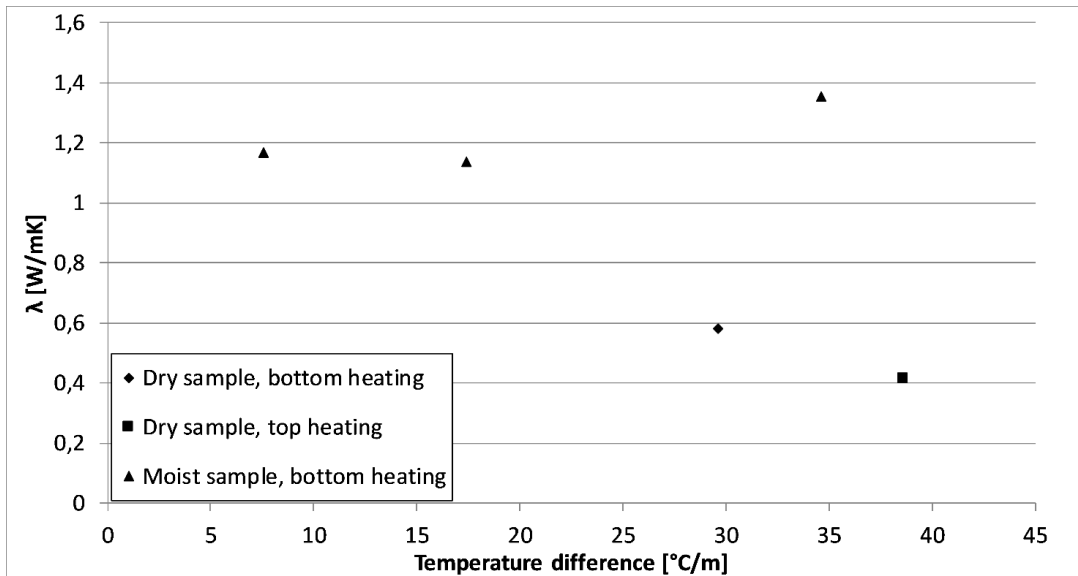


**Figure 8.** Summary of the tests on the CrA3 material (sub-ballast material).

The results of bottom heating were much more interesting than top heating tests. All the results can be found in the previously mentioned figures and tables. The bottom heating caused thermal conductivity to increase in all tested materials that were dry. However, there were significant differences in the growth of thermal conductivity. The thermal conductivity growth in CrA2 materials was only a little above 0.1W/mk with large temperature differences. Similar behavior was noticeable in CrA3 material in which the thermal conductivity increased from 0.4 W/mk value to 0.6 W/mK. With the coarsest material, CrA1 thermal conductivity with bottom heating was 0.89 W/mk, which was tested with the lowest temperature difference. That measured value was more than twice compared to top heating and, in addition, the thermal conductivity increased with increasing temperature difference.

Based on the results, it can be said that CrA1 material was the only one in which natural convection clearly happened. The results of CrA2 material also support this observation, because the thermal conductivity remained almost the same, although the temperature difference was doubled. The interesting detail in dry sample tests was the effect of the test order. It seemed that when the medium started moving, the convection appeared to be stronger with lower temperature differences as well. The great differences between different tests in CrA1 material also led to only one CrA3 dry bottom heating test, because it was obvious that the achieved thermal conductivity difference, 0.2W/mK, was not so significant even when the temperature difference was as great as 29.6 °C

In its natural state, a material always contains some moisture, so it was decided to also test wet material samples. In the wet test, water was led into the aggregate by a thin pipe through the side of the apparatus, from which it flowed to an aluminium tray underneath the sample. Adding water to the sample increased the thermal conductivity of all tested samples.

The smallest changes were detected in CrA2-material, where the thermal conductivity increased to 0.8–1.0 W/mK, which was almost twice that of the dry top heating result. The increase of thermal conductivity was moderate, although the temperature gradients used were high. With CrA3-material, which was the most interesting, the thermal conductivity increased to 1.2–1.4 W/mK with the moist sample. These results are about three times higher than those obtained in the dry top. The coarsest material CrA1 achieved values between 1.5–3.0 W/mK, which were many times higher compared to the ones resulting from top heating tests. After the moisture tests, the top of the samples were wet, which indicated the water flow in the sample by natural convection or diffusion. It seems probable that there is rain like phenomenon in apparatus, where the water evaporates at the bottom, rises up, condensates on top, and rains down.

The CrA1 material sample was also tested in a situation where the top heat transfer slab was lifted 50 mm above the sample, leaving a clear air gap between the sample and the top slab. The results of this test with moist railway ballast material are presented in table 2. The test at a temperature difference of 5.6 °C was the most uncertain in terms of results, because the readings of the heat flux sensors had stabilized, although small changes were still indicated by the temperature sensors in the sample. This not only suggests that, at small temperature differences, heat transfer is slow, in accordance with Fourier's law, but also that stabilization takes a lot of time. It is also possible that convection cells are not a stable process at all. The results may also be affected by the temperature of the test environment. The results from an open top surface also seem to fall mainly on the curve of a wet sample to complement missing points. This probably suggests that a slab removed 50 mm from the top surface of the sample does not constitute the type of open top surface situation met in critical Rayleigh number analysis.

## **Discussion**

### ***Computational analysis based on the theory of convection***

In a computational analysis, the test results were compared to values calculated with Rayleigh Equation 1 and the Nusselt number. The intrinsic permeability included in the formula was a problematic quantity, because it is difficult to determine for highly water permeable coarse materials. Intrinsic permeability can, however, be calculated from water permeability with the Kozeny-Carman formula (Johansen 1975). The intrinsic permeability of a material can also be assessed by other methods. Goering et al. (2000) chose to use the Fair & Hatch method (1933) presented by Bear (1972). In this method, intrinsic permeability is assessed on the basis of porosity, particle shape parameter, share of the studied fraction in the material, and average geometric grain size.

In this study, the water permeability of CrA2 (5/16 mm) crushed rock aggregate was measured in an aggregate laboratory to establish the intrinsic permeability of the material. However, the material proved so coarse that, even at a low pressure difference, the amount of water flowing through the

material exceeded the capacity of the test apparatus. For this reason, no attempts were made to measure the water permeability of the coarser sub-ballast material and railway ballast. The intrinsic permeability determined by the measurements,  $1.38 \cdot 10^{-8} \text{ m}^2$  (calculated with a water permeability value of  $1.04 \cdot 10^{-1} \text{ m/s}$ ), was also proven too small by the computational analysis.

Dry state computational analysis was used to seek a suitable magnitude of intrinsic permeability for the materials on the basis of literature. Then, the built calculation model was matched to the achieved test results. In the dry state tests, it went reasonably well. On the basis of literature, railway ballast was assigned an intrinsic permeability of  $8 \cdot 10^{-7} \text{ m}^2$ , which, judging by the results, was quite close to the correct value. Based on the calculated Rayleigh number, no convection should occur, for instance, in CrA2 material, but thermal conductivity did increase somewhat in the tests. With the CrA2 material, the results matched best when intrinsic permeability was  $3.5 \cdot 10^{-7} \text{ m}^2$ . This value is slightly higher than the value calculated with the water permeability value.

The assessment of the intrinsic permeability of CrA2 and CrA3 materials involves a lot of uncertainty, because determining the quantities necessary for calculating the Rayleigh number in the wet state tests is difficult. The medium in the sample was unsaturated water vapor, whose degree of saturation varied somewhat within the sample. Determining the parameters of this mix proved to be impossible in practice. Evaporation and condensation of water also occurred in the wet state tests, leading to the transfer of a lot of temperature energy during change of state.

During the study, some doubt arose as to whether addition of water to the sample could cause diffusion of water vapor. Water vapor diffusion is a well-known phenomenon in building physics. For example, according to Hagentoft (2001), the ratio between water content and partial pressure of water can be determined on the basis of the general gas law with Formula 3.

$$p_v = 461,4 \cdot (T + 273,15) \cdot v \quad (3)$$

, where

$p_v$ = partial pressure of water vapour [Pa]

T= temperature in centigrade

v= air water content [ $\text{kg/m}^3$ ]

Moreover, according to Hagentoft (2001), it must also be taken into account that air temperature affects maximum water content. For example, air can contain a maximum of about  $5 \text{ g/m}^3$  of humidity at  $0 \text{ }^\circ\text{C}$ , but at  $20 \text{ }^\circ\text{C}$ , as much as  $17 \text{ g/m}^3$ . The respective partial pressures of water vapor are about 630 Pa and 2300 Pa, which means that water vapor flows by diffusion from hot to cold, according to Fick's law. This may partly explain the results of the CrA2 material and the higher thermal conductivity in the wet state. The density of the moving medium must also be considered, since humid air is lighter than dry air (Rogers & Yau 1989), whereby the differences in density due to water vapor may also increase the effect of convection. However, it is difficult to include these effects in a computational analysis.

Table 5 shows estimates of critical temperature differences based on the test results and computational analysis. The critical Rayleigh number affects critical temperature differences, since the boundary surfaces of the material samples were practically closed in the test. When the top surface is open, convection is possible at a smaller Rayleigh number. In dry weather, the critical temperature differences are about 7% lesser than those in the table, if the mean temperature is 0 °C instead of 20 °C. Ambient temperature has a marked impact on the parameters in wet state analyses and may cause wide variation in results. The results also reveal the dependence of the critical temperature difference on the test run, since the Nusselt number did not usually increase in direct proportion to temperature difference. However, when interpreting the results, it should be borne in mind that field measurements at the Hippi test site detected a temperature gradient of about 9 °C/m during the observation period. In nature, the size of the temperature gradient depends largely on the observation point, since the temperature gradient near the surface may also be clearly higher when temperature sinks rapidly. The calculations with the 2.6m thick layer, which is highly used in Northern Finland to insulate the subsoil from frost, led to very low critical temperature differences.

**Table 5.** Critical temperature differences estimated by computational analysis for 1 m and 2.6 m thick layers.

| Material        | Closed/open | Dry/moist | Test run<br>$\Delta T$ [°C ] | Nu[-] | T <sub>crit</sub> 1 m [°C ] | T <sub>crit</sub> 2,6 m [°C ] |
|-----------------|-------------|-----------|------------------------------|-------|-----------------------------|-------------------------------|
| Railway ballast | closed      | dry       | 10                           | 1,6   | 6                           | 2.3                           |
| Railway ballast | closed      | moist     | 6                            | 3     | 2                           | 0.8                           |
| Railway ballast | open        | dry       | 10                           | 1.6   | 4                           | 1.5                           |
| Railway ballast | open        | moist     | 6                            | 3     | 1.3                         | 0.5                           |
| Sub-ballast     | closed      | moist     | 15                           | 1.7   | 9                           | 3.5                           |
| Sub-ballast     | open        | moist     | 15                           | 1.7   | 6                           | 2.3                           |
| Sub-ballast     | open        | moist     | 35                           | 2.1   | 12                          | 4.6                           |

### ***The new grading curves for sub-ballast material***

Based on this study and partly compaction analysis of crushed rock aggregates (Kalliainen et al. 2011), the Finnish Transport Agency now uses new grading limits that are presented in the Figure 9. New grading curves are cutting the coarse side granularity of material and allowing more 0.063...4 mm particles. This kind of grading would result to denser structures, which eliminates the possibility of medium flowing.

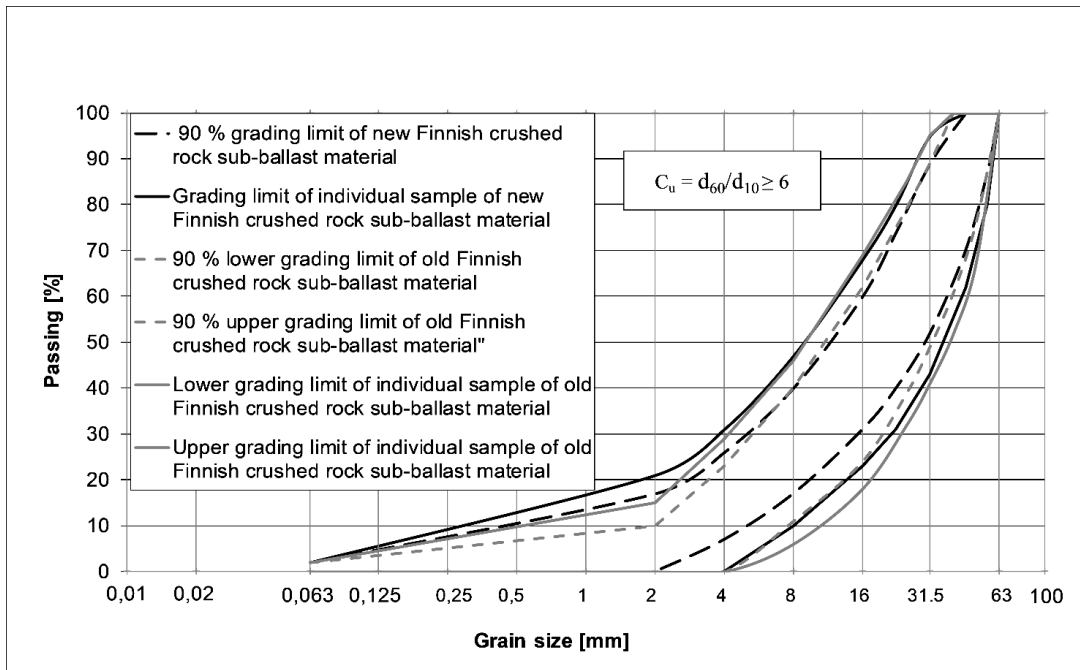


**Figure 9.** New and old grading curves of sub-ballast material. The new curves limit the amount of coarse fractions in the sub-ballast material.

## Conclusion

The results of the laboratory tests prove that natural convection can significantly alter the thermal conductivity of coarse material. Railway ballast (CrA1) proved susceptible to convection, even at small temperature differences, with dry air as the medium, but this phenomenon was not observed with the 5/16 mm crushed rock aggregate (CrA2) and sub-ballast material (CrA3). The moving medium was found to be of great importance, since the addition of water changed the thermal behavior of materials. Water vapor had the greatest impact on railway ballast, but distinct convective heat transfer also started to occur in sub-ballast material when water was added. Besides convection, water vapor diffusion is also likely to be a significant factor, since temperature differences causes a vapor pressure gradient in the sample and moving water vapor carries heat away. The transfer of heat in connection with diffusion may also be increased by a possible change of state of water (Farouki 1986, Kane et al. 2001). The ambient temperature also has a great influence on the moving of water vapor (Jabro 2009).

The laboratory tests of this study do not fully correspond to the actual situation in the field, since a 1 m<sup>3</sup> closed box has several boundary surfaces that do not exist in a railway embankment. These boundary surfaces may change the behavior of convection. Most laboratory tests were carried out while the sample was closed within the airtight test apparatus. Even the situation where the top slab

was lifted 50 mm corresponded to a closed situation in the light of the results. In nature, the top surface is completely open and exposed to winds. The test results also suggest that when the medium starts circulating in the material, it will also continue to circulate at smaller temperature differences. This is only logical, because the forces resisting movement are greater when a material is at rest. It is also probable that trains moving at high speed also promote the flow of medium near the surface.

Based on this study, the following main results can be pointed out:

- The increase of effective thermal conductivity caused by natural convection is a true and significant phenomenon.
- The railway ballast material (CrA1) permits significant convective heat transfer. With small temperature gradients, the thermal conductivity was more than twice compared to conduction-only situation. This kind of material cannot be used in railway substructure in cold regions if the subsoil is frost-susceptible material.
- The critical temperature differences for 1m and 2.6 m thick layers was also calculated. The calculated values for the thicker layer were low compared to the measured gradients from Hippi's test site. This indicates that there is potential for natural convection.
- In environments like in Finland, it is not reasonable to use coarser sub-ballast material, and the height of substructure should not be increased with coarse materials, as it runs the risk of natural convection. The coarse side limits of grading sub-ballast material are now quite near for possible natural convection. The segregation during material placement in sites can also lead to some risks. The presented new grading limits (in discussion) are reducing the possibility of natural convection.
- The water in structures have a great influence on material heat transfer properties, because of natural convection and diffusion. The importance of drainage should be regarded.

### **Data Availability statement**

Some or all data, models, or code that support the findings of this study are available from the corresponding author upon reasonable request. The supplementary data includes temperature and heat flux measurements during tests. The most important data and parameters has been published in this paper.

### **Acknowledgements**

The authors are grateful to the Finnish Transport Agency for funding this study.

### **References**

Bear, J. 1972. *Dynamics of Fluids in Porous Media*. New York, USA: American Elsevier Pub Co.

Côté, J., Fillion, M-H., Konrad, J-M. 2011. "Intrinsic permeability of materials ranging from sand to rock-fill using natural air convection tests". *Canadian Geotechnical Journal*, 48(5): 679–690. <https://doi.org/10.1139/t10-097>

- Fair, G.M., Hatch, L.P. 1933. "Fundamental factors governing the streamline flow of water through sand". *Journal American Water Works Association*, 25: 1551–1565.
- Farouki, O.T. 1986. *Thermal properties of soils: Series on Rock and Soil Mechanics 11*. Clausthal-Zellerfeld, Germany: Trans Tech Publications.
- Finnish Rail Administration. 2004. *SFS-EN 13450 Aggregates for railway ballast, national guidelines*. Helsinki, Finland: Finnish Rail Administration (in Finnish).
- FSA (Finnish Standards Association). 2014. *Characterisation of track geometry quality, Railway Applications, Track Geometry quality, part 6. SFS-EN13848-6*. Helsinki, Finland: FSA.
- FuJun, N., MingHao, L., GuoDong, C., ZhanJu, L., Jing, L., GuoAn, Y. 2015. "Long-term thermal regimes of the Qinghai-Tibet Railway embankments in plateau permafrost regions". *Science China, Earth Sciences*, 58(9): 1669–1676. <https://doi.org/10.1007/s11430-015-5063-0>
- Goering, D.J. 1998. "Experimental investigation of air convection embankments for permafrost-resistant roadway design". *Proceedings of the 7th International Permafrost Conference*, 318–326. Yellowknife, Canada: Collection Nordicana, Quebec.
- Goering, D.J., Instanes, A., Knudsen, S. 2000. "Convective heat transfer in railway embankment ballast". *International Symposium on Ground Freezing and Frost Action in Soils*, 31–36. Ground Freezing 2000, Louvain, Belgium.
- Hagetoft, C-E. 2001. *Introduction to Building Physics*. Lund, Sweden: Studentlitteratur AB.
- Jabro, J.D. 2009. "Water Vapor Diffusion Through Soil as Affected by Temperature and Aggregate Size". *Transport in Porous Media*, 77(3): 417–428. <https://doi.org/10.1007/s11242-008-9282-0>
- Jernbaneverket 1999. *Laerebok i jernbaneteknikk*, L521, Kapittel vol. 6, Frost. Utgitt. 39p.
- Johansen, O. 1977. *Varmeledningsevne av jordarter*. Institute of Kjoleteknikk, 231 p. Draft translation 637: *Thermal conductivity of soils*, U.S Army Cold regions research and engineering laboratory. 291p.
- Kalliainen, A., Kolisoja, P., Luomala, H. & Nurmikolu, A. 2011. "Density and Bearing Capacity of Railway Track Subballast". *Proceedings of International Symposium on Railway Geotechnical Engineering*, GEORAIL 2011, Paris, France.
- Kane, D.G., Hinkel, K.M., Goering, D.J., Hinzman, L.D., Outcalt, S.I. 2001. "Non-conductive heat transfer associated with frozen soils". *Global and Planetary Change*, 29(3–4): 275–292. [https://doi.org/10.1016/S0921-8181\(01\)00095-9](https://doi.org/10.1016/S0921-8181(01)00095-9)

Kersten, M.S. 1949. *Thermal properties of soils*, Engineering Experiment Station, Bulletin 28. University of Minnesota.

Lapwood, E.R. 1948. "Convection of a fluid in a porous medium". *Mathematical Proceedings of the Cambridge Philosophical Society*, 44(4): 508–521.

Mills, I. (1993). *Quantities, units, and symbols in physical chemistry*. Oxford, UK: Blackwell Scientific Publications.

Mu, Y., Ma, W., Liu, Y., Sun, Z. 2010. "Monitoring investigation on thermal stability of air-convection crushed-rock embankment". *Cold Regions Science and Technology*, 62(2): 160–172. <https://doi.org/10.1016/j.coldregions.2010.03.007>

Nurmikolu, A. 2004. *Murskatun kalliokiviaineksen hienoneminen ja routivuus radan rakennekerroksissa, Kirjallisuusselvitys [Degradation and Frost Susceptibility of the Crushed Rock Aggregate in Track Structure, Literature Review]*. Publications of the Finnish Rail Administration A4/2004. Helsinki, Finland: Finnish Rail Administration.

Qian, J., Yu, Q.H., You, Y.H., Hu, J., Guo, L. 2012. "Analysis on the convection cooling process of crushed-rock embankment of high-grade highway in permafrost regions". *Cold Regions Science and Technology*, 78 :115–121. <https://doi.org/10.1016/j.coldregions.2012.01.010>

Rogers R.R. and Yau, M.K. 1989. *A Short Course in Cloud Physics*. Oxford, UK: Pergamon press.

Wang, A., Ma, W. 2012. "The optimal design principles and method of crushed-rock based embankment in cold regions". *Proceedings of the International Conference on Cold Regions Engineering*. <https://doi.org/10.1061/9780784412473.001>